Endogenous triggers of inflammation in the pathogenesis of autoimmunity



Anna Maria Marzeda

Wolfson College

University of Oxford

A thesis submitted for the degree of

Doctor of Philosophy

December 2021

“Success is not final, failure is not fatal:

it is the courage to continue that counts.”

Acknowledgements

First and foremost, I would like to express my deepest gratitude to my supervisor, Professor Kim Midwood. Kim, you are an exceptional mentor and an outstanding scientist - I am eternally thankful that you believed in me and gave me a chance, and for all your support and guidance over these years. It was a truly extraordinary experience to learn from you and grow as a professional, and as a person.

I would also like to thank my co-supervisor, Professor Wyatt Yue. Thank you Wyatt for all your insightful comments and excellent advice, and for making sure I am not only surviving, but thriving.

I wish to thank all the past and present members of the Midwood Group – I am grateful for all your help and advice. It was an absolute pleasure working with you!

I would like to extend my thanks to all students, researchers and support staff at the Kennedy Institute of Rheumatology. Thank you all for making Kennedy such an amazing place to do science.

I am grateful to the Kennedy Trust for Rheumatology Research, which sponsored this project.

To my colleagues and friends, Kristina Zec, Ana Espirito Santo, Carl Lee, Claire Deligne, Martha Gschwandter, Ewaldus Compeer, Anastasios Chanalaris and Valentina Gifford, I would like to say: thank you so very much! For all the scientific discussions, your career advice, but most importantly – for holding the light high for me in the darkest of hour. I could not have made it without your support and encouragement.

Finally, thanks to my family and friends, for their unwavering support and relentless fascination with my work. Thank you for motivating me to never give up.

I would like to end by expressing my utmost gratitude and reverence to my wonderful parents, Iwona and Tomasz Marzeda. I would never have achieved this without their love and support. *Mamo i Tato – dziekuje!*

Thank you all who made this possible.

Anna Marzeda

Statement of Originality

I declare that all data, words, figures, and results included herein are my own work and have not been submitted for another award, degree, or diploma at any other university or learning institution. I certify that this thesis is the result of my own work and all collaborations have been acknowledged at the appropriate locations within the text.

Sub-chapter 1.3 Tenascin-C: a matrix protein with diverse immunomodulatory capabilities, was adapted from my own literature review:

Marzeda AM, Midwood KS. Internal Affairs: Tenascin-C as a Clinically Relevant, Endogenous Driver of Innate Immunity. J Histochem Cytochem. 2018 Apr; 66(4):289-304.

All of the included sections were authored by myself. Permission to include this publication as part of the thesis was obtained from my co-author and supervisor, Professor Kim S. Midwood. This publication is included at the end of this thesis for reference.

This project was completed at the Kennedy Institute of Rheumatology, Nuffield Department of Orthopaedics, Rheumatology and Musculoskeletal Sciences, University of Oxford.

Abstract

Damage-associated molecular patterns (DAMPs) are a group of molecules released following stress and injury, which alert the body to intrinsic danger, trigger inflammation and promote tissue repair. However, it is of vital importance to tightly control responses to DAMPs, in order to prevent excessive pathological inflammation.

Herein, I describe a universal molecular determinant that marks DAMPs for detection by Toll-like receptor 4 (TLR4). Employing comparative analysis of sequence and structural modelling, I identify a positively charged feature present on the surface of the extracellular matrix protein tenascin-C, and many other stress response proteins containing fibrinogen-like globe (FBG) domain. I then experimentally confirm that this cationic ridge is necessary for receptor binding, activation of immune response *in vitro*, and induction of inflammation *in vivo*. Therefore, I discover a novel subset of endogenous TLR4 ligands.

Furthermore, I demonstrate that the FBG domain from tenascin-C (FBG-C) not only elicits the first wave of immune response, but also reprograms cell responses to subsequent threats in health and disease. I reveal how exposition of primary human monocytes to tenascin-C modulates further cytokine release in response to a variety of pathogenic ligands detected by a number of different receptors, and in response to cell stimulation with cytokines and DAMPs, including re-exposure to tenascin-C. This phenomenon is temporally controlled, cytokine specific, and regulated on the level of transcription. Finally, in a cellular model designed to mimic accumulating tissue levels of DAMPs, such as observed in the joints of people with rheumatoid arthritis (RA), I establish that cell tolerance is not broken by repeated, long-term exposure to tenascin-C.

However, monocytes from people with RA exhibit intrinsic differences in response to tenascin-C compared to healthy controls.

Altogether, my data reveal how monocyte activation of TLR4 by tenascin-C induces protective responses designed to prevent opportunistic infection upon tissue injury, and to limit cytokine synthesis during repair. Understanding more about immune re-programming by inflammatory triggers such as tenascin-C may offer the opportunity to reinstate control over dysregulated cytokine networks driving both infectious and chronic ‘sterile’ inflammatory diseases.

Table of contents

List of figures **10**
List of tables **12**
Abbreviations **13**
Chapter 1 Introduction **16**
1.1 The innate immune system – first line of defence against danger **17**
1.1.1 Sensing and eliminating the invader 17
1.1.2 Remembering past threats: innate immune memory? 20
1.1.3 Endotoxin tolerance – preventing immune overreaction 20
1.1.4 Trained immunity – potentiating response to re-infection 26
1.1.5 Conclusions: tolerance and training – two sides of the same coin 30
1.2 Danger-associated molecular patterns (DAMPs) – signals of threat from within **33**
1.2.1 PAMPs and DAMPs in health and disease 35
1.2.2 Endogenous triggers in innate immune memory 37
1.2.3 Unanswered questions in the danger versus stranger model of immunity 40
1.3 Tenascin-C: a matrix protein with diverse immunomodulatory capabilities **42**
1.3.1 Tenascin-C up close: a diverse interaction partner 42
1.3.2 The pro-inflammatory capabilities of tenascin-C 43
1.3.3 Tenascin-C and the resolution of inflammation 49
1.3.4 The wider picture: conclusions from animal models 50
1.3.5 Tenascin-C in the clinic 57
1.4 Hypotheses and Objectives **64**
Chapter 2 Materials and methods **68**
2.1 Materials **69**
2.1.1 Reagents 69
2.1.2 Buffers 73
2.2 Methods **74**
2.2.1 *In silico* analysis of homology and protein modelling 74
2.2.2 Cloning 77
2.2.3 Expression 81
2.2.4 Protein purification 83
2.2.5 Protein quality control 84
2.2.6 Protein activity in vitro 86
2.2.7 Solid phase binding assay 88
2.2.8 Protein activity *in vivo* 89
2.2.9 Induction of innate immune memory 90
2.2.10 Measurement of innate immune memory effects 93

2.2.11 Epigenetic re-modelling studies 97
2.2.12 RA samples 99
2.2.13 Statistics 101
Chapter 3 Fibrinogen-related proteins (FRePs) as novel TLR4 activators 102
3.1 Introduction 103
3.2 Results 104
3.2.1 Amino acid sequence analysis of the 24 human FRePs 104
3.2.2 Structural analysis of the 24 human FRePs 110
3.2.3 FBG domain cloning, expression and purification 115
3.2.4 FBG domain activity *in vitro* 118
3.2.5 FBG domain binding to TLR4 122
3.2.6 FBG domain activity *in vivo* 123
3.3 Discussion 125
3.3.1 *In silico* analysis of human FRePs 125
3.3.2 Recombinant protein preparation 129
3.3.3 Activity in human macrophages 131
3.3.4 Binding to TLR4 135
3.3.5 Induction of inflammation *in vivo* 137
3.3.6 Conclusions 139
Chapter 4 Innate immune memory induced by tenascin-C 141
4.1 Introduction 142
4.2 Results 144
4.2.1 FBG-C de-sensitises human macrophages to LPS 144
4.2.2 Establishment of the memory assay 149
4.2.3 FBG-C induces innate immune tolerance 160
4.2.4 FBG-C induced tolerance: a protein dependent effect 168
4.2.5 FBG-C induced memory is not limited to re-activation of TLR4 pathway 176
4.2.6 FBG-C induced memory is effector-specific and temporally regulated 182
4.2.7 Transcriptional analysis of effector molecules in FBG-C induced memory 186
4.2.8 Epigenetic re-programing in FBG-C induced memory 197
4.3 Discussion 207
4.3.1 Investigating memory effects *in vitro* in human immune cells 208
4.3.2 FBG-C vs LPS in innate immune memory: same, but different? 212
4.3.3 The importance of cell viability in innate immune memory research 215
4.3.4 Complexity of FBG-C induced tolerance/training 217
4.3.5 Understanding re-programming underlying FBG-C induced memory 222
4.3.6 Conclusions 225

Chapter 5 Tenascin-C induced memory in the context of rheumatoid arthritis 228
5.1 Introduction 229
5.2 Results 235
5.2.1 Induction of memory in sustained model of inflammation 235
5.2.2 Innate immune memory in RA blood monocytes 244
5.3 Discussion 249
5.3.1 RA-specific extrinsic factors are not enough to block memory 250
5.3.2 RA cells: intrinsically different, but tolerised as well 253
Chapter 6 Final discussion 256
6.1 Conclusions 257
6.2 Clinical relevance 261
6.3 Future work 264
Appendix 266
Bibliography 272

List of figures

Figure 1.1 Selected pattern recognition receptors and their ligands 19
Figure 1.2 Tenascin-C modulates physiological and pathological inflammation 61
Figure 1.3 Fibrinogen molecule 65
Figure 3.1 Simplified domain organization of human fibrinogen-related proteins (FRePs) 104
Figure 3.2 TLR4-binding epitope identified in the tenascin family 106
Figure 3.3 Localization of the TLR4-binding epitope in tenascin-C 106
Figure 3.4 The linear epitopes of loops 5, 7 and 10 of FBG-C are not conserved in human FRePs 109
Figure 3.5 Subdomain organization of the FBG domain 111
Figure 3.6 Conserved cationic ridge in fibrinogen related proteins (FRePs) 113
Figure 3.7 Protein purification strategy 116
Figure 3.8 Recombinant FBG domain quality control 117
Figure 3.9 FBG domains from predicted TLR4-activating FRePs induce pro-inflammatory cytokine release 120
Figure 3.10 Cytokine release induced by FBG domains is TLR4-dependent and not due to LPS contamination 121
Figure 3.11 FIB-G and FIC-1 bind to TLR4 122
Figure 3.12 FBG domains of FIB-G and FIC-1 induce inflammation *in vivo* 124
Figure 3.13 Recently published crystal structures of FBG domains from TN-C, ALP-3, ALP-4, ALP-2 and ALP-6 confirm structural accuracy of modelled cationic ridge 128
Figure 3.14 Additional positively charged residue in FIC-2 may contribute to the induction of cytokine release 132
Figure 4.1 LPS de-sensitises primary human macrophages 147
Figure 4.2 FBG-C de-sensitises primary human macrophages 148
Figure 4.3 Memory assay protocol 150
Figure 4.4 Optimization of LPS induced tolerance control I 153
Figure 4.5 Optimization of LPS induced tolerance control II 154
Figure 4.6 Optimization of β-glucan induced training control I 157
Figure 4.7 Optimization of β-glucan induced training control II 158
Figure 4.8 FBG-C induces tolerance, but not training, to LPS 161
Figure 4.9 LPS induces tolerance to FBG-C 163
Figure 4.10 β-glucan does not induce training to FBG-C 165
Figure 4.11 FBG-C induces tolerance to FBG-C 167
Figure 4.12 Cell viability during PRIME step 171
Figure 4.13 Cell viability during TRIGGER step 172
Figure 4.14 Cell viability - photos 173
Figure 4.15 FBG-C induced tolerance is protein dependent and not due to LPS contamination 175
Figure 4.16 FBG-C induced memory is not contained to the activation of TLR4 pathway I 179

Figure 4.17 FBG-C induced memory is not contained to the activation of TLR4 pathway II . 181
Figure 4.18 Time course memory assay protocol 183
Figure 4.19 Memory effects are effector-specific and temporally regulated..... 185
Figure 4.20 Transcriptional regulation of memory - assay protocol 186
Figure 4.21 Transcriptional regulation of memory - primary response 188
Figure 4.22 Transcriptional regulation of memory – secondary response I 192
Figure 4.23 Transcriptional regulation of memory – secondary response II 193
Figure 4.24 Secondary challenge contributes to the FBG-C generated IL-6 superinduction ... 195
Figure 4.25 FBG-C induced tolerance/superinduction is protein dependent..... 196
Figure 4.26 Epigenetic probe library testing – assay protocol..... 197
Figure 4.27 Epigenetic probes alter TNF tolerance 199
Figure 4.28 Epigenetic probes alter IL-6 superinduction 200
Figure 4.29 STRING interaction network analysis of proteins involved in the establishment of TNF tolerance 201
Figure 4.30 STRING interaction network analysis of proteins involved in the establishment of IL-6 superinduction 202
Figure 4.31 Gene ontology (GO) enrichment analysis 204
Figure 4.32 Chromatin immunoprecipitation – assay protocol 206
Figure 4.33 Proposed regulation mechanisms of FBG-C and LPS generated IL-6 superinduction 223
Figure 5.1 Tolerance during prolonged exposure to FBG-C I..... 237
Figure 5.2 Tolerance during prolonged exposure to FBG-C II 240
Figure 5.3 Induction of tolerance by citrullinated FBG-C..... 243
Figure 5.4 Primary immune response in rheumatoid arthritis patients blood monocytes..... 245
Figure 5.5 Innate immune memory effects in rheumatoid arthritis patients blood monocytes I 246
Figure 5.6 Innate immune memory effects in rheumatoid arthritis patients blood monocytes II 247

List of tables

Table 1.1 Examples of damage-associated molecular patterns (DAMPs) with their respective receptors 34
Table 1.2 Tenascin-C as a modulator of cellular behaviour in inflammation 45
Table 1.3 Tenascin-C in mouse models of inflammatory diseases 56
Table 2.1 cDNA clones of human FRePs purchased from Sino Biological 69
Table 2.2 Accession numbers of the 24 human FRePs 75
Table 2.3 Available crystal structures of FBG domains 76
Table 2.4 Sequence details of cloned FBG domains 78
Table 2.5 Sequences of primers designed for cloning of FBG domains 79
Table 2.6 Composition of PCR mixes 80
Table 2.7 Protocol of PCR 80
Table 2.8 Parameters of expressed recombinant FBG domains 82
Table 2.9 Composition of RT reaction mix 94
Table 2.10 RT reaction protocol 94
Table 2.11 TaqMan Assays IDs 95
Table 2.12 Composition of TaqMan qPCR reaction mix 95
Table 2.13 Protocol of TaqMan qPCR 95
Table 2.14 Small molecule epigenetic probes tested 98
Table 2.15 Details of study participants suffering from RA 99
Table 2.16 Details of healthy control participants 100
Table 3.1 FBG domain sequence identity in human FRePs 105
Table 3.2 Accession numbers and used abbreviations of 24 human FRePs 108
Table 3.3 Conservation of epitopes involved in TLR4 activation in human FRePs 114
Table 3.4 Recombinant protein yields 116
Table 4.1 Immune triggers used to interrogate FBG-C induced cross-tolerance 177

Abbreviations

ACPA, anti-citrullinated protein antibody

ANOVA, analysis of variance

ATP, adenosine triphosphate

BCG, Bacillus Calmette–Guérin

BSA, bovine serum albumin

C/EBPβ, CCAAT/enhancer binding protein-β

CALEB, chicken acidic leucine-rich EGF-like domain-containing brain protein

CAMP, cathelicidin antimicrobial peptide

CBB, coomassie brilliant blue

CCL, C–C motif chemokine ligand

CD, cluster of differentiation

ChIP, chromatin immunoprecipitation

CIRP, cold-inducible RNA binding protein

CLR, C-type lectin receptor

CSPG5, chondroitin sulfate proteoglycan 5

CTCF, CCCTC-binding factor

CXCL5, C-X-C motif chemokine 5

DAMP, damage-associated molecular pattern

DC, dendritic cell

DKK1, Dickkopf-related protein 1

DMARD, disease-modifying antirheumatic drug

DMSO, dimethyl sulfoxide

ECM, extracellular matrix

EDA, extra domain A

EDTA, ethylenediaminetetraacetic acid

EGF-L, epidermal growth factor-like

EGFR, epidermal growth factor receptor

ELISA, enzyme-linked immunosorbent assay

ET, endotoxin tolerance

FBG, fibrinogen-like globe

FBS, fetal bovine serum

FNIII, fibronectin type III-like repeats

FReP, fibrinogen-related protein

GM-CSF, granulocyte-macrophage colony-stimulating factor

GSK3, glycogen synthase kinase 3

HC, healthy control

HIF-1, hypoxia-inducible factor 1

HIV, human immunodeficiency virus

HKCA, heat killed *Candida albicans*

HKEC, heat killed *Escherichia coli*

HKSA, heat killed *Staphylococcus aureus*

HLA, human leukocyte antigen

HMGB1, high mobility group box 1

HMGN1, high mobility group nucleosome-binding protein 1

HMW, high molecular weight

HRP, horseradish peroxidase

IFN, interferon

IL, interleukin

IPTG, isopropyl ß-D-1-thiogalactopyranoside

IRAK, interleukin-1 receptor-associated kinase

IRF3, interferon regulatory factor 3

LAL, limulus amebocyte lysate

LB, lysogeny broth

LBP, lipopolysaccharide binding protein

LDH, lactate dehydrogenase

LPS, lipopolysaccharide

LTA, lipoteichoic acid

Mab, monoclonal antibody

M-CSF, macrophage colony-stimulating factor

MAPK, mitogen-activated protein kinase

MARCO, macrophage receptor with collagenous structure

MD-2, myeloid differentiation factor-2

MDP – muramyl dipeptide

MDSC, myeloid-derived suppressor cells

MMP, matrix metalloproteinase

MRC1, mannose receptor C-type 1

MST, microscale thermophoresis

mTOR, mammalian target of rapamycin

MTT, 3-(4,5-dimethylthiazol-2-yl)-2,5-diphenyltetrazolium bromide

MyD88, myeloid differentiation factor-2

NF-κB, nuclear factor kappa-light-chain-enhancer of activated B cells

NLR, nucleotide-binding oligomerization domain-like receptor

NMR, nuclear magnetic resonance

NOD2, nucleotide-binding oligomerization domain-containing protein 2

OD, optical density

OVA, ovalbumin

oxLDL, oxidised low-density lipoprotein

PAD, protein-arginine deiminase

PAGE, polyacrylamide gel electrophoresis

PAMP, pathogen-associated molecular pattern

PBMC, peripheral blood mononuclear cell

PBS, phosphate-buffered saline

PCR, polymerase chain reaction

PI3K, phosphatidylinositol 3-kinase

PMB, polymyxin B

PRR, pattern recognition receptor

PTPN22, protein tyrosine phosphatase non-receptor type 22

RA, rheumatoid arthritis

Rag1, recombination activating gene 1

RAGE, receptor for advanced glycation endproducts

RF, rheumatoid factor

RLR, retinoic acid-inducible gene-I-like receptors

RPM, revolutions per minute

RPMI, Roswell Park Memorial Institute

RT, room temperature

RT qPCR, real time quantitative PCR

SAR, systemic acquired resistance

SCID, severe combined immunodeficiency

SDS, sodium dodecyl sulfate

SHIP, Src homology 2 (SH2) domain containing inositol polyphosphate 5-phosphatase

SLE, systemic lupus erythematosus

SOCS1, suppressor of cytokine signalling 1

STAT4, signal transducer and activator of transcription 4

TCR, T-cell receptor

TEMED, tetramethylethylenediamine

TGF-β, transforming growth factor beta

TI, trained immunity

TLR, Toll-like receptor

TMB, 3,3',5,5'-tetramethylbenzidine

TNF, tumour necrosis factor

TNFR, TNF receptor

TRAF, TNF receptor associated factor

TRIF, Toll/interleukin-1 receptor domain-containing adapter inducing interferon-β

1

Introduction

Contents

1.1 The innate immune system – first line of defence against danger 17

1.1.1 Sensing and eliminating the invader 17

1.1.2 Remembering past threats: innate immune memory? 20

1.1.3 Endotoxin tolerance – preventing immune overreaction 20

1.1.4 Trained immunity – potentiating response to re-infection 26

1.1.5 Conclusions: tolerance and training – two sides of the same coin 30

1.2 Danger-associated molecular patterns (DAMPs) – signals of threat from within ... 33

1.2.1 PAMPs and DAMPs in health and disease 35

1.2.2 Endogenous triggers in innate immune memory 37

1.2.3 Unanswered questions in the danger versus stranger model of immunity 40

1.3 Tenascin-C: a matrix protein with diverse immunomodulatory capabilities 42

1.3.1 Tenascin-C up close: a diverse interaction partner 42

1.3.2 The pro-inflammatory capabilities of tenascin-C 43

1.3.3 Tenascin-C and the resolution of inflammation 49

1.3.4 The wider picture: conclusions from animal models 50

1.3.5 Tenascin-C in the clinic 57

1.4 Hypotheses and Objectives 64

1.1 The innate immune system – first line of defence against danger

The human body is in a state of permanent siege, invisible to the naked eye. On a daily basis hordes of diverse pathogens seeking a host come in contact with our skin and mucosa, and are inhaled or ingested. In response to this constant threat we have evolved a sophisticated immune system, comprising two distinct, yet closely collaborating, sub-systems: innate and the adaptive immunity. The latter provides responses tailored to the specific invading pathogen, such as T cell cytotoxicity and the production of antibodies by B cells, granting long-lasting protection in the event of re-infection. However, mounting of the adaptive responses requires time, and the enemy has extraordinary replication properties – for example a single *Escherichia coli* bacterium is capable of dividing up to 2-3 times every hour [1], and thus producing millions of cells within a few hours. Thus, non-specific, yet swift mechanisms of innate immunity are essential, providing protection during the first critical phase of the invasion [2].

1.1.1 Sensing and eliminating the invader

The first obstacle on the road to successful invasion by a pathogen is the epithelium. The skin epidermis and the mucosal membranes lining respiratory, digestive, reproductive and urinary tracts provide a physical barrier separating the host system from the external environment [3]. Additionally, the secretion of sweat, saliva and mucus by the epithelial tissues helps lower pH and mechanically remove the pathogens. The epithelium also serves as a niche for the commensal microbiota in symbiotic relationship with the host. These microbiota further impede pathogen spread through competition for space and nutrients, and through production of antimicrobial substances [4].

When this physical barrier is breached, the defensive function of the innate immune system is executed through a combination of humoral- and cell-mediated mechanisms. Immediately, the surface of pathogen cells is bound by opsonins, a varied

group of molecules serving as tags for elimination. The complement system is activated and a proteolytic cascade leads to formation of membrane pores and disintegration of opsonin-tagged invaders [5]. Moreover, broad-spectrum antimicrobial peptides such as defensins [6] and cathelicidins [7] are produced by innate immune and epithelial cells to reinforce host defences by destroying bacterial membrane integrity and disrupting cell metabolism.

The innate immune responses are coordinated by circulating and tissue-resident cells including monocytes and macrophages, neutrophils and other granulocytes, dendritic cells and natural killer cells. To detect the presence of a pathogen, innate immune cells utilize pattern recognition receptors (PRRs). PRRs are structurally versatile proteins and can be divided into four major families: membrane-bound Toll-like receptors (TLRs) and C-type lectin receptors (CLRs), and intracellular NOD-like receptors (NLRs) and RIG-like receptors (RLRs) [8]. PRRs sense pathogen-derived molecular motifs, collectively referred to as pathogen-associated molecular patterns (PAMPs). PAMPs comprise motifs found on various molecules produced exclusively by microorganisms, and not by the host, and therefore are promptly recognized as non-self. As these molecules are essential for pathogen survival, and any alterations could bring functional impairment or lethality, PAMPs remain highly conserved among large groups of pathogens [2]. For example, lipopolysaccharide (LPS), a PAMP sensed by TLR4, is the main component of the outer membrane in Gram-negative bacteria, and is vital for the protection of the bacterial cell from external environment [9]. Examples of PAMPs with their respective PRRs are presented in Fig. 1.1.

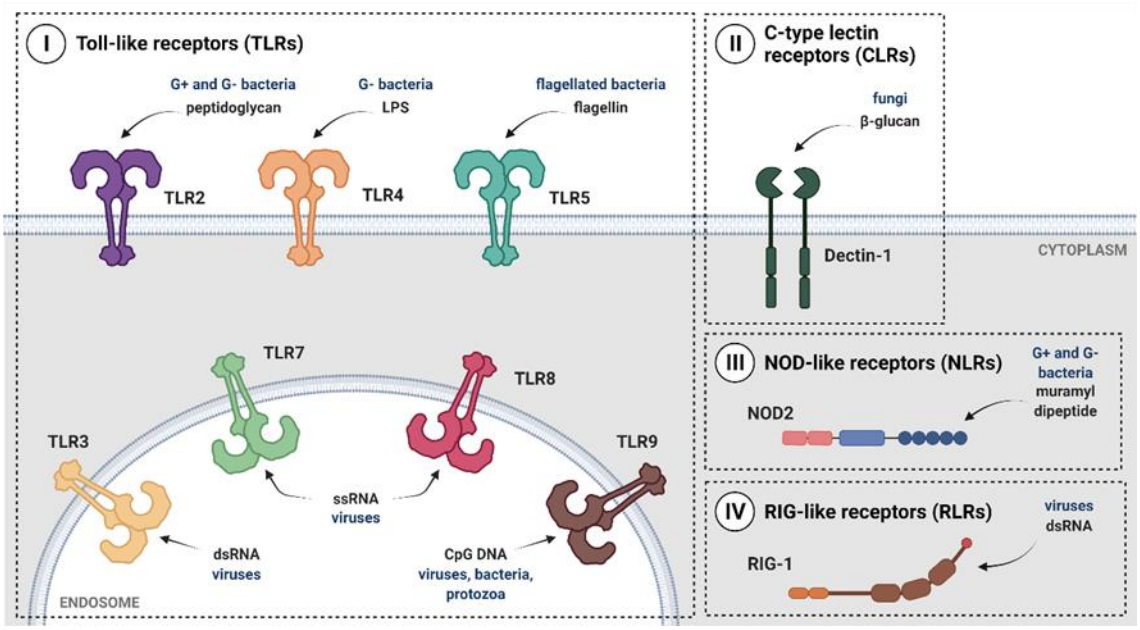


Figure 1.1 Selected pattern recognition receptors and their ligands. Pattern recognition ligands (PRRs) comprise of four major families: membrane-bound Toll-like receptors (TLRs) and C-type lectin receptors (CLRs), and intracellular NOD-like receptors (NLRs) and RIG-like receptors (RLRs). Examples of each of the families, with respective agonists and their origins, are presented above. G+, Gram positive; G-, Gram negative; ds, double stranded; ss, single stranded; NOD, nucleotide-binding oligomerization domain; RIG, retinoid acid-inducible gene.

The binding of PAMP ligands by PRRs triggers signalling cascades that result in transcriptional activation of genes required for the antimicrobial response [10]. Following detection of PAMPs, the cell-mediated response of the innate immune compartment is driven by three predominant mechanisms. Firstly, activated leukocytes express cytokines and chemokines, such as tumour necrosis factor (TNF) and interleukin 6 (IL-6), pleiotropic signalling molecules that promote inflammation and drive cellular infiltration. Furthermore, some innate immune cells, particularly macrophages, neutrophils and dendritic cells, are capable of neutralizing pathogens through a process called phagocytosis. Phagocytes recognize complement components and opsonins on the surface of a pathogen, engulf and internalize it, and eventually destroy the microbial cell through lysis. Finally, innate effector cells provide instruction to the adaptive immune system allowing for the development of targeted immune response and long-term immune memory. This is mostly executed by dendritic cells, and also to some extent by

macrophages, which following capture of a pathogen are capable of antigen processing and presentation to the lymphocytes. Additionally, cytokines and immune mediators produced by innate immune cells also regulate adaptive immune responses, for example by increasing the efficiency of antigen presentation, inducing chemotaxis of lymphocytes and stimulating their maturation [11]. Whilst these immediate responses of the innate immune system are well established, emerging data has highlighted a novel, longer term aspect of innate biology.

1.1.2 Remembering past threats: innate immune memory?

Conventionally, immunological memory has been considered to be a distinctive attribute of the adaptive immune system. Adaptive immune cells, lymphocytes, carry antigen specificity, and following recognition of the invading pathogen are expanded, allowing for potent tailored cytotoxic and antibody responses on re-infection [2]. However, an antibody and clonal selection based system is absent in about 97% of living species [12]. It seems inconceivable that plants and invertebrates, equally endangered with a plethora of pathogenic microorganisms, would not develop acquired defense mechanisms allowing for more efficient pathogen clearance. Thus, one could speculate that capability to retain some sort of memory on past infections is likely to have evolved outside of the classical adaptive system present in vertebrates. Indeed, a constantly growing body of evidence supports the idea that the innate immune system also possesses the ability to store information about recent encounters with pathogens to provide an adjusted response to future immune triggers.

1.1.3 Endotoxin tolerance – preventing immune overreaction

In the beginning of the 20th century neurological disorders, such as neurosyphilis, and psychiatric conditions, e.g. psychosis, were treated with so called ‘fever therapy’. This involved induction of fever by intentional inoculation with malaria

(the method was awarded the Nobel Prize in 1927) or injection of other pyrogenic (fever inducing) agents, for example typhoid fever vaccine [13]. It was observed that patients receiving the vaccine exhibited attenuated responses to repeated vaccination over time, and required increasing doses of the vaccine to elicit febrile reaction [14]. This puzzling effect was further examined in rabbits, revealing that repetitive administration of bacterial preparations indeed caused quick and progressive reduction of their capability to induce fever [15]. The same effects were observed *in vivo* using purified bacterial endotoxin (or LPS) [16], and this hyporesponsive state was since referred to as endotoxin tolerance (ET).

Further *in vivo* investigation demonstrated rabbits tolerised with multiple doses of endotoxin are not only protected from induction of febrile responses, but are also resistant to lethal effects of LPS [17]. Moreover, induction of ET by pre-treatment with low doses improved survival of mice [18, 19] and rats [20, 21] following challenge with a lethal dose of LPS. Such reduced toxicity could be explained when induction of pro-inflammatory cytokines by LPS was demonstrated to be suppressed in tolerised animals. Serum levels of TNF, IL-1β, and IL-6 in response to endotoxin administration were found to be markedly decreased in tolerised mice [19, 22, 23], rats [21], and rabbits [24]. Inhibition of TNF and IL-6 release in ET was also reported in a clinical trial with healthy human volunteers [25].

A breakthrough was made when transfer of LPS-susceptible macrophages permitted induction of ET in LPS resistant mice, demonstrating the crucial role of macrophages in the generation of tolerance [18]. Since this study, impaired cytokine production in ET has been widely reported in monocytes and macrophages *in vitro*, and *ex vivo* in cells isolated from tolerant animals (comprehensively reviewed in [14]). Amongst these published data, suppression of TNF release following re-challenge with

endotoxin emerges as a common shared feature, observed consistently in murine (peritoneal macrophages [26-31], splenocytes [28, 32], bone marrow derived macrophages [33, 34]) and human (peripheral blood mononuclear cells [35-37], monocytes [38-40], monocyte derived macrophages [35, 40]) primary cells, and cell lines alike (mouse [30, 41] and human THP-1 [36, 38, 40, 42, 43]). However, secretion of other inflammatory mediators, such as IL-6 and IL-1β, has been reported to be both suppressed and augmented in ET (reviewed in [44]). For example, in an *in vitro* study with healthy human blood monocytes, secondary stimulation of LPS tolerised cells resulted in inhibition of TNF, and significant increase of IL-6 and IL-1β [45]. What is more, tolerant human monocytes were characterized *in vitro* by enhanced phagocytic capacity, yet impaired antigen presentation [46]. This provides the first clue to the complexity of ET, and hints that is not simply a state of complete unresponsiveness.

Since its discovery, molecular mechanisms mediating LPS tolerance have been a subject of scientific debate. Traditionally, the tolerant state observed in endotoxin stimulated cells was suggested to be a result of disabled LPS signalling through its receptor, TLR4. For LPS to activate a TLR4-mediated response, three additional host proteins are required: LPS binding protein (LBP), cluster of differentiation 14 (CD14), and myeloid differentiation protein-2 (MD-2). LBP transports LPS in the direct vicinity of the cell and CD14 delivers the molecule to MD-2 bound to TLR4 [47]. The formation of the signalling platform, composed of two copies of the LPS-MD2-TLR4 complex, results in triggering of a downstream signalling cascade through an adaptor protein MyD88, allowing for activation of the NF-κB pathway, and resulting in pro-inflammatory cytokine production. LPS induced signalling can also stimulate MyD88-independent pathway through the engagement of adaptor molecule Toll/IL-1R domain-containing adaptor-inducing IFN-β (TRIF), which activates the interferon regulatory

factor 3 (IRF3) transcription factor, leading to upregulation of type I interferons [48]. Indeed, the receptor complex, and downstream signalling molecules were implied to be affected in ET. In mouse peritoneal macrophages *in vitro* stimulation with LPS caused a decrease in surface expression of TLR4 within hours, and this suppression was still sustained after 24 h [49]. However, other studies demonstrated the level of TLR4 surface expression was not reduced in peripheral blood mononuclear cells 24 h post [50], and in Chinese hamster ovary cells 5 h post exposure to LPS [51]. Varied observations were published on TLR4 gene expression in human, mouse and rat cells, with mRNA reported to be decreased, unchanged, or increased [52]. Expression of the TLR4 co-receptor, CD14, was also found to be augmented in a human monocytic cell line [53, 54], and its surface expression in human THP-1 cells and mouse macrophages was increased, or remained unchanged [49, 55]. Finally, levels of MD-2 mRNA in LPS tolerance were shown to be both upregulated in human monocytes [56], and downregulated in peripheral blood mononuclear cells [50]. Collectively, these data do not support sequestering of TLR4 and its co-receptors from the cell surface as the mechanistic cause of LPS tolerance.

Upon re-challenge with LPS, impaired NF-κB activation was repeatedly shown in tolerant cells [44], and is sometimes reported as proof of tolerance induction alongside TNF suppression. For instance, inefficient phosphorylation and degradation of NF-κB inhibitors, preventing nuclear translocation of this transcription factor, in response to LPS was demonstrated in tolerised mouse macrophages [57], human THP-1 cells [55, 58], and in blood monocytes isolated from patients during Gram-negative sepsis [59]. Upstream in the signalling cascade, a number of negative regulators of the MyD88-dependent signalling cascade was identified as relevant in ET (reviewed in [60]), that could explain diminished NF-κB activity. For example, the SH2-containing inositol

phosphatase (SHIP), inhibiting NF-κB through reduction of phosphatidylinositol 3-kinase (PI3K) activity [61], was shown to be upregulated in tolerised mouse macrophages [62], and in human monocytes [63]. Furthermore, SHIP was demonstrated to be essential for the induction of ET in SHIP−/− bone marrow derived macrophages [62], and following shRNA knockdown of SHIP-1 in THP-1 cells [64]. Other molecules, such as IRAK-M, A20, and SOCS1, where also found to be elevated in ET [65, 66], and their knockdown caused impaired acquisition of tolerance in mouse macrophages [67, 68], or in human THP-1 cells [69]. In addition, defects in the components of MyD88 - NF-κB pathway were also associated with the tolerant phenotype. A short splice variant of MyD88, characterised by diminished capacity to activate downstream signalling, was upregulated in monocytes from septic patients [70]. Dysregulation of NF-κB protein composition, with increase of the inactive p50 homodimer, and a decrease of the p50/p65 active heterodimer, was observed in a human monocytic cell line [54], and in peripheral blood mononuclear cells from patients with severe sepsis [71], and after major trauma [72].

However, as alluded to above, tolerance induced by LPS is not a state of complete immunoparalysis, and tolerised cells are not simply transcriptionally inactive. In naïve myeloid cells activation of TLR4 signalling by LPS leads to expression of a variety of genes, including cytokine mediators of inflammation, but also antimicrobial peptides, coagulation factors, molecules involved in tissue repair, and regulators of cell metabolism [73]. Upon acquisition of ET some of the LPS response genes, such as pro-inflammatory cytokines, become silenced and can no longer be induced by further stimulation with endotoxin; these are sometimes referred to as tolerisable genes, e.g. IL-6 and IL-1β. Meanwhile, other, non-tolerisable genes, for example cathelicidin-related antimicrobial peptide (CAMP), or scavenger macrophage receptor with collagenous

structure (MARCO), continue to be expressed [74]. Therefore, receptor downregulation, or negative regulation of signalling cascades, are unlikely to be exhaustive explanation of observed ET effects.

The most recent advances in the field demonstrate that this altered transcriptomic profile of tolerised cells is a result of an extensive epigenetic reprogramming. DNA methylation, and acetylation and methylation of histone tails were shown to alter chromatin architecture and its accessibility, and thus regulate gene transcription. These modifications, or marks, can be both repressive, for example di-methylation of histone H3 at lysine 9 (H3K9me2) and tri-methylation of H3 at lysine 27 (H3K27me3), and activating, like acetylation of H4 (H4Ac) and tri-methylation of H3 at lysine 4 (H3K4me3) [75]. In ET, extensive epigenetic re-modelling in promoter and enhancer regions of LPS response genes were demonstrated in tolerised human monocytes, resulting in transcriptional activity that could explain observed tolerant phenotype [39, 74, 76]. For example, enhanced repressive marks, H3K9me2 and DNA methylation, and reduction of phosphorylation of histone H3 at serine 10 (p-H3S10), linked with open chromatin, were found at TNF gene promoter in LPS tolerised THP-1 cells [42, 77].

It is also important to mention that LPS-elicited production of immune mediators, such as TNF, IL-1β and IL-6, is being controlled beyond gene transcription, through post-transcriptional regulatory mechanisms. These include RNA-binding proteins (RBPs) and microRNAs (miRNAs), which can bind to transcribed mRNA, regulate its stability, and modulate cytokine translation (reviewed in [78]). Furthermore, RBPs and miRNAs were found to promote acquisition of ET phenotype by inducing mRNA decay and translation inhibition of tolerised effector genes. In THP-1 cells, miR-221 together with RBPs TTP and AUF1 were demonstrated to drive TNF transcript

degradation, while miR-579 and miR-125b recruited TIAR and were responsible for the arrest of protein synthesis [79]. Members of the miR-181 family were shown to target both TNF and IL-6 mRNA, and miR-181 inhibition could improve transcript half-life and rescue cytokine production in human and mouse cells *in vitro* [80, 81]. On the other hand, enhanced transcript stability and translation efficiency has been proposed to contribute to the continued expression of non-tolerisable anti-inflammatory genes, such as secretory interleukin-1 receptor antagonist, observed in tolerised THP-1 cells [82]. Finally, miR-146a and miR-155, two miRNAs targeting different downstream components of the TLR signalling cascade, were also identified to be important in the establishment of ET [83].

ET is the first discovered and undoubtedly most widely investigated memory-like behaviour in the innate immune compartment, yet monocyte/macrophage tolerance is not an LPS-specific phenomenon. A hyporesponsive state can also be induced by other TLR ligands, such as Pam3CSK4 (TLR2 agonist), lipoteichoic acid (TLR2), poly(I:C) (TLR3), flagellin (TLR5), and R848 (TLR7/8) [34, 84, 85]. What is more, LPS and other triggers can induce so called cross-tolerance, that is confer the state of tolerance to a non-identical secondary stimulus [86]. This is perhaps not so surprising in light of findings describing genome-wide epigenetic reprogramming in ET – repressive marks would thwart transcriptional re-activation of specific TLR-inducible genes, regardless of the source of secondary signal.

Altogether, these data support the idea that LPS induced tolerance is more than a refractory state resulting from receptor desensitisation. Rather, it emerges as a functional adaptation, allowing for most efficient, context dependent response of innate immune cells facing a constant threat from a multitude of different pathogens.

1.1.4 Trained immunity – potentiating response to re-infection

In contrast to vertebrates, invertebrates and plants lack adaptive immunity and depend on innate immune response for defense against pathogens [87]. However, experimental data shows that besides rapid non-specific and short-lived response to pathogens, those organisms appear to be additionally protected from secondary infection in the future [88]. For example, tobacco plants exposed to tobacco mosaic virus displayed enhanced resistance to re-infection introduced in more distal tissue [89]. This was found to be a result of enhanced expression of pathogenesis-related genes, stimulated by salicylic acid signalling [90, 91]. Such disseminated protection is known as systemic acquired resistance (SAR), and confers a long-lasting immunity against a broad spectrum of plant pathogens (reviewed in [92]). Furthermore, in *Drosophila melanogaster* challenge with a sub-lethal dose of *Streptococcus pneumoniae* enhanced fly survival following a re-infection with the same pathogen. The protection was life-long, required a functional Toll pathway, and was mediated by *Drosophila* phagocytes [93]. These data corroborate the presence of memory-like mechanisms in the absence of traditional adaptive immunity.

In humans, the first hint of a non-specific enhanced protection against infection comes from observation following vaccination. The bacille Calmette-Guérin (BCG), a live attenuated vaccine against tuberculosis, has been shown to improve mortality rates of immunized children by protecting from infections with pathogens other than *Mycobacterium tuberculosis* [94]. In addition to BCG, vaccines against influenza, measles and yellow fever were also demonstrated to produce broad heterologous protection from infection, not specific for the type of vaccine used (reviewed in [95]).

Studies using mice models reported similar non-related protection from infection following treatment with BCG, and highlighted lymphocyte independent

aspects of this phenomenon. BCG vaccinated mice with cyclophosphamide suppressed lymphocyte activity were protected from subsequent *Candida albicans* and *Staphylococcus aureus* infection [96]. Similarly, BCG vaccination granted immunity to infection with the parasite *Schistosoma mansoni* in nude mice [97], and protected SCID mice from lethal *C. albicans* challenge [98]. Altogether, this points to the existence of distinct type of memory in the innate immune compartment of invertebrates that reinforces their resistance to re-infection, designated trained immunity (TI).

Experimental studies in mice have shown protective TI-like effects can be also induced by *C. albicans,* and specific isolated peptidoglycan PAMPs; β-glucan, a component of yeast cell wall, and muramyl dipeptide (MDP), mycobacterium cell wall constituent. *C. albicans* was demonstrated to confer immunity to re-infection in wild-type [99], and in Rag1-deficient mice [100]. β-glucan from *Saccharomyces cerevisiae* increased survival following intravenous challenge with *Staphyloccocus aureus* in healthy AKR/J mice, and animals with lymphocytic leukemia [101]. Mice treated with MDP acquired enhanced resistance to infection with *Klebsiella pneumoniae* [102], *Pseudomonas aeruginosa* [103], and *C. albicans* [104]. This non-specific protection in trained mice was found to be dependent on macrophages, evidenced by adoptive transfer of spleen macrophages from *C. albicans* trained into naïve mice granting protection against systemic re-challenge [105]; and a result of enhanced production of pro-inflammatory cytokines, with increased levels of GM-CSF, TNF, IFN-γ, and IL-1 detected in serum and splenocytes cultures [106].

Since these studies, training with *C. albicans* [100], β-glucan [100, 107], and MDP [84] have been demonstrated *in vitro,* and with BCG *in vitro* and *ex vivo* [98, 107] in primary human monocytes. Gold standard *in vitro* protocol in the field includes primary stimulation, sometimes also called training or priming, with a pathogenic trigger

inducing TI, followed by an intermittent period of recovery, and then simulation of re-infection by secondary challenge (re-stimulation, re-challenge) with a non-related stimuli, frequently LPS or Pam3CSK4. Cells trained in this way display markedly increased pro-inflammatory cytokine release, for example monocytes trained with β-glucan upregulate production of TNF and IL-6 in response to LPS [39, 100, 107]. Trained phenotype also involves rewiring of cell metabolism, with the shift from oxidative phosphorylation to aerobic glycolysis through the activation of mammalian target of rapamycin (mTOR)/hypoxia-inducible factor-1α (HIF-1α) pathway being fundamental for acquisition of enhanced immune response, as demonstrated in human monocytes primed with β-glucan [108]. Increase in glycolysis was also observed in BCG training, following LPS re-stimulation of human monocytes *in vitro*, or mouse splenocytes *ex vivo* [109].

Induction of TI is triggered by activation of PRR signalling; β-glucan is a dectin-1 agonist [110], while MDP works through NOD2 [111]. Monocytes isolated from dectin-1 deficient individuals fail to induce β-glucan training [112]. Mechanistically, TI was demonstrated to be a result of extensive transcriptional re-modelling in trained cells, modulated by alteration of epigenetic landscape that warrants transcriptional accessibility of immune response genes [39, 76, 98, 100]. Amongst the open chromatin histone marks examined, H3K4me3 appears to be particularly important for the induction of TI. Priming with β-glucan has been demonstrated to cause a genome-wide increase in H3K4me3, including on promoters of TNF and IL-6, and treatment with histone methyltransferase inhibitor could prevent the augmentation of LPS-elicited pro-inflammatory cytokine release [100]. Furthermore, an intriguing interplay between transcriptomic, metabolic and epigenetic pathways has been described in TI. The transcriptomic activation caused by the training stimulus leads to accumulation of metabolites that can serve as

intermediates for the enzymes conducting epigenetic modifications. Those modifications, including on regulatory elements of metabolic genes, are in turn responsible for the functional reprogramming resulting in trained phenotype [113].

What is more, a fascinating link was discovered between TI and endotoxin tolerance. Treatment of LPS tolerised human monocytes with β-glucan reverted the ET phenotype, and restored production of pro-inflammatory cytokines. ET could also be reversed in monocytes after *in vivo* induction of tolerance in an experimental model of endotoxemia. On molecular level, reversal of tolerance by β-glucan was conferred through induction of chromatin re-modelling promoting transcriptional activation of LPS response genes [76].

1.1.5 Conclusions: tolerance and training – two sides of the same coin

The aforementioned examples demonstrate the widespread presence of innate immune mechanisms in nature. The change of reactivity of innate immune cells induced by first exposure to microbiological triggers can both repress (tolerance) and potentiate (training) the secondary immune response. Despite the apparently opposing functional results, both tolerance and training are actually caused by extensive transcriptional, epigenetic and metabolic reprogramming, and can be viewed as two sides of the same coin.

The altered expression of immune related genes observed in training and tolerance discussed above has been widely described in the context of innate immune response reshaping. However, emerging data suggests that modulation of cytokine production by myeloid cells can further impact the function of adaptive immune cells, such as polarization of T cells. For example, trained cells upregulate IL-6 and IL-1β, two cytokines known to promote Th17 differentiation [114, 115]. Indeed, PBMCs obtained following BCG vaccination exhibited enhanced IL-17 and IL-22 secretion in response to

re-stimulation, implying an improved Th17 response [116]. Moreover, increased production of IFN-γ by BCG trained cells might point to an expansion of Th1 cell population [98, 116]. Memory phenotype induced in macrophages by helminth pathogen *Fasciola hepatica* involves augmented secretion of IL-10 and IL-1 receptor antagonist (IL-1RA), but reduced release of TNF and IL-12 [117]. In the adaptive immune compartment, IL-10 is a pleiotropic cytokine with numerous anti-inflammatory functions, involving promoting differentiation of Tregs [118] and suppressing Th17 pro-inflammatory responses [119]. IL-1RA blocks IL-1β signalling [120], while IL-12 drives Th1 polarization [121]. Correspondingly, suppression of Th1 and Th17 responses was observed when *F. hepatica* trained macrophages were cultured with spleen and lymph node cells [117]. In addition to IL-1β regulation, production of T cell polarizing cytokines IL-10 (downregulation [122] or upregulation [123]) and IL-12 (downregulation [28, 74, 124]) was also reported to be altered in LPS tolerised cells, and thus one could speculate that balance between Tregs and effector Th1 and Th17 cells might be shifted as a result of ET phenotype. Furthermore, antigen presentation is impaired in ET, with a decreased expression of MHC class II and co-stimulatory molecule CD86 [125]. While the full extent of the influence innate immune memory phenotypes might have on the adaptive immune responses is yet to be uncovered, these data serve as a reminder of a close relationship between the two arms of the immune system that should be carefully considered before drawing conclusions on the systemic impact of tolerance and training..

It is unlikely for a phenomenon to be so ubiquitous without having an important physiological function. Indeed, innate immune memory is postulated to be an evolutionary adjustment that allows for more effective response to changing environment. While it is crucial to promptly sense and react to invasion, persistent exposition to pathogenic triggers might lead to excessive, prolonged induction of

immune response. Acquisition of tolerance following the primary exposure prevents the cells from propagating deleterious inflammation and might serve as a protective switch-off mechanism in conditions like sepsis. On the other hand, potentiation of response can be a way of reinforcing non-specific defences against re-infection.

However, it is hypothesized that maladaptive innate immune memory mechanisms could also be implicated in disease pathology [108]. For example, endotoxin tolerance might be contributing to post-sepsis immunoparalysis, increasing the risk of opportunistic infections. Moreover, trained immunity is speculated to play a role in induction and maintenance of chronic inflammatory diseases, such as RA, SLE or type 1 diabetes (reviewed in [126]). Further in-depth investigation is necessary to fully understand the importance of innate immune memory in health and disease, and might lead to development of novel targeted immunotherapies.

1.2 Danger-associated molecular patterns (DAMPs) – signals of threat from within

Traditionally, the primary function of the innate immune system was considered to be the recognition and elimination of non-self entities, as discussed above. However, infection is not the sole threat to an organism's homeostasis. Inflammatory responses are also activated by entities of non-microbiological origin, for example by a wide variety of endogenous stimuli generated as a result of cellular stress and tissue damage. These signals include molecules released upon cell death and components of damaged extracellular matrix, which are vital for triggering pathways designed to clear cellular debris and restore tissue integrity [127, 128]. Furthermore, the immune system can be activated by inorganic irritants, such as asbestos [129]; by deposits of endogenous molecules, such as amyloid beta [130] and cholesterol [131]; and by tumour-associated antigens [132]. In relation to PAMPs, non-pathogenic molecules eliciting an immune response have been termed damage-associated molecular patterns, or DAMPs. Triggering of immune responses by DAMPs is a result of sensing by PRRs, the same receptors that recognize PAMPs. For example, TLR4, receptor responsible for detecting bacterial LPS, is also activated by a number of endogenous molecules, such as biglycan [133], fibronectin extra domain A (EDA) [134], and fibrinogen [135] (more examples of DAMPs and their respective PRRs are presented in Table 1.1). As DAMPs are host-derived molecules, in healthy tissues they are required to be kept apart from PRRs in order to avoid unnecessary activation. In physiological conditions, DAMPs are downregulated, separated in specific cellular compartments, or sequestered in the extracellular matrix (ECM) [127]. For instance, tenascin-C, an endogenous ligand of TLR4, is absent in healthy tissue, but synthesised de novo in response to injury and inflammation [136]. CpG rich mitochondrial DNA, compartmentalized in the

mitochondria, is released into the circulation by cells following injury, where it can be taken up and activate TLR9 [137]. Finally, fragments of hyaluronan, a major component of the ECM, accumulate during matrix degradation, and stimulate immune response through TLR4 and TLR2 [138].

Table 1.1 Examples of damage-associated molecular patterns (DAMPs) with their respective receptors. EDA, extra domain A; NLRP3, NLR family pyrin domain containing 3; RAGE, receptor for advanced glycation end products.

DAMP	Receptor
β-defensin-3	TLR1/TLR2 [139]
Biglycan	TLR2, TLR4 [133], NLRP3 [140]
Fibronectin EDA	TLR4 [134]
Fibrinogen	TLR4 [135]
HMGB1	TLR2, TLR4, RAGE [141-143]
Hyaluronan	TLR2, TLR4 [138]
Mitochondrial DNA	TLR9 [137]
Neutrophil elastase	TLR4 [144]
S100 proteins	TLR2, TLR4, RAGE [145-147]
Serum amyloid A	TLR2, TLR4 [148, 149]
Tenascin-C	TLR4 [136]
RNA	TLR3 [150], TLR7, TLR8 [151]

While the induction of inflammation by PAMPs is relatively well understood, the mode of action of DAMPs remains elusive. What we do know is that upon sensing by PRRs DAMPs induce production of pro-inflammatory cytokines and chemokines, driving recruitment of leukocytes to the site, and promoting inflammation [152]. Such immune response provides pre-emptive protection, in case the wound is no longer sterile. What is more, DAMPs can also prime adaptive immunity. Following DAMP stimulation, activated innate immune cells become efficient antigen presenting cells, and can provide

co-stimulatory signals to lymphocytes when other, applicable antigen emerges, for example pathogenic, tumour-associated, or altered self antigen [153].

Therefore, responses triggered by endogenous and pathogenic triggers are partially overlapping. However, while the detection of PAMPs is a signal for the immune system to fight the invading pathogen, DAMPs are crucial molecules for the stimulation of tissue repair. In the first, inflammatory stage of wound healing, DAMP induced inflammation and resulting leukocyte infiltration is essential for clearing of cellular debris. As the dead tissue is removed from the site of injury, immune mediators elicited by DAMPs contribute to leukocyte switching from pro-inflammatory to a repair programme, allowing for inflammation resolution. Then, pro-reparative macrophages and other innate immune cells guide fibroblasts to synthesise ECM components, such as collagen, and stimulate keratinocytes to proliferate and migrate. As a result, ECM is regenerated and tissue integrity restored [154, 155].

Hence, the innate immune system does not simply discriminate between harmful foreign and benign self. Rather, it can comprehend the context of detected threat, discriminating endogenous injury signals from PAMPs, and mounting a timed, adequate response aimed at tissue regeneration, and not limited to acute inflammation.

1.2.1 PAMPs and DAMPs in health and disease

As discussed above, detection of PAMPs by PRRs is an unequivocal signal of infection, and a pre-requisite to activate pro-inflammatory and antimicrobial responses aimed at containing and eliminating the pathogen. PRRs evolved to recognize conserved motifs from the various microorganisms threatening our survival, such as pathogenic bacteria, fungi, protozoa, and also viruses [8]. Therefore, PAMP sensing by PRR is an essential protective mechanism in all infectious diseases. For example, during a urinary tract infection with Gram-negative bacteria *E. coli*, LPS is detected by TLR4, while

TLR5 recognizes bacterial flagellin [156]. *Streptococcus pneumoniae*, Gram-positive bacterium causing respiratory tract infections and meningitis, triggers immune response in consequence of virulence factors lipoteichoic acid and peptidoglycan ligating TLR2 [157]. Following phagocytic uptake of protozoan parasites from the *Plasmodium* genus, the cause of malaria, parasitic DNA rich in CpG is sensed in the endosomes by TLR9 [158]. Furthermore, defects in the pattern recognition system and downstream signalling cascades are often associated with increased susceptibility to infectious diseases [8].

'Sterile' inflammation induced by DAMPs, allowing for execution of effective tissue repair, is also critically important for maintaining homeostasis of the system. However, in spite of this beneficial physiological function, DAMPs can also drive detrimental pathological processes. DAMPs, initially exposed or upregulated as a result of injury, require to be promptly removed by phagocytes following completion of the pro-inflammatory phase of healing, to allow for completion of tissue repair. If this does not happen, and/or if these endogenous triggers are not downregulated, and continue to be highly expressed, immune responses are persistently activated. Inflammation cannot be resolved, and chronic inflammatory conditions can develop [159]. DAMP induced dysregulated inflammation has been implicated in a variety of pathologies, such as autoimmune diseases (for example rheumatoid arthritis [160] and systemic lupus erythematosus [161]), metabolic disorders (diabetes [162], atherosclerosis [163]), or neurodegenerative diseases (Alzheimer's disease [164], Parkinson's disease[165]). Sustained firing of inflammatory pathways by DAMPs can also cause disordered tissue remodelling (instead of physiological regeneration), or tissue fibrosis. The excessive fibrotic tissue, comprised of ECM components produced by DAMP-activated fibroblasts, accumulates in the sites of inflammation and damage, resulting in scarring and impaired organ function [166]. Altogether, while sterile inflammation has an extracellular role in

physiological tissue repair and regeneration, excessive DAMP induced inflammation that fails to be resolved is harmful for the host, and can contribute to the development of inflammatory diseases.

1.2.2 Endogenous triggers in innate immune memory

Various PAMPs are capable of inducing both inhibiting, and potentiating, innate immune memory. One could deliberate if a similar aptitude is shared by endogenous triggers of innate immune response. After all, not only do they signal through the same type of receptors, the PRRs, but also require equivalent, if not tighter, control to prevent immune overreaction. Indeed, there is evidence that certain DAMPs might also be able to induce a refractory functional state similar to ET. These include high-mobility group box protein 1 (HMGB1) [167], high-mobility group nucleosome-binding protein 1 (HMGN1) [168], cold-inducible RNA-binding protein (CIRP) [169], as well as S100 A8 and A9 proteins [170].

HMGB1 is a DNA-binding protein involved in regulation of gene transcription in the nucleus; yet when released outside of the cell it can bind to TLR4 and receptor for advanced glycation end products (RAGE), and activate pro-inflammatory cytokine production [171]. In THP-1 cells priming with HMGB1 was shown to reduce TNF release following LPS [167] or LTA [172] stimulation. Decrease in serum TNF levels in response to LPS challenge could also be observed in vivo in mice pre-treated with HMGB1 [167]. Likewise HMGB1, HMGN1 binds to nucleosomal DNA and contributes to chromatin architecture; extracellular HMGN1 can also stimulate TLR4 signalling [173]. It has been reported that HMGN1 can induce hyporesponsiveness to LPS in human PBMCs, with reduced production of IL-6 and TNF. What is more, priming with HMGN1 could also induce tolerance to Pam3CSK4 and flagellin [168]. Intracellular CIRP is an RNA chaperone controlling translation in response to diverse types of cellular stress,

while extracellular has a role as a DAMP agonist of TLR4 [174]. Recently, eCIRP has been demonstrated to promote tolerance to LPS in mouse peritoneal macrophages in vitro and ex vivo. Surprisingly, this is depending on eCIRP interaction with a novel receptor, IL-6R, and not TLR4 [169]. Finally, the two members of the S100 protein family, S100A8 (also known as myeloid related protein 8, or MRP8) and S100A9 (MRP14) are small calcium binding proteins released in response to tissue damage and activating TLR4 [175]. Human primary monocytes primed with S100A8 or S100A9 displayed tolerance to re-challenge with the same stimulus, but also cross-tolerance to LPS and LTA [170].

On the other hand, endogenous molecules can also induce potentiation of immune response. LDL is the main particle carrying cholesterol in the bloodstream and its modified version, oxLDL, is known to promote inflammation [176]. In an in vitro study with primary human monocytes oxLDL has been shown to augment production of IL-6 and TNF in response to LPS and Pam3CSK4 [177]. Moreover, induction of hyperresponsive phenotype was reported in mice fed high fat diet. Trained animals had markedly increased serum levels of pro-inflammatory cytokines following administration of LPS; analogous effect was observed with bone marrow cells and splenocytes re-stimulated *ex vivo* [178].

Overall, not only pathogenic factors, but also a number of endogenous molecules, released or processed in response to cellular stress and trauma, are capable of inducing memory in the innate immune compartment. Furthermore, emerging evidence corroborates the similarity of DAMP- and PAMP-dependent memory acquisition, both resulting from epigenetic re-programming [170, 177].

The above examples of endogenous inducers of memory are relatively recent discoveries, however one other molecule has been implicated to have tolerising

properties as early as 1988 – the pro-inflammatory cytokine TNF [179]. It has been first observed in rats and mice that administration of TNF is protective from subsequent injections of normally lethal doses of TNF [179, 180]. Tolerised mice were shielded from TNF-induced inflammation-related symptoms such as fever, gastrointestinal toxicity, liver injury, anorexia, hypertension and hypothermia [181]. In vitro, stimulation of monocytes and macrophages with TNF could induce tolerance to itself, as well as cross-tolerance to LPS.

Further investigation has shown that cells primed with TNF undergo a very specific transcriptomic remodelling. Production of a subset of pro-inflammatory cytokines is reduced or tolerised following re-stimulation (referred to as absolute tolerance), such as TNF, IL-1β, IL-6 and IL-8; others are non-tolerisable, but also not further induced, and simply continue to be expressed at the same level (induction tolerance), like IL-18 and IL-32 [182]. TNF-induced de-sensitization is triggered by activation of TNFR1, however in mice blockade of the glucocorticoid receptor also had a negative impact on the development of tolerant phenotype [183].

Mechanistically, two different models have been proposed regarding the acquiring of TNF tolerance, depending on the concentration used for priming. Low doses of TNF result primarily in the regulation of a group of tolerisable genes, and this is controlled by glycogen synthesis kinase 3 (GSK3, a serine/threonine kinase), which can phosphorylate interaction partners p65 and transcription factor CCAAT/enhancer binding protein (C/EBP) β, hence repressing transcription [182, 184]. Higher doses affect a larger part of the transcriptome, and cause both absolute and induction tolerance. GSK3 is also involved in the high-dose TNF tolerance, however the key player in this condition is A20 deubiquitinase, a negative regulator of NF-kB signalling [182]. Additionally, in a

separate study looking at TNF/LPS cross-tolerance GSK3 was demonstrated to augment A20 expression [185].

TNF is one of the major mediators of inflammation induced as a result of PAMP/DAMP sensing by PRRs. A burning question emerges in regards to its tolerising properties – is it possible that autocrine/paracrine activity of TNF released in response to TLR4 activation by LPS is contributing to acquisition of hyporesponsive state in endotoxin tolerance? This has been interrogated in THP1 cells with the use of TNF neutralizing antibody, and TNF receptors targeting antibodies: anti-TNFR1 and anti-TNFR2. Antibody blockade of TNF signalling prior to priming with LPS had no effect on endotoxin tolerance induction [186]. Thus, induction of endotoxin tolerance is not dependant on the primary TNF response to LPS.

Hence, the available data corroborates the protective memory mechanisms induced in innate immune cells regulate not only pathogenic, but also endogenously driven immune responses. However, DAMPs are a varied group of molecules, and substantial further work is needed to fully understand the aspects of cellular reprograming distinct to, and shared between the endogenous triggers, and between DAMPs and PAMPs.

1.2.3 Unanswered questions in the danger versus stranger model of immunity

Many questions around the danger model of immunity remain unanswered, not least how the identity of endogenous inflammatory molecules is defined, and the mechanisms by which their activity must be tightly regulated to avoid catastrophic autoimmune destruction. Addressing these questions will not only provide insight into an intriguing immunological puzzle, but may also open new therapeutic avenues to treat inflammatory diseases of non-infectious origin, where pathology is driven by endogenous inflammatory stimuli. In this thesis I will explore these immunological

aspects including: 1) the molecular determinants that make DAMPs dangerous, 2) how DAMP-mediated inflammation in regulated, and 3) the contribution of DAMP-mediated inflammation to chronic 'sterile' inflammation. Work in the Midwood lab has focused on understanding the pro-inflammatory activity of the extracellular matrix molecule tenascin-C, as an archetypal DAMP, as well as investigating the role of this molecule in inflammatory diseases including RA and how targeting at this level might ameliorate chronic joint inflammation in people with RA, whilst leaving intact host defence against infection. I will use tenascin-C as an exemplar DAMP for further study.

1.3 Tenascin-C: a matrix protein with diverse immunomodulatory capabilities

Tenascin-C is a large hexameric protein of the extracellular matrix that exhibits limited expression in healthy tissues, but which is rapidly upregulated upon tissue damage. Typically, its expression is transient, with mRNA downregulated and protein cleared by the time tissue repair is complete [187]. However, persistent expression of tenascin-C is associated with a wide variety of pathological conditions, where it accumulates at sites of inflammation, for example, in autoimmune, fibrotic, and metabolic diseases, and in many cancers [188]. Possessing an intricate molecular architecture that facilitates an extensive interactome, tenascin-C is a versatile modulator of a plethora of cellular functions.

1.3.1 Tenascin-C up close: a diverse interaction partner

Tenascin-C is characterized by a distinct domain organization. An assembly domain at the N-terminus, responsible for the formation of the six-armed oligomer known as the hexabrachion, is followed by a series of epidermal growth factor-like (EGF-L) repeats, constitutively expressed and alternatively spliced fibronectin type III-like repeats (FNIII), and a C-terminal fibrinogen-like globe (FBG). This complex structure enables tenascin-C to establish a wide variety of molecular interactions (reviewed in [189]). Tenascin-C is an important regulator of the matrix itself, modulating its assembly and the biophysical properties of tissue. Within the extracellular matrix, tenascin-C binding partners include collagen, fibronectin, periostin, fibrillin-2, and proteoglycans: perlecan, aggrecan, neurocan, and phosphacan/receptor protein tyrosine phosphatase β/ζ. Tenascin-C also binds to proteins exposed on the cell surface, such as syndecan 4, contactin, glypican, annexin II, and CALEB/CSPG5. It can further directly influence internal cell signalling by binding to cell surface receptors such as epidermal growth

factor receptor (EGFR), Toll-like receptor 4 (TLR4), and integrins. Moreover, tenascin-C is able to bind numerous growth factors, including members of the fibroblast growth factor family and the transforming growth factor beta (TGF-β) superfamily. This multitude of interactions makes tenascin-C a diverse modulator of cellular behaviour, such as proliferation, migration, adhesion, and differentiation, capable of producing highly context- and cell-type-specific responses.

1.3.2 The pro-inflammatory capabilities of tenascin-C

To date, three main binding partners have been identified to be responsible for the inflammatory effects of tenascin-C: TLR4, and integrins α9β1 and αVβ3. The impact of tenascin-C activation of these receptors is summarized in Table 1.2.

TLR4 is a cell surface receptor present on leukocytes and stromal cells. It was first identified as the PRR responsible for mediating innate immune responses to the potent bacterial virulence factor, lipopolysaccharide (LPS) or endotoxin, but it also has a growing number of endogenous activators; this list includes tenascin-C, biglycan, fibrinogen, and S100 proteins, among many others [190]. The most widely reported effect of TLR4 activation by tenascin-C is the induction of soluble pro-inflammatory mediators, such as IL-6, IL-8, and TNF. This has been observed in a number of cell types, including macrophages [136, 191-193], DCs [194], fibroblasts [136, 195], and chondrocytes [196]. More recently, tenascin-C signalling through TLR4 has been implicated in inflammasome priming. Inflammasomes are multiprotein, intracellular complexes that drive specific inflammatory responses including the release of IL-1β and IL-18, and induction of pyroptosis, a type of programmed cell death [197]. Typically, inflammasomes require two separate signals for activation: the first “priming” signal comprises PRR-driven pro-cytokine production and synthesis of inflammasome components; this is followed by inflammasome assembly and caspase-1-mediated

maturation and release of bioactive IL-1β and IL-18 [198]. Stimulation of rat epicardium–derived cells with tenascin-C induced TLR4-dependent pro-IL-1β transcription, implicating elevated tenascin-C expression in rat cardiac tissue following ischemic injury as a potential priming step for inflammasome assembly that can be driven by adenosine or ATP-mediated purinergic stimulation in this cell type [199]. In addition, increased levels of secreted mature IL-1β could be detected in cell culture medium of mouse bone marrow–derived DCs stimulated with tenascin-C [194], indicating that tenascin-C may be capable of driving IL-1 synthesis in the absence of an exogenous second signal. However, a direct link between tenascin-C activation of TLR4 and purinergic signalling, or the requirement for any other second signal, has not been investigated.

Tenascin-C upregulation therefore would be expected to increase tissue levels of pro-inflammatory cytokines and chemokines, orchestrating innate immune cell recruitment and activation. In addition, a number of reports suggest that tenascin-C-mediated cytokine release is also important for creating a microenvironment permissive for selective T-cell polarization. DCs derived from tenascin-C-deficient mice exhibited diminished pro-inflammatory cytokine release in response to LPS stimulation, and a reduced capacity to drive naive T cells toward Th17, but not Th1, Th2, or Treg, cell differentiation [200]. Stimulation of DCs with exogenous tenascin-C promoted their ability to drive the generation of Th17 cells, and this effect could be ablated with anti-IL-6 and anti-TLR4 antibodies, suggesting that IL-6 synthesis induced by tenascin-C activation of TLR4 is a key determinant of T-cell subset polarization [194]. Interestingly, tenascin-C also stimulated chondrocyte secretion of prostaglandin E2 [196], a complex mediator of inflammation known to be involved in Th17 polarization [201, 202].

Table 1.2 Tenascin-C as a modulator of cellular behaviour in inflammation.

Receptor	Cell Type	TN-C Source	Response	TN-C Domain	Evidence	Pathway	Reference
TLR4	Primary human macrophages	Recombinant human full-length TN-C purified from HEK cells; recombinant human TN-C domains[a,b]	↑ IL-6, IL-8, and TNF	FBG	anti-TLR4 Ab and TLR4 KO mouse macrophages	NF-kB Myd88-dependent	[136]
	Human synovial fibroblasts		↑ IL-6		Myd88 and TLR4 KO mouse embryonic fibroblasts		
	Primary human chondrocytes	Full-length TN-C purified from human glioblastoma cell line[a,b]	↑ IL-6, IL-8, prostaglandin E2, nitrate, and ADAMTS4		TLR4 inhibitor TAK242		[196]
	Mouse bone marrow neutrophils		↑ MMP-9		TLR4 KO neutrophils		[203]
	Human THP-1-derived macrophages	Recombinant human TN-C purified from mouse myeloma cell line	↑ macrophage differentiation into foam cells		anti-TLR4 Ab	↑ CD36, oxLDL scavenger receptor	[204]
	Mouse bone marrow–derived DCs	Full-length TN-C purified from human glioblastoma cell line	↑ IL-6, IL-1α, and IL-1β; ↑ IL-17 in cocultures of naive T cells and DCs		TLR4 inhibitor TAK242	NF-kB	[194]
	Human peripheral blood monocyte–derived macrophages	Recombinant human FBG domain[a,b]	↑ IL-6, IL-8, TNF, IL-10, collagen (expression and phosphorylation), MMP-1, and MMP-14	FBG	anti-TLR4 Ab and TLR4 inhibitor TAK242	p38, JNK, and NF-kB	[191]
	Human and mouse fibroblasts	Full-length TN-C purified from human glioblastoma cell line[b]	↑ type I collagen, αSMA, and TLR4		TLR4 inhibitor TAK242, Myd88 blocking peptide, and TLR4 KO cells	NF-kB Myd88-dependent	[205]
	Human cardiac myofibroblasts	Full-length TN-C purified from human glioblastoma cell line, recombinant human FBG domain[a,b]	↑ IL-6 and MMP-3	FBG	anti-TLR4 Ab (for IL-6)		[195]
	Mouse macrophage cell line Human hepatoma cell line		↑ IL-6, TNF ↑ epithelial-mesenchymal transition		TLR4 inhibitor VIPER		[192]
	Primary human macrophages	Recombinant human FBG domain[a,b]	↑ IL-6, IL-8, and TNF	FBG	anti-TLR4 Ab and TLR4 inhibitor TAK242		[193]
α9	Mouse synovial macrophages	Recombinant FNIII3 domain (RGD to RAA)	↑ IL-6, IL-1α, IL-1β, TNF, CCL2, CCL3, CCL4, CXCL2, and CXCL5	FNIII3	anti-α9 Ab and mutant FNIII3 (removed α9 binding sequence) (IL-6 reduced)		[206]
	Mouse synovial fibroblasts		↑ IL-6, IL-1α, CCL2, CCL4, CXCL5, CXCL12, and MMP-9 ↓ MMP-2		anti-α9 Ab (IL-6 reduced)		
	Mouse dendritic cells	Full-length TN-C purified from human glioblastoma cell line, recombinant mutant FNIII3 domain (RGD to RAA)	↑ IL-6, IL-23, Th17 differentiation	FNIII3	anti-α9 Ab and mutant FNIII3	NFκB, MEK/ERK	[207]
αVβ3	Mouse peritoneal macrophages		↑ IL-6, IL-1β, and TNF		NFκB inhibitor (all cytokines), two different αVβ3 inhibitors and anti-β3 Ab (NFκB phosphorylation and IL-6 upregulation)	NFκB	[208]

"TN-C source" column was left blank if no details about source and type of used tenascin-C were given in the article. Abbreviations: TN-C, tenascin-C; TLR4, toll-like receptor 4; HEK, human embryonic kidney; IL, interleukin; TNF, tumor necrosis factor; FBG, fibrinogen-like globe; KO = gene knockout; NFκB, nuclear factor kappa-light-chain-enhancer of activated B cells; ADAMTS4, a disintegrin-like and metalloproteinase with thrombospondin motifs-4; TAK242, small-molecule inhibitor of TLR4; MMP, matrix metalloproteinase; THP-1 = monocyte-like acute monocytic leukemia-derived cell line; oxLDL, oxidized low-density lipoprotein; DC, dendritic cell; JNK, c-Jun N-terminal kinase; αSMA, alpha-smooth muscle actin; FNIII3, third fibronectin type III repeat; RAA, tripeptide Arg-Ala-Ala; CCL, C-C motif chemokine ligand; CXCL, chemokine receptor; MEK, mitogen-activated protein kinase kinase; ERK, extracellular signal–regulated kinase.

[a]Limulus amebocyte lysate (LAL) test has been used to measure endotoxin contamination in protein samples.

[b]Preincubation with polymyxin B has been used as endotoxin contamination control.

Wider profiling of the impact of tenascin-C activation of TLR4 in primary human macrophages highlighted functional consequences beyond cytokine synthesis. Comparison of macrophages activated by tenascin-C, or by a pathogenic ligand, LPS, revealed overlapping, but distinct downstream impacts on cell behaviour. While both ligands induce classical NFκB and mitogen-activated protein kinase (MAPK) signalling, LPS drove macrophages toward an aggressive phenotype designed to fight infection, characterized by high levels of pro-inflammatory cytokines and tissue degrading matrix metalloproteinases, while tenascin-C favoured the upregulation of extracellular matrix protein expression and phosphorylation, resulting in macrophage behaviour more suited to tissue repair [191]. Tenascin-C has also been shown to help drive macrophages to become foam cells. Tenascin-C potentiated oxidized low-density lipoprotein (oxLDL)–induced foam cell formation, in a TLR4-dependent manner. Tenascin-C was also upregulated upon macrophage stimulation by oxLDL, and was capable of inducing the expression of CD36, a scavenger receptor involved in LDL uptake, suggesting the existence of a positive feedback loop promoting the generation of these cells key to the development of atherosclerosis [204]. These data collectively show that tenascin-C profoundly influences macrophage polarization, that it induces a macrophage phenotype quite different to that induced by pathogenic activation of TLR4, and that macrophage subsets created by tenascin-C activation can differ depending on context.

An increasingly wide range of cell types are reported to respond to tenascin-C via activation of TLR4. In murine bone marrow isolated neutrophils, tenascin-C has been shown to upregulate the expression of matrix metalloproteinase (MMP)-9 in a TLR4-dependent manner [203]. Activation of the TLR4/tenascin-C axis has been also reported to induce epithelial-mesenchymal transition and promote migration of human hepatoma cell line [192]. Tenascin-C also induces TLR4-mediated cytokine synthesis in

fibroblasts. For example, in synovial fibroblasts it promotes high levels of IL-6 secretion, although it does not induce IL-8 in these cells, in contrast to macrophages [136]. Moreover, other outputs have been reported in tenascin-C-activated stromal cells. TLR4-dependent activation of primary human foreskin fibroblasts by tenascin-C induces synthesis of type I collagen and alpha-smooth muscle actin [205]. These data support a role for tenascin-C not only in triggering immune cell–mediated inflammation but also in stromally driven defense responses, suggesting that this matrix molecule contributes to both inflammatory processes immediately following tissue damage and subsequent tissue remodelling by activating cell-type-specific responses via TLR4.

That tenascin-C drives very different TLR4-mediated inflammatory signalling than LPS supports the idea that the immune system is able to distinguish different alarm signals using common sensors, to activate distinct, tailored responses to particular threats, that is, injury versus infection. However, it is not yet clear on the molecular level how different outputs arise from activation of the same PRR. We still do not fully understand how tenascin-C binds to and activates TLR4. What we do know is that the binding site comprises three distinct epitopes within the FBG domain of tenascin-C [193], and that the classical LPS co-receptors, myeloid differentiation protein-2 (MD-2) and CD14, are not essential for TLR4 activation by tenascin-C [136].

In addition to TLR4, tenascin-C activation of two other cell surface receptors has been shown to drive inflammatory responses. Integrins α9β1 and αVβ3 are transmembrane receptors capable of binding to a number of matrix proteins, including fibronectin and tenascin-C. The binding of tenascin-C by both integrins induces pro-inflammatory cytokine synthesis, with the interaction site responsible for the observed effects pinpointed to the third FNIII repeat for α9β1 [206]. Although αVβ3 is known to bind to two different sites within tenascin-C, the third FNIII repeat [209] and the FBG

domain [210], it is still unknown which of them, if any, is responsible for conferring the pro-inflammatory activity. In murine synovial macrophages and fibroblasts, tenascin-C-induced α9 integrin–mediated signalling upregulates a wide array of pro-inflammatory molecules, including IL-6, IL-1α, CCL2, CCL4, and CXCL5 [206]. α9 integrin activation by tenascin-C is also involved in Th17 cell differentiation through induction of IL-6 and IL-23 in DCs. In this study, stimulation of IL-6 secretion by tenascin-C was shown to be a synergistic effect of both α9 integrin- and TLR4-mediated signalling [207]. The outcome of αVβ3 activation by tenascin-C was studied in peritoneal macrophages, where it resulted in the upregulation of IL-6, IL-1β, and TNF. This effect of tenascin-C on cytokine secretion could be ablated with an NF-κB inhibitor [208]. These data show that tenascin-C can induce cytokine synthesis by activating more than one receptor family; how this interplay is mediated on the cellular level remains to be elucidated, but such receptor redundancy may illustrate the importance of tenascin-C as a danger signal, ensuring that it does not go unnoticed at times of cellular stress.

In addition to its influence through binding to membrane receptors, tenascin-C may also indirectly modulate intracellular inflammatory signalling. In a human glioblastoma cell line, tenascin-C downregulates the Wnt inhibitor DKK1, resulting in increased classical Wnt signalling by stabilization of β-catenin [211]. Tenascin-C also interacts with Wnt3a, and human adenocarcinoma cell line cells plated on tenascin-C in the presence of Wnt3a exhibit enhanced classical Wnt signalling. Interestingly, when cells were incubated with soluble tenascin-C, the signalling was markedly reduced [212]. This might suggest that while soluble tenascin-C would sequester Wnt ligands, within the ECM it could be responsible for accumulating ligands close to the cell surface enabling signalling activation. Due to the fact that a complex crosstalk exists between Wnt and NF-κB pathways [213], regulation of Wnt signalling by tenascin-C could exert

both positive and negative modulation of the inflammatory response. Furthermore, evidence is emerging that supports a role for tenascin-C in PRR-mediated responses to pathogen invasion. In murine bone marrow–derived macrophages, rapid upregulation of tenascin-C upon LPS detection by TLR4 controls the maturation of the micro-RNA miR-155. Impaired maturation of miR-155 in the absence of tenascin-C prevents effective translation of LPS-induced pro-inflammatory cytokines including TNF [214]. Finally, tenascin-C is capable of interfering with HIV transmission. Tenascin-C present naturally in human breast milk was shown to bind HIV-1 Envelope protein, neutralizing the infectious properties of this virus in reporter cell lines and peripheral blood mononuclear cells [215]. This cooperative impact of microbiological and endogenous alarm signals demonstrates an amazing complexity of signalling within the innate immune system.

1.3.3 Tenascin-C and the resolution of inflammation

The induction of tenascin-C expression is a transient process during the progression of inflammation; it is not detectable following the completion of tissue repair. However, persistent tenascin-C expression is associated with chronic inflammation, where the pro-inflammatory properties of tenascin-C mediated by interactions with both TLR4 and the integrins might offer an interesting insight into the mechanism of its involvement in inflammatory diseases. Upregulated as a result of tissue damage, cellular stress, and inflammatory mediators, and subsequently exacerbating the inflammatory response, tenascin-C is likely to activate a positive feedback loop driving disease. At this point, the vital importance of strict control over tenascin-C expression becomes evident, and the factors regulating tissue levels of tenascin-C have recently been reviewed [188, 189, 216].

The question arises whether tenascin-C plays an active role during the resolution of inflammation, or whether its disappearance from tissues simply creates a less pro-

inflammatory environment. Tenascin-C has been shown to bind to TGF-β [217], a factor that plays a key role in the resolution of inflammation [218], and interactions with tenascin-C might increase local concentrations or activity of this immunosuppressive factor. Moreover, tenascin-C has been shown itself to exert immunosuppressive effects on lymphocytes. A number of studies found tenascin-C to be capable of arresting T-cell activation induced by various stimuli [219-223]. The blocking of anti-CD3 MAb/fibronectin-induced activation of human peripheral blood T cells by tenascin-C was shown to be mediated through the alternatively spliced repeats A1 and A2 within FNIII domain and was caused by a blockade of TCR/CD3 complex internalization [222]. In addition, in murine CD4+ and CD8+ splenocytes activated with a cocktail of IL-2 and anti-CD3 and anti-CD28 beads, tenascin-C-mediated reorganization of the actin cytoskeleton was implicated in regulating T-cell behaviour [223]. On the whole, these data add to the evidence supporting tenascin-C as a sophisticated regulator of inflammation, capable of conveying both pro- and anti-inflammatory responses.

1.3.4 The wider picture: conclusions from animal models

The intricate inflammatory functions of tenascin-C described in vitro prompt questions about the significance of its contribution to inflammation in vivo. The macroscopic effects of tenascin-C gene deletion have been examined using two independently generated knockout mice [224, 225]. Surprisingly, few gross phenotypic differences could be detected in the tenascin-C knockout (TNC KO) animals, compared with wild type. They were born alive and fertile, normal in size, and exhibited standard development and lifespan. Abnormalities in TNC KO mice were observed during tissue repair following corneal [226, 227] and myocardial [228] injury, including reduced macrophage infiltration, delayed myofibroblast recruitment, and reduced TGF-β, fibronectin, and collagen synthesis, resulting in delayed healing. These phenotypes

stimulated further interest in the protein's relevance during pathological conditions. Indeed, investigation of inflammatory responses in TNC KO mice challenged with experimental disease has provided considerable insight into the role of tenascin-C in immunity in vivo (summarized in Table 1.3).

In line with the pro-inflammatory capabilities of tenascin-C reported in vitro, tenascin-C persistently emerges as a key player in chronic inflammation in vivo. The reduction of pro-inflammatory cytokine secretion and subsequent diminished inflammatory cell recruitment as a result of tenascin-C deficiency have been shown to exert a protective effect in a number of inflammatory disease models. Tenascin-C ablation in transgenic mice overexpressing mutated amyloid precursor protein resulted in suppression of Alzheimer's disease–specific inflammation. Lower levels of pro-inflammatory mediators, such as TNF, IL-1β, and IL-6, and higher levels of anti-inflammatory mediators, such as IL-10, MRC1, and CCL2, in the central nervous system were associated with reduced amyloid deposition and ameliorated Alzheimer's disease pathology [229]. Knockout of tenascin-C was reported to reduce immune cell infiltration and prevent brain edema and blood–brain barrier disruption following insult in a surgical subarachnoid haemorrhage model [230, 231]. Remarkable anti-inflammatory effects of tenascin-C deficiency were also reported in models of joint inflammation. During acute inflammation induced by zymosan, the resolution of synovial inflammation was significantly quicker in TNC KO animals compared with wild type. Furthermore, tenascin-C-deficient mice were protected from prolonged synovitis, and cartilage and bone destruction, in a model of erosive arthritis induced by methylated BSA [136]. During this erosive arthritis, tenascin-C deficiency resulted in decreased cytokine synthesis in the joint, including attenuated IL-6 and IL-23 expression, and this altered cytokine profile created a microenvironment that could not support Th17 polarization,

manifesting in significantly reduced IL-17 expression [200]. TNC KO mice also exhibited a decrease in the production of IL-17 by Th17 cells during experimental autoimmune encephalomyelitis, a mouse model of multiple sclerosis, accompanied by a reduction in the number of interferon gamma (IFNγ)–producing Th1 cells [232]. Moreover, during ovalbumin (OVA)-induced bronchial asthma, TNC KO animals exhibited significantly attenuated allergic inflammation, with reduced eosinophil infiltration and reduced levels of IgE levels. This dampening of the inflammatory response was shown to be a result of impaired differentiation of Th2 cells, leading to a decrease in the expression of the classical type 2 cytokines, IL-5 and IL-13 [233]. These studies support in vitro data suggesting that tenascin-C can modulate T cell polarization, but highlight that tenascin-C exerts complex and highly context-specific effects, affecting T-cell subsets shown to orchestrate particular pathologies: Th2 in asthma [234], Th17 in RA [235], and Th17 and Th1 in autoimmune encephalomyelitis [236].

In addition to exacerbating inflammatory responses, tenascin-C has been shown to play a particularly deleterious role promoting tissue fibrosis. For example, in the cardiovascular system, tenascin-C deficiency relieves postsurgical neointimal hyperplasia [237, 238] and improves cardiac function after myocardial infarction [239]. Moreover, in a concanavalin A–induced hepatitis model, a reduction in collagen expression and deposition was observed in the livers of TNC KO mice. This was associated with reduced secretion of inflammatory mediators IFNγ, TNF, and IL-4, and lower lymphocyte and neutrophil infiltration into the liver, as well as a significant downregulation of TGF-β expression compared with wild-type mice [240]. Impaired TGF-β signalling, with diminished nuclear translocation of Smad-2 and Smad-3, was also shown to protect tenascin-C-deficient animals from lung fibrosis in a bleomycin-induced acute lung injury model [241]. Moreover, a decrease in TGF-β expression and

attenuation of collagen deposition caused reduced dermal and pleural thickening, as well as accelerated resolution of inflammation, in the absence of tenascin-C in bleomycin-induced mouse models of systemic sclerosis [205]. Consistent with in vitro studies, these data indicate that tenascin-C impacts both the immune and the stromal compartment during inflammatory disease models, and suggest that enhanced fibrosis may be mediated at least in part by raising tissue levels of TGF-β, enabling this factor to exert fibrogenic effects by promoting fibroblast activation, and stimulating excessive production of extracellular matrix [242]. Finally, liver tissue regeneration was enhanced as a result of tenascin-C ablation in a model of hepatic ischemia/reperfusion injury. In the absence of tenascin-C, the secretion of IL-6, IL-1β, and CXCL2 was decreased and the recruitment of leukocytes impaired. This inflammatory phenotype was accompanied by attenuated catabolic processes, with depleted necrosis, lower levels of apoptotic markers, and decreased expression and activation of MMP-9, an extracellular matrix–degrading enzyme [203], suggesting tenascin-C can impact tissue fibrosis by both promoting matrix deposition and inhibiting matrix removal.

These data indicate that tenascin-C expression in experimental models contributes to prolonged inflammation and fibrosis during disease pathogenesis. However, a number of studies provide evidence supporting a positive role for tenascin-C during inflammation in vivo. Following renal injury in a snake venom–induced model of proliferative glomerulonephritis, an inflammatory kidney disease, TNC KO animals showed drastically impaired renal regeneration, with increased proteinuria and scar tissue formation, decreased mesangial cells proliferation, and aberrant patterns of TGF-β, collagen, and fibronectin expression. The severity of observed abnormalities resulted in death of all knockout animals within 4 months, despite the injury being reversible in wild-type controls [243]. Tenascin-C has been also reported to attenuate inflammation in

chemically induced dermatitis. Tenascin-C-null mice exhibited increased swelling and prolonged polymorphonuclear cell infiltration. During post insult regeneration, a disorganization of extracellular matrix and formation of elastosis-like structures were observed [244]. A significant delay in tissue regeneration was also observed in tenascin-C-deficient mice in a surgical degenerative knee osteoarthritis model. In contrast to controls, the injured cartilage could not be regenerated in TNC KO animals, and the defects were filled with fibrous tissue. Moreover, age-related spontaneous articular cartilage degeneration was accelerated in knockout animals [245].

Collectively, these studies confirm tenascin-C is a potent regulator of inflammation and fibrosis in vivo. However, these data also highlight that tenascin-C displays a remarkable functional dichotomy; in some models, it positively influences tissue repair, protecting from excessive inflammation and remodelling, and preventing fibrotic tissue formation. In contrast, in other models, it is capable of driving chronic inflammation and promoting pro-fibrotic responses often to the detriment of the organism. Temporal control of tissue levels of tenascin-C might be of importance here; where expression is downregulated tenascin-C mediated inflammation and repair can proceed in a controlled manner, while persistent expression of tenascin-C would fuel pro-inflammatory and pro-fibrotic responses. Another key influencing factor might be the tissue microenvironment where expression of distinct tenascin-C splicing variants, differential proteolytic processing, and the presence of different tenascin-C receptors exposed on the cell surface would also be expected to shape the context of tenascin-C-mediated responses.

In considering the role of tenascin-C in inflammation in vivo, more intriguing questions continue to emerge. Tenascin-C has been shown to contribute to the immune response to LPS-induced sepsis. TNC KO animals were protected from systemic

inflammation following the cytokine storm caused by LPS administration, supporting a role for tenascin-C in host defense against infection in vivo. Interestingly, this phenotype in tenascin-C-deficient mice could be partially rescued by bone marrow transplant from wild-type littermates [214], highlighting that both myeloid and stromally derived tenascin-C participate in these immune responses. Within the bone marrow compartment, a decrease in cell colony–forming capacity has been reported in TNC KO animals, yet the steady-state haematopoiesis was not affected [246]. However, tenascin-C-deficient mice did exhibit impaired hematopoietic recovery as a result of a bone marrow ablation by irradiation [247]. Tenascin-C was also shown to regulate bone marrow–mediated angiogenesis. In addition, a recent study found that tenascin-C expressed in the bone marrow, but not the myocardium, was responsible for the attenuation of fibrosis in a mouse model of cardiac hypertrophy. TNC KO animals showed an exacerbation of inflammation and impaired cardiac function following the transverse aortic constriction surgery. This phenotype could be rescued by a bone marrow transplant from a wild-type donor, and simultaneously, a transplant from a tenascin-C-null donor to a wild-type recipient resulted in a declined cardiac function [248]. Together, these data pose questions about the site of action of tenascin-C during inflammation, suggesting a role not only locally, at the site of inflammation, but also distally, impacting inflammatory cell behaviour at sites some distance from pathology. These data also raise a cautionary note that it will be important to take into account the background strain of mice used in studies, as different strains of mice are known to exhibit different immune compartment biases that could define the ultimate impact of tenascin-C deletion in vivo.

Table 1.3 Tenascin-C in mouse models of inflammatory diseases.

Pathology	Model	Tenascin-C Deficiency Effect	Ref.
Tenascin-C deficiency alleviating inflammatory response			
Alzheimer's disease	Mutated APP-overexpression AD model	↓ proinflammatory cytokine synthesis and amyloid deposits in the brain	[229]
Asthma	Ovalbumin-induced bronchial asthma model	↓ inflammatory cell infiltration, goblet cell production, IL-5, IL-13, MCP-1, and MMP-9 expression, levels of IgE, airway hyperresponsiveness	[233]
Cancer	Transgenic metastatic breast cancer model	Altered tumor organization ↑ macrophage infiltration	[249]
	Xenografting melanoma model	↓ tumor size and vascularization, VEGF expression	[250]
	Transgenic pancreatic cancer model	↓ tumor vascularization, vessel leakage, level of tumor cell–specific marker insulin mRNA ↑ levels of Wnt pathway inhibitor DKK1	[251]
Hepatic ischemia/ reperfusion injury	Warm hepatic IRI model	↑ liver regeneration, ↓ necrosis, levels of apoptotic markers, IL-1β, IL-6, CXCL2, and MMP-9 expression, impaired leukocyte recruitment, altered expression of adhesion molecules	[203]
Liver fibrosis	Concanavalin A–induced hepatitis model	↓ collagen expression and deposition, inflammatory cell infiltration, IFNγ, TNF, IL-4, and TGF-β production, numbers of αSMA positive cells	[240]
Lung fibrosis	Bleomycin-induced acute lung injury model	↓ collagen deposition, numbers of αSMA and Smad2/3-positive fibroblasts, fibroblast–myofibroblast transformation	[241]
Multiple sclerosis	MOG-induced experimental autoimmune encephalomyelitis model	↓ number of IFNγ producing Th1 cells and IL-17 production by Th17 cells	[232]
Myocardial infarction	Surgical MI model	↓ collagen deposition, myocardial stiffness ↑ cardiac function	[239]
Neointimal hyperplasia	Surgical aortomy model	↓ aorta scaring, cell migration and proliferation, deposition of proteoglycans	[237]
Rheumatoid arthritis	Zymosan-induced acute arthritis model	↑ resolution of paw swelling, no synovitis, no cell infiltration	[136]
	mBSA-induced erosive arthritis model	↑ synovial inflammation resolution, no fibrin or cell aggregation, no pannus formation, no proteoglycan loss, no chondrocyte death, no cartilage or bone erosion	
Subarachnoid hemorrhage	Surgical SAH model	↓ brain edema, blood-brain barrier disruption	[230]
		↓ cerebral vasospasm and inflammatory cell infiltration	[231]
Systemic sclerosis	Bleomycin-induced pulmonary fibrosis model	↓ fibrosis scores, pleural thickening, numbers of fibrotic foci, inflammatory cell infiltration, collagen deposition, numbers of αSMA- and Smad2-positive fibroblasts	[205]
	Bleomycin-induced dermal fibrosis model	↑ resolution of fibrotic dermis thickening ↓ inflammatory cell infiltration, collagen, fibronectin, IL-6, MCP-1, and TGF-β expression, Smad-2/3 activation	
	Tsk dermal fibrosis model	↓ hypodermis thickening, collagen and αSMA deposition	
Tenascin-C deficiency disturbing tissue remodeling			
Dermatitis	chemically induced ear dermatitis model	↑ ear thickening, disorganized ECM, prolonged granulocyte infiltration, formation of elastosis-like structures	[244]
Glomerulonephritis	Habu-snake venom induced proliferative glomerulonephritis model	Abnormal regeneration, ↑ proteinuria and scar tissue formation, ↓ mesangial cells proliferation, PDGF-BB expression, abnormal TGF-β, collagen and fibronectin expression	[243]
Osteoarthritis	spontaneous age-related knee OA model	↑ articular cartilage degeneration	[245]
	surgical degenerative knee OA model	Delayed cartilage regeneration	

Abbreviations: APP, β-amyloid precursor protein; AD, Alzheimer's disease; IL, interleukin; MCP-1, monocyte chemotactic protein 1; MMP, matrix metalloproteinase; VEGF, vascular endothelial growth factor; DKK1, Dickkopf-1; IRI, ischemia/reperfusion injury; CXCL2, C-X-C motif chemokine ligand 2; IFNγ, interferon gamma; TNF, tumor necrosis factor; TGF-β, transforming growth factor beta; αSMA, alpha-smooth muscle actin; MOG, myelin oligodendrocyte glycoprotein; MI, myocardial infarction; mBSA, methylated BSA; SAH, subarachnoid hemorrhage; ECM, extracellular matrix; PDGF-BB, platelet-derived growth factor chain B dimer; OA, osteoarthritis.

1.3.5 Tenascin-C in the clinic

In humans, a missense mutation in the TNC gene is responsible for autosomal dominant hearing loss, caused by irreversible abnormalities in developing cochlea [252]. Polymorphisms in the gene have been also associated with increased risk of asthma, rhinoconjunctivitis, and Achilles tendinopathy [253-255]. However, it is the wild-type protein that attracts most interest as a potential target for diagnostics and therapy.

Successful treatment of a disease must be preceded by a correct diagnosis. This is often challenging, as signs and symptoms can be nonspecific, or their severity highly subjective. Hence the widespread use of biomarkers, easily measurable objective factors indicating the medical state of the patient. Biomarkers can be employed to predict disease incidence and severity, treatment outcome, or surgical intervention effects. Although tenascin-C is upregulated in a number of human pathologies, it has been most thoroughly studied in the context of cancer, and was shown largely to correlate with metastasis and indicate poor prognosis. So far its prognostic significance has been confirmed in breast, lung, and bladder cancer, glioma, squamous cell carcinoma, melanoma, and colorectal and hepatocellular carcinoma (reviewed in [256]). Recently, tenascin-C levels have been investigated as a diagnostic factor in preeclampsia, a hypertensive disorder of pregnancy and one of the most common cause of maternal deaths worldwide [257]. Consistent with its involvement in driving inflammation, tenascin-C has also been widely considered as a biomarker of patient inflammatory status in a number of chronic inflammatory diseases.

A screen of tenascin-C in sera from patients suffering diverse conditions, including cancer, malaria, and sepsis (from a routine chemistry laboratory of a large hospital), found a positive correlation between the levels of tenascin-C and C-reactive protein (CRP), highlighting that elevated serum tenascin-C is associated with pathological inflammation, but is not disease specific [258]. Subsequent studies have

shown that circulating tenascin-C levels correlate with disease activity in inflammatory conditions including ulcerative colitis, Crohn's disease, and systemic lupus erythematosus (SLE) [259, 260]. The clinical relevance of tenascin-C was particularly evident in SLE, as it was found to be a better predictive factor of disease aggravation (so-called "flare") than conventionally used biomarkers, potentially allowing for quicker identification of the need to escalate immunosuppressive therapy. The diagnostic value of tenascin-C was also investigated in arthritis, revealing upregulation in the synovial fluid of osteoarthritis patients, with levels correlating to disease severity [261]. Similarly, tenascin-C was elevated in RA, although here tenascin-C did not correlate with the levels of CRP in synovial fluid [262]. Upon further investigation, markedly raised circulating levels of tenascin-C in RA patients correlate with joint erosion [263]. Moreover, in RA, a subset of autoantibodies recognizing a citrullinated epitope in the FBG domain of tenascin-C could be detected years before any manifestation of the disease and thus could help in early clinical diagnosis [264], as well as predicting among people presenting with early synovitis, those whose inflammation will not resolve but who will go on to develop RA [265]. Tenascin-C has been also considered an attractive candidate biomarker in cardiac pathologies (reviewed in [266]). For example, tenascin-C has been proven a useful biomarker in a retrospective study on Kawasaki disease. Serum levels of tenascin-C were shown to predict the risk of acquiring resistance to the high-dose intravenous immunoglobulin therapy, implemented in Kawasaki disease to reduce pathological chronic inflammation, and also subsequent development of coronary artery lesions, one of the most dangerous complications of the acute form of the disease [267]. Moreover, in line with in vitro data highlighting the pro-fibrotic activity of tenascin-C, this matrix molecule could also be useful in the stratification of patients with conditions caused by pathological cardiac tissue remodelling. High tenascin-C levels in patients suffering from

hypertrophic cardiomyopathy correlated with high incidence of heart failure, a potential cause of premature death that is hard to predict with echocardiographic examination [268]. In addition, in systemic sclerosis, a disease driven by persistent fibrosis, significantly elevated tenascin-C expression was found in skin biopsies from patients with inflammatory subset of the disease. What is more, tenascin-C levels were also markedly higher in circulation of patients with both early- and late-stage disease [205]. Together, these data highlight tenascin-C as a prospective diagnostic target in a number of inflammatory and fibrotic conditions, useful in predicting disease progression and determining patient response to treatment.

Tenascin-C is an immunomodulatory protein that plays a key role in physiological tissue repair, but which can also drive pathological inflammation and fibrosis (Fig. 1.2). While an increasing body of data support a role for tenascin-C in influencing inflammation, this field is still in its infancy. Although tenascin-C impacts immune signalling in a wide range of cell types, the details of these signalling pathways remain to be fully defined in each target cell, from distinct immune populations to stromal cell lineages, and the molecular basis of the cell-type-specific responses reported so far to be dissected. Furthermore, there may be as yet uncovered roles for tenascin-C in impacting other effector cells that may provide a fuller picture of how this matrix molecule orchestrates inflammation. For example, myeloid-derived suppressor cells (MDSCs), a heterogeneous population of immature myeloid cells capable of inhibiting T cell–mediated inflammation, are emerging as key players in immune responses underlying tissue repair [269] as well as cancer [270] and autoimmune diseases such as RA, inflammatory bowel disease, or SLE [271]. Due to their unique immune suppressive potential, MDSCs are emerging as potential cellular immunotherapeutic agents [272]. The expansion of MDSCs can be stimulated by activation of the TLR4 pathway [273],

for example, in the lungs where MDSCs induced by activation of TLR4 signalling by LPS inhibit Th2 effector functions [274]. In a mammary carcinoma mouse model, S100A8/A9 proteins, endogenous TLR4 activators, have been shown to induce MDSCs accumulation in tissue, albeit this was triggered by binding to glycoprotein receptors on the cell surface [275]. These data raise the intriguing possibility that MDSCs may respond to tenascin-C and that this interaction could serve as a natural means of turning off tenascin-C-driven inflammation. Whether this is the case, and whether this mechanism goes awry in chronic or pathological inflammation, remains to be seen.

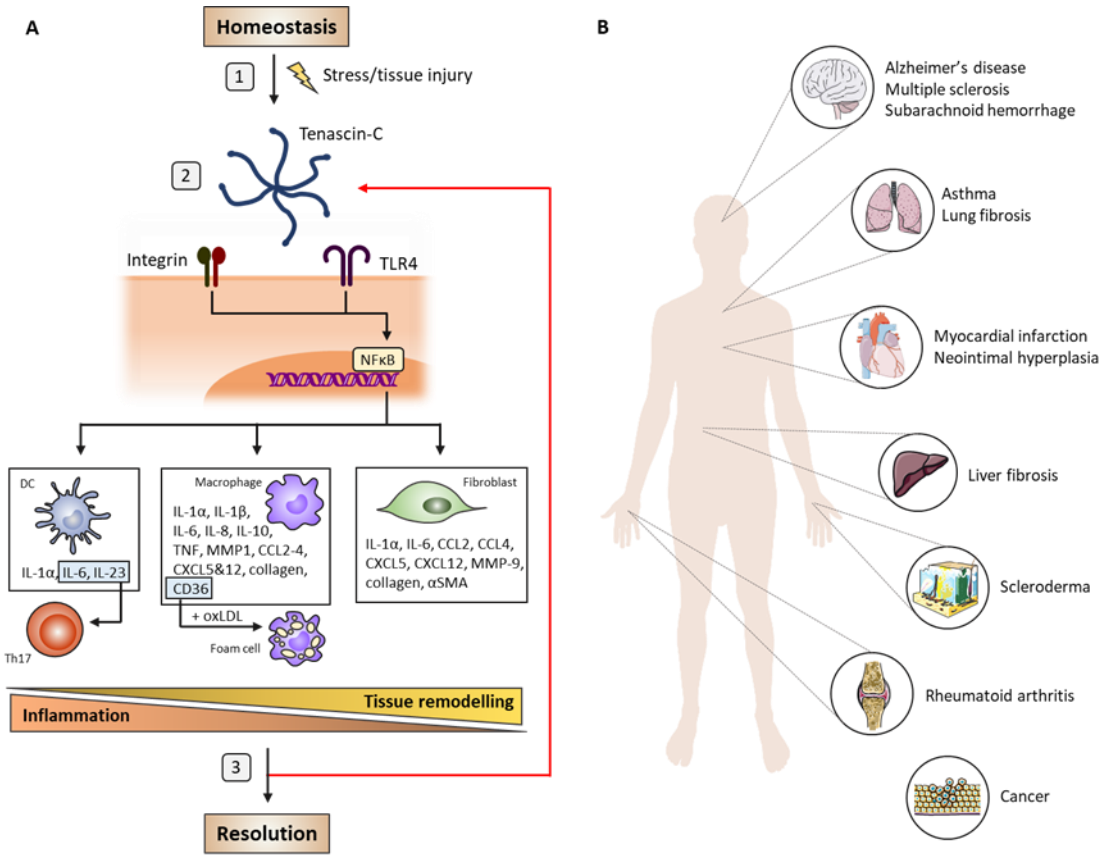


Figure 1.2 Tenascin-C modulates physiological and pathological inflammation. A Tenascin-C, upregulated upon cellular stress or tissue injury, is capable of binding to TLR4 and integrins α9β1 and αVβ3 on the cell surface and inducing NFκB-mediated gene expression. In macrophages and DCs, tenascin-C stimulates the secretion of a wide array of proinflammatory cytokines and chemokines, provoking an inflammatory response. Among these soluble mediators, IL-1β, IL-6, and IL-23 promote the differentiation of Th17 cells. Tenascin-C also polarizes myeloid cell phenotypes in a context-specific manner, for example, generating reparative macrophages or facilitating lipid uptake, promoting macrophages to form foam cells. In fibroblasts, tenascin-C stimulates expression of a different subset of mediators; this includes the cytokine IL-6 but also molecules such as αSMA, TGF-β and high levels of collagen that promote tissue remodeling. Tenascin-C is also capable of inhibiting naive T-cell activation. Typically, tenascin-C expression is downregulated, allowing for the resolution of inflammation and completion of tissue repair. However, a number of questions regarding the mode of action of tenascin-C still need answering: 1. What are the exact mechanisms leading to tenascin-C upregulation? 2. Does the form of tenascin-C (hexabrachion/monomer/domains cleaved by proteolytic enzymes) influence receptor binding and activation? 3. How exactly, and why, is tenascin-C expression downregulated and protein cleared from the tissue? Answering each of these questions will be crucial to understanding how and why persistent expression of tenascin-C leads to a chronic inflammation that can trigger the development of a number of inflammatory diseases, summarized in **B**. TLR4, toll-like receptor 4; NFκB, nuclear factor kappa-light-chain-enhancer of activated B cells; DC, dendritic cell; IL = interleukin; αSMA, alpha-smooth muscle actin; TGF-β, transforming growth factor beta; TNF, tumor necrosis factor; MMP, matrix metalloproteinase; CCL, C-C motif chemokine ligand; CXCL, chemokine receptor; oxLDL, oxidized low-density lipoprotein.

Due to its unique properties and characteristic expression pattern, tenascin-C has long been regarded as an attractive therapeutic candidate for targeting in clinics. A substantial part of ongoing work focuses on utilizing tenascin-C as a “postcode” for delivery of therapeutics directly to the tumour microenvironment with the means of aptamer or antibody technologies (reviewed in [276]). However, we are yet to explore applications targeting the pro-inflammatory potential of tenascin-C. To regain control over detrimental inflammation fuelled by tenascin-C, two main strategies could be implemented. The first approach might involve regulation of tenascin-C production at the level of mRNA transcription and protein expression. This would in principle resolve the key issue underlying tenascin-C pathology - its misregulated expression. Global inhibition of tenascin-C expression, however, would ablate all the effects exerted by this large multimodular molecule in all tissues, which would include undesirable, prolonged engagement of pro-inflammatory signalling, but which also might prevent desirable functions, for example, those supporting physiological tissue remodelling. The restricted pattern of prolonged expression of tenascin-C in the adult to pathological sites may make this a viable option. Moreover, the phenotype of the tenascin-C knockout mouse implies a level of redundancy for this molecule during development, and its absence does not have a profound effect in reported cases of acute tissue repair, suggesting an association with immune persistence that may provide an avenue to treat chronic diseases without significantly affecting underlying biology. Alternatively, elucidating mechanisms that control the induction of tenascin-C expression at the transcriptional level, or tissue removal at the protein level, would provide information that might enable manipulation in a tissue- or disease-specific manner, adding a further level of refinement to this approach.

The second approach would involve targeting tenascin-C signalling by specifically preventing its activation of receptors that mediate undesirable inflammatory signalling. However, this strategy also comes with its own challenges. Little is known about how different domains in tenascin-C interact with each other at the functional level; for example the extent of synergy between domain signalling is unclear, nor do we know how individual interactions are influenced by the structural context of the molecule as a whole. We also have limited knowledge of the different ligand binding modes of this matrix molecule; this includes understanding whether interactions are mediated as a result of ligand binding exclusively to a unique epitope within tenascin-C, or to more general motifs with multiple potential ligands, or whether a combination of both possibilities exists. For example, RGD sequences bind to more than one combination of integrin dimers, and integrins can also bind to non-RGD containing motifs in tenascin-C. In addition, one site among the tripartite TLR4-binding epitope within tenascin-C comprises an exposed cationic ridge [193], which might conceivably interact with other charged molecules. Understanding more about how this multimodular molecule binds to its wide range of ligands therefore is key to understanding not only its biological complexity but also inhibitor development.

In this thesis I will endeavour to further elucidate how interaction of tenascin-C immunogenic domain, FBG, with its ligand, TLR4, drives immune responses, and how those responses are regulated to avoid chronic inflammation.

1.4 Hypotheses and Objectives

Endogenous danger signals play a crucial physiological function of alerting the host to stress and stimulating tissue repair, yet their activity must be tightly regulated in order to avoid sustained inflammation that might lead to catastrophic autoimmune destruction. In this thesis I will address 3 aims: 1) dissecting widespread molecular determinants of danger, 2) exploring innate memory induced in response to endogenous immune stimuli, and 3) comparative analysis of the response to DAMPs in healthy individuals, compared to the responses of people with RA.

AIM 1: Tenascin-C, fibrinogen, and other FBG domain-containing proteins

The C-terminal FBG domain of tenascin-C has been identified as a TLR4 agonist. This domain derives its name from fibrinogen, a soluble plasma glycoprotein complex that is an essential component in the coagulation cascade [277]. The full length fibrinogen molecule is a rod-shaped homodimer, comprising two copies each of α, β and γ chains. Both ɣ and β chains possess the characteristic globular domain exposed on either end of the complex [278] (Fig. 1.3). Fibrinogen is an important factor in maintaining tissue homeostasis and wound healing. Not only is fibrinogen involved in thrombogenesis, providing a substrate for fibrin polymerization and promoting platelet aggregation [279], but it also contributes to the immune response by triggering signalling through the integrins and TLR4 [280].

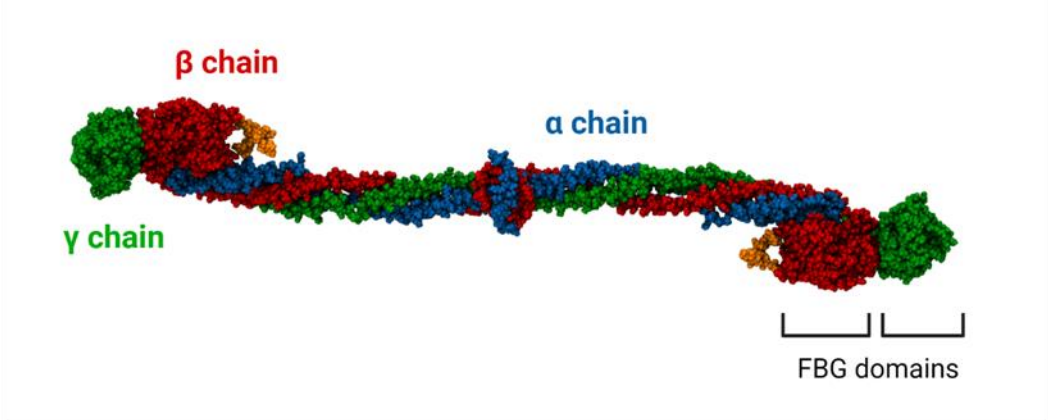


Figure 1.3 Fibrinogen molecule. Van der Waals representation of the fibrinogen structure (PDB ID 3GHG). Fibrinogen is a large molecule consisting of 2 symmetrical units, each comprising one copy of α, β and γ chains. Fibrinogen chain α is shown in blue, chain β – in red, and chain γ – in green. Globular FBG domains at the C-terminus of chain β and chain γ are marked for one of the symmetric units. Image adapted from Köhler *et al.*, PLoS Comput Biol 2015.

FBG is an archaic and well conserved domain, identified in organisms as far back in the phylogenetic tree as sea sponges [281]. It is a widespread domain in eukaryotes, present in over 2,500 molecules, collectively referred to as fibrinogen-related proteins, or FRePs. In humans, a total of 24 different FRePs exist. Aside from fibrinogen, tenascin-C and other tenascin family members, human FRePs include ficolins, angiopoietins, and angiopoietin-like proteins, among others. Despite homology in the C-terminal globe, FRePs exhibit diverse architecture of the N-terminus and have unique ways of modulating cell behaviour. However, multiple human FRePs appear to be stress response proteins, like tenascin-C. They are upregulated following injury and infection, and involved in a number of tissue repair mechanisms, such as coagulation, induction of inflammation and angiogenesis (reviewed in [282]). This functional similarity of diverse proteins sharing a common structural feature might point to the FBG serving as a universal signal alarming the body about danger.

The 24 human FRePs are stress response proteins that share a C-terminal globular domain, FBG. Among them, fibrinogen and tenascin-C are known TLR4 agonists, capable of eliciting pro-inflammatory response. I hypothesized that a common

motif exists in the FBG domains from FRePs that is responsible for TLR4 ligation. To interrogate this hypothesis, my objectives were to analyse the sequence and structure of FBG domains from human FRePs, and investigate if molecules sharing distinct features can bind to, and activate TLR4; and elicit immune responses *in vitro* and *in vivo*.

The activity and immunogenicity of FRePs will be tested using:

– a solid phase TLR4 binding assay;
– induction of cytokine secretion in primary human macrophages;
– assessment of mouse joint damage following intraarticular administration.

AIM 2: Induction of immune memory by tenascin-C

Pathogenic virulence factors are known to not only generate a first wave of immune responses, but also induce cellular re-programing that regulates innate cell responses to future threats. This phenomenon comprises potentiation of responses, or training, for example by yeast β-glucan [100]; and suppression – e.g. LPS tolerance. A limited number of endogenous molecules were also demonstrated to induce innate immune training and tolerance.

In the second part of my thesis, I aimed to investigate if FBG domain from tenascin-C, an archetypal DAMP stimulating inflammation, possesses the capability to induce memory mechanisms, and, if so, how are those mechanisms regulated. For this purpose I will employ an *in vitro* memory assay using primary human monocytes, a gold standard technique widely used in the field of innate immune memory research. With this assay, I will interrogate induction of tolerance and/or training by FBG-C through measurement of cytokine secretion. In addition, I will examine generation of cross-memory to other pathogenic and endogenous triggers, the effector specificity of memory effects, and temporal aspects of memory development. Furthermore, I will evaluate expression of immune mediators in the memory assay by quantitation of cytokine

mRNA. Finally, I will perform chromatin immunoprecipitation to detect alterations in chromatin structure that can affect gene expression; and I will target epigenetic pathways using a library of small molecule inhibitors.

Aim 3: DAMP induced immune responses in autoimmunity

Tenascin-C was demonstrated to accumulate in the arthritic joint, and its pro-inflammatory capabilities were implicated in RA progression. I hypothesised that activation of TLR4 signalling by the FBG domain from tenascin-C induces regulatory memory that protects from excessive inflammation; and that this mechanism malfunctions in people who develop autoimmune conditions like RA. To interrogate this hypothesis, my aim was to investigate if FBG-C induced signalling generates a tolerant phenotype in the context of RA. I will execute this with two approaches:

- examination of innate immune memory during a model of sustained inflammation with healthy human monocytes;
- comparison of immune responses induced in healthy monocytes and in cells isolated from individuals suffering from RA.

2

Materials and methods

Contents

2.1 Materials 69

2.1.1 Reagents 69

2.1.2 Buffers 73

2.2 Methods 74

2.2.1 *In silico* analysis of homology and protein modelling 74

2.2.2 Cloning 77

2.2.3 Expression 81

2.2.4 Protein purification 83

2.2.5 Protein quality control 84

2.2.6 Protein activity in vitro 86

2.2.7 Solid phase binding assay 88

2.2.8 Protein activity in vivo 89

2.2.9 Induction of innate immune memory 90

2.2.10 Measurement of innate immune memory effects 93

2.2.11 Epigenetic re-modelling studies 97

2.2.12 RA samples 98

2.2.13 Statistics 101

2.1 Materials

2.1.1 Reagents

Molecular biology

dNTP mix, Phusion HF Buffer, Phusion Hot Start II DNA Polymerase, GeneRuler DNA Ladder, DNA Loading Dye and GeneJET Gel Extraction Kit were purchased from Thermo Scientific. T4 DNA ligase, ligase buffer, primers and agarose were purchased from Invitrogen. Restriction enzymes (NdeI, XhoI and NotI) and CutSmart Buffer were purchased from New England BioLabs. pET32b vector was purchased from Merck. pET21d vector was purchased from Novagen. Plasmid miniprep kit was purchased from Qiagen. illustra PuReTaq Ready-To-Go PCR Beads were purchased from GE Healthcare Life Sciences. cDNA clones of human FRePs were purchased from Sino Biological (details of clones used are presented in Table 2.1). Fibrinogen ɣ chain IMAGE consortium cDNA clone (ID: 3935073) was purchased from GE Healthcare Dharmacon. Angiopoietin-like protein 6 cDNA clone (ID: OHu17260) was purchased from GenScript.

Table 2.1 cDNA clones of human FRePs purchased from Sino Biological.

Protein	Gene	RefSeq ID	Catalogue no.
Angiopoietin-like 1	ANGPTL1	NM_004673.3	HG10776-M
Angiopoietin-like 2	ANGPTL2	NM_012098.2	HG11014-M
Angiopoietin-like 4	ANGPTL4	NM_139314.1	HG10563-M
Ficolin-1	FCN1	NM_002003.2	HG10930-M
Ficolin-2	FCN2	NM_004108.2	HG10574-M

Protein production, quality control and activity testing

Trizma base, EDTA, sodium chloride, SDS, glycine, bromophenol blue, ammonium persulfate, TEMED, Tween 20, IPTG, Triton X-114, cystamine, 2-hydroxyethyldisulfide, sodium thiosulfate and BSA were purchased from Sigma. LB broth base and LB/agar were purchased from Invitrogen. Hydrochloric acid, glycerol and carbenicillin were purchased from Merck. ProBond nickel-chelating resin was purchased from Life technologies. Urea, acetic acid, PBS x10, sodium carbonate and formalin were purchased from VWR. Methanol, formic acid and silver nitrate were purchased from Ficher Scientific. TMB substrate was purchased from KPL. Mab hTLR4 (clone HTA125) was purchased from Invivogen. 30% acrylamide/bisacrylamide and anti-mouse IgG-HRP Ab (cat. no. 170-6516) were purchased from Biorad. Tetra-His Ab (cat. no. 34670) was purchased from Qiagen. Recombinant human TLR4 and Streptavidin-HRP were purchased from R&D systems. β-mercaptoethanol was purchased from MP Biomedicals. Sodium hydroxide and Coomassie Brilliant Blue G-250 were purchased from Fluka. Capture and detection anti-human IL-6, IL-8 and TNF antibodies were purchased from BD Pharmingen. Amersham ECL Western Blotting Detection Reagent was purchased from GE Healthcare.

Cell isolation and culture

Histopaque-1077 was purchased from Sigma. EasySep Human Monocyte Enrichment Kit without CD16 Depletion was purchased from Stemcell Technologies. RPMI 1640 was purchased from Lonza. RPMI 1640 (Dutch modified), ACK Lysing Buffer, fetal bovine serum (FBS), phosphate buffered saline (PBS), penicillin/streptomycin, GlutaMAX, sodium pyruvate and gentamicin were purchased from Gibco. Ethylenediaminetetraacetic acid (EDTA) was purchased from Sigma. M-CSF was purchased from Peprotech. MTT was purchased from Invitrogen. CytoTox 96 Non-

Radioactive Cytotoxicity Assay was purchased from Promega. Pooled human serum was kindly provided by Dr Henk Schipper (Monaco Group, Kennedy Institute, University of Oxford).

Cell stimulation

LPS from *E. coli*, serotype EH100 (Ra) (TLR grade) was purchased from Enzo Life Sciences. TAK242 (CLI-095) TLR4 inhibitor, Pam3CSK4, Poly(I:C) HMW, ultrapure flagellin from *S. typhimurium*, muramyldipeptide, CpG oligonucleotides, heat killed *C. albicans*, heat killed *E. coli* O111:B4 and heat killed *S. aureus* were purchased from Invivogen. LPS from *E. coli*, serotype O55:B5 and serotype O111:B4, Polymyxin B and proteinase K were purchased from Sigma. β-glucan solution was kindly provided by Prof. David Williams (East Tennessee State University). Oxidised low density lipoprotein from human plasma (oxLDL) was purchased from Invitrogen. Recombinant human TNF-α was purchased from BioLegend. Recombinant human IL-1α (Stemcell Technologies) was kindly provided by Carl Lee (Nanchahal Group, Kennedy Institute, University of Oxford).

RNA isolation and mRNA quantitation

RNeasy Micro Kit was purchased from Qiagen. High-Capacity cDNA Reverse Transcription Kit, TaqMan Universal PCR Master Mix and TaqMan Gene Expression Assays were purchased from Applied Biosystems.

Chromatin immunoprecipitation

iDeal ChIP-qPCR Kit, ChIP grade antibodies against CTCF (cat. no. C15410210, lot no. A2354-0010), H3K4me3 (cat. no. C15410003, lot no. A8034D), H3K27me3 (cat. no. C15410195, lot no. A0824D) and RNA polymerase II (cat. no. C15200004, lot no. 001-13) were purchased from Diagenode. Formaldehyde solution was purchased from Sigma.

Epigenetic probes testing

Library of epigenetic probes was kindly provided by Cassandra Adams and Tryfon Zarganis-Tzitzikas (Centre for Medicines Discovery, University of Oxford). Dimethyl sulfoxide (DMSO) was purchased from Sigma.

2.1.2 Buffers

TAE buffer: 40 mM Tris, 20 mM acetic acid, 1 mM EDTA

Agarose DNA gel: 1% (w/v) agarose in TAE buffer

TN buffer: 50 mM Tris, 150 mM NaCl, pH 8.0

Urea-Tris buffer: 8 M urea, 20 mM Tris, pH 8.0

4x Separating gel buffer: 1.5 M Tris-HCl, 0.4% (w/v) SDS, pH 8.8

4x Stacking gel buffer: 0.5 M Tris-HCl, 0.4% (w/v) SDS, pH 6.8

10x Running buffer: 248 mM Tris, 1.92 M glycine, 1% (w/v) SDS

2x Loading buffer: 125 mM Tris, 4.1% (w/v) SDS, 20% (v/v) glycerol, 5% (v/v) mercaptoethanol, 0.001% (w/v) bromophenol blue, pH 6.8

4% Stacking gel: 125 mM Tris, 4% acrylamide/bis-acrylamide, 0.1% (w/v) ammonium persulfate, 0.1% (v/v) TEMED, pH 6.8

12% Separating gel: 375 mM Tris, 12% acrylamide/bis-acrylamide, 0.1% (w/v) ammonium persulfate, 0.1% (v/v) TEMED, pH 8.8

CBB staining solution: 0.1% (w/v) Coomassie Brilliant Blue G-250, 50% (v/v) methanol, 20% (v/v) acetic acid

De-staining solution: 30% (v/v) methanol, 1% (v/v) formic acid

PBST: 1x PBS, 0.05% (v/v) Tween 20

TNC buffer: 50 mM Tris, 150 mM NaCl, pH 8.0

2.2 Methods

2.2.1 *In silico* analysis of homology and protein modelling

Sequence alignment

Protein sequences were obtained from UniProt Knowledgebase (accession numbers are presented in Table 2.2). Multiple sequence alignments were performed using Clustal Omega 1.2.1 and coloured according to the Clustal colour scheme.

Homology modelling

Available crystal structures of FBG domains from human FRePs were obtained from RCSB PDB database (identification numbers are presented in Table 2.3). Where crystal structures were not available, homology models of FBG domains were generated using SWISSMODEL using fibrinogen ɣ chain crystal structure 1FID as a template. Protein models were coloured and structurally analysed using Pymol Molecular Graphics System.

Table 2.2 Accession numbers of the 24 human FRePs.

Protein	Accession no.
Angiopoietin 1	Q15389
Angiopoietin 2	O15123
Angiopoietin 4	Q9Y264
Angiopoietin-like protein 1	O95841
Angiopoietin-like protein 2	Q9UKU9
Angiopoietin-like protein 3	Q9Y5C1
Angiopoietin-like protein 4	Q9BY76
Angiopoietin-like protein 5	Q86XS5
Angiopoietin-like protein 6	Q8NI99
Angiopoietin-like protein 7	O43827
Fibrinogen α chain	P02671
Fibrinogen β chain	P02675
Fibrinogen γ chain	P02679
Fibrinogen-like protein 1	Q08830
Fibroleukin	Q14314
FIBCD-1	Q8N539
Ficolin-1	O00602
Ficolin-2	Q15485
Ficolin-3	O75636
Microfibril-associated glycoprotein 4	P55083
Tenascin-C	P24821
Tenascin-R	Q92752
Tenascin-W	Q9UQP3
Tenascin-X	P22105

Table 2.3 Available crystal structures of FBG domains.

Protein	PDB ID
Angiopoietin 1	4EPU
Angiopoietin 2	1Z3U
Angiopoietin-like protein 3	6EUA
Angiopoietin-like protein 4	6EUB
FIBCD-1	4M7H
Fibrinogen α chain	1FZD
Fibrinogen β chain	1FZA
Fibrinogen γ chain	1FID
Ficolin-1	2JHM
Ficolin-2	4R9J
Ficolin-3	2J5Z
Tenascin-C	6QNV

2.2.2 Cloning

Primers were designed to introduce an N-terminal hexa-histidine tag and flanking restriction sites (sequence details of cloned FBG domains are presented in Table 2.4, designed primers are presented in Table 2.5). FBG sequences were amplified by PCR using full-length cDNA clones as templates (composition of PCR mix is presented in Table 2.6, PCR protocol is presented in Table 2.7). PCR products were purified (separated on 1% agarose gel, excised and extracted from gel using GeneJET kit). Purified inserts and vectors were digested for 1h at 37°C with restriction enzymes in CutSmart Buffer. Enzymes were then inactivated by incubating for 20 min at 80°C. Digested inserts and plasmids were purified (separated on 1% agarose gel, excised and extracted from gel using GeneJET kit) and ligated by incubation with T4 DNA ligase o/n at RT. 2 µL of post-ligation mix was then used to transform competent *E. coli* TOP10 cells by heat shock (incubation for 50 s at 42°C, followed by 2 min on ice). Transformed cells were plated on LB/agar plates with 100 µg/mL carbenicillin, selective antibiotic for pET series vectors, and incubated o/n at 37°C. 10-20 randomly selected colonies were analysed with colony PCR using illustra PuReTaq Ready-To-Go PCR Beads and insert-specific primers (protocol according to manufacturer's instruction) (Supplementary figure 1). Positive clones were amplified, plasmid DNA was isolated and sequenced.

Table 2.4 Sequence details of cloned FBG domains.

Protein	Gene	Accession number	FBG size [bp]	Domain boundaries
ALP-1	ANGPTL1	AF107253	663	811-1473
ALP-2	ANGPTL2	AF125175	675	826-1500
ALP-4	ANGPTL4	AF169312	684	599-1282
ALP-6	ANGPTL6	NM_031917.2	660	943-1602
FIB-G	FGG	BC021674	804	556-1359
FIC-1	FCN1	AK314867	658	363-1016
FIC-2	FCN2	HUMSLP35	654	296-949

Table 2.5 Sequences of primers designed for cloning of FBG domains.

Protein	FORWARD primer	REVERSE primer	PCR product [bp]
ALP-1	CAC CAT ATG CAT CAT CAT CAT CAT CAT TTC ATC AAT GAA GGA CCA TTC	GCT CTC GAG TTA GTC AAT AGG CTT GAT CAT CAT CTG AAC	702
ALP-2	AAA CAT ATG CAT CAT CAT CAT CAT CAT GAC AAG CCG TCG GGC CCA TG	GCT CTC GAG TTA GTG GAA GGT GTT GGG GTT CGG TC	714
ALP-4	AAA CAT ATG CAT CAT CAT CAT CAT CAT AGC CGC CTG CAC CGG CTG C	ACT CTC GAG TTA GGA GGC TGC CTC TGC TGC CAT G	723
ALP-6	CAC CAT ATG CAT CAT CAT CAT CAT CAT ACC AAG CCT GTG GGC CCG TG	GCT CTC GAG TTA CAG CTT CAG GGG CCG AAT GAG CAT ATG C	699
FIB-G	CAC CC ATG GCA CAT CAT CAT CAT CAT CAT CAA ATC CAT GAT ATC ACT GG	GTT CTC GAG TTA AAC GTC TCC AGC CTG TTT GGC TCC C	843
FIC-1	CAC CAT ATG CAT CAT CAT CAT CAT CAT CAG TCG TGT GCG ACA GGC CCA C	GCT CTC GAG TTA GGC GGG CCG CAC CTT CAT CTC TG	693
FIC-2	CAC CAT ATG CAT CAT CAT CAT CAT CAT CAG CCG TGC CTG ACA GGC CC	GCT CTC GAG TTA GGC AGG TCG CAC CTT CAT CTC TG	693

Table 2.6 Composition of PCR mixes.

5x Phusion HF Buffer	1x
dNTP Mix 10 mM	200 µM
FORWARD primer 5 µM	0.5 µM
REVERSE primer 5 µM	
cDNA clone template	100 ng
Phusion Hot Start II HF DNA Polymerase 2 U/µL	1 U
MiliQ H_2O	up to 50 µL

Table 2.7 Protocol of PCR.

Cycle step	Temperature	Time	No of cycles
Initial denaturation	98°C	30 s	1
Denaturation	98°C	10 s	35
Annealing/extension	72°C	30 s	
Final extension	72°C	7 min	1

2.2.3 Expression

Small scale

Clones with confirmed DNA identity were transformed into expression strain *E. coli* BL21 and protein expression was tested in small scale. For that, 4 mL of LB with 100 μg/mL carbenicillin (LB/carbenicillin) was inoculated with 80 μL of o/n culture of selected clones and incubated at 37°C with shaking until OD_{600nm} reached 0.6. 1 mL of culture was collected (unstimulated control) and IPTG was added to a final concentration of 1 mM to induce expression for 4 h at 37°C with shaking. 1 mL of culture was collected and cell pellet was separated by centrifugation at 5000 x g for 5 min. The pellet was washed twice with 1 mL of PBS, re-suspended in 200 μL of PBS and sonicated. After centrifugation at for 5 min soluble fraction (supernatant) and insoluble fraction (pellet) was collected and protein expression was analysed with sodium dodecyl sulphate polyacrylamide gel electrophoresis (SDS-PAGE) (Supplementary figure 2). For each FBG domain, the clone producing highest yield of recombinant protein was chosen for future work. Glycerol stocks of selected clones were prepared by mixing 0.5 mL of o/n bacterial culture with 0.5 mL of 50% glycerol and stored at -80°C.

Large scale

10 mL of LB/carbenicillin was inoculated with glycerol stock of selected clone and incubated o/n at 37°C with shaking at 200 RPM. The next morning, o/n culture was added to 1 L of LB/carbenicillin and incubated at 37°C with shaking at 200 RPM until OD_{600nm} reached 0.6. IPTG to final concentration 1 mM was added to induce expression for 4 h at 37°C with shaking at 200 RPM. Bacterial culture was then centrifuged at 3500 RPM for 15 min, pellet was collected, washed with TN buffer and stored at -20°C until further processing. Parameters of expressed recombinant FBG domains are presented in Table 2.8.

Table 2.8 Parameters of expressed recombinant FBG domains.

Protein	Size [aa]	Molecular weight [kDa]	Theoretical pI	Extinction coefficient [M^{-1} cm^{-1}]
ALP-1	227	26.58	6.51	77600
ALP-2	231	27.38	7.88	91580
ALP-4	234	26.52	8.72	57200
ALP-6	226	26.08	6.87	81610
FBG-C	234	26.98	8.78	52620
FIB-G	275	31.00	6.27	74620
FIC-1	224	25.17	6.30	56755
FIC-2	224	25.53	6.66	55265

2.2.4 Protein purification

Bacterial pellet from 0.5 L culture was defrosted, re-suspended in 20 mL of TN buffer and sonicated (4 times 30 s, amplitude 40%). Insoluble fraction was collected by centrifugation at 10000 RPM for 15 min in 4°C. The pellet was then solubilized in 40 mL of urea-Tris buffer by brief sonication and incubated overnight in 4°C with constant rotation. The next morning, solution was centrifuged again, passed through 0.8 μm syringe filter and passed twice through 5 mL of nickel beads equilibrated with urea-Tris buffer. Flow-through was collected and beads were washed with 50 mL of urea-Tris buffer, then ice cold 125 mL urea-Tris with 0.1% (v/v) Triton X-114 (LPS removal buffer) and finally 50 mL ice cold urea-Tris. Then, protein was eluted with urea-Tris containing 300 mM imidazole. 5 fractions of 5 mL were collected and protein concentration was measured with NanoDrop. Fractions containing protein were pooled together and diluted to 0.5 L with urea-Tris buffer. Cystamine was added to 20 mM and protein was dialysed against 2 L of TN buffer supplemented with 5 mM β-mercaptoethanol and 1 mM 2-hydroxyethyldisulphide for two days and then 2 L of TN buffer for two days at 4°C (buffer was changed every day). Refolded protein was then applied to 1.2 mL nickel beads equilibrated with TN buffer. Beads were washed with 125 mL of ice cold TN buffer with 0.1% (v/v) Triton X-114, and then 100 mL ice cold TN buffer. Protein was eluted with TN buffer supplemented with 300 mM imidazole. 5 fractions of 1 mL were collected and protein concentration was measured by NanoDrop. Efficiency of purification was assessed with SDS-PAGE (Supplementary figures 3 and 4). Fractions containing protein were dialysed twice against 2 L of TN buffer for 2 h and o/n at 4°C to remove imidazole. Purified protein was stored at -80°C.

2.2.5 Protein quality control

SDS-PAGE

Protein samples were separated on hand-casted 10-well 12% polyacrylamide gels. Gels were placed in gel tank (ATTO) filled with Running buffer. Protein samples were mixed with equal volume of 2x Loading buffer and incubated for 5 min at 100°C. 10-20 µL of boiled samples and 6 µL of pre-stained protein ladder (weight marker) was loaded per well. Electrophoresis was run at 130 V until the visible bromophenol blue line reached the lower edge of the gel.

Coomassie staining

To visualise protein bands following the SDS-PAGE, gels were incubated with CBB staining solution for 30 min at RT with moderate agitation. To de-stain the background gels were incubated with De-staining solution.

Silver staining

1 µg of purified proteins were separated by SDS-PAGE and gels were fixed with 50% methanol, 5% acetic acid solution for 1 h at RT or o/n at 4°C. Next, gels were washed once in 50% methanol for 10 min and twice in water for 10 min. Gels were then sensitized with 0.02% (w/v) sodium thiosulfate for 1.5 min and washed twice in water for 1 min. Silver staining was performed by incubation in 0.1% (w/v) silver nitrate for 1 h at 4°C. Gels were then washed twice in water for 1 min and developed by incubation in 2% (w/v) sodium carbonate, 0.04% (v/v) formalin until bands were clearly visible. Reaction was stopped by incubation in 5% acetic acid for 5 min. Results are presented in Supplementary figure 5.

Western blotting

10 µL of test expression samples or 1 µg of purified proteins were separated by SDS-PAGE and transferred to nitrocellulose membrane using Trans-Blot Turbo Transfer System (BioRad) according to manufacturer's instructions. Membrane was blocked for 1 h with 5% (w/v) BSA in PBST and then incubated o/n at 4°C with Tetra-His antibody diluted 1:10000 in 2% (w/v) BSA in PBST. Next, membrane was washed 3 times with PBST for 10 min, incubated with anti-mouse IgG-HRP antibody diluted 1:20000 in 2% (w/v) BSA in PBST for 1 h and washed 3 times with PBST for 10 min. All incubation and washing steps were performed with vigorous agitation of the membrane. To detect protein bands chemiluminescence was induced with Amersham ECL and captured on X-ray film. Results are presented in Supplementary figure 5.

Circular dichroism spectroscopy

Secondary structure was analysed using J-815 Circular Dichroism Spectrometer (Jasco). Spectra were measured in the range from 190 nm to 250 nm at 20°C. Each sample was measured 5 times and averages were plotted using Spectra Manager II software. Results are presented in Supplementary figure 6.

LPS contamination testing

LPS contamination was measured using Endpoint Chromogenic LAL Assay or Recombinant Factor C Assay (Lonza) according to manufacturer's instructions. Only samples containing below 10 pg/mL of LPS were used in subsequent experiments.

2.2.6 Protein activity in vitro

Human primary macrophage preparation

Peripheral blood mononuclear cells (PBMCs) were isolated from leukocyte cones obtained from NHS Blood and Transfusion (NHSBT) at the John Radcliffe Hospital, Oxford (cat. code NC24) by density gradient separation using Histopaque. Next, monocytes were isolated from PBMC fraction by counter-flow centrifugation using Beckman Coulter's Centrifugal Elutriation System. Cells were plated (1 million cells/mL) in RPMI 1640, 5% FBS, 1% penicillin/streptomycin and differentiated into macrophages for 5 days with 100 ng/mL of M-CSF. Differentiated macrophages were collected by scraping and plated in 96-well plates at 1 x 10^5 cells/well in RPMI 1640, 3% FBS and 1% penicillin/streptomycin to rest for 48 h.

Macrophage stimulation

Rested macrophages were stimulated with increasing concentration of LPS or recombinant FBG proteins. As a control for LPS contamination, the different stimuli were pre-incubated for 30 min with 10 μg/mL polymyxin B (PMB; final concentration) on ice. Alternatively, cells were stimulated with proteins denatured by boiling for 1 h, or treated with 10 times diluted mix of proteinase K in TNC buffer (3 μL proteinase K in 147 μL TNC buffer) for 1 h at 37°C, followed by boiling for 15 min, and incubation with PMB for 30 min. To assess TLR4 dependency, cells were pre-incubated with 3μM of selective TLR4 inhibitor TAK242 for 6 h at 37ºC prior to cell stimulation. After 24h, the medium was collected and stored at -20°C. To examine cell viability MTT assay was performed after each stimulation. After removal of conditioned medium, wells were refilled with fresh medium and 10% (v/v) MTT was added. Cells were incubated for 2 h at 37°C and then lysed with 10% (w/v) SDS, 0.01 M HCl. Plates were then incubated o/n

at 37°C to allow the solubilisation of formazan crystals and absorbance at 570 nm was measured using FluoStar Omega plate reader.

Cytokine ELISA

Levels of pro-inflammatory cytokines IL-6, IL-8 and TNF in post-stimulation media were measured by ELISA. Plates were coated o/n at 4°C with 50 µL of capture antibody diluted in PBS: anti-IL-6 1:500, anti-IL-8 1:250, anti-TNF 1:125. Plates were washed 3 times with PBST and blocked with 100 µL of 2% (w/v) BSA in PBS for 1 h at RT. Plates were washed 3 times with PBST and incubated for 2 h at RT with 50 µL of medium samples diluted in 0.5% (w/v) BSA in PBS: 10x for IL-6, 600x for IL-8, 2x for TNF. Plates were washed 3 times with PBST and incubated with 50 µL of biotinylated detection Ab diluted 1:1000 in 0.5% (w/v) BSA in PBS for 1 h at RT. Plates were washed 3 times with PBST and incubated with 50 µL of Streptavidin-HRP diluted 1:400 in 0.5% (w/v) BSA in PBS for 1 h at RT. Plates were washed 3 times with PBST and 50 µL of TMB substrate was added. Reaction was stopped with 50 µL of 6% sulphuric acid. Absorbance was measured at 450 nm using FluoStar Omega plate reader and data analysed using Omega software.

2.2.7 Solid phase binding assay

Binding assay was performed by Dr Lorena Zuliani-Alvarez. Nunc Maxisorp 96 well plates (Thermo Scientific) were coated o/n at 4°C with 1 μg/mL solution of recombinant FBG proteins in PBS. Unspecific binding was blocked with 10% (w/v) BSA in PBST for 2 h at RT. Decreasing concentrations of recombinant TLR4 in 2% (w/v) BSA in PBST were added and incubated for 2 h at RT. TLR4 binding was detected with mAb anti-human TLR4 at 1 ug/mL in 2% (w/v) BSA in PBST for 1 h at RT. Samples were then incubated with secondary antibody anti-mouse IgG-HRP diluted 1:1000 in 2% (w/v) BSA in PBST for 1 h at RT. Signal was developed with TMB substrate incubated for 10 min in the dark. Reaction was stopped using 6% (v/v) sulphuric acid solution and plates were measured at 450 nm using FluoStar Omega plate reader.

2.2.8 Protein activity *in vivo*

Animals

8 week old male DBA/1 mice were purchased from Charles River and allowed to acclimatize for 7 days. All animals were fed standard rodent chow and water ad libitum, and were housed (< six mice/cage) in sawdust-lined cages in an air-conditioned environment with 12 h light/dark cycles. All animal procedures were approved by the institutional ethics committee and the UK Home Office.

FBG injection

Intra-articular injections were carried out by Dr Fiona McCann and Dr Claire Deligne as described previously. Briefly, mice were anesthetized by inhaled isoflurane. Mice were then injected with 1 μg FBG in 10 μL of sterile PBS into the right knee joint using a sterile BD micro-fine 30G insulin syringe. Control mice received an injection of 10 μL PBS alone. At day 3 mice were euthanized, and the knee joints were excised and fixed in 10% (v/v) buffered formalin, decalcified, with 10% EDTA and processed to paraffin.

Histology

Coronal tissue sections (4 μm thick) were cut at 7 depths throughout the joint 80 μm apart and stained with hematoxylin and eosin or Safranin-O to assess joint pathology. Histological analysis was performed by Dr Claire Deligne. Each joint was scored as described: 0 = normal; 1 = cell infiltration with no signs of joint erosion; 2 = inflammation with the presence of erosions limited to discrete foci; and 3 = severe and extensive joint erosion with loss of architecture. Investigator performing the analysis was blinded to the experimental groups. The mean score for each animal in an experimental group was calculated by averaging the histopathologic scores in at least five section depths per joint.

2.2.9 Induction of innate immune memory

Human primary monocyte isolation

PBMCs were isolated from leukocyte cones obtained from NHSBT at the John Radcliffe Hospital, Oxford (cat. code NC24) by density gradient separation using Histopaque. Cells were then washed with PBS, and platelet contamination was removed by centrifugation at 200 RCF. Remaining red blood cells were lysed using ACK Lysing Buffer. Next, monocytes were isolated from purified PBMC fraction by immunomagnetic negative selection using EasySep Human Monocyte Enrichment Kit without CD16 Depletion according to manufacturer's instructions. Cells were plated at 5 x 10^5 cells/mL in RPMI 1640 (Dutch modified) supplemented with 2 mM GlutaMAX, 1 mM sodium pyruvate, and 50 µg/mL gentamicin, in 96-well plates (200 µL, 1 x 10^5 cells per well). Following seeding, cells were left to rest for a minimum of 1 h before stimulation.

Monocyte stimulation

Detailed descriptions of the different variations of memory assays are included throughout the text in chapters 4 and 5. Rested monocytes were stimulated with various concentrations of LPS O55:B5, β-glucan, or recombinant FBG-C protein. As a control for LPS contamination, FBG-C was pre-incubated for 30 min with 10 µg/mL polymyxin B on ice. Additionally, cells were stimulated with FBG-C denatured by boiling for 60 min at 90°C. In the citrullination experiment, cells were stimulated with FBG-C treated with PAD2, or heat inactivated PAD2 (citrullination protocol described below). After 24h, medium was collected and stored at -20°C. Next, cells were washed, and then rested for different amounts of time and re-stimulated, or immediately re-stimulated with LPS O55:B5 at 10 ng/mL or FBG-C at 1 µM. In the cross-tolerance experiment, monocytes were re-stimulated with a selection of 15 different pathogenic and endogenous triggers.

During rest and secondary stimulation, medium was supplemented with 10% pooled heat inactivated human serum, or left serum free. After 24h of secondary stimulation, culture medium was again collected and stored at -20°C.

FBG-C citrullination

All citrullination was performed by Dr Anja Schwenzer. FBG-C domain was citrullinated with human PAD2 enzyme in TNC buffer (50 mM Tris, 150 mM NaCl, 10 mM $CaCl_2$, pH 8) supplemented with 5 mM dithiothreitol for 3 hours at 37°C. As a control, sham citrullination was performed by incubating FBG-C with heat-inactivated PAD2. Citrullination was confirmed using Western blotting with a monoclonal human anti-modified citrulline (AMC) antibody (Modiquest Research, clone C4) diluted 1:500.

Cell viability measurement

To examine cell viability, the MTT assay was performed after stimulation. Following medium collection, fresh serum free medium with 10% (v/v) MTT was added to the wells. Cells were incubated for 22 - 24 h at 37°C and then lysed with 10% (w/v) SDS, 0.01 M HCl. Plates were then incubated o/n at 37°C to allow the solubilisation of formazan crystals and absorbance at 570 nm was measured using FluoStar Omega plate reader.

Cell viability was also measured in culture media and lysed cell cultures after 4 h and at the end of primary and secondary stimulation by quantitation of lactate dehydrogenase (LDH) using CytoTox 96 Non-Radioactive Cytotoxicity Assay (Promega) according to the manufacturer's protocol. Briefly, assay reagent was added to culture media or cell lysates prepared using included lysis buffer, and samples were incubated for 30 min at RT, protected from light. Next, absorbance at 490 nm was measured using FluoStar Omega plate reader.

Images of cell cultures were acquired using EVOS XL Core Imaging System (AMG) at 10x magnification. Images were processed using ImageJ software.

2.2.10 Measurement of innate immune memory effects

Cytokine ELISA

Levels of pro-inflammatory cytokines IL-6, IL-8 and TNF in culture media were measured by ELISA as described in paragraph 2.2.6.

RNA isolation

Total RNA was isolated from monocytes using RNeasy Micro Kit (Qiagen) according to the manufacturer's instructions. Briefly, stimulated monocytes were lysed in the plate and lysates from triplicate wells were pooled together. To improve recovery, carrier RNA was added and samples were homogenised by vortexing. Nucleic acids were then precipitated with ethanol, and samples applied to silica-based spin columns. Following treatment with DNase I and washing, RNA was eluted in nuclease-free water. RNA concentration was measured using NanoDrop. Isolated RNA was used immediately for reverse transcription. Any remaining RNA was stored at -80°C.

Reverse transcription

Isolated RNA was reverse transcribed into cDNA using High-Capacity cDNA Reverse Transcription Kit (Applied Biosystems) according to manufacturer's instructions. 30 – 50 ng RNA per reaction was used. Composition of reverse transcription (RT) reaction mix is presented in Table 2.9, incubation protocol is presented in Table 2.10. Obtained cDNA was stored at -20°C.

Table 2.9 Composition of RT reaction mix.

10x RT Buffer	1x
25x dNTP Mix (100 mM)	4 mM
10x RT Random Primers	1x
RNA	10 µL
MultiScribe Reverse Transcriptase (50 U/µL)	50 U
Nuclease-free H_2O	up to 20 µL

Table 2.10 RT reaction protocol.

Cycle step	Temperature	Time
1	25°C	10 min
2	37°C	120 min
3	85°C	5 min

TaqMan qPCR

TNF and IL-6 mRNA was quantified by standard curve qPCR using FAM-conjugated TaqMan primers and probes (TaqMan Gene Expression Assays used are listed in Table 2.11) and TaqMan Universal PCR Master Mix. GAPDH was used as a control reference gene. qPCR was performed using ViiA7 instrument (Applied Biosystems), according to the manufacturer's recommendations (composition of reaction mixes is presented in Table 2.12 and cycling protocol is presented in Table 2.13).

Table 2.11 TaqMan Assays IDs.

Gene	Assay ID
TNF	Hs00174128_m1
IL-6	Hs00174131_m1
GAPDH	Hs02758991_g1

Table 2.12 Composition of TaqMan qPCR reaction mix.

TaqMan Universal PCR Master Mix (2x)	1x
TaqMan Gene Expression Assay (20x)	1x
cDNA template	0.5 µL
Nuclease-free H_2O	up to 10 µL

Table 2.13 Protocol of TaqMan qPCR.

Cycle step	Temperature	Time	No of cycles
UNG incubation	50°C	2 min	1
Polymerase activation	95°C	10 min	1
Denaturation	95°C	15 s	40
Annealing/extension	60°C	1 min	

qPCR data analysis

qPCR data was analysed using the delta Ct (ΔCt) method. Average threshold cycle (Ct) values were obtained from the ViiA7 software following a qPCR run, and ΔCt and relative expression values were calculated:

ΔCt = average gene of interest Ct – average reference gene Ct

*Relative expression (% reference gene) = 2 ^ (- ΔCt) * 100%*

2.2.11 Epigenetic re-modelling studies

Chromatin immunoprecipitation

Chromatin immunoprecipitation was performed using iDeal ChIP-qPCR Kit according to manufacturer's instructions. Briefly, monocytes were isolated as described in paragraph 2.2.9 and seeded in 10 cm culture dishes at 1 x 10^6 cells/mL, 8 x 10^6 cells per dish, in medium supplemented with 10% human serum. Following stimulation, cells were fixed for 8 min by addition of Fixation Buffer supplemented with formaldehyde (final formaldehyde concentration 1%). Cells were then lysed, and chromatin was isolated and sheared with Bioruptor Pico (Diagenode) for 7 cycles (30 s on, 30 s off). Immunopreciptitation was performed o/n using ChIP-grade antibodies against RNA Polymerase II, H3K4me3, H3K27me3, and CTCF bound to Protein A-coated magnetic beads. 1 µg (RNA Pol II, H3K4me3 and IgG control) or 1.5 µg (H3K27me3 and CTCF) antibody per IP was used. Captured DNA was washed, eluted, decrosslinked, and stored at -20°C.

Epigenetic probe library

Monocytes were isolated and seeded as described in paragraph 2.2.9 and then pre-incubated with epigenetic probes at 1 µM in DMSO/PBS (final DMSO concentration in culture 0.01%) for 24 h. Probe list with targets is presented in Table 2.14. At the end of pre-incubation period, FBG-C at 1 µM or LPS O55:B5 at 100 ng/mL was added for 24 h. After that, medium was collected, cells washed, and fresh medium supplemented with 10% human serum was added. Next, cells were re-stimulated with LPS O55:B5 at 10 ng/mL for 24 h, medium was collected and MTT assay performed as described in paragraph 2.2.9. Collected media were stored at -20°C.

Table 2.14 Small molecule epigenetic probes tested. MT, methyltransferase; KDM, lysine demethylase; Kme, methyl-lysine reader; BRD, bromodomain; Rme, methyl-arginie reader.

Probe	Target	Probe	Target	Probe	Target
SGC 0946	MT: DOT1L	MS 023 dihydrochloride	MT: PRMT type 1	VinSpinIn	Kme/Rme: Spindlin family
GSK J4	KDM: JMJD3/UTX	NVS-CECR2-1	BRD: CECR2	BAY-850	BRD: ATAD2A
UNC 1215	KME: L3MBTL3	BAY 299	BRD: BRPF2/TAF1	GSK4027	BRD: PCAF/GCN5
SGC-CBP30	BRD: CREBBP/EP300	TP 472	BRD: BRD9/7	GSK484	PAD4
I-CBP 112	BRD: CREBBP/EP300	TP 064	MT: PRMT4	GSK8814	BRD: ATAD2/2B
(R)-PFI 2 hydrochloride	MT: SETD7	GSK 591 dihydrochloride	MT: PRMT5	LLY-507	MT: SMYD2
UNC 1999	MT: EZH2/H1	BAY 598	MT: SMYD2	PFI-4	BRD: BRPF1B
PFI 3	BRD: SMARCA2/4	A 395	KME: EED	SGC-iMLLT1	BRD: YEATS domain
UNC 0642	MT: G9a/GLP	GSK 343	MT: EZH2	WM-1119	KAT6A
A 366	MT: G9a/GLP	A 196	MT: SUV420H1/H2	NVS-MLLT1	BRD: YEATS domain
BAZ2-ICR	BRD: BAZ2A/2B	GSK 6853	BRD: BRPF1B	SGC6870	MT: PRMT6
OICR 9429	WDR5	L Moses dihydrochloride	BRD: PCAF/GCN5	UNC6934	Kme: NSD2-PWWP1
OF 1	BRD: BRPF1/2/3	BAY 6035	MT: SMYD3	GSK-J1	KDM: JmjD3
GSK LSD 1 dihydrochloride	KDM: LSD1	GSK 864	IDH1 mutant	IOX2	HIF PHD
SGC 707	MT: PRMT3	LLY 283	MT: PRMT5	IOX1	2OG oxygenase
NI 57	BRD: BRPF1/2/3	SGC 3027	MT: PRMT7	PFI-1	BRD: BET family
BI 9564	BRD: BRD9/7	MRK 740	MT: PRDM9	UNC0638	MT: G9a/GLP
I-BRD9	BRD: BRD9	BI 9321	Kme: NSD3-PWWP1	NVS-BPTF-1	BRD: BPTF
GSK 2801	BRD: BAZ2A/2B	LP99	BRD: BRD9/7		
MS049 oxalate salt	MT: PRMT4/6	TP238	BRD: CECR2/BPTF		

2.2.12 RA samples

Human subjects

Whole blood was obtained from 8 patients diagnosed with RA recruited for the Birmingham Early Arthritis Cohort (BEACON) study. Participants recruited were treatment naïve, or treated with hydroxychloroquine, methotrexate, or both. None of the subjects were receiving biologic disease modifying drugs. The participants' details are presented in Table 2.15. Samples were obtained with written, informed consent and approval from the University of Birmingham Local Ethical Review Committee in compliance with the Declaration of Helsinki.

Table 2.15 Details of study participants suffering from RA. F, female; M, male; HCQ, hydroxychloroquine; MTX, methotrexate.

Donor no	Age [years]	Gender	Disease duration [weeks]	Treatment
RA 1	73	F	6.7	None
RA 2	81	F	30.2	None
RA 3	69	F	187.6	None
RA 4	41	F	266.7	HCQ
RA 5	50	M	324.5	MTX + HCQ
RA 6	54	F	31.5	None
RA 7	58	F	318.5	MTX
RA 8	72	M	466.3	HCQ

Control blood obtained from 6 healthy volunteers was purchased from Cambridge Bioscience. Healthy participants' details are presented in Table 2.16.

All whole blood samples used in this study were collected into EDTA-coated tubes and transported in ambient conditions.

Table 2.16 Details of healthy control participants.
F, female.

Donor no	Age [years]	Gender
HC 1	60	F
HC 2	51	F
HC 3	57	F
HC 4	52	F
HC 5	52	F
HC 6	59	F

Monocyte isolation and stimulation

Monocytes were isolated from whole blood, stimulated, and cytokine secretion in culture media was analysed as described in paragraph 2.2.9.

2.2.13 Statistics

Data analysis was performed using GraphPad Prism software. Multiple group datasets were analysed by one-way analysis of variance (ANOVA), followed by Dunnett multiple comparisons tests. Two-tailed paired T-test was used for comparisons involving only two groups. *In vivo* data was analysed by a Mann-Whitney non-parametric test. Two-way ANOVA and Sidak multiple comparisons testing was used to analyse data from the citrullination experiment. Patient samples and healthy controls data was analysed using two-tailed unpaired T-test. P values lower than 0.05 were considered significant.

3

Fibrinogen-related proteins (FRePs) as novel TLR4 activators

Contents

3.1 Introduction 103

3.2 Results 104

3.2.1 Amino acid sequence analysis of the 24 human FRePs 104

3.2.2 Structural analysis of the 24 human FRePs 110

3.2.3 FBG domain cloning, expression and purification 115

3.2.4 FBG domain activity *in vitro* 118

3.2.5 FBG domain binding to TLR4 122

3.2.6 FBG domain activity *in vivo* 123

3.3 Discussion 125

3.3.1 *In silico* analysis of human FRePs 125

3.3.2 Recombinant protein preparation 129

3.3.3 Activity in human macrophages 131

3.3.4 Binding to TLR4 135

3.3.5 Induction of inflammation *in vivo* 137

3.3.6 Conclusions 139

3.1 Introduction

Previous work on the tenascin family of proteins by Dr Lorena Zuliani-Alvarez revealed that the capability of tenascin-C to bind to and activate TLR4 is conferred by three sites in loops 5, 7 and 10 of the C-terminal FBG domain [283]. Amongst these sites a linear epitope comprising several cationic residues in loop 5 (KTRYKLK) was essential for TLR4 activation. The aim of the first part of my project was to examine if these three sites are conserved in other FBG domain-containing proteins and identify novel TLR4 activators.

In humans there are 24 different proteins that contain an FBG domain, collectively called fibrinogen-related proteins (FRePs). I analysed the amino acid sequences of the FBG domains from all human FRePs and discovered little conservation between loops 5, 7 and 10. Moreover, I observed that the linear KTRYKLK TLR4 binding epitope in loop 5 is an exclusive attribute of tenascin family proteins. However, I also found that these loop 5 residues contributed to a distinct positively charged ridge exposed on the surface of the FBG domain of tenascin-C. I identified this sequence feature in 13 of the 24 human FRePs and predicted that it constitutes a common structural TLR4-binding epitope. To interrogate my hypothesis, I chose FBG domains from 7 different FRePs, which I cloned, expressed and purified, and then used to examine TLR4 activation *in vitro* and *in vivo*. I demonstrated that recombinant FBG domains possessing the cationic ridge bind to TLR4 in a solid phase binding assay, induce TLR4-dependent pro-inflammatory cytokine release in primary human macrophages and stimulate inflammation *in vivo*. Thus, I discovered a structural TLR4-binding epitope universal for FBG domain-containing proteins, which enabled me to identify 11 putative novel endogenous TLR4 activators and experimentally validate 6 of them.

3.2 Results

3.2.1 Amino acid sequence analysis of the 24 human FRePs

FRePs are a group of molecules comprising members of different protein families including tenascins, angiopoietins, angiopoietin-like proteins, fibrinogens and ficolins, as well as fibrinogen C domain-containing protein 1, fibrinogen-like protein 1, fibroleukin and microfibril-associated protein 4. FRePs from different families exhibit distinct domain organisations (Fig. 3.1) and execute diverse functions. For example fibrinogens play an important role in blood coagulation [284], ficolins activate lectin complement pathway [285], and angiopoietins are growth factors involved in angiogenesis [286]. The defining characteristic of FRePs is the possession of a C-terminal FBG domain. These domains exhibit 30-40% sequence identity compared to the fibrinogen ɣ chain (Table 3.1) [282].

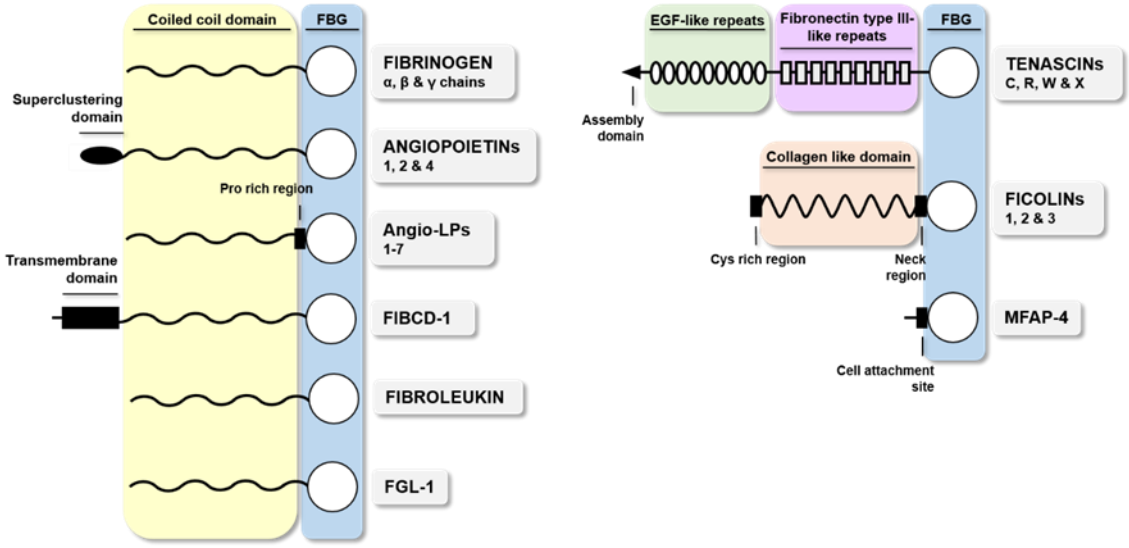


Figure 3.1 Simplified domain organization of human fibrinogen-related proteins (FRePs). The 24 human FRePs comprise tenascins, angiopoietins, angiopoietin-like proteins (Angio-LPs), fibrinogens and ficolins, as well as fibrinogen C domain-containing protein 1 (FIBCD-1), fibrinogen-like protein 1 (FGL-1), fibroleukin and microfibril-associated protein 4 (MFAP-4). FRePs from different protein families possess a diverse range of N-terminal sequences, but share a common FBG domain at the C-terminus of the protein.

Table 3.1 FBG domain sequence identity in human FRePs. Average sequence identity of FBG domains from FReP families in comparison to fibrinogen ɣ chain [282]. FIBCD-1, fibrinogen C domain-containing protein-1.

FAMILY	SEQUENCE IDENTITY [%]
Tenascins	31.6
Angiopoietins	37.4
Angiopoietin-like proteins	36.8
FIBCD-1	38.4
Fibroleukin	38.7
Ficolins	39.3

Fibrinogen was the first FReP implicated as a TLR4 ligand [135], although in this study the exact domain of this large molecule involved in driving TLR4 activation was not identified. A study of tenascin-C was the first to reveal the FBG domain as responsible for activation of TLR4 [136]. Further study of tenascin-C, -R, -W and -X by Dr Lorena Zuliani-Alvarez showed that among the family members tenascin-R and tenascin-W, but not tenascin-X, are also capable of activating TLR4. Using comparative sequence analysis combined with protein engineering, Dr Zuliani-Alvarez pinpointed 3 distinct sites in the FBG domain contributing to interaction of tenascin-C with the receptor. These comprised a positively charged epitope (KTRYKLK) in loop 5, a triad of polar (D and N) and hydrophobic (I) residues in loop 7 and an extended cationic loop 10 (Fig. 3.2 and Fig. 3.3). While all 3 sites facilitate binding to TLR4, the loop 5 epitope is crucial for the activation of the receptor [283].

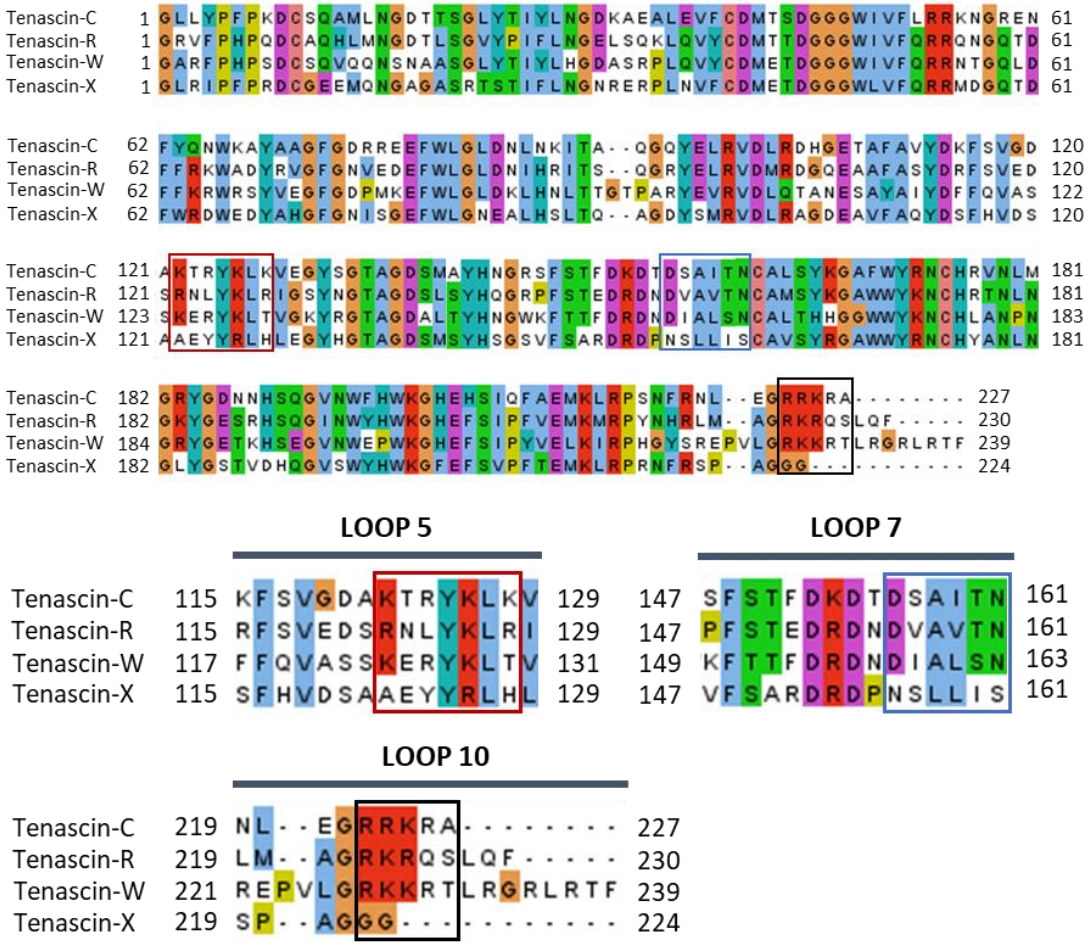


Figure 3.2 TLR4-binding epitope identified in the tenascin family. Multiple sequence alignment of the FBG domains from tenascin family members. Cationic loop 5 epitope (KTRYKLK) is highlighted in red box, loop 7 epitope (polar: D and N, and hydrophobic: I residues) – in blue box and cationic loop 10 epitope (RRKRA) – in black box. The alignment was coloured according to the Clustal colour scheme. Light blue - hydrophobic, red - positively charged, green - polar, pink - conserved column of cysteine, violet - negatively charged, orange - glycine, yellow - proline, cyan - aromatics.

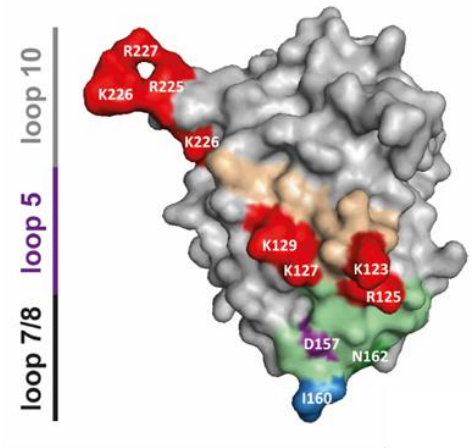


Figure 3.3 Localization of the TLR4-binding epitope in tenascin-C. Homology model of the FBG domain of tenascin-C, built using structure of fibrinogen γ (PDB ID: 1FID) as a template, highlighting the TLR4-binding epitope in loop 5, loop 7, and loop 10. The sequence of loop 5 is depicted in pale orange, within which positively charged residues are coloured red. Positive residues in the C-terminal loop 10 are also coloured red. The sequence of loop 7 is presented in pale green, within which the triad of polar and hydrophobic residues are coloured purple, dark green, and blue. Image adapted from Zuliani-Alvarez *et al.*, Nat Commun 2017.

To investigate if the TLR4 activation epitope identified in the tenascin family is also present in FBG domains from other FRePs, their amino acid sequences were compared. Multiple sequence alignment of FBG domains from all 24 human FRePs (accession numbers are presented in Table 3.2) revealed limited sequence conservation in loops 5, 7 and 10 (Fig. 3.4). The cationic loop 5 epitope and the extended cationic loop 10 C-terminus were found exclusively in tenascins-C, -R and -W, whereas the polar and hydrophobic residues in loop 7 were also present in three other FRePs, angiopoietin-like protein 1 (ALP-1), fibrinogen β chain (FIB-B) and microfibril-associated glycoprotein 4 (MFAP-4). Altogether, this analysis demonstrated that the previously identified TLR4 binding epitope is specific for tenascin family members.

Table 3.2 Accession numbers and used abbreviations of 24 human FRePs.

Protein	Abbrev.	Accession no
Tenascin-C	FBG-C	P24821
Tenascin-R	FBG-R	Q92752
Tenascin-W	FBG-W	Q9UQP3
Tenascin-X	FBG-X	P22105
Angiopoietin-1	ANG-1	Q15389
Angiopoietin-2	ANG-2	O15123
Angiopoietin-4	ANG-4	Q9Y264
Angiopoietin-like protein 1	ALP-1	O95841
Angiopoietin-like protein 2	ALP-2	Q9UKU9
Angiopoietin-like protein 3	ALP-3	Q9Y5C1
Angiopoietin-like protein 4	ALP-4	Q9BY76
Angiopoietin-like protein 5	ALP-5	Q86XS5
Angiopoietin-like protein 6	ALP-6	Q8NI99
Angiopoietin-like protein 7	ALP-7	O43827
Fibrinogen C domain-containing protein 1	FIBCD-1	Q8N539
Fibrinogen α chain	FIB-A	P02671
Fibrinogen β chain	FIB-B	P02675
Fibrinogen γ chain	FIB-G	P02679
Fibrinogen-like protein 1	FGL-1	Q08830
Fibroleukin (Fibrinogen-like protein 2)	FGL-2	Q14314
Ficolin-1	FIC-1	O00602
Ficolin-2	FIC-2	Q15485
Ficolin-3	FIC-3	O75636
Microfibril-associated protein 4	MFAP-4	P55083

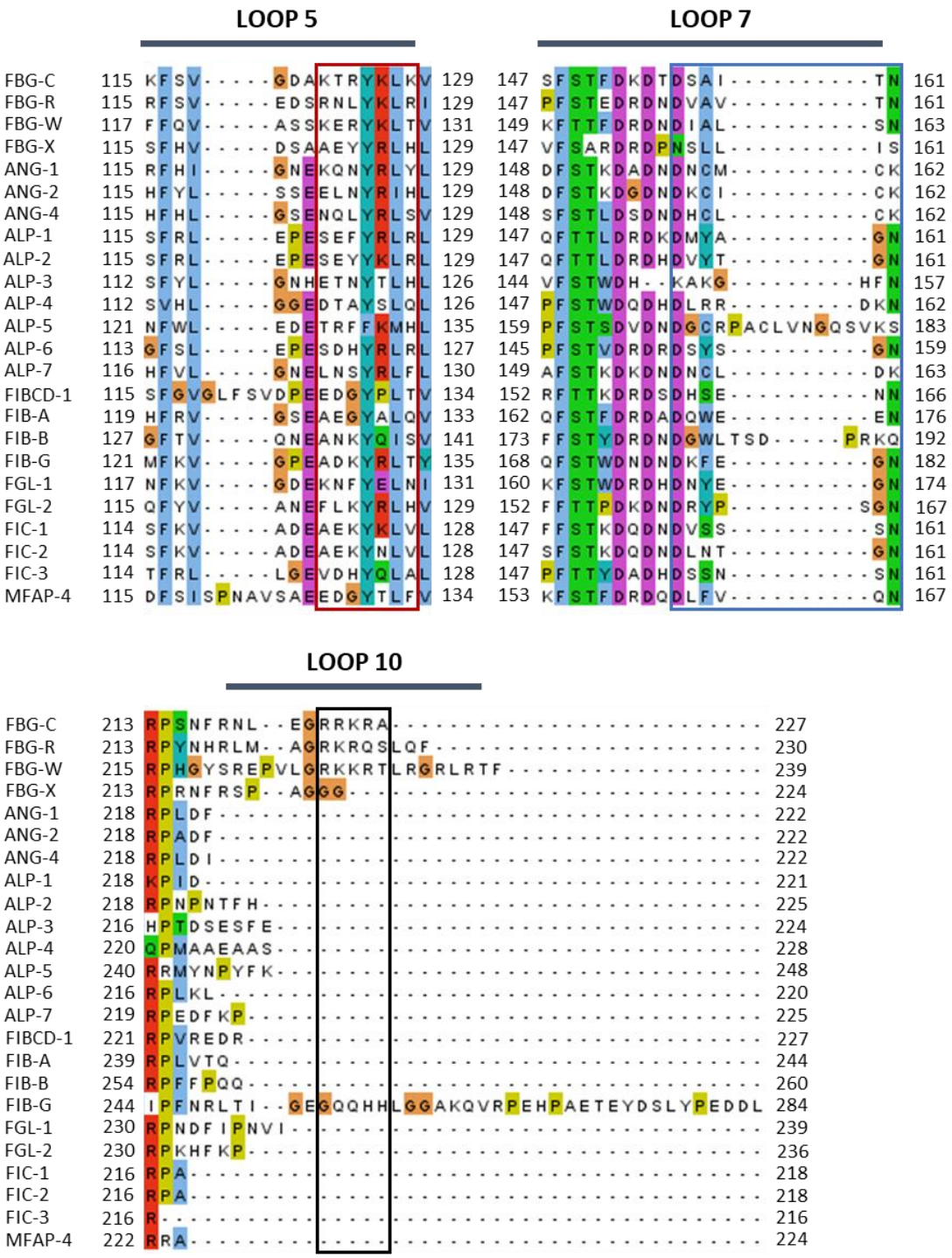


Figure 3.4 The linear epitopes of loops 5, 7 and 10 of FBG-C are not conserved in human FRePs. Multiple sequence alignment of FBG domains from 24 human FRePs was performed. Sequences aligned with the tenascin cationic loop 5 epitope (KTRYKL) are highlighted in red box, loop 7 epitope (polar: D and N, and hydrophobic: I residues) – in blue box and cationic loop 10 epitope (RRKRA) – in black box. The alignment was coloured according to the Clustal colour scheme. Light blue - hydrophobic, red - positively charged, green - polar, pink - conserved column of cysteine, violet - negatively charged, orange - glycine, yellow - proline, cyan - aromatics.

3.2.2 Structural analysis of the 24 human FRePs

Protein-protein interactions often involve not merely linear, but also conformational epitopes, which are formed from multiple segments of residues non-adjacent in the polypeptide chain. Therefore mapping protein binding interfaces often involves an evaluation of the 3D structure space. To look for common structural features between tenascins and other FRePs, tertiary structures of the FBG domains were analysed. Where a crystal structure of a protein was not available, a homology model was constructed based on the crystal structure of the fibrinogen ɤ chain (PDB ID: 1FID) (PDB IDs of all crystal structures used in the process of the analysis are listed in Table 2.2).

All FBG domains from the 24 human FRePs exhibited the characteristic FBG domain fold described initially in the fibrinogen ɤ chain [287], which comprises 3 distinct subdomains: A, B and P (Fig. 3.5). At the N-terminus, approximately 50 residues form subdomain A, consisting of short antiparallel twisted β sheets and a short α-helix. The central subdomain B is made predominantly of a multi-stranded antiparallel β sheet and 2-3 α-helices connected by loops. Residues located at the very C-terminus of the protein contribute to one strand of the subdomain B β sheet. Subdomain P is the least structurally organised and is composed mostly of loops.

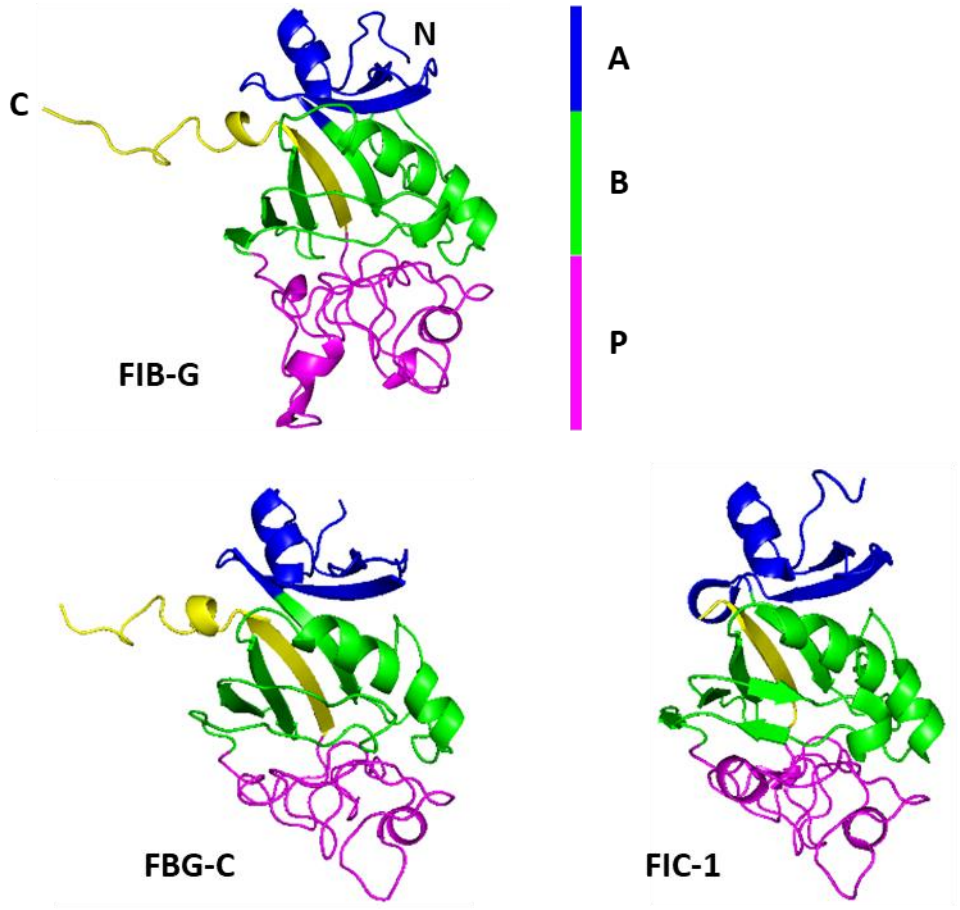


Figure 3.5 Subdomain organization of the FBG domain. Subdomain organization of the FBG domain from 3 human FRePs, FIB-G (PDB ID: 1FID), FIC-1 (PDB ID: 2JHM) and FBG-C (model built using 1FID as template). The FBG domain consists of 3 distinct subdomains: A (in blue), B (in green and yellow) and P (in magenta). Subdomain A is located at the N-terminus (N) of the domain and is the smallest; subdomain B is central and is made up from residues in the middle (in green) and also at the C-terminus (in yellow) of the domain; subdomain P has the least regular structural organization.

Electrostatic interactions between proteins are crucial for molecular recognition and assembly of biologically active complexes [288]. Therefore, surface charge distribution on the FBG molecules was examined next. The KTYRKLK epitope in loop 5 of tenascin-C, -R and –W, family members that activate TLR4, was identified to form a cationic ridge on the surface of the protein, together with 2-3 other positively charged residues located in neighbouring loops 6 and 7 of these FBG domains (Fig. 3.6). In the FBG domain of tenascin-X, the family member that does not activate TLR4, this region was relatively sparse in positive charge, comprising only 2 cationic residues. In some of

the other human FRePs, non-contiguous positively charged residues derived from loops 5, 6 and 7 of the FBG domain sequence formed a similar cationic ridge to the TLR4-activating tenascins. In other FRePs no or few positive charges were observed in this region, resembling tenascin-X. Given previous data [283] showing that a minimum of 3 cationic residues in the loop 5 epitope is required for TLR4 activation, I hypothesised that any FReP with 3 or more positive charges in this cationic ridge would activate TLR4, and that any FReP with 2 or less positive charges in this ridge would not. Using this categorization, 10 putative TLR4 agonists and 10 putative non-binders were revealed (Table 3.3). Interestingly, the predicted TLR4 activation epitope was not present consistently within all studied protein families. For example, cationic ridge could be observed in angiopoietin-1 and angiopoietin-2, but not angiopoietin-4. This could suggest that, like tenascins, members of a single FReP family may differ distinctly in their capabilities to activate immune responses.

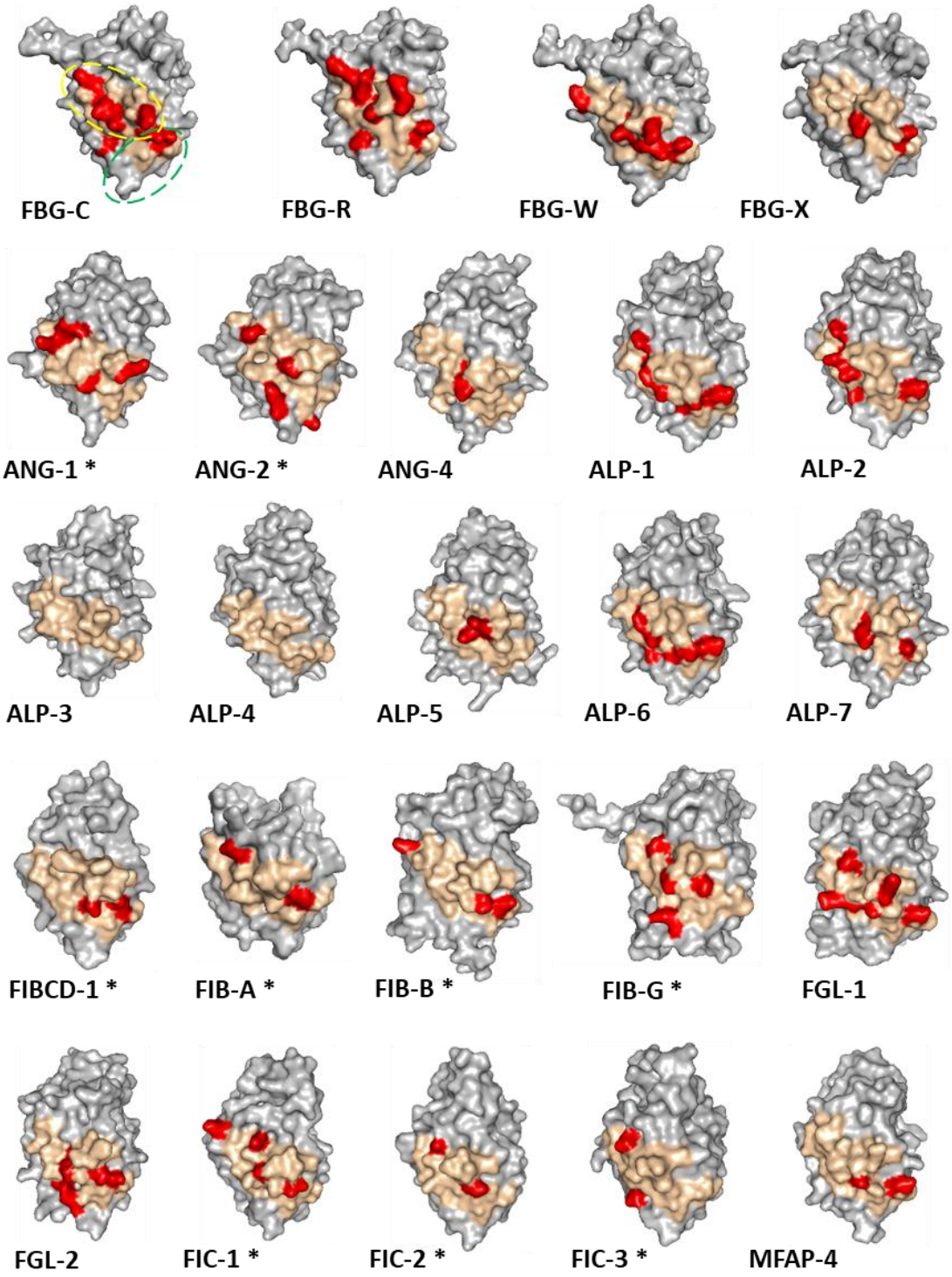


Figure 3.6 Conserved cationic ridge in fibrinogen related proteins (FRePs). The cationic ridge present in FBG-C is conserved in a subset of FRePs which possess a comparable conformational epitope comprised of residues from loops 5, 6 and 7. Crystal structures (*) or homology models of the FBG domains of all human FRePs shown. The region created by residues from loops 5, 6 and 7 on the surface of each FBG domain is shown in pale orange, within which positively charged residues are coloured red. In FBG-C, localization of loop 5 is marked with yellow dotted line, and loop 7 with green dotted line.

Table 3.3 Conservation of epitopes involved in TLR4 activation in human FRePs. Comparison of the structures (*crystal structure available) or homology models of the FBG domains from the 24 human FRePs. Cationic ridge: the number of positively charged residues within the region exposed on the surface of the FBG domain around loops 5, 6 and 7. Loop 7: the presence (+) or absence (-) of a triad of polar and hydrophobic residues. Cationic C-terminal: the presence (+) or absence (-) of an extended loop 10 containing a cluster of positive charges. FBG domains were designated potential TLR4 activators if they possessed a cationic ridge comprising 3 or more positively charged residues. CONFIRMED, ability to activate TLR4 has been experimentally confirmed previously [283].

	Protein	Cationic ridge	Loop 7	Cationic C-terminal	Predicted TLR4 activator
	FBG-C	7	+	+	YES (CONFIRMED)
	FBG-R	6	+	+	YES (CONFIRMED)
	FBG-W	6	+	+	YES (CONFIRMED)
	FBG-X	2	-	-	NO (CONFIRMED)
*	**ANG-1**	4	-	-	YES
*	**ANG-2**	4	-	-	YES
	ANG-4	1	-	-	NO
	ALP-1	5	+	-	YES
	ALP-2	5	-	-	YES
*	**ALP-3**	0	-	-	NO
*	**ALP-4**	0	-	-	NO
	ALP-5	2	-	-	NO
	ALP-6	5	-	-	YES
	ALP-7	2	-	-	NO
*	**FIBCD-1**	2	-	-	NO
*	**FIB-A**	2	-	-	NO
*	**FIB-B**	3	+	-	YES
*	**FIB-G**	4	-	-	YES
	FGL-1	5	-	-	YES
	FGL-2	5	-	-	YES
*	**FIC-1**	4	-	-	YES
*	**FIC-2**	2	-	-	NO
*	**FIC-3**	2	-	-	NO
	MFAP-4	2	+	-	NO

3.2.3 FBG domain cloning, expression and purification

In order to experimentally confirm that this cationic ridge is a TLR4 activation epitope, 7 FBG domains from different FRePs were selected for functional testing. FIB-G, a predicted activator, was chosen based on the literature showing that full-length fibrinogen is an established endogenous ligand of TLR4 [135, 289]. To test the predicted opposing TLR4-activation properties in closely related members of same protein families, representatives of ficolins (FIC-1, a predicted activator, and FIC-2, a predicted non-activator) and angiopoietin-like proteins (ALP-1, ALP-2 and ALP-6, predicted activators, and ALP-4, a predicted non-activator) were selected. Ficolins are a protein family with a known role in the innate immune system, capable of activating the complement pathway [285]. Thus, it was an intriguing concept to consider if FIC-1 might also trigger immune responses through activation of TLR4. The functions of angiopoietin-like proteins remain more elusive, with implications of involvement in angiogenesis, metabolism, inflammation and cancer [290]. Demonstrating an interaction with TLR4 could therefore contribute to very novel understanding of molecular pathways responsible for the observed effects of angiopoietin-like proteins.

The 7 candidate FBG domains were sub-cloned, expressed and purified as described previously for FBG-C [136, 283]. Briefly, sequences of the FBG domains were sub-cloned into expression vector incorporating an N-terminal hexa-histidine tag, and over-expressed in *E. coli*. Recombinant proteins were then purified from the inclusion body fraction in a three-step protocol using immobilized metal affinity chromatography with nickel resin (Fig. 3.7). All chromatography steps included a Triton X-114 wash in order to remove LPS contamination [291]. This unified production protocol resulted in varied yields of purified proteins (Table 3.4). Complete expression and purification

protocol is described in Chapter 2, pages 81-83. Primers used for cloning are presented in Table 2.4. Sequence details of cloned domains are described in Table 2.3.

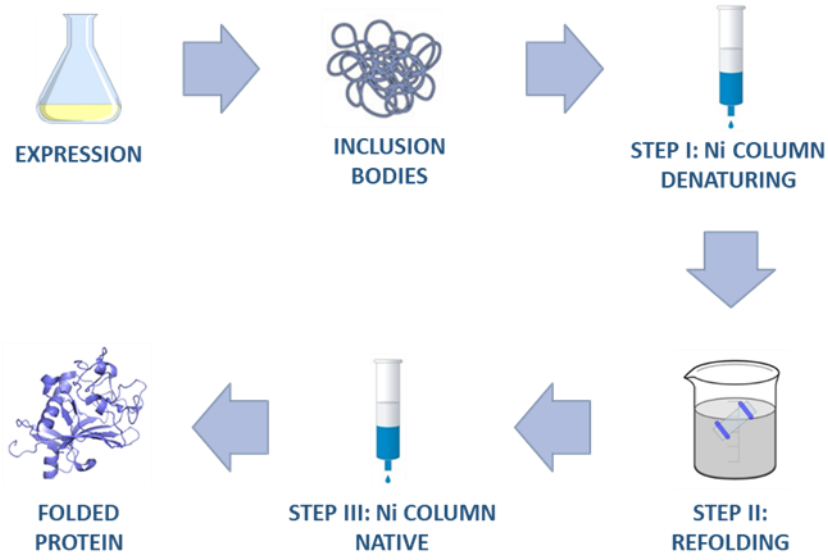


Figure 3.7 Protein purification strategy. FBG domains containing hexa-histidine tag were expressed in *E. coli* strain BL21, bacterial pellet was sonicated and inclusion body fraction (IB) was isolated by centrifugation. Next, IBs were dissolved in urea buffer and purified using nickel chromatography in denaturing conditions (STEP I). Eluted proteins were diluted and refolded by dialysis (STEP II). Finally, proteins were concentrated using nickel chromatography in native conditions (STEP III), yielding pure folded protein.

Table 3.4 Recombinant protein yields. Approximate yields of recombinant FBG domains obtained with the described 3 step purification protocol. Protein amounts were quantified with NanoDrop.

FBG DOMAIN	YIELD [mg protein/0.5 L of culture]
FBG-C	8 - 12
FIB-G	18 - 20
ALP-1	1 - 1.5
ALP-2	0.3 - 0.5
ALP-4	1 – 1.5
ALP-6	0.7 – 1
FIC-1	4 - 8
FIC-2	4 – 6.5

Prior to activity testing, quality control of purified recombinant FBG domains was performed. Protein purity was confirmed with silver-stained SDS-PAGE gels, and protein identity with western blotting using an anti-histidine tag antibody (Fig. 3.8 A, Supplementary fig. 4). Native folding of the proteins was confirmed by circular dichroism (CD) spectroscopy (Fig. 3.8 B, Supplementary fig. 5). Complex asymmetric molecules, such as proteins, interact with light beams and differentially absorb right- and left-circularly polarized light, producing distinct spectra. CD spectra are dependent on the secondary structure composition and polypeptide chain conformation, and therefore can be used to monitor protein folding. Spectra were obtained for the newly produced FBG domains (Fig. 3.8 B, green line), which were comparable to the data obtained previously for validated, active FBG-C by Dr Zuliani-Alvarez. Following thermal denaturation of the proteins this characteristic spectra could no longer be observed (Fig. 3.8 B, red line). Finally, LPS contamination was tested using a commercial endotoxin contamination testing kit. Samples typically contained less than 3 pg/mL and any fractions containing more than 10 pg/mL of endotoxin were excluded from future work.

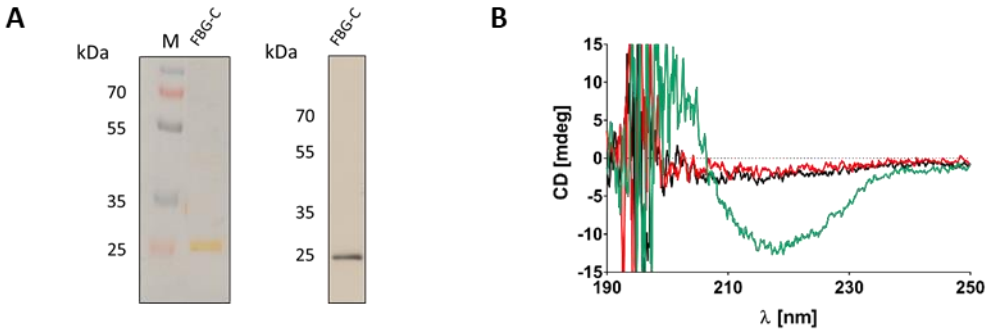


Figure 3.8 Recombinant FBG domain quality control. Example quality control of FBG-C. **A.** The purity of obtained protein was assessed by silver staining and western blotting with anti-His Tag antibody. **B.** Folding of purified proteins was assessed by circular dichroism. Folded FBG domains generate a distinct negative peak between 210 nm and 230 nm, which is no longer observed following thermal denaturation of the protein. Green line, protein sample; red line, protein sample boiled; black line, buffer.

3.2.4 FBG domain activity *in vitro*

Upon activation of TLR4 in human macrophages downstream signalling cascades are activated that result in the production of pro-inflammatory cytokines, such as IL-6, IL-8 and TNF. The induction of these cytokines in human primary macrophages has been previously used to confirm the activity of the tenascin family members [136, 283]. Here, the same method was utilised to evaluate the activity of purified recombinant FBG domains *in vitro*.

To obtain cells, peripheral blood mononuclear cells were isolated from human blood by density gradient centrifugation over ficoll and further purified by elutriation (a counterflow centrifugation technique), yielding highly enriched monocytes. Macrophages were differentiated from monocytes by culturing for 5 days with macrophage colony-stimulating factor and then stimulated with increasing concentrations of purified FBG domain proteins. Due to lower purification yields of some proteins not all could be applied at a concentration of 5 µM, hence the highest available concentration for each of the domains was used for stimulation. After 24 h of stimulation levels of IL-6, IL-8 and TNF were measured in culture medium by ELISA (Fig. 3.9). Complementary MTT assays were performed for each macrophage experiment to confirm applied stimuli did not affect cell viability.

All of the predicted TLR4 activators that were tested, FIB-G, FIC-1, ALP-1, ALP-2 and ALP-6, induced dose-dependent cytokine release. Among the two predicted non-binders, ALP-4 induced no cytokine activity, while stimulation with FIC-2 resulted in production of low levels of IL-6 and IL-8.

To demonstrate that the observed cytokine release is receptor dependent, a selective TLR4 inhibitor TAK242 was used [292]. Incubation of macrophages with

TAK242 for 6 h prior to stimulation abolished FBG domain-induced pro-inflammatory cytokine production (Fig. 3.10 A). The measured cytokine levels were not significantly reduced by a pre-treatment with an endotoxin neutralizing agent polymyxin B (PMB), indicating cytokine release is due to FBG activity and not LPS contamination (Fig. 3.10 B). Disruption of the structural fold with high temperature rendered FBG-C and FIC-1 entirely incapable of inducing cytokine production. Interestingly, FIB-G exhibited some degree of resistance towards thermal denaturation and the heat-denatured protein could induce low levels of IL-6, albeit significantly reduced in comparison to intact domain. Alongside heat denaturation, another method to validate a protein induced effect is proteolytic cleavage with proteinase K [293], which digest and fragments amino acid chains, and destroys protein structure. Hence further on this technique has been used instead to test ALP-1, ALP-2, ALP-6 and FIC-2. Protease treatment of the proteins resulted in decreased levels of IL-6 (however this was not statistically significant for ALP-2 and FIC-2). Altogether, this data shows that the structural integrity of the predicted TLR4 activators is necessary for their pro-inflammatory activity *in vitro*.

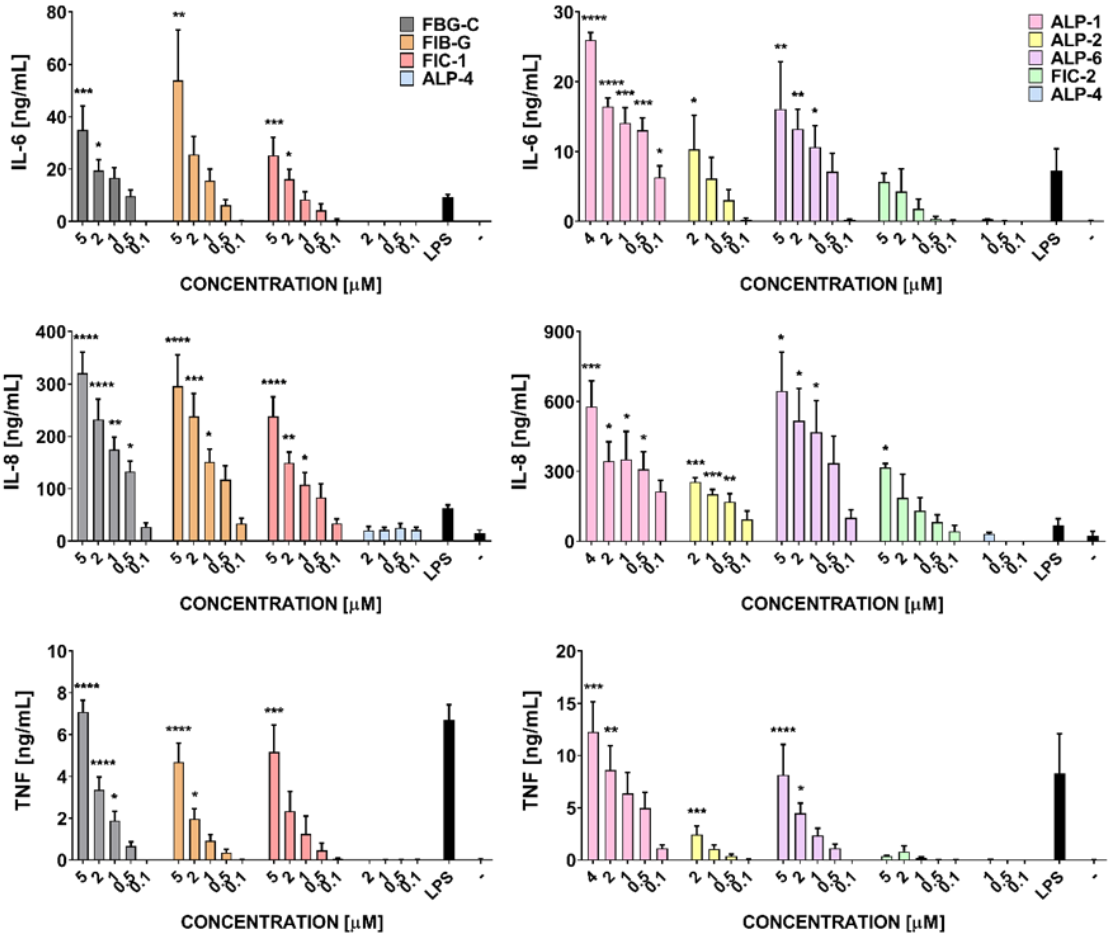


Figure 3.9 FBG domains from predicted TLR4-activating FRePs induce pro-inflammatory cytokine release. Primary human macrophages were stimulated with decreasing concentrations of FBG domains (starting at highest available concentration for each domain), LPS at 1 ng/mL or were left unstimulated (-) for 24h, and IL-6, IL-8 and TNF levels were measured by ELISA. Stimulation experiments were performed in two batches (FBG-C/FIB-G/FIC-1/ALP-4 and ALP-1/ALP-2/ALP-6/FIC-2/ALP-4), with separate groups of donors, and are presented on separate sets of graphs. Data are shown as mean ± SEM from at least 3 independent donors. Data was analysed using one-way ANOVA vs non-stimulated, *p<0.05, **p<0.01, ***p<0.001, ****p<0.0001.

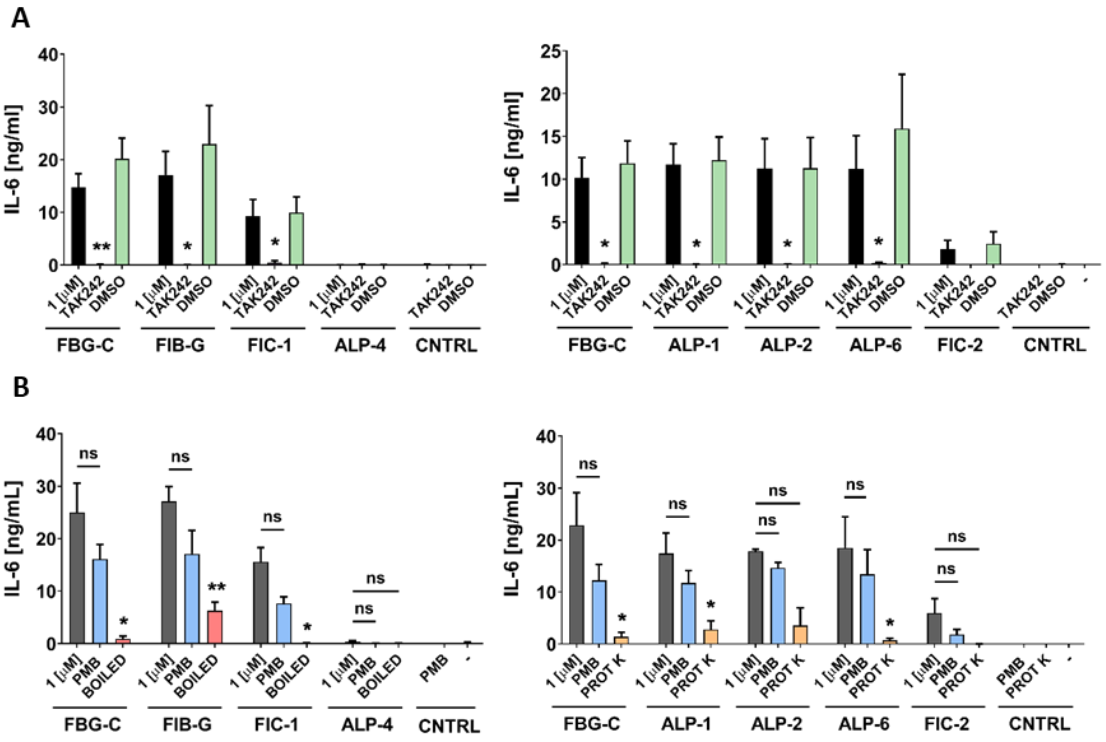


Figure 3.10 Cytokine release induced by FBG domains is TLR4-dependent and not due to LPS contamination. Primary human macrophages were stimulated with FBG domains at 1 µM for 24h. **A.** Prior to stimulation cells were incubated for 6 h with selective TLR4 inhibitor TAK-242 (TAK242), DMSO control (DMSO) or left without any inhibitor (1 [µM]). TAK-242 only (CNTRL TAK242), DMSO only (CNTRL DMSO), and unstimulated (CNTRL -) controls were included. **B.** Prior to stimulation protein samples were incubated with polymyxin B (PMB), boiled (BOILED), treated with proteinase K (PROT K) or left unprocessed (1 [µM]). Polymyxin B only (CNTRL PMB), proteinase K only (CNTRL PROT K), and unstimulated (CNTRL -) controls were included. Cytokine release was measured by ELISA. Data are shown as mean ± SEM from at least 3 independent donors. Data was analysed using paired t-test vs NO INH (A) or PROTEIN (B), *$p < 0.05$, **$p < 0.01$.

3.2.5 FBG domain binding to TLR4

The binding of FBG domains from tenascin family members to TLR4 has been previously assessed with the use of a solid phase binding assay [283]. FBG domains from selected FRePs were examined using the same method, performed by Dr Lorena Zuliani-Alvarez. Briefly, recombinant FBG domains bound to ELISA plates were incubated with the extracellular domain of TLR4. Following washing of unbound receptor, bound TLR4 was detected with the use of a monoclonal anti-TLR4 antibody. The predicted TLR4 agonists FIB-G and FIC-1 could bind TLR4, albeit with lower affinity than FBG-C. No binding was observed for predicted non-binder ALP-4 and non-binding tenascin, tenascin-X, which was used as a negative control (Fig. 3.11).

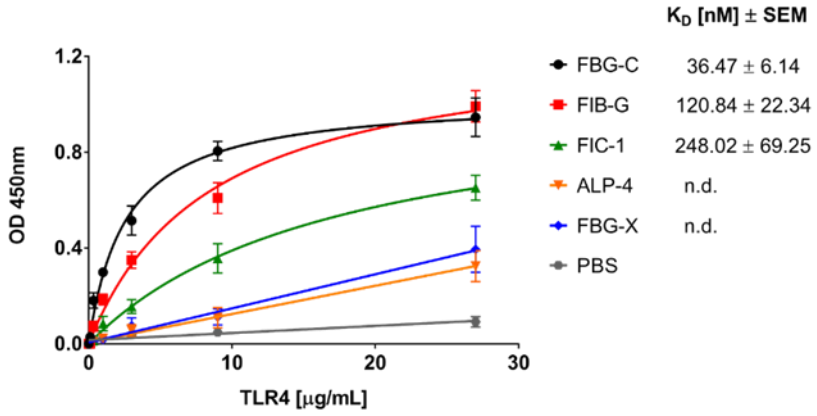


Figure 3.11 FIB-G and FIC-1 bind to TLR4. Binding to TLR4 was measured in a solid phase binding assay. 96 well plates were coated with 1 µg/mL of FBG-C, FBG-X, FIB-G, FIC-1 and ALP-4, or PBS, and incubated with increasing doses of TLR4. TLR4 was then detected using a monoclonal anti-TLR4 antibody. Curves were fitted in GraphPad Prism using one binding site hyperbola equation. Data are shown as mean ± SEM from 3 independent experiments. N.d., not determined.

3.2.6 FBG domain activity *in vivo*

FBG-C has previously been shown to induce synovial inflammation following intra-articular injection in mice [136]. To determine whether other recombinant FRePs also drive inflammation *in vivo*, 1 µg of FIB-G, FIC-1 or ALP-4 was injected into mouse knee joint by Dr Fiona McCann and Dr Claire Deligne. FBG-C was used as a positive control and a mutant of FBG-C, lacking the cationic residues in the loop 5 epitope and thus not able to activate TLR4 [283], was used as a negative control. Injection of an equal volume of PBS buffer alone was also performed to exclude potential effects caused by the procedure itself. As described previously for FBG-C [136], mice were culled 3 days after injection, knee joints harvested and histological analysis was performed by Dr Claire Deligne. Predicted binders FIB-G and FIC-1 induced immune cell infiltration, cartilage destruction and bone erosion whilst ALP-4 did not (Fig. 3.12).

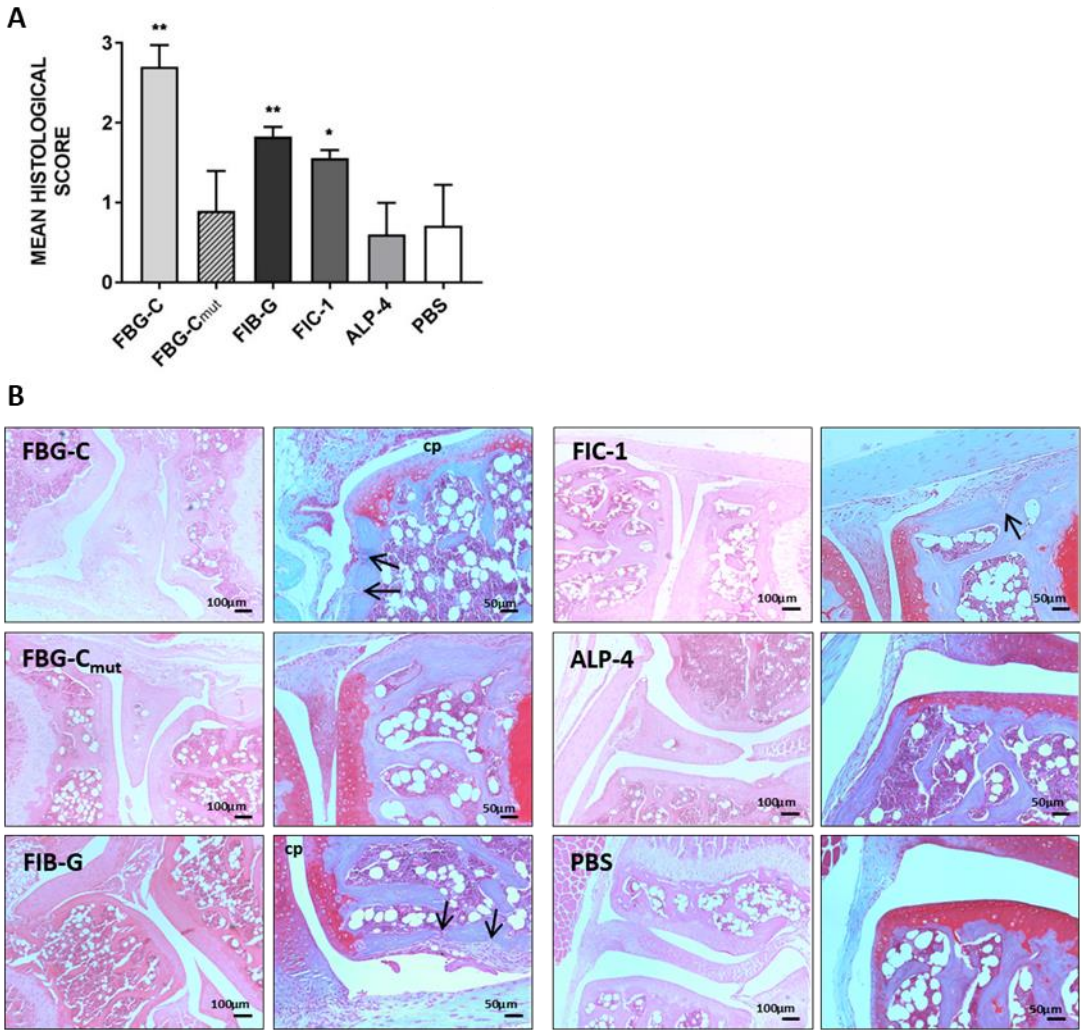


Figure 3.12 FBG domains of FIB-G and FIC-1 induce inflammation *in vivo*. Synovial inflammation was assessed 3 days post injection of each protein (1 µg) or PBS alone into the knees of DBA-1 mice. **A.** The histological score was calculated as the mean of seven sections from each knee joint per mouse. n = 5 mice per group except for FIC-1 (n = 4). Mann–Whitney non-parametric test vs. PBS, *$p < 0.05$, **$p < 0.01$. **B.** Images show representative sections stained by haematoxylin and eosin (left panels) or safranin-O (right panels). Mice injected with FBG-C, FIB-G, and FIC-1 exhibit cell infiltration into a thickened synovial lining layer, cellular invasion into the subchondral bone (arrows indicate bone erosion) and loss of articular cartilage proteoglycan (cp), pathological features not observed in mice injected with FBG-C mutant (FBG-C_{mut}, FBG-C with mutation removing the loop 5 binding epitope) or ALP-4. Scale bar left panels: 100 µM, right panels: 50 µM.

3.3 Discussion

In this chapter the FBG domains from all 24 human FRePs were analysed *in silico* in the search for common motifs that could be responsible for conferring the ability to activate TLR4. A structural feature, called the cationic ridge, shared by many FRePs, was identified as a potential universal TLR4 binding epitope. Based on the presence of this ridge a subset of novel endogenous TLR4 activators was predicted, and the ability of six of these candidates to activate TLR4 was confirmed experimentally by investigating receptor binding, activation *in vitro* and induction of inflammation *in vivo*.

3.3.1 *In silico* analysis of human FRePs

In this project, simple *in silico* sequence-based methods were used that allowed for the analysis and prediction of protein structure, interaction and functions. Those methods should be treated with caution due to their approximate nature and need to be confirmed experimentally. However, they can provide initial suggestions and enable the analysis of larger datasets that might be difficult to process using traditional *in vitro* techniques due to resources and time constraints.

Firstly, to analyse the amino acid sequences of all human FRePs, a multiple sequence alignment was performed using Clustal Omega [294]. The generated alignment demonstrated that the extended C-terminal is exclusive to the tenascins and the critical loop 5 epitope possesses no more than 2 cationic residues in non-tenascin FRePs, which was shown previously to be insufficient to trigger receptor activation [283]. The strongest conservation could be observed in the loop 7 epitope, with the aspartic acid conserved in 19 out of 20 non-tenascin FRePs, the asparagine in 14 (although in 2 cases it is substituted by serine or glutamine, also polar residues) and a hydrophobic (isoleucine or similar) in 9. The alignment also exposed a several residue long insertion in the loop 7 epitope of ALP-5 and FIB-B. Altogether, it proved the previously discovered linear TLR4 binding

epitope as a whole cannot be found beyond the tenascin family. Based on this data, no other FReP could be anticipated to activate TLR4. However, an idea was conceived that perhaps a common feature responsible for receptor binding and activation can be found in FRePs on a structural level.

Due to the fact that a limited number of FBG domains from FRePs had crystal structures solved at the time this analysis was prepared, it was necessary to perform homology modelling. This was executed using SWISS-MODEL [295], using FIB-G structure (PDB ID: 1FID) as template. Investigation of structural organization of tenascin family members and other FRePs led to discovery of a cationic ridge that was hypothesized to be a universal structural TLR4-binding epitope. Based on the comparison of the charge distribution within this region in both binding and non-binding members of the tenascin family, and FBG-C mutagenesis data showing at least 3 cationic residues are necessary in loop 5 epitope for receptor activation [283], a decision was made to label all FRePs with 3 or more lysines/arginines located in loops 5, 6 and 7 as possessing the cationic ridge. Application of this cut off led to prediction of 10 prospective endogenous TLR4 ligands, all but FIB-G being entirely novel and not previously linked to this receptor.

Following the completion of the modelling, more crystal structures of FBG domains were published: FBG-C (PDB ID: 6QNV), ALP-3 (6EUA), ALP-4 (6EUB) (Fig. 3.13). I have also collaborated with Dr Jesse Coker (DPhil student of Midwood, Marsden and Yue) on the project that resulted in the determination of crystal structures for ALP-2 (6Y41) and ALP-6 (6Y43) [296]. The crystal structure of FBG-C, a confirmed TLR4 activator, demonstrated the modelled charge distribution was accurate. What is more, it showed that arginine 147 is surface-exposed, and thus potentially accessible to form interactions. Likewise, the location of cationic residues within the ridge region of

ALP-2 and ALP-6 structures is in accordance with the models. In the structures of ALP-3 and ALP-4 no additional positively charged residues could be assigned to the cationic ridge. Altogether, the newly published crystal structures corroborate entirely the accuracy of the described cationic ridge.

Since the discovery of the first member of ALP family, ALP-1, nearly two decades ago [297], a growing body of evidence established the role of ALPs in angiogenesis, inflammation, carcinogenesis and cancer metastasis [290]. Additionally, ALP-3, ALP-4, ALP-5, and ALP-8, the only member of the ALP family entirely devoid of the FBG domain, were also shown to be involved in the regulation of lipid metabolism. Interestingly, it appears that the observed cationic ridge divergence in the ALP family seem to overlap the division in protein functionality, with the predicted TLR4 non-binders acting as not only angiogenic, but also metabolic regulators, with a potential as therapeutic targets in lipid disorders [298].

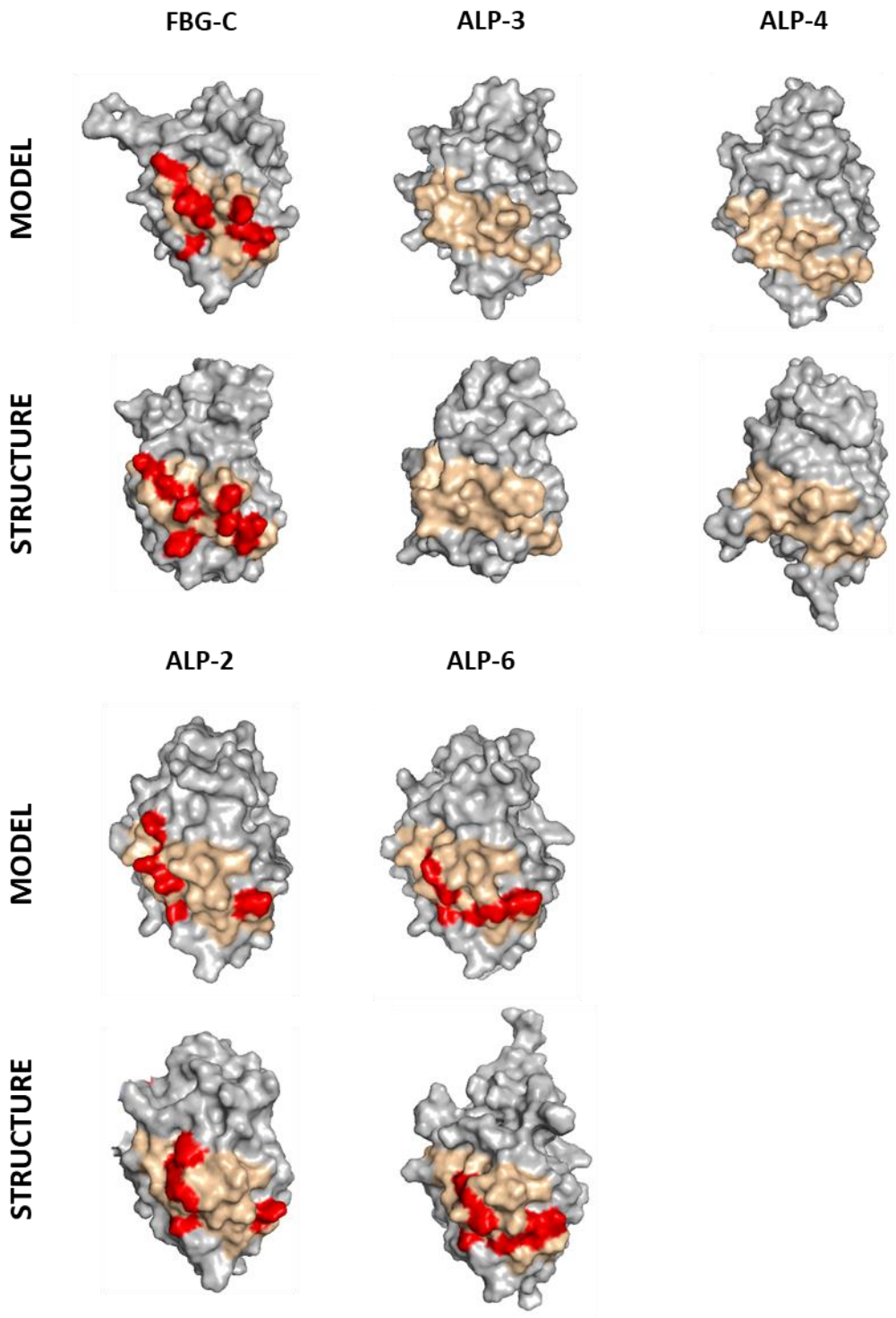


Figure 3.13 Recently published crystal structures of FBG domains from TN-C, ALP-3, ALP-4, ALP-2 and ALP-6 confirm structural accuracy of modelled cationic ridge. MODEL, structural models build on the crystal structure of the fibrinogen γ chain (PDB ID: 1FID). **STRUCTURE**, published crystal structures. The cationic ridge region created by residues from loops 5, 6 and 7 on the surface of each FBG domain is shown in pale orange, within which positively charged residues are coloured red. In the structure of FBG-C C-terminal loop 10 is missing due to the use of a truncated construct to produce protein for crystalization.

3.3.2 Recombinant protein preparation

Despite structural similarities and use of consistent preparation protocols, the protein yields differed substantially between the seven FBG domains. A high degree of variability could be observed on three different stages of protein preparation: expression, binding to nickel resin and refolding by dialysis. While the exact nature of poor over-expression of human recombinant proteins might be difficult to establish, a possible explanations include the toxicity of the produced protein to the bacterial expression strain or codon usage bias. Low binding of the tagged protein to the resin can be caused by formation of secondary structures resistant to urea denaturation that prevent exposition of the tag to interact with the resin. Finally, the composition and pH of buffer used during the refolding step might not universally fit produced FBG domains that greatly vary in isoelectric point, leading to instability and precipitation. However, due to the fact that obtained amounts of protein were enough for activity/binding testing, a decision was consciously made to accept low yields, provided that final product was comparably pure and correctly folded across the different samples, for the initial screen of FBG proteins. The procedure could be optimized for individual FBG domains in the future that might be needed in greater quantities for further investigation.

A significant difficulty during the production of recombinant proteins is the possibility of contamination with LPS, a potent virulence factor. This issue is particularly problematic if the proteins are to be used for the study of the immune responses, in live cell assays or *in vivo*. Thus, it is crucial that sufficient care is taken to remove the initial contamination and limit subsequent exposure to LPS (e.g. through contaminated labware or buffers). During the purification of FBG domains for this study successful removal of endotoxin was performed with the use of Triton X-114, a detergent capable of facilitating the dissociation of LPS molecules from the protein [291]. Triton X-114 treatment was

always followed by an extensive wash with the purification buffer, as this detergent can be toxic to the cells in culture [299]. The employed method allowed consistently clean protein samples, with LPS levels below 10 pg/mL. To further exclude potential contamination during sample storage and handling, FBG domains were pre-incubated with polymyxin B, an LPS neutralizing agent, prior to stimulation.

3.3.3 Activity in human macrophages

The activity of the selected candidates was tested using primary human macrophages differentiated from blood monocytes with M-CSF. All of the 5 predicted TLR4 activators: FIB-G, FIC-1, ALP-1, ALP-2 and ALP-6 induced dose-dependent production of pro-inflammatory cytokines IL6, IL-8 and TNF, while one of the predicted non-activators, ALP-4, had no effect on cytokine release. This data supports the hypothesis that presence of the cationic ridge is necessary for the FBG domain to activate immune response *in vitro*. However, contrary to the predictions, the other anticipated non-activator, FIC-2, was observed to induce release of IL-6 and IL-8, but not TNF (Fig. 3.9). In search of an explanation for the weak response induced by a predicted non-binder, the charge distribution on the surface of FIC-2 molecule was investigated once more, revealing a positively charged residue adjacent to the cationic ridge region (Fig. 3.14). It is possible that the detected arginine 183, collectively with two originally identified lysines (186 and 193), is sufficient to allow for some form of interaction with the receptor. A question arises whether activation of TLR4 by endogenous triggers is a discrete event, with clear on and off receptor states, or rather a more continuous process, where through currently unknown mechanism weak interaction results in blunted, but detectable responses.

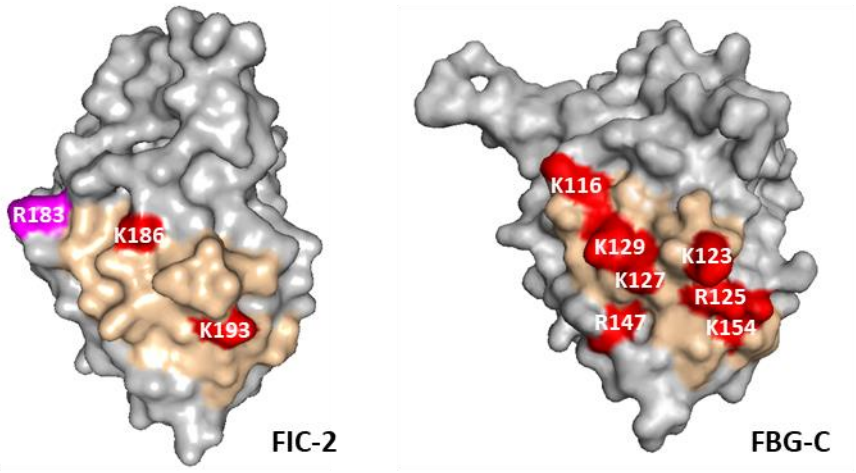


Figure 3.14 Additional positively charged residue in FIC-2 may contribute to the induction of cytokine release. Upon re-investigation of charge distribution on the surface of FIC-2 additional positively charged residue was identified adjacent to the cationic ridge region. It is possible that arginine 183 (in magenta), together with the two originally identified lysines, can enable FIC-2 to form a weak interaction with TLR4, inducing low levels of cytokine release. Charge distribution on FBG-C molecule is shown for comparison. The cationic ridge region created by residues from loops 5, 6 and 7 on the surface of each FBG domain is shown in pale orange, within which positively charged residues are coloured red.

Signalling through TLR4 can be inhibited with the use of blocking antibodies or small molecule compound TAK-242 [292]. TAK-242 specifically binds to intracellular part of TLR4 and prevents the activation of signalling cascade by disrupting the interaction between the receptor and its adaptor molecules. Here, TAK-242 was used to prove that the induction of cytokine release by FRePs is a result of activation of signalling through TLR4. Indeed, pre-treatment with the inhibitor rendered human macrophages no longer responsive to FIB-G, FIC-1, FIC-2, ALP-1, ALP-2 and ALP-6, proving the direct connection between their pro-inflammatory effects *in vitro* and TLR4 activation.

Due to the fact that TLR4 is a sensitive sensor of bacterial endotoxin, exceptional care was taken to prevent endotoxin contamination in the recombinant protein samples. However, as an additional precaution, pre-incubation of protein with an LPS neutralizing agent PMB was used during stimulation of macrophages. PMB is a naturally occurring antibiotic produced by a soil bacterium *Paenibacillus polymixa*.

Chemically a cyclic cationic polypeptide, it binds to negatively charged lipid A in an LPS molecule and prevents its detection by TLR4 [300]. Thus, it can be used to neutralize potential endotoxin contamination in protein samples [301]. Addition of PMB to recombinant FBG samples did not significantly change the levels of cytokines released by primary human macrophages, allowing to exclude endotoxin as the cause of their observed pro-inflammatory activity.

Exposure to high temperatures can lead to irreversible destruction of protein structure, affecting the ability to form interactions and, in consequence, causing loss of biological function. To prove that the structural organization of the FBG domain, that is the characteristic fold with exposed cationic ridge, is necessary for the activation of pro-inflammatory response, FBG-C, FIB-G and FIC-1 samples were boiled prior to stimulation of human macrophages. While heat denaturation rendered FBG-C and FIC-1 fully inactive, FIB-G displayed considerable thermal stability. This is quite surprising, as so called D region in fibrinogen molecule, consisting of FBG domains from chain β and ɣ, precipitates in temperatures above 60°C [302]. This observed heat resistance of FIB-G is difficult to explain as it is still not fully understood how different types of intra-protein interactions influence thermostability, and it is not uncommon for homologous protein to have drastically different heat sensitivity [303]. An alternative explanation is that the observed weak signal is due to cell activation by epitopes exposed following denaturation of the protein structure. It is known that heat-treatment of proteins and denatured protein aggregation can result in formation of new epitopes, capable of eliciting immune responses [304, 305]. Subsequently, instead of thermal denaturation proteolytic cleavage was used to test ALP-1, ALP-2, ALP-6 and FIC-2. For that proteinase K was used, a serine protease with broad substrate specificity isolated from the fungus *Tritirachium album* [306]. Compared to boiling, proteinase K treatment

destroys not only secondary and tertiary, but also primary structure of the protein, producing random shorter peptides. Proteolytic cleavage with proteinase K of all of the tested FBG domains markedly reduced their capability to induce pro-inflammatory cytokine release.

In summary, FBG domains possessing the cationic ridge were shown to: 1) induce dose-dependent production of pro-inflammatory cytokines in primary human macrophages, 2) that can be abolished with a selective TLR4 inhibitor TAK-242, 3) is not a result of LPS contamination, and 4) depends on structural integrity of the protein. This constitutes a strong body of evidence supporting the hypothesis of the cationic ridge being a universal epitope responsible for activation of signalling through TLR4.

3.3.4 Binding to TLR4

A number of biophysical methods can be used to acquire information on the interaction between a receptor and its ligand using recombinant proteins, including surface plasmon resonance (SPR), bio-layer interferometry (BLI), isothermal titration calorimetry (ITC), microscale thermophoresis (MST), as well as nuclear magnetic resonance (NMR) and X-ray crystallography. Here, a simple solid-phase assay was used that allowed for the measurement of binding affinities of candidate TLR4 agonists. The assay did not require any prior ligand labelling nor specific equipment, and was used successfully before to examine the binding of the tenascin family members to TLR4 [283]. Binding affinity, or the strength of a binding interaction between the two partners, can be described by an equilibrium dissociation constant (K_D). K_D is a concentration of ligand at which half of the receptor sites are occupied. The higher the K_D value, the weaker the interaction, and thus binding strength of different ligands can be compared. K_D values calculated for tested ligands show that both FIB-G (120.84 nM) and FIC-1 (248.02 nM) bind to TLR4 with lower affinities than FBG-C (36.47 nM). This could be potentially explained by the fact that both lack the loop 7 and the C-terminus epitopes that have been shown to stabilise the binding to the receptor in tenascins [283]. FIB-G and FIC-1 also possess fewer positively charged residues in the cationic ridge region compared to FBG-C. To put the obtained affinities in a broader context, the affinities of some examples of non-FReP binding partners of TLR4 have been quantified at 28 nM for biglycan-TLR4 complex (measured using MST) [307] and 19.6 nM for surfactant protein A-TLR4 complex (measured using SPR) [308]. The binding affinity of LPS and TLR4 is higher, with K_D of 3 nM calculated for a three way lipid A-TLR4-MD-2 complex (measured using an immunoprecipitation binding assay) [309]. In general endogenous ligands of TLR4 seem to be characterized by slightly lower binding affinities than LPS.

This might be a manifestation of how the immune system uses a common sensor, yet can elicit adequate response depending on the threat detected. One could speculate that a pathogenic trigger binds to the receptor with higher affinity to induce a swift and potent reaction to prevent the spreading of infection. On the other hand, endogenous triggers are a signal of tissue damage, and should promote non-aggressive responses, such as clearing of the debris and matrix remodelling, and perhaps that could be achieved by binding of the receptor with lower affinity.

3.3.5 Induction of inflammation *in vivo*

Full length tenascin-C has been repeatedly shown to be an important pro-inflammatory factor *in vivo*. Tenascin-C deficiency has a protective effect in mouse models of various inflammatory diseases, alleviating immune responses [310]. What is more, upon injection into a mouse joint, FBG domain from tenascin-C induces acute inflammation, characterized by immune cell infiltration, destruction of cartilage tissue and erosion of bone [136]. The predicted TLR4 activators FIB-G and FIC-1 caused similar effects following intra-articular injection, although the observed joint inflammation was less severe, and the predicted non-binder ALP-4 was inert.

Both fibrinogen and ficolin-1 have been previously linked to pathologies of inflammatory origin. Fibrinogen is a known acute-phase response protein, and has been shown *in vivo* to be a regulator of inflammation in diseases such as atherosclerosis, Alzheimer's disease and RA [280]. However, the pro-inflammatory potential of fibrinogen has been attributed mostly to its interaction with the integrins. For example, mice expressing mutant form of fibrinogen, incapable of binding to its partner integrin $\alpha_M\beta_2$, exhibited markedly reduced disease severity in a collagen induced arthritis model [311]. Fibrinogen also has a clinical relevance in arthritis. Presence of autoantibodies against citrullinated peptides, such as fibrinogen fragments, is a marker of early RA with high diagnostic value [312].

Mice deficient in ficolin B, a murine orthologue of FIC-1, are protected from a collagen antibody-induced arthritis model [313]. In the same model of arthritis, administration of an anti-ficolin-1 antibody ameliorated the symptoms of joint inflammation [314]. A connection between FIC-1 and RA has also been described in humans. Single nucleotide polymorphisms in FCN1 gene coding ficolin-1, located in the promoter and FBG domain coding region (albeit not causing any change in the amino

acid sequence) were shown to have significant association with RA [315]. Moreover, serum levels of FIC-1 were found to be elevated in RA patients [314].

It is possible that some of the observed *in vivo* disease relevant effects of those proteins are a consequence of their capability to bind to and activate TLR4. While future work will be required to confirm this, the FReP-TLR4 interaction could be a novel target in the treatment of inflammatory diseases such as RA.

3.3.6 Conclusions

A positively charged structural feature exposed on the surface of an FBG domain has been shown to confer the capability to bind and activate TLR4, leading to activation of immune responses and promotion of inflammation *in vivo*. A total of 13 human proteins from diverse families possess this cationic ridge, provoking many questions in regards to functionality and purpose of such universal pro-inflammatory motif.

First of all, do all cationic ridge containing proteins serve a common role? Are they all simply danger signals, alerting the body of tissue damage and activating repair mechanisms? Is it possible that different FRePs can induce different responses by the means of diverse mode of TLR4 activation or engagement of various co-receptors? It has been shown that classic co-receptors essential for LPS induced signalling through TLR4, MD-2 and CD14, are not required for the effects induced by FBG-C [136]. It remains to be seen if any other molecules are necessary for cationic ridge-possessing proteins to activate TLR4. It is also conceivable that the observed responses are a result of integration of signalling through TLR4 and some other receptor within one cell, or within a population of cells.

Secondly, it might seem puzzling that this structural TLR4 epitope is so abundant in human proteins. If all are indeed to be sensed as danger signals, it might be practical for a PRR to have a strictly limited number of recognized epitopes, preventing unwanted activation of immune responses. One might also wonder why only certain members of a protein family are marked with a PRR activation epitope. In the case of ficolins, while all play a role in the activation of the lectin complement pathway, FIC-2 and FIC-3 are serum proteins, whilst FIC-1 circulates at much lower levels and is found predominantly bound to the surface of monocytes and neutrophils. As FIC-2 produced

only weak cytokine release, the only ficolin that can induce a potent immune response is the one predominantly present in the tissue, and not periphery. It might be that this motif has evolved to only play a role in local inflammation, and so FRePs present in high quantities in circulation should not be marked with the cationic ridge. The expression pattern of TLR4 activating FRePs might also be a way of preventing the trigger of detrimental constant systemic inflammation. For example, FBG-C, the archetypal pro-inflammatory FReP, is virtually absent in adult healthy tissues and only expressed at sites of damage or infection. Additionally, an FBG domain constitutes only a small part of a FReP, and many FRePs multimerize, for example tenascin-C forms hexamers, ficolins form trimers which then further associate into higher oligomeric structures, and fibrinogen is built from 2 of each chain α, β and ɣ. It is possible that proteolytic cleavage resulting in the release of the domain is necessary for the activation of the pro-inflammatory potential of the protein. As a matter of fact, proteinase treatment of fibrinogen does result in TLR4-dependent allergic airway inflammation [316]. The activation thresholds for the FBG to have an observable effect in the tissue might also depend on the local accumulation of protein, for example by tethering in the extracellular matrix. Finally, certain specific switch off mechanisms might also contribute to restraining FReP-induced inflammation. In the next chapter, the capability of FBG-C to desensitize innate immune cells to sensing of subsequent triggers will be explored.

In conclusion, the discovery of a universal TLR4 epitope contributes to our knowledge of the complexity of endogenously triggered inflammation. However, the exact mode of action and relevance in physiological responses and pathological conditions of the novel TLR4 ligands are yet to be fully understood.

4

Innate immune memory induced by tenascin-C

Contents

4.1 Introduction 142

4.2 Results 144

4.2.1 FBG-C de-sensitises human macrophages to LPS 144

4.2.2 Establishment of the memory assay 149

4.2.3 FBG-C induces innate immune tolerance 160

4.2.4 FBG-C induced tolerance: a protein dependent effect 168

4.2.5 FBG-C induced memory is not limited to re-activation of TLR4 pathway 176

4.2.6 FBG-C induced memory is effector-specific and temporally regulated 182

4.2.7 Transcriptional analysis of effector molecules in FBG-C induced memory 186

4.2.8 Epigenetic re-programing in FBG-C induced memory 197

4.3 Discussion 207

4.3.1 Investigating memory effects *in vitro* in human immune cells 208

4.3.2 FBG-C vs LPS in innate immune memory: same, but different? 212

4.3.3 The importance of cell viability in innate immune memory research 215

4.3.4 Complexity of FBG-C induced tolerance/training 217

4.3.5 Understanding re-programming underlying FBG-C induced memory 222

4.3.6 Conclusions 225

4.1 Introduction

In the innate immune compartment, a number of virulence factors have been shown to induce "memory", defined as an altered response of the immune cells to subsequent stimuli following exposure to primary stimulation. This phenomenon comprises either a potentiated response (training), which can be induced by a component of yeast cell wall, β-glucan, or a diminished response (tolerance), for example induced by bacterial LPS. Training and tolerance play vital protective roles, such as preventing secondary infections or restricting excessive detrimental inflammation in sepsis. However, these are not simply states of immune over-sensitivity or inertia, but rather complex functional adaptations resulting from broad transcriptional, epigenetic and metabolic re-programming.

While memory generated by pathogenic stimuli has been extensively studied, little is known about innate immune memory induced by non-infectious triggers. In the second part of my project I aimed to investigate whether one of the endogenous ligands of TLR4, the FBG domain from tenascin-C (FBG-C), is also capable of driving innate immune memory, and, if so, to shed light on the molecular basis of the FBG-C induced memory.

In the course of my work on human macrophages, I observed that stimulation with LPS or recombinant FBG-C causes loss of the capability to produce TNF in response to immediate re-stimulation. To explore this further, I performed a literature review, and then optimised a memory assay in primary human monocytes based on the gold standard model used to examine β-glucan and LPS as classic training and tolerance controls. Utilizing this memory assay I determined that FBG-C is capable of generating innate immune tolerance to re-challenge. Moreover, I established that FBG-C induced memory comprises both enhanced and diminished responses, is temporally regulated and effector-

specific, and is not limited to re-activation of the TLR4 pathway. To better understand the mechanisms behind the observed effects I performed gene expression analysis of two key cytokines that were differentially regulated following FBG-C activation, and employed a library of small molecule epigenetic inhibitors, revealing how secondary inflammatory responses are altered at the transcriptional level, and highlighting potential epigenetic modifiers that control these pathways. Altogether, I discovered and characterized innate immune memory induced by FBG-C, and provided insight into the cellular re-programming underlying this phenomenon.

4.2 Results

4.2.1 FBG-C de-sensitises human macrophages to LPS

Lipopolysaccharide (LPS) is a large glycolipid serving as the key component of the outer membrane in Gram-negative bacteria. Structurally, LPS contains 3 distinct domains: lipid A, core oligosaccharide and O antigen, and is responsible for creating a permeability barrier protecting bacterial cell from harmful molecules (e.g. antibiotics) that might be present in its direct environment. Lipid A, the most conserved region, is a potent activator of host immune response and is often the major factor behind bacteria pathogenicity [9]. Following sensing of lipid A by TLR4, immune cells produce mediators including pro-inflammatory cytokines (TNF, IL-1, IL-6), reactive oxygen species, and prostaglandins [317]. On a systemic level, exposure to LPS causes fever (febrile response), and can lead to potentially fatal septic shock [318]. Due to the fact that bacterial LPS is capable of inducing immune response so powerful it can actually be toxic to the host organism, and that it is an integral part of pathogen cell, and not a secreted virulence factor, it has been historically referred to as endotoxin.

It has been established decades ago that repeated injection of LPS in rabbits de-sensitises the animals, which is characterized by consecutive gradual decrease in febrile response to the challenge [15]. Similarly, patients recovering from infectious diseases, as well as volunteers exposed to pathogens, manifested reduced fever as a result of LPS administration [319]. Finally, markedly diminished cytokine production could be observed in immune cells primed, and then re-stimulated with LPS *in vitro* [14]. This refractory state has been termed LPS (or endotoxin) tolerance.

To confirm LPS induced tolerance can be reproduced in this study, the macrophage assay implemented in Chapter 3 to test FReP activity was adjusted. Cells were isolated and differentiated as described before, but then exposed to sequential

repeated stimulation instead of only one stimulation. Macrophages were first stimulated with decreasing concentrations of LPS (10 ng/mL – 10 fg/mL) for 24h, upon which culture medium was collected, cells washed, and then re-stimulated with LPS at 10 ng/mL for 24h. Published data shows that LPS at 10 ng/mL or higher induces tolerance [26-29, 31, 33, 35, 39, 42], while some studies in murine macrophages also demonstrate that lower doses, 1 ng/mL - 5 pg/mL, can induce potentiation of cytokine response to re-stimulation [320-323]. The range of concentrations used for primary stimulation was thus chosen to have a chance of observing both effects. 10 ng/mL is a commonly used concentration for re-stimulation [26-28, 31, 35, 39, 42, 321]. As a control, cells were left untreated in the first 24h, and then stimulated with LPS for the next 24h [-/+]. Additionally, sample left unstimulated throughout the duration of the experiment was also included [-/-]. TNF release in the medium after the first stimulus (at 24h) and after the second (at 48h) was measured, and cell viability was tested using MTT assay at the end of the experiment (at 48h).

As expected, stimulation of macrophages with LPS in the first 24h induced a dose dependent secretion of TNF, while unstimulated cells [-] did not produce the cytokine (Fig. 4.1 A). Following re-stimulation with LPS, dose dependent inhibition of TNF secretion was observed in cells stimulated in the first 24h, compared to initially unstimulated control [-/+]. However, potentiation of TNF release could not be observed even at low doses. No spontaneous cytokine release was detected in samples that remained untreated for 48h [-/-] (Fig. 4.1B). Cell viability was not significantly different in any of the tested conditions (Fig. 4.1 C).

Next, the assay was used to verify if FBG-C, an endogenous activator of TLR4, has the potential to generate a similar de-sensitization. For this purpose, cells were stimulated with decreasing concentrations of recombinant FBG-C domain (1 μM –

100 pM), or LPS at 1 ng/mL, and then re-stimulated with LPS at 10 ng/mL. In the first 24h, cells responded to primary stimulation with FBG-C and LPS by producing TNF, and no cytokine release was detected in the unstimulated sample [-] (Fig. 4.2 A). Then, a dose-dependent suppression of secondary response to LPS was observed in cells stimulated with FBG-C in the first 24h, in comparison to unstimulated control [-/+]. TNF secretion by cells stimulated with LPS, and re-stimulated with LPS, was fully blocked, as observed before. Cells left untreated for 48h [-/-] produced very little background TNF (Fig. 4.2 B). MTT measured in the treated samples was not significantly different compared to unstimulated control [-/-] (Fig. 4.2 C). Thus, the first piece of evidence was obtained that FBG-C is capable of inhibiting TNF response, similar to LPS tolerance in human macrophages.

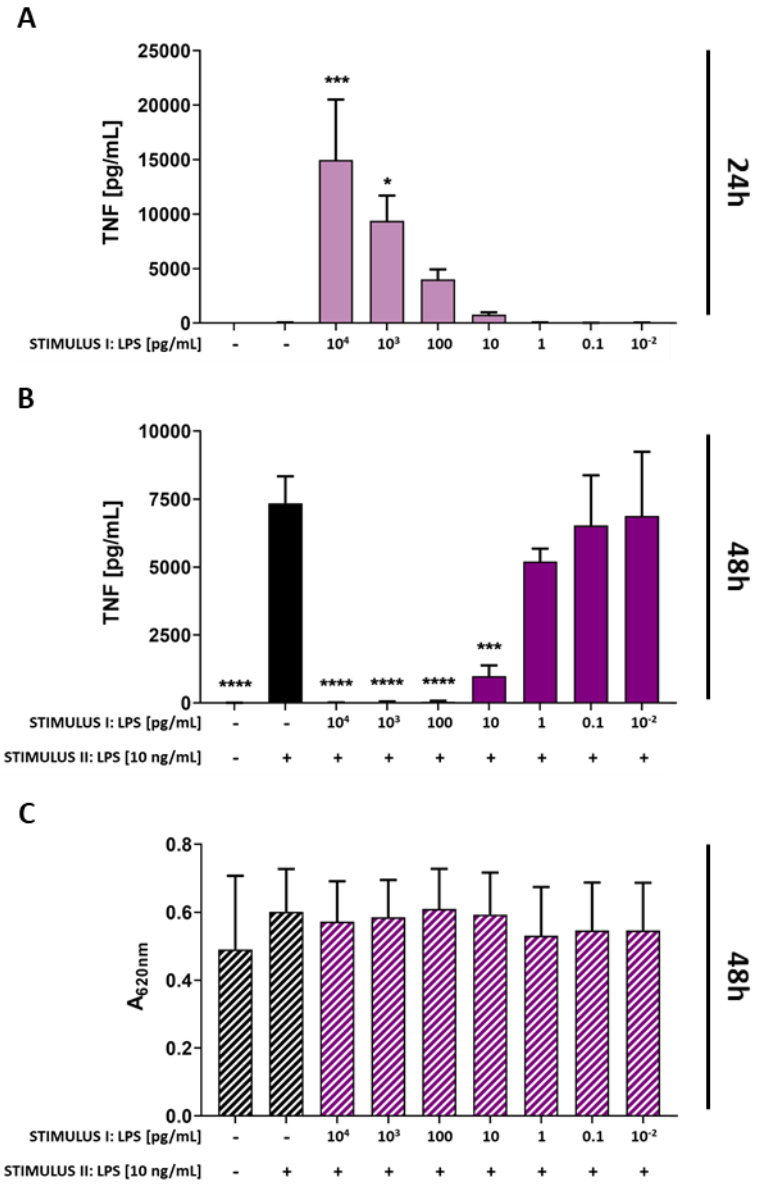


Figure 4.1 LPS de-sensitises primary human macrophages. Primary human macrophages were stimulated for 24h with decreasing concentrations of LPS (STIMULUS I) or left unstimulated [-]. Medium was then collected for analysis, fresh medium was added and cells were re-stimulated for 24h with 10 ng/mL of LPS (STIMULUS II, [+]) or left unstimulated [-]. TNF levels in the media after STIMULUS I (**A**) and after STIMULUS II (**B**) were measured by ELISA. MTT assay was performed to asses cell viability after STIMULUS II (**C**). Data are shown as mean ± SEM from 3 independent donors. Data was analysed using one-way ANOVA vs unstimulated [-] (**A**) and [-/-] (**C**) or unstimulated and re-stimulated with LPS [-/+] (**B**), *$p < 0.05$, ***$p < 0.001$, ****$p < 0.0001$.

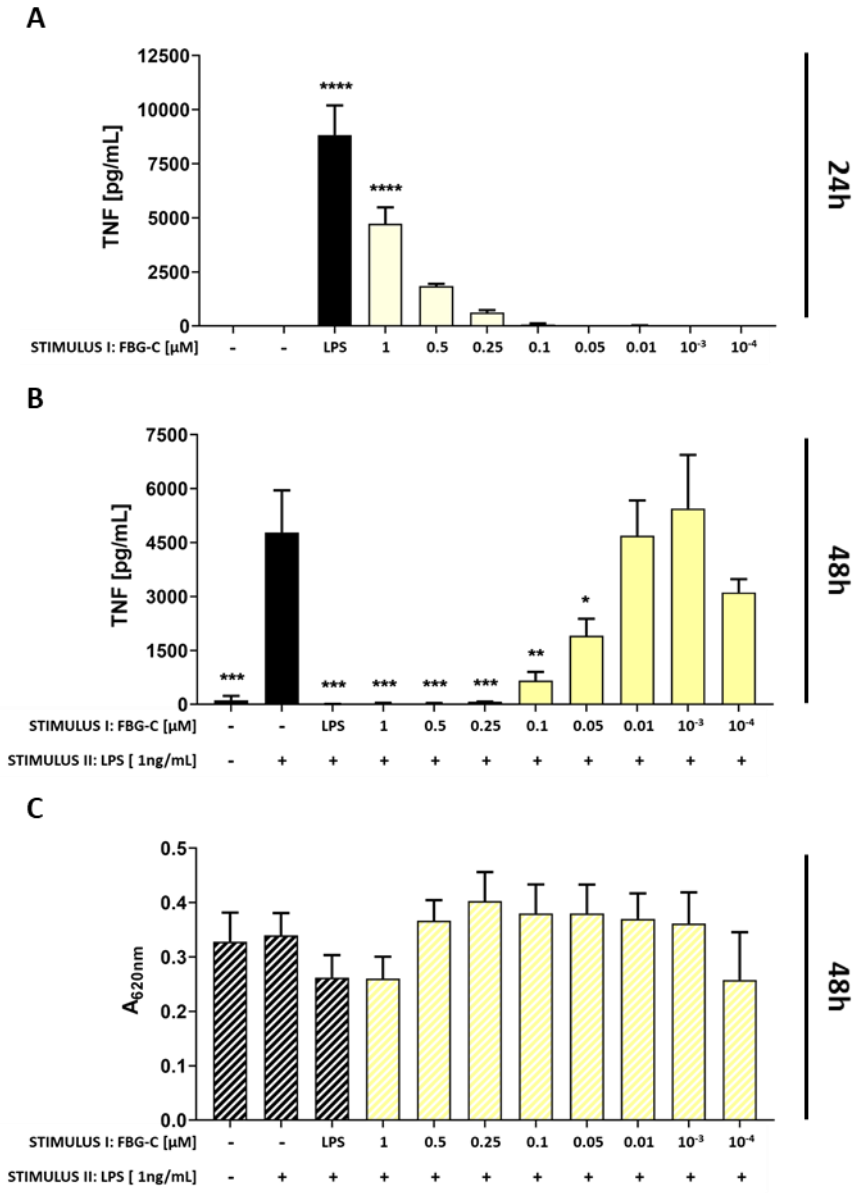


Figure 4.2 FBG-C de-sensitises primary human macrophages. Primary human macrophages were stimulated for 24h with decreasing concentrations of FBG-C or with LPS at 1 ng/mL (STIMULUS I) or were left unstimulated [-]. Medium was then collected for analysis, fresh medium was added and cells were re-stimulated for 24h with 1 ng/mL of LPS (STIMULUS II, [+]) or were left unstimulated [-]. TNF levels in media after STIMULUS I (**A**) and after STIMULUS II (**B**) were measured by ELISA. MTT assay was performed to asses cell viability after STIMULUS II (**C**). Data are shown as mean ± SEM from 3 independent donors. Data was analysed using one-way ANOVA vs unstimulated [-] (**A**) and [-/-] (**C**) or unstimulated and re-stimulated with LPS [-/+] (**B**), *$p < 0.05$, **$p < 0.01$, ***$p < 0.001$, ****$p < 0.0001$.

4.2.2 Establishment of the memory assay

In addition to the phenomenon of LPS tolerance, it has become evident more recently that pathogenic triggers also have the ability to induce a hyperresponsive phenotype in human immune cells. This concept was first conceived due to the non-specific protection conferred by the Bacillus Calmette–Guérin (BCG) vaccine [324]. It was later demonstrated that PBMCs isolated from the blood of BCG vaccinated individuals exhibit enhanced cytokine secretion in response to stimulation with a variety of pathogens [98]. Studies in monocytes and macrophages established BCG, but also *C. albicans* and β-glucan, can cause augmented cytokine responses to secondary challenge *in vitro* [100]. Such exacerbated immune response in the innate compartment is referred to as trained immunity, and its acquisition - training.

β-glucan, a component of fungi cell wall sensed by the host through the C-type lectin receptor dectin-1, remains the most widely used agent to investigate trained immunity. β-glucan training and LPS tolerance are often considered to be opposing forms of the same process - innate immune memory. Thus, these two classic triggers were utilised to develop an innate immune memory protocol that could be used to study FBG-C induced memory. Based on a literature review of methods used in the past two decades, an experimental protocol in primary human monocytes was designed, consisting of two stimulation steps separated by a rest period (Fig. 4.3). The cells were first stimulated for 24h (PRIME), during which primary response would be induced and memory acquisition initiated. After 24h, medium was collected, cells washed, and fresh medium added, to remove the priming stimulus. Cells were then rested for 5 days, and one medium change at day 5 was included. At day 6 a second stimulus was added to cells for 24h (TRIGGER), and altered secondary responses were assessed using ELISA detection of TNF and IL-6, the most commonly reported immune mediators to be affected in innate immune

memory. A wide range of concentrations of the memory inducing stimuli (PRIME) was tested (LPS at 100 ng/mL – 100 fg/mL, and β-glucan at 100 – 0.1 µg/mL), encompassing doses reported in the literature [39, 100]. In addition, two variations of published protocols were compared, distinguished by the absence (Fig. 4.3 A) or presence (Fig. 4.3 B) of serum during the PRIME step [39, 76, 178, 325]. The addition of human serum in this protocol is aimed at providing physiological levels of growth factors that drive differentiation of monocytes into macrophages [39, 326].

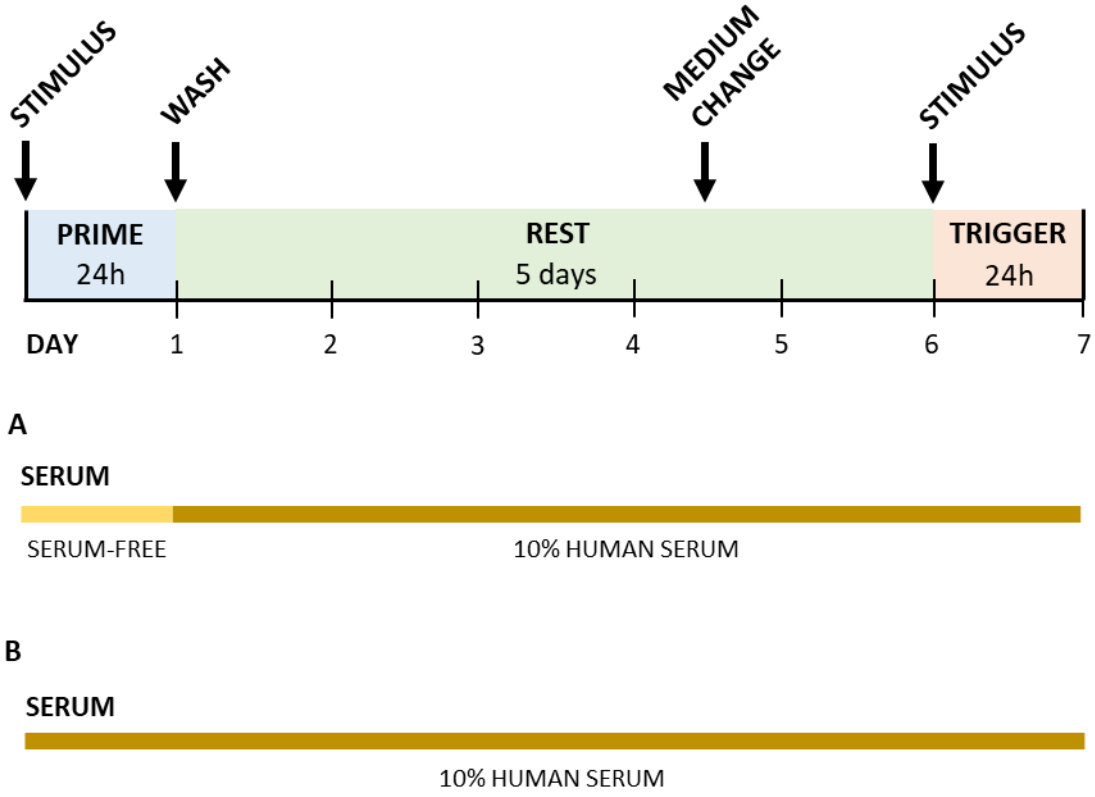


Figure 4.3 Memory assay protocol. Primary human monocytes were seeded in a 96 well plate and stimulated for 24h with training or tolerizing agents (PRIME). Medium was then collected, cells washed with PBS and fresh medium added. Cells were rested for 5 days (REST), with one medium change during the resting period. On day 6 cells were re-stimulated (TRIGGER) for 24h, after which time medium was collected for analysis and cell viability assays were performed. Two variations of the protocol were tested: PRIME step performed in serum-free medium, while REST and TRIGGER in medium supplemented with 10% human serum (**A**); medium supplemented with 10% human serum was used during the whole protocol (**B**).

Stimulation of monocytes with increasing doses of LPS in serum free medium during the PRIME step induced dose dependent release of TNF and IL-6, demonstrating the cells are responsive to this trigger in the first 24h of the memory assay. No spontaneous cytokine secretion was detected in unstimulated cells (-) (Fig. 4.4 A). At day 7, unprimed and unstimulated cells (-/-) produced very low or low levels of TNF and IL-6, respectively. In the unprimed and LPS re-stimulated sample (-/+) both TNF and IL-6 were induced, demonstrating that monocytes remain capable of responding to stimulation during the TRIGGER step in the absence of priming. However, in cells primed with LPS, release of TNF and IL-6 following re-stimulation was inhibited. This effect was dose dependent, with higher concentrations of LPS during the PRIME step generating more potent suppression of LPS induced cytokine release during the TRIGGER step. Additionally, suppression of cytokine secretion was more pronounced for TNF than IL-6, with nearly complete inhibition of TNF observed compared to approximately 50% inhibition of IL-6, in cells primed with the highest concentration of LPS (100 ng/mL) compared to the unprimed, re-stimulated control (-/+). Increase of cytokine secretion could not be distinguished in cells primed with low, or very low doses of LPS (Fig. 4.4 B). In the MTT assay performed at the end of day 7 no significant differences in cell viability were observed across all the tested conditions (Fig. 4.4 C).

Priming of monocytes with LPS in serum supplemented medium also resulted in dose dependent production of TNF and IL-6 at 24h, whereas no cytokine release could be detected in the unprimed sample (-) (Fig. 4.5 A). After 7 days, almost no TNF was released by unprimed and unstimulated cells (-/-), but induction of TNF was observed in the unprimed, re-stimulated control (+/-). In cells primed with LPS, release of TNF following re-stimulation was inhibited in a dose dependent manner, with the two highest concentrations of LPS during priming (100 and 10 ng/mL) generating a nearly complete

suppression of cytokine release. Moderate induction of IL-6 following LPS stimulation was seen in unprimed cells (-/+; 1300 pg/mL) over the background cytokine secretion measured in the unprimed, unstimulated sample (-/-; 900 pg/mL). In cells primed with LPS, release of IL6 following re-stimulation was similar to cells which had not been primed (-/+). Here again increase of cytokine secretion could not be identified, regardless of the LPS concentration used for priming (Fig. 4.5 B). Cell viability measured by MTT assay was not significantly different in any of the tested conditions (Fig. 4.5 C).

A number of differences were observed in the data collected using protocols in which cells were primed in the absence (Fig. 4.4) or presence (Fig. 4.5) of serum. Firstly, LPS induced cytokine release measured at 24h was higher in cells cultured in medium supplemented with serum. Cells primed with LPS in the presence of serum produced up to 10,000 pg/mL of TNF and 50,000 pg/mL IL-6 (Fig. 4.5 A), while monocytes grown without serum produced a maximum of 3,500 pg/mL of TNF and 25,000 pg/mL of IL-6 (Fig. 4.4 A). However, at day 7, higher levels of cytokines were detected in the protocol that omitted serum during priming. In response to LPS, unprimed cells secreted 1,500 pg/mL of TNF and 3,500 pg/mL of IL-6 when no serum was present during the first 24h of the protocol (Fig. 4.4 B), and as little as 200 pg/mL of TNF and 1,500 pg/mL of IL-6 if serum was present throughout the whole duration of the protocol (Fig. 4.5 B). Furthermore, cell viability assessed with MTT assay was higher in the no serum PRIME protocol (Fig. 4.4 C; OD of approximately 0.15 – 0.25) compared to priming with serum (Fig. 4.5 C; OD $\leq$ 0.1). Finally, while LPS induced TNF suppression was observed in both versions of the protocol, inhibition of IL-6 release could be detected in the no serum PRIME protocol (Fig. 4.4 B), but not in the fully serum supplemented protocol (Fig. 4.5 B).

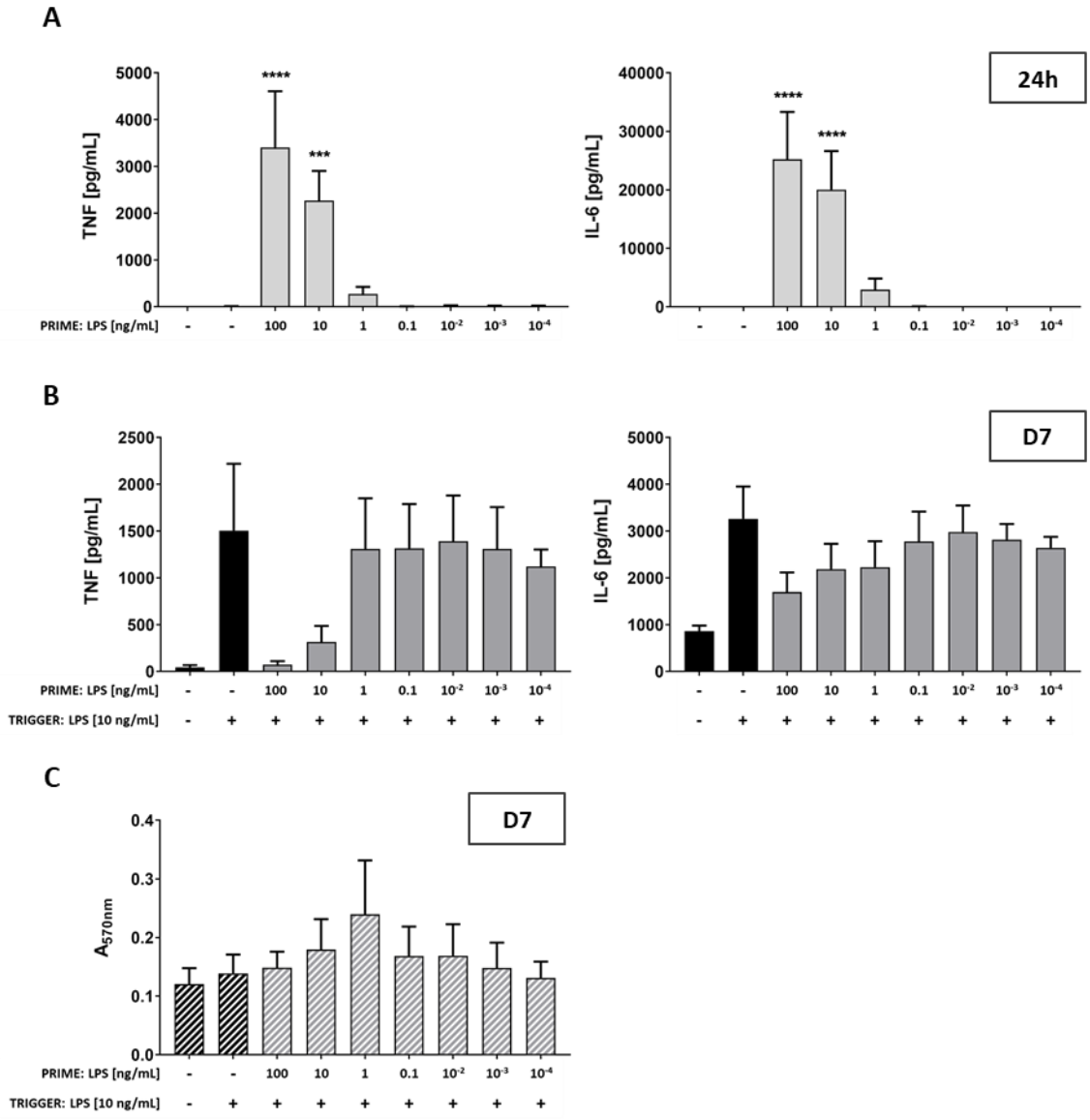


Figure 4.4 Optimization of LPS induced tolerance control I. Cells were primed for 24h with decreasing concentrations of LPS or left unstimulated [-] in serum free medium. After 5 days of rest in medium supplemented with 10% human serum, cells were then re-stimulated with LPS at 10 ng/mL [+], or left unstimulated [-]. TNF and IL-6 levels in media at 24h (**A**) and at day 7 (**B**) were measured by ELISA. MTT assay was performed to asses cell viability at day 7 (**C**). Data are shown as mean ± SEM from 3 independent donors. Data was analysed using one-way ANOVA vs unstimulated [-] (**A**) and [-/-] (**C**) or unstimulated and re-stimulated with LPS [-/+] (**B**), *$p < 0.05$, **$p < 0.01$, ***$p < 0.001$, ****$p < 0.0001$.

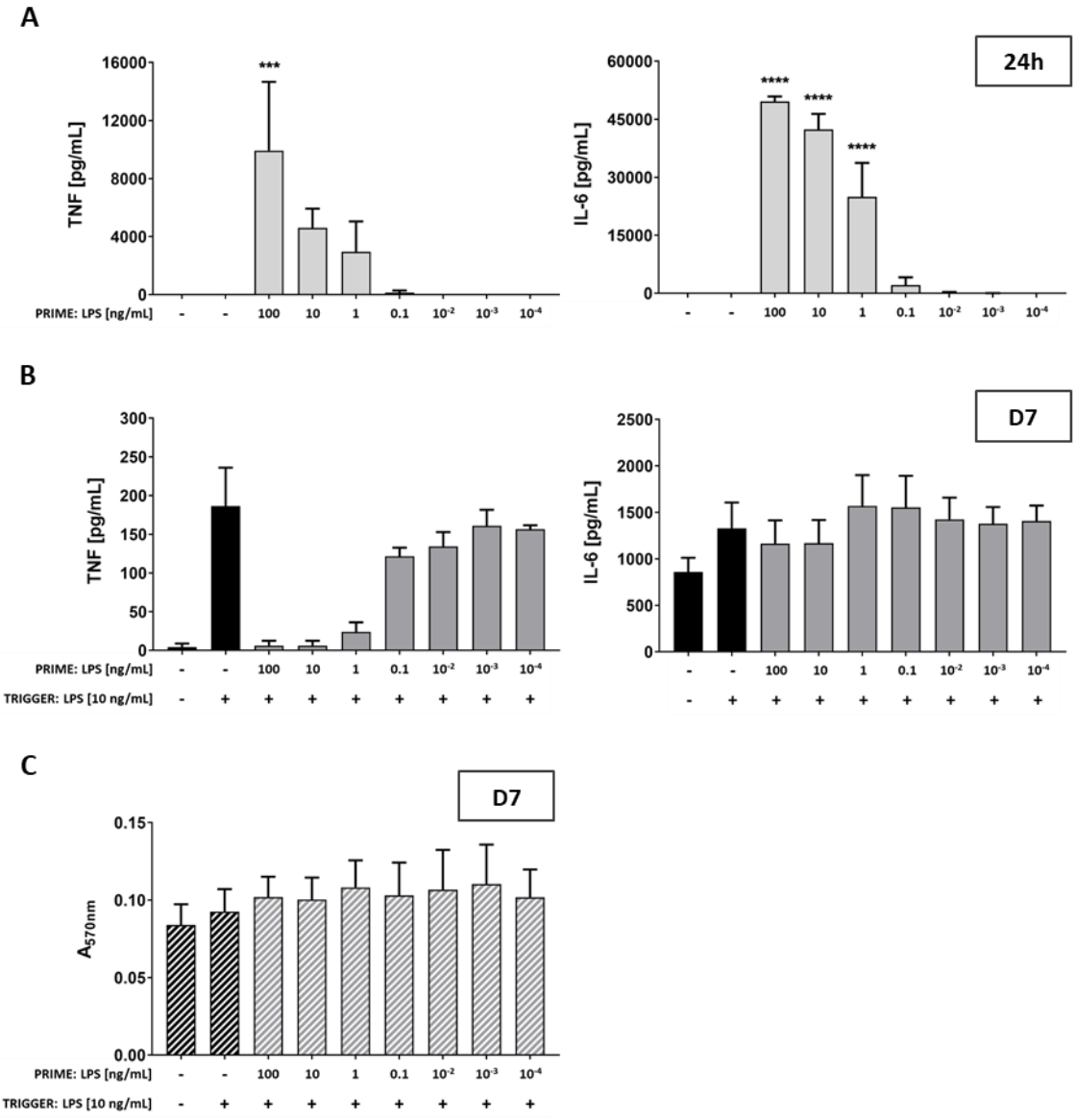


Figure 4.5 Optimization of LPS induced tolerance control II. Cells were primed for 24h with decreasing concentrations of LPS or left unstimulated [-] in medium supplemented with 10% human serum. After 5 days of rest in serum supplemented medium, cells were then re-stimulated with LPS at 10 ng/mL [+], or left unstimulated [-]. TNF and IL-6 levels in media at 24h (**A**) at day 7 (**B**) were measured by ELISA. MTT assay was performed to asses cell viability at day 7 (**C**). Data are shown as mean ± SEM from 3 independent donors. Data was analysed using one-way ANOVA vs unstimulated [-] (**A**) and [-/-] (**C**) or unstimulated and re-stimulated with LPS [-/+] (**B**), *p < 0.05, **p < 0.01, ***p < 0.001, ****p < 0.0001.

Next, to confirm if β-glucan training can be reproduced in the memory protocol, monocytes were primed with decreasing doses of this stimulus, and then re-stimulated with LPS at 10 ng/mL. In cells primed in the absence of serum, stimulation with β-glucan did not induce production of TNF or IL-6, and no spontaneous release of these cytokines could be detected in unprimed cells [-] (Fig. 4.6 A). At day 7, unstimulated cells [-/-] did not secrete TNF, and produced low levels of IL-6. As observed previously, unprimed cells re-stimulated with LPS [-/+] were responsive, producing both TNF and IL-6. In comparison, β-glucan primed cells re-stimulated with LPS secreted significantly more TNF and IL-6 than the unprimed, re-stimulated control [-/+]. This effect was dose dependent, with highest concentrations of β-glucan generating 3 to 4 fold increase in cytokine release in response to LPS re-stimulation (Fig. 4.6 B). Additionally, higher MTT signal was measured at the end of the protocol in cells primed with β-glucan, compared to unstimulated control [-/-]. This increase was statistically significant in samples primed with β-glucan at 100 – 10 μg/mL (Fig. 4.6 C).

Priming of the cells with β-glucan in the presence of human serum induced low levels of TNF and IL-6, but no cytokine release was detected in unstimulated samples [-] (Fig. 4.7 A). Unstimulated cells at day 7 [-/-] produced no TNF, and low background levels of IL-6. Re-stimulation of unprimed cells with LPS [-/+] resulted in weak induction of TNF and IL-6 secretion over the unstimulated control [-/-]. Following re-stimulation, cells primed with β-glucan at 100 – 5 μg/mL released increased levels of both cytokines, compared to the unprimed, re-stimulated sample [-/+] (Fig. 4.7 B). In the MTT assay performed at the end of the protocol, β-glucan primed cells generated a stronger signal than the unstimulated cells [-/-] (Fig. 4.7 C).

Comparison of the data collected in cells primed in serum free (Fig. 4.6) or serum supplemented (Fig. 4.7) medium revealed similar differences to what has been

observed during LPS tolerance testing (Fig. 4.4 and 4.5, respectively). In the PRIME step, cells stimulated with β-glucan in the presence of serum could produce up to 1000 pg/mL of both TNF and IL-6 (Fig. 4.7 A), while priming in the absence of serum did not induce any cytokine secretion (Fig. 4.6 A). Then at day 7, overall TNF and IL-6 release was higher if serum was excluded during priming. Following re-stimulation with LPS, unprimed cells produced approximately 1,500 pg/mL of TNF and 3,000 pg/mL of IL-6 when no serum was present in the first 24h of the protocol (Fig. 4.6 B), and less than 200 pg/mL of TNF and 1,500 pg/mL of IL-6 when serum was supplemented throughout the duration of the experiment (Fig. 4.7 B). Cells primed with β-glucan without serum could make up to 9,000 pg/mL of TNF and 10,000 pg/mL of IL-6 in response to re-stimulation with LPS (Fig. 4.6 B), while only about 2,500 pg/mL of TNF and 4,000 pg/mL of IL-6 if primed in the presence of serum (Fig. 4.7 B). Finally, absorbance measured in the MTT assay at day 7 was also higher for the samples with no serum during the PRIME step, with 0.12 – 0.15 (Fig. 4.6 C) vs 0.1 (Fig. 4.7 C) in the control samples, and 0.4 – 0.5 (Fig. 4.6 C) vs 0.3 – 0.4 (Fig. 4.7 C) in the β-glucan primed samples.

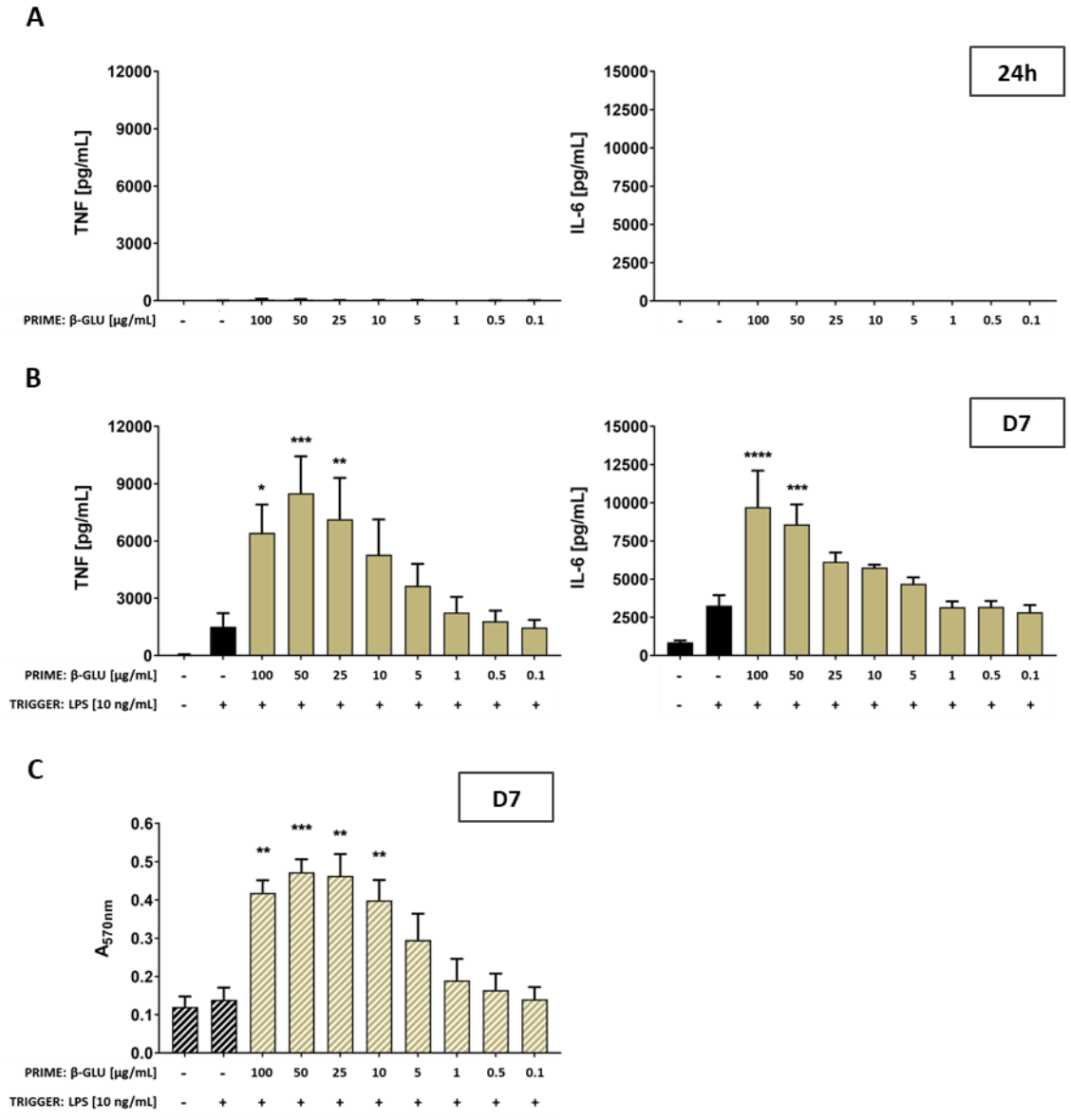


Figure 4.6 Optimization of β-glucan induced training control I. Cells were primed for 24h with decreasing concentrations of β-glucan or left unstimulated [-] in serum free medium. After 5 days of rest in medium supplemented with 10% human serum, cells were then re-stimulated with LPS at 10 ng/mL [+], or left unstimulated [-]. TNF and IL-6 levels in media at 24h (**A**) and day 7 (**B**) were measured by ELISA. MTT assay was performed to asses cell viability at day 7 (**C**). Data are shown as mean ± SEM from 3 independent donors. Data was analysed using one-way ANOVA vs unstimulated [-] (**A**) and [-/-] (**C**) or unstimulated and re-stimulated with LPS [-/+] (**B**), *p < 0.05, **p < 0.01, ***p < 0.001, ****p < 0.0001.

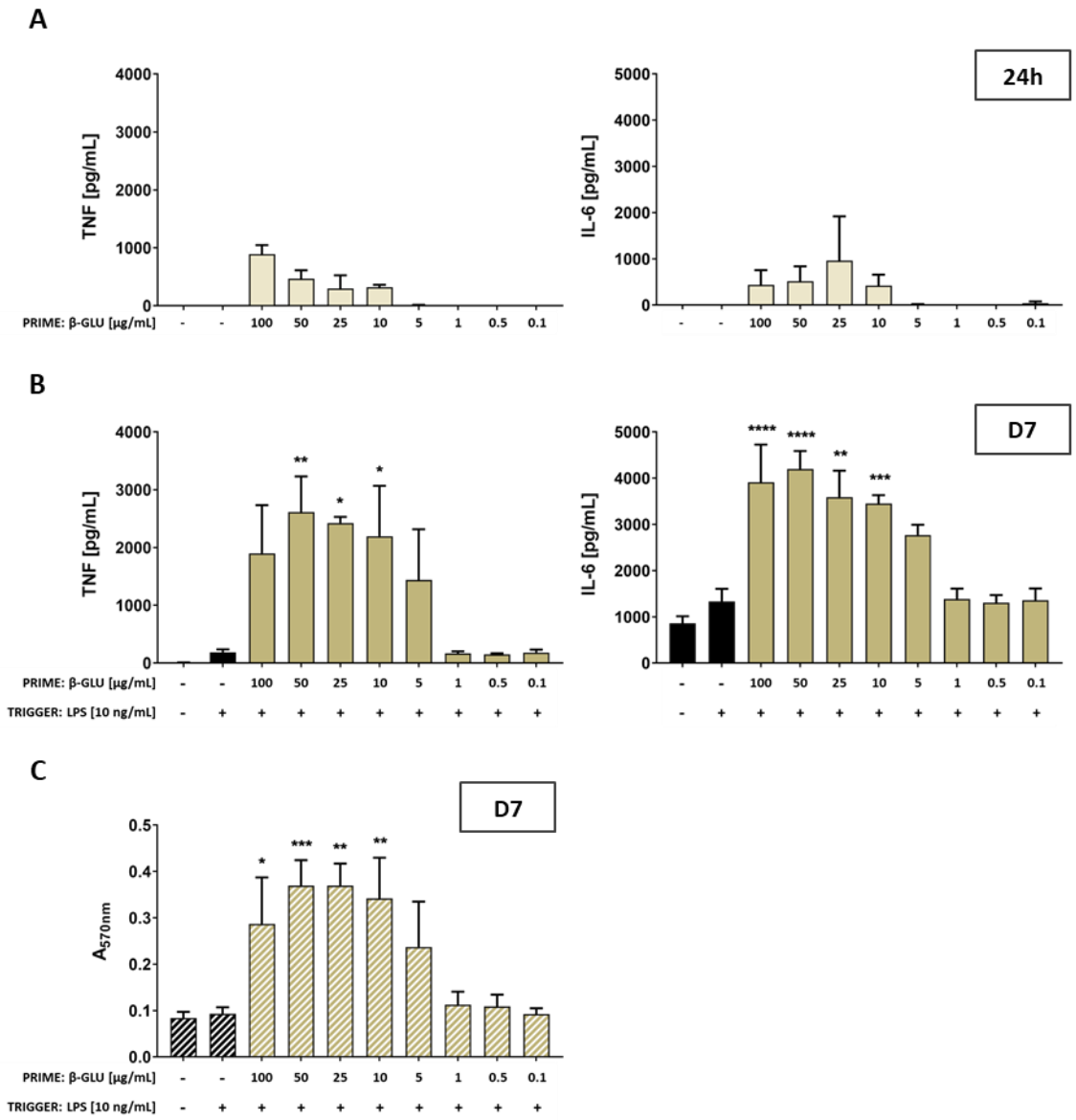


Figure 4.7 Optimization of β-glucan induced training control II. Cells were primed for 24h with decreasing concentrations of β-glucan or left unstimulated [-] in medium supplemented with 10% human serum. After 5 days of rest in serum supplemented medium, cells were then re-stimulated with LPS at 10 ng/mL [+], or left unstimulated [-]. TNF and IL-6 levels in media at 24h (**A**) and at day 7 (**B**) were measured by ELISA. MTT assay was performed to asses cell viability at day 7 (**C**). Data are shown as mean ± SEM from 3 independent donors. Data was analysed using one-way ANOVA vs unstimulated [-] (**A**) and [-/-] (**C**) or unstimulated and re-stimulated with LPS [-/+] (**B**), *p < 0.05, **p < 0.01, ***p < 0.001, ****p < 0.0001.

In conclusion, the protocols used here enabled replication of published data demonstrating LPS tolerance and β-glucan training. Due to the more effective inhibition (LPS) and potentiation (β-glucan) observed during the secondary response, and higher MTT measurement, in cells cultured without serum during the first 24h of the protocol,

it was decided to exclude serum during the PRIME step in future work (protocol as presented on Fig. 4.3 A). Priming with LPS at 100 ng/mL and β-glucan at 10 µg/mL was incorporated in all subsequent memory experiments to serve as classic tolerance and training controls. In the next paragraphs suppression of cytokine production following re-stimulation will be referred to as tolerance, while potentiation will be termed training, regardless of the inducing stimuli.

4.2.3 FBG-C induces innate immune tolerance

Subsequently, the optimized memory protocol was employed to interrogate the capability of FBG-C to induce innate immune memory, and to assess if this stimulus can produce either tolerance or training, or both, depending on the dose used. Monocytes were primed with decreasing concentrations of recombinant FBG-C (5 µM – 1 nM) in serum free medium, and then re-stimulated with LPS at 10 ng/mL. At 24h, no cytokine release was detected in unprimed controls [-], and cells stimulated with FBG-C secreted TNF and IL-6 in a dose-dependent manner (Fig. 4.8 A), similarly to what has been shown previously in human macrophages in paragraph 4.2.2 (Fig. 4.2 A), and in published literature [193]. After 7 days, very low levels of TNF and low levels of IL-6 were detected in the unstimulated sample [-/-], and unprimed, re-stimulated cells [-/+] responded by producing both cytokines. In comparison to this control [-/+], cells primed with FBG-C secreted significantly less TNF and IL-6 in response to LPS re-stimulation. This effect was striking, with FBG-C generating up to 100% suppression of TNF and 90 - 97% suppression of IL-6 release following re-stimulation with LPS, compared to cytokine levels produced by unprimed, re-stimulated cells [-/+]. Observed inhibition of cytokine release was also dose dependent, with higher concentrations of FBG-C during priming inducing more effective reduction of TNF and IL-6 secretion in response to LPS. Suppression of cytokine production compared to unprimed, re-stimulated control [-/+] was observed for all tested FBC-C concentrations, and no potentiation of TNF or IL-6 release could be detected (Fig. 4.8 B). Cell viability in FBG-C primed samples was not significantly affected compared to the unprimed controls ([-/-] and [-/+]) (Fig. 4.8 C). Induction of LPS tolerance and β-glucan training was effective in monocytes used in the course of this experiment (Fig. 4.8 D). Hence, FBG-C was demonstrated to induce innate immune tolerance, but not training, to LPS.

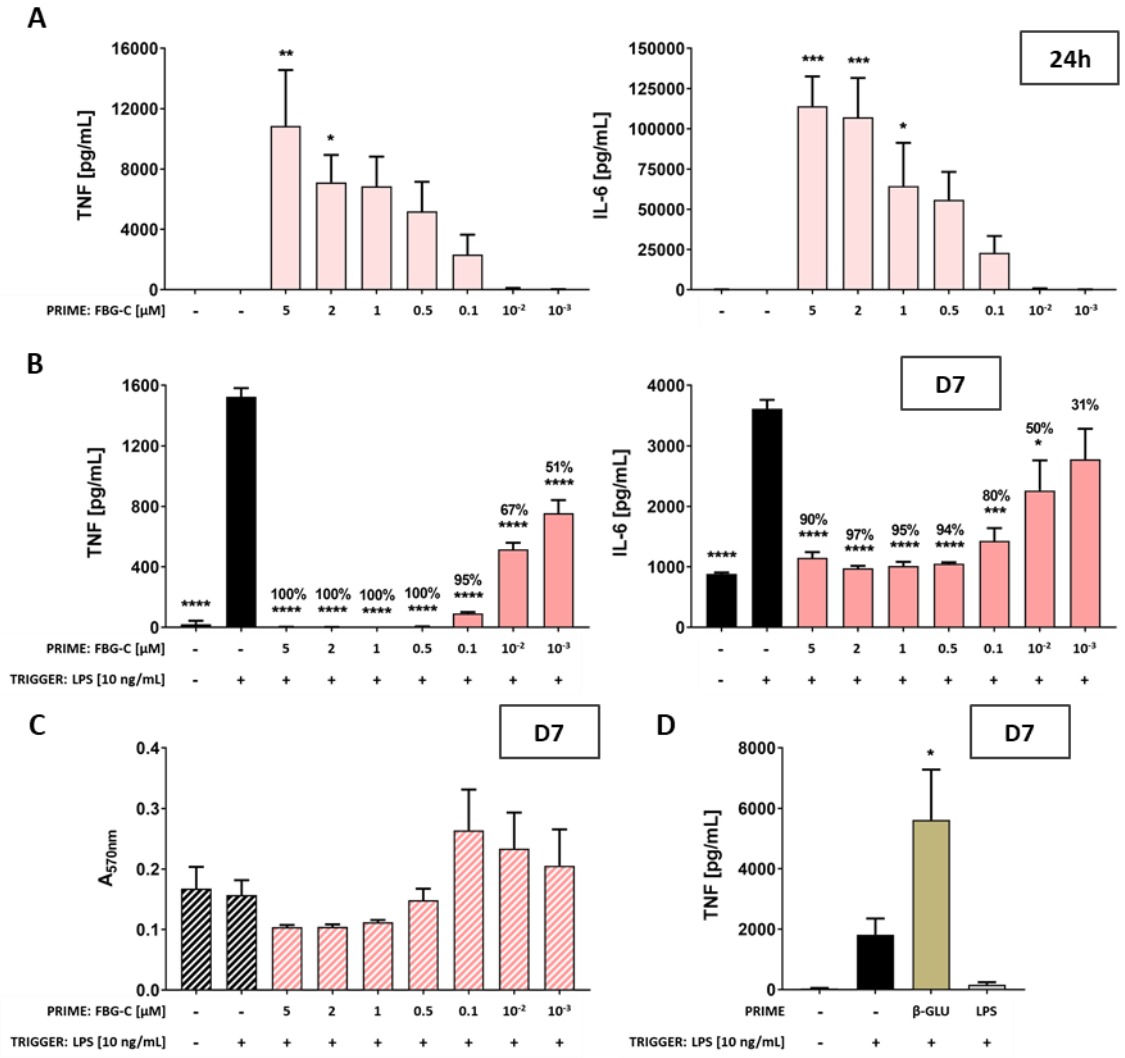


Figure 4.8 FBG-C induces tolerance, but not training, to LPS. Cells were primed for 24h with decreasing concentrations of FBG-C or left unstimulated [-] in serum free medium. After 5 days of rest in medium supplemented with 10% human serum, cells were then re-stimulated with LPS at 10 ng/mL [+], or left unstimulated [-]. TNF and IL-6 levels in media at 24h (**A**) and at day 7 (**B**) were measured by ELISA. MTT assay was performed to asses cell viability at day 7 (**C**). As a control, cells were also assayed for the induction of training by β-glucan and tolerance by LPS (**D**). Data are shown as mean ± SEM from 3 independent donors. Data was analysed using one-way ANOVA vs unstimulated [-] (**A**) and [-/-] (**C**) or unstimulated and re-stimulated with LPS [-/+] (**B**), *p < 0.05, **p < 0.01, ***p < 0.001, ****p < 0.0001. Percent inhibition of unstimulated and re-stimulated with LPS [-/+] normalized to unstimulated control [-/-] was shown above the bars (**B**).

Stimulation with LPS is known to induce tolerance to LPS, and in the previous paragraph FBG-C was demonstrated to induce tolerance to LPS. To further examine the specificity of LPS tolerance with regards to the secondary stimulus, monocytes were primed with LPS at 100 ng/mL, and then re-stimulated with decreasing doses of FBG-C. Following the primary stimulation with LPS, cells secreted TNF and IL-6, while no cytokine release was detected in the unprimed samples [-], as expected (Fig. 4.9 A). At day 7, low background levels of cytokines were quantified in the unstimulated sample [-/-], and unprimed, LPS re-stimulated cells [-/LPS] responded by producing TNF and IL-6, while LPS tolerance was observed in LPS primed, LPS re-stimulated positive control [+/LPS]. In unprimed, FBG-C re-stimulated samples dose dependent secretion of TNF and IL-6 was measured. Finally, cytokine release by LPS primed cells in response to re-stimulation with FBG-C was inhibited in comparison to unprimed cells re-stimulated with the same dose of FBG-C (Fig 4.9 B). No difference in cell viability assessed with MTT assay was observed between primed and unprimed cells (Fig. 4.9 C). Therefore, LPS was shown to induce tolerance to FBG-C.

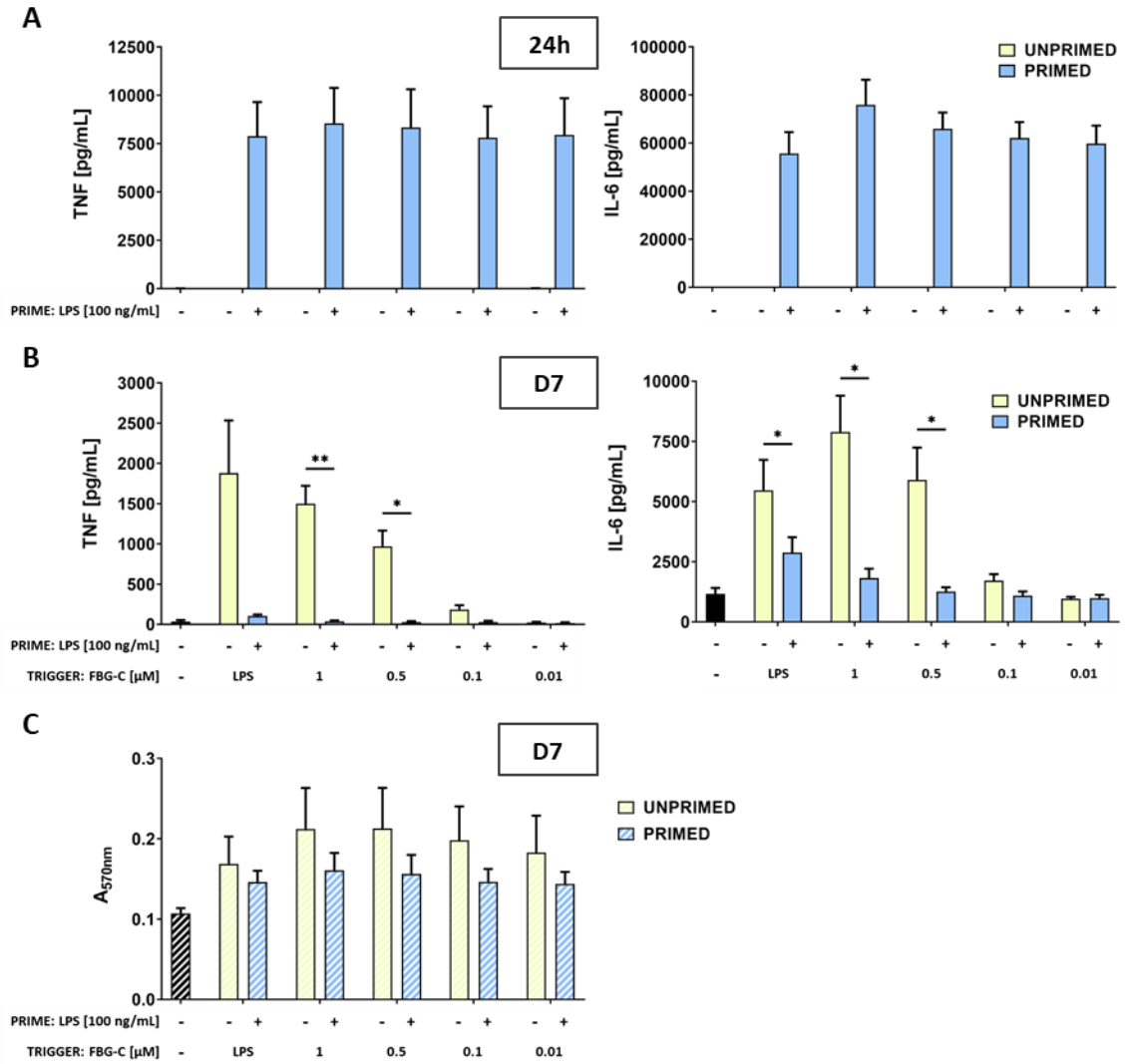


Figure 4.9 LPS induces tolerance to FBG-C. Cells were primed for 24h with LPS at 100 ng/mL [+] or left unprimed [-] in serum free medium. After 5 days of rest in medium supplemented with 10% human serum, cells were then re-stimulated with decreasing concentrations of FBG-C, LPS at 10 ng/mL or left unstimulated [-/-]. TNF and IL-6 levels in media at 24h (**A**) and at day 7 (**B**) were measured by ELISA. MTT assay was performed to asses cell viability at day 7 (**C**). Data are shown as mean ± SEM from 4 independent donors. Data was analysed using one-way ANOVA between the primed samples (**A**) or T-test between primed and unprimed (**B** and **C**); *p < 0.05, **p < 0.01.

As demonstrated above, FBG-C induces tolerance to LPS (Fig. 4.8), and LPS induces tolerance to FBG-C (Fig. 4.9). In addition, *C. albicans* β-glucan is known to induce training to LPS. To investigate if β-glucan can also train cell responses towards FBG-C, monocytes were primed with β-glucan (β-GLU) at 10 µg/mL, and then re-stimulated with decreasing doses of FBG-C. As observed previously, stimulation with β-glucan [+] did not induce production of TNF or IL-6, and no spontaneous release of these cytokines could be detected in unprimed cells [-] (Fig. 4.10 A). At the end of day 7, no TNF and low levels of IL-6 were secreted by unstimulated monocytes [-/-]. Classic training could be observed, with β-glucan primed, LPS re-stimulated cells [+/LPS] producing more cytokines than the unprimed, LPS re-stimulated control [-/LPS]. In response to re-stimulation with FBG-C, dose dependent release of TNF and IL-6 was detected, similar in β-glucan primed and unprimed samples (Fig. 4.10 B). No differences in cell viability was observed between unstimulated [-/-] and unprimed, re-stimulated samples, regardless of the secondary stimulus used. However, MTT signal was significantly increased in all β-glucan primed cells (Fig. 4.10 C). This experiment indicates that β-glucan does not induce training to FBG-C.

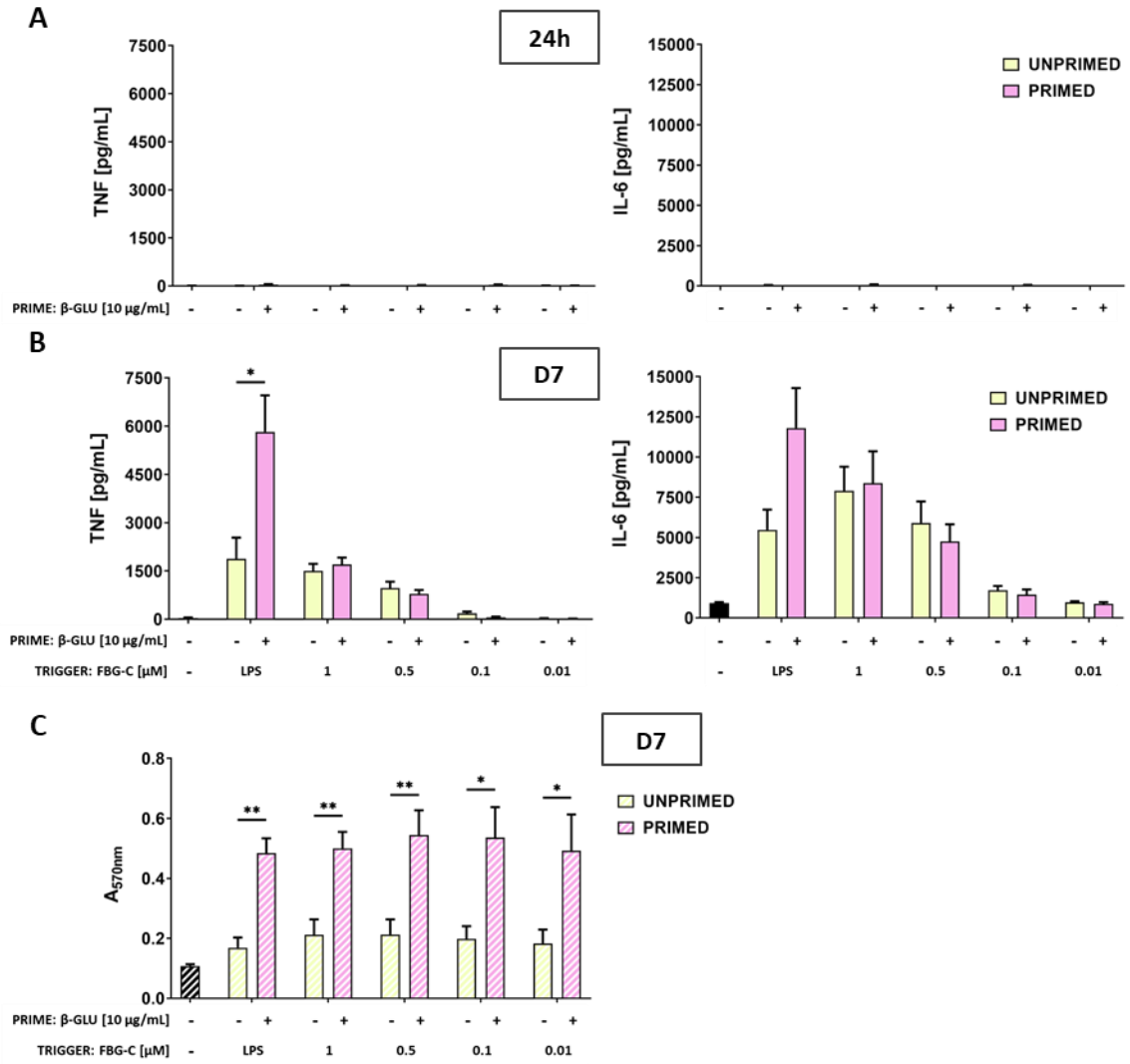


Figure 4.10 β-glucan does not induce training to FBG-C. Cells were primed for 24h with β-glucan (β-GLU) at 10 µg/mL [+] or left unprimed [-] in serum free medium. After 5 days of rest in medium supplemented with 10% human serum, cells were then re-stimulated with decreasing concentrations of FBG-C, LPS at 10 ng/mL or left unstimulated [-/-]. TNF and IL-6 levels in media at 24h (**A**) and at day 7 (**B**) were measured by ELISA. MTT assay was performed to asses cell viability at day 7 (**C**). Data are shown as mean ± SEM from 4 independent donors. Data was analysed using one-way ANOVA between the primed samples (**A**) or T-test between primed and unprimed (**B** and **C**); *p < 0.05, **p < 0.01.

So far, the study of the interplay between endogenous FBG-C and pathogenic stimuli revealed LPS can generate a state of tolerance, protecting from excessive inflammation, towards both a subsequent re-infection (re-stimulation with LPS) and tissue injury (re-stimulation with FBG-C). FBG-C was also demonstrated to tolerise innate immune cells to LPS, however it was not known if FBG-C could induce tolerance to itself, a phenomenon that could be of importance in repetitive tissue damage and during pathological chronic inflammation. To investigate this, monocytes were primed with decreasing concentrations of FBG-C, and then re-stimulated with FBG-C at 1 μM. Primary stimulation with FBG-C induced a dose dependent release of TNF and IL-6 at 24h, and no cytokines were produced by unprimed cells [-] (Fig. 4.11 A). Low background cytokine secretion was detected in unstimulated samples [-/-] at day 7, and unprimed cells responded to re-stimulation with FBG-C [-/+] by producing TNF and IL-6. In cells primed with FBG-C and re-stimulated inhibition of cytokine release was observed, compared to the unprimed, re-stimulated sample [-/+]. This suppression of cytokine response was the most effective at highest concentrations of FBG-C used during priming, with 1 – 0.1 μM inducing a complete blockade of TNF, and over 79% inhibition of IL-6 secretion. The cytokine responses of cells primed with lowest doses of FBG-C were not significantly different compared to the unprimed, re-stimulated control [-/+] (Fig. 4.11 B). Cell viability measured at the end of the protocol was lower in cells primed with FBG-C at 1 and 0.5 μM compared to the unprimed, re-stimulated control [-/+], although this was not statistically significant (Fig. 4.11 C). Monocytes used in this experiment displayed efficient classic LPS tolerance and β-glucan training (Fig. 4.11 D). Altogether, FBG-C was shown to induce tolerance not only to LPS, but also to itself.

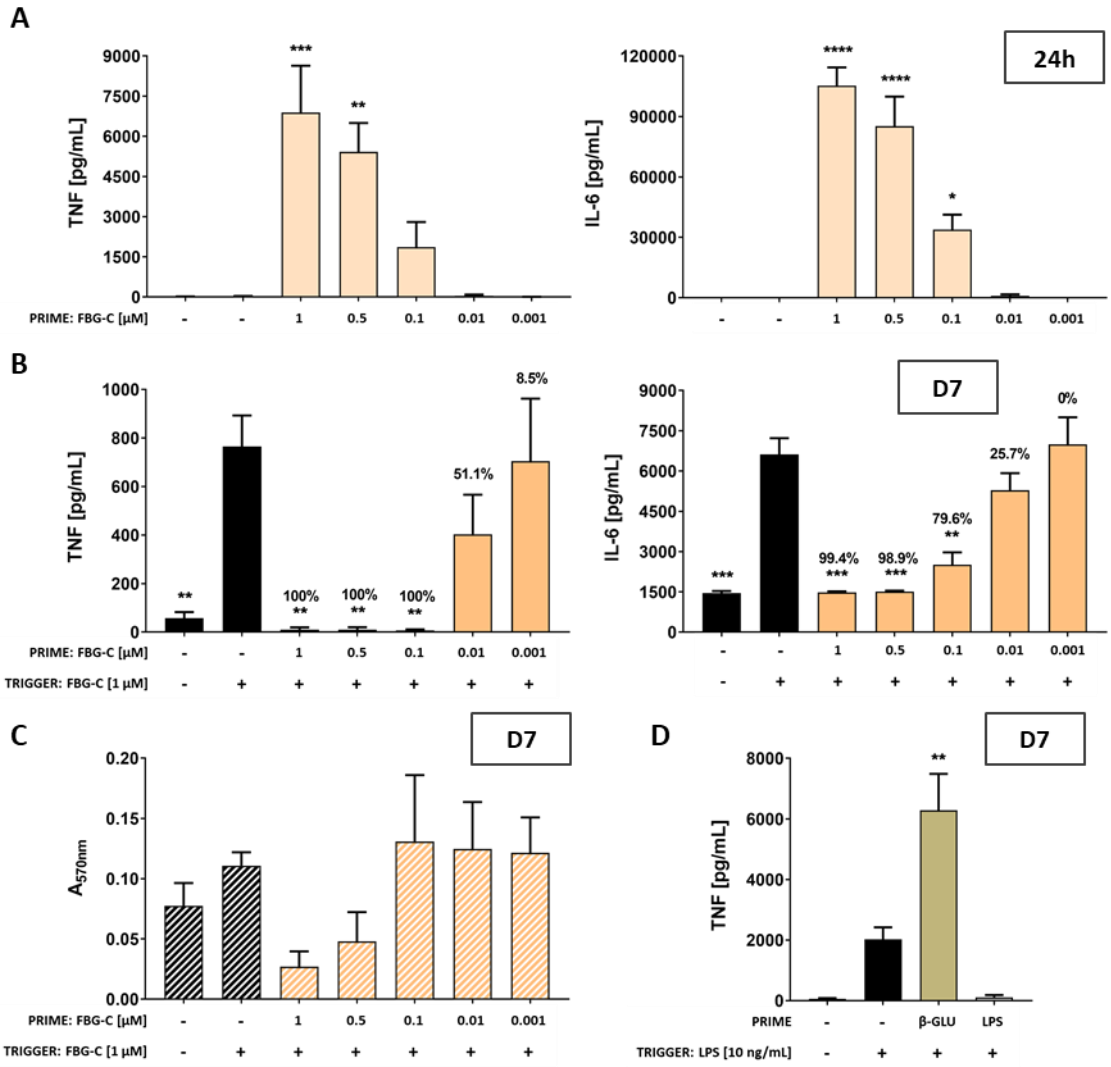


Figure 4.11 FBG-C induces tolerance to FBG-C. Cells were primed for 24h with decreasing concentrations of FBG-C or left unstimulated [-] in serum free medium. After 5 days of rest in medium supplemented with 10% human serum, cells were then re-stimulated with FBG-C at 1 µM [+], or left unstimulated [-]. TNF and IL-6 levels in media at 24h (**A**) and at day 7 (**B**) were measured by ELISA. MTT assay was performed to asses cell viability at day 7 (**C**). As a control, cells were also assayed for the induction of training by β-glucan and tolerance by LPS (**D**). Data are shown as mean ± SEM from 3 independent donors. Data was analysed using one-way ANOVA vs unprimed [-] (**A**) or unprimed and re-stimulated with LPS [-/+] (**B**, **C** and **D**), *p < 0.05, **p < 0.01, ***p < 0.001, ****p < 0.0001. Percent inhibition of unstimulated and re-stimulated with LPS [-/+] normalized to unstimulated control [-/-] was shown above the bars (**B**).

4.2.4 FBG-C induced tolerance: a protein dependent effect

The assessment of tolerance and training in paragraph 4.2.3 depends on measurement of cytokine release in medium after 7 days of culture, and changes in cell viability could partially account for quantified inhibition or potentiation of cytokine responses. In cells tolerised with FBG-C at 1 and 0.5 μM, and re-stimulated with FBG-C, cell viability measured by MTT assay was decreased compared to the control, albeit this was not statistically significant. However, in cells primed with lower dose of FBG-C, 0.1 μM, MTT signal was not affected, and tolerance was equally efficient (Fig. 4.11). On the other hand, β-glucan primed samples consistently display an enhanced MTT signal, regardless of the type and concentration of secondary stimulus (Fig. 4.10). In a previously published study investigating innate immune training in human monocytes, cell numbers in sample stimulated with β-glucan for 24h, followed by 6 days of rest, were demonstrated to be higher than in the unstimulated control [107].

Therefore, a memory experiment was performed, involving induction of FBG-C tolerance to FBG-C and LPS, as well as classic β-glucan training and LPS tolerance positive controls. To obtain more data on the cytotoxicity of the employed triggers in the memory protocol, a lactate dehydrogenase (LDH) assay was performed at 4h and 24h into PRIME and TRIGGER steps. Release of LDH, a cytosolic enzyme, into culture medium is a sign of membrane damage, and thus an indicator of cell cytotoxicity [327]. LDH was quantified in culture medium and lysed cells that remained adherent to the culture plate after removal of medium. In parallel, in cells from the same donor, an MTT assay was performed at the end of PRIME and TRIGGER steps. However, both MTT and LDH assays, as well as many other techniques aimed at measuring cell viability and cytotoxicity, are dependent on the metabolic activity of the cells [328]. This can pose a serious problem if utilised stimuli affect the cell metabolism. In fact, β-glucan is known

for inducing an extensive metabolic re-programming, involving a switch from oxidative phosphorylation to glycolysis [112, 113]. Thus, images of the stimulated cell cultures were also acquired using bright-field microscopy, in order to visually assess cell density at the start and at the end of the memory protocol.

The analysis of cell viability during priming revealed little cytotoxicity in the first 4h for all stimuli, evidenced by very low levels of released LDH, with the majority of LDH retained in adherent cells (Fig. 4.12 A). At 24h, a modest increase in LDH release was observed for the highest doses of FBG-C, which was only significantly higher than the unstimulated control [-] at 1 μM. Corresponding decreases in adherent LDH and MTT were observed for this condition, although the difference was not statistically significant in comparison to the unstimulated sample [-] (Fig. 4.12 B and C). Then, analysis of LDH and MTT at day 7 enabled assessment of cytotoxicity following re-stimulation. Little LDH secretion was detected at 4h in unstimulated sample [-/-], and this was higher than, or equal to the release measured in all other tested conditions. No significant differences in adherent cells were observed between the unprimed, FBG-C primed, and LPS primed samples. However, LDH levels in β-glucan primed adherent cells were significantly higher than in the unstimulated control [-/-] (Fig. 4.13 A). Analogous observations were made at 24h, with all the cultured cells releasing low levels of LDH, and all unprimed, FBG-C primed, and LPS primed adherent cells retaining similar amounts of the enzyme, while in β-glucan primed adherent cells this measurement was significantly higher (Fig. 4.13 B). No statistically significant differences between the samples were detected in the MTT assay at 24h, however the signal was higher in β-glucan primed cells (Fig. 4.13 C).

Surprisingly, while only low levels of LDH release were observed throughout the protocol, signifying little cytotoxicity was induced by the employed stimuli, overall amounts of LDH detected in lysed adherent cells were higher during the PRIME than the

TRIGGER step. This could suggest loss of cells, or a general decrease in cell metabolism. Photos taken at the beginning of the protocol show dense culture consisting of round cells of equal size. In comparison, at day 7 unstimulated culture [-/-] was much more sparse, with both round and elongated cells differing in size. The unprimed, FBG-C primed, and LPS primed samples, regardless of the secondary stimulus, demonstrated cell density similar to the unstimulated control [-/-]. Proportion of elongated cells was the highest in the FBG-C primed cultures re-stimulated with FBG-C or LPS. β-glucan primed, LPS re-stimulated culture showed the highest cells density and the most cell aggregation at day 7, however loss of cells could also be observed in this sample compared to the start of the protocol (Fig. 4.14).

Together the above data indicate that cell numbers decrease over the course of the memory protocol, and this is unlikely due to the cytotoxicity of the memory inducing stimuli, but rather a result of prolonged culture involving multiple cell handling steps (change of medium and washing). However, the decrease is similar in FBG-C and LPS primed cultures and the unprimed controls. β-glucan primed cultures display the least cell loss and highest viability measurements, which is probably linked to the metabolic activation of the cells induced by this stimulus, and possibly a stronger adherence to the culture vessel.

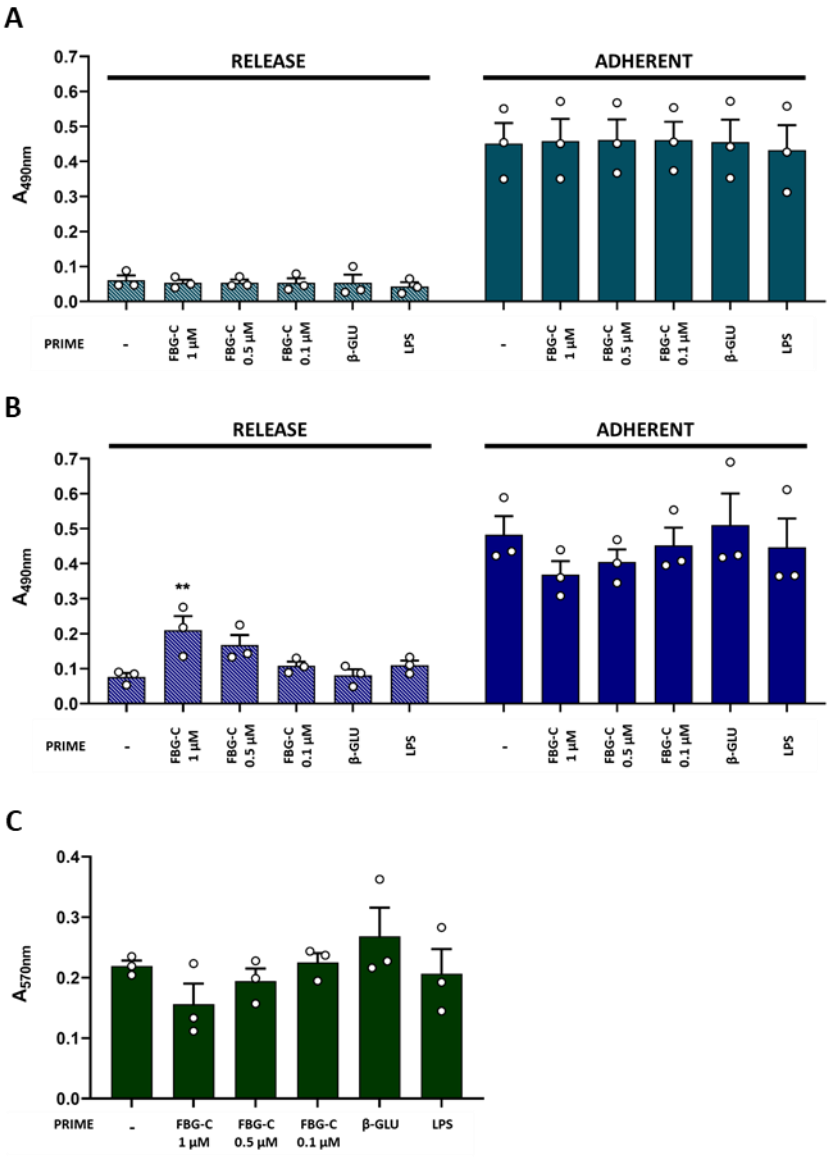


Figure 4.12 Cell viability during PRIME step. Cells were primed for 24h with decreasing concentrations of FBG-C, β-glucan at 10 µg/mL [β-GLU], LPS at 100 ng/mL or left unprimed [-] in serum free medium. To measure cell viability, LDH assay in culture medium (RELEASE), and in lysed adherent cells (ADHERENT) were performed 4h (**A**) and 24h (**B**) post stimulation start. MTT assay was also performed 24h post stimulation start (**C**). Data are shown as mean ± SEM from 3 independent donors. Data was analysed using one-way ANOVA vs unstimulated [-], **$p < 0.01$.

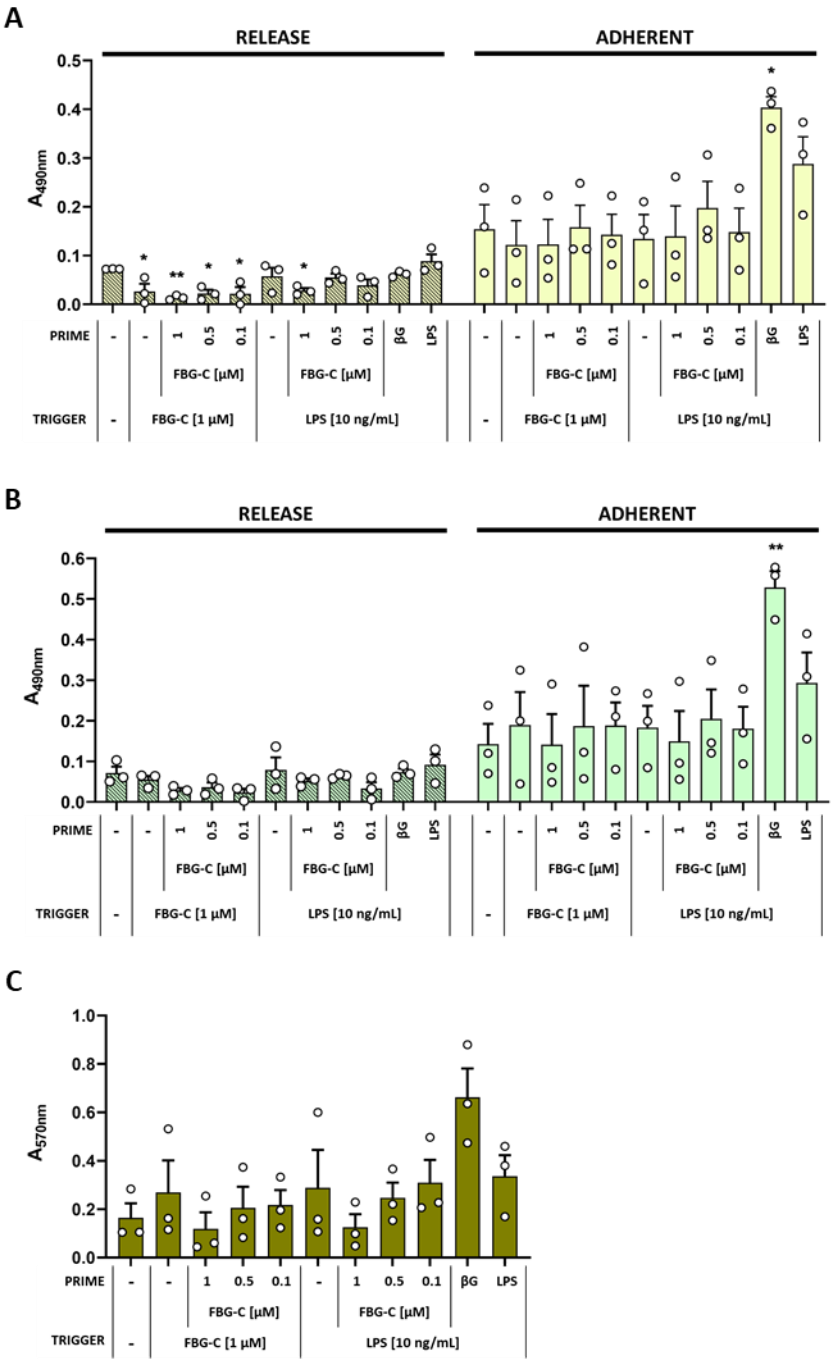


Figure 4.13 Cell viability during TRIGGER step. Cells were primed for 24h with decreasing concentrations of FBG-C, β-glucan at 10 µg/mL [βG], LPS at 100 ng/mL or left unprimed [-] in serum free medium. After 5 days of rest in medium supplemented with 10% human serum cells were then re-stimulated with FBG-C at 1 µM, LPS at 10 ng/mL or left unstimulated [-/-]. To measure cell viability, LDH assay in culture medium (RELEASE) and in lysed adherent cells (ADHERENT) were performed 4h (**A**) and 24h (**B**) into TRIGGER step. MTT assay was also performed at the end of the protocol (**C**). Data are shown as mean ± SEM from 3 independent donors. Data was analysed using one-way ANOVA vs unstimulated [-/-], **$p < 0.01$.

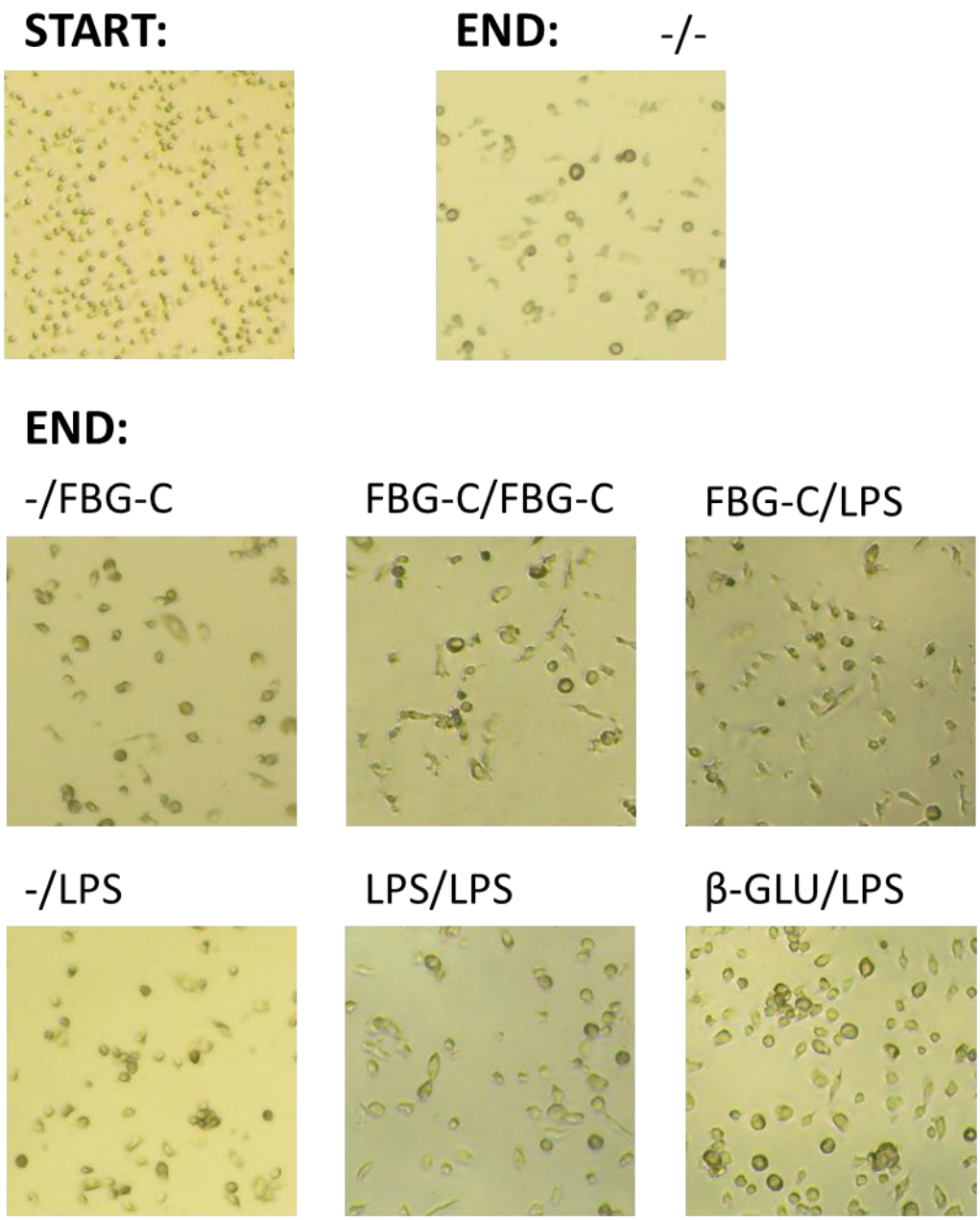


Figure 4.14 Cell viability - photos. Cells were primed for 24h with FBG-C at 1 μM, β-glucan at 10 μg/mL, LPS at 100 ng/mL or left unprimed [-] in serum free medium. After 5 days of rest in medium supplemented with 10% human serum cells were then re-stimulated with FBG-C at 1 μm, LPS at 10 ng/mL, or left unstimulated [-/-]. Photos were taken at the end of the protocol. 3 independent donors were analysed, picture shown is representative for each condition.

Tolerance induced by FBG-C is manifested by inhibition of TNF and IL-6 release, like the classic LPS tolerance. FBG-C used in this study is a recombinant protein produced in bacteria, and introduction of traces of endotoxin during protein preparation could have an impact on the observed memory effects. To validate that FBG-C induced tolerance is an exclusively protein dependent effect, and not due to LPS contamination, incubation of FBG-C with an endotoxin neutralizing agent PMB, or digestion with proteinase K was implemented before priming, as described previously in Chapter 3. Analysis of cell media at day 7 of the memory protocol revealed that induction of tolerance in sample primed with FBG-C treated with PMB was not affected. Inhibition of TNF and IL-6 release upon re-stimulation with LPS was observed in these cells, similarly to cells primed with FBG-C alone. When FBG-C was digested with proteinase K [PROT K], response of primed cells was not significantly lower than the unprimed, re-stimulated control. Cytokine secretion was not supressed in control samples primed with PMB or proteinase K alone (Fig. 4.15 A). Cell viability measured by MTT was not significantly different in any of the tested conditions (Fig. 4.15 B). Tolerance and training could be induced in cells used in this experiment by the classic stimuli LPS and β-glucan (Fig. 4.15 C).

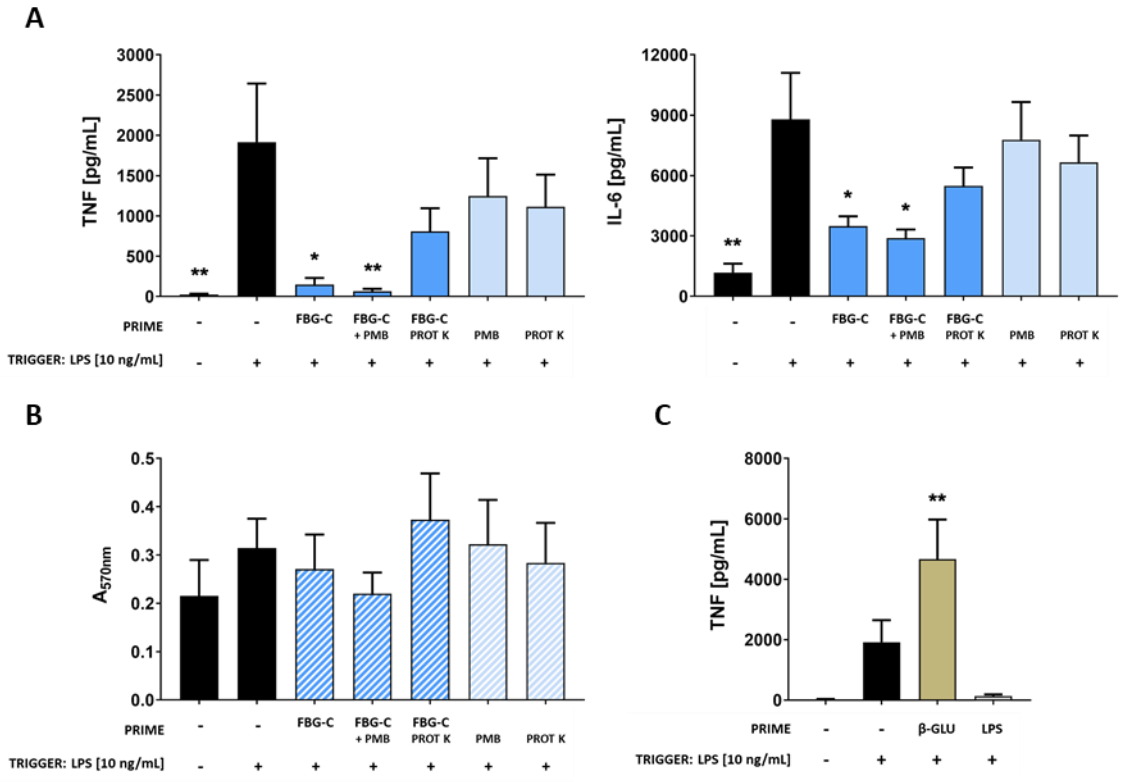


Figure 4.15 FBG-C induced tolerance is protein dependent and not due to LPS contamination. Cells were primed for 24h with FBG-C at 1 μM alone [FBG-C], pre-treated with PMB [FBG-C + PMB], digested with proteinase K [FBG-C + PROT K], PMB alone [PMB], proteinase K alone [PROT K] or left unprimed [-] in serum free medium. After 5 days of rest in medium supplemented with 10% human serum cells were then re-stimulated with LPS at 10 ng/mL [+], or left unstimulated [-/-]. TNF and IL-6 levels in media at the end of the protocol were measured by ELISA (**A**). MTT assay was performed to asses cell viability at the end of the experiment (**B**). Cells were also assayed for the induction of training by β-glucan and tolerance by LPS (**C**). Data are shown as mean ± SEM from 5 independent donors. Data was analysed using one-way ANOVA vs unprimed, re-stimulated with LPS [-/+], *$p < 0.05$, **$p < 0.01$.

In summary, the above control experiments confirm that tolerance induced by FBG-C cannot be ascribable to loss of cell viability or contamination with LPS, but requires structural integrity of the FBG-C protein.

4.2.5 FBG-C induced memory is not limited to re-activation of TLR4 pathway

In paragraph 4.2.3 priming of the monocytes with FBG-C was shown to induce tolerance in response to secondary challenge with FBG-C or LPS, and that priming cells with LPS induced tolerance to secondary challenge with FBG-C. Both LPS and FBG-C are activators of TLR4. However, the literature shows that LPS induces tolerance spanning beyond the TLR4 pathway, or 'cross tolerance'. For example LPS priming induces tolerance to secondary stimulation with the TLR2 agonist lipoteichoic acid [85]. To explore the extent of FBG-C cross-tolerance, cells were primed with FBG-C, and then re-stimulated with a wide variety of immune triggers, including pathogenic and endogenous ligands of diverse PRR receptors, whole pathogens, and cytokines (complete list of triggers presented in Table 4.1).

Table 4.1 Immune triggers used to interrogate FBG-C induced cross-tolerance.

Trigger	Receptor
LPS serotype EH100	TLR4
LPS serotype O111:B4	TLR4
Pam3CSK4	TLR2/TLR1
Poly(I:C)	TLR3
Flagellin	TLR5
CpG	TLR9
β-glucan	Dectin-1
Muramyl dipeptide	NOD2
Heat killed *C. albicans*	various
Heat killed *E. coli*	various
Heat killed *S. aureus*	various
Oxidised LDL	various
Fibrinogen ɣ FBG	TLR4
TNF	TNFR1 and TNFR2
IL-1α	IL-1RI and IL-1RII

Unprimed cells, treated with protein vehicle control (TN buffer and PMB) in the PRIME step, produced TNF in response to re-stimulation with different types of LPS (TLR4 ligands), Pam3CSK4 (P3CSK4; TLR2/TLR1 ligand) and flagellin (FLA; TLR5 ligand). However, very low levels of TNF secretion were detected in unprimed samples re-stimulated with poly(I:C) (agonist of TLR3), CpG (TLR9 agonist), β-glucan (dectin-1 agonist) and muramyl dipeptide (MDP; agonist of NOD2), indicating monocytes do not respond to these stimuli by producing TNF. In comparison to the unprimed controls, significant inhibition of TNF release was observed in FBG-C primed cells re-stimulated with LPS, P3CSK4 and flagellin, demonstrating FBG-C induces tolerance towards these stimuli (Fig. 4.16 A). Strong induction of IL-6 in unprimed cells was observed following

re-stimulation with LPS serotype EH100, and weaker stimulation of IL-6 production was detected for LPS serotype O111:B4 and flagellin. Unprimed cells re-stimulated with other immune triggers produced low, background levels of IL-6, equal to what has been consistently measured in unstimulated controls at day 7, signifying IL-6 is not induced in response to these stimuli. Statistically significant suppression of IL-6 secretion in FBG-C primed vs unprimed cells was observed following re-stimulation with LPS EH100, corroborating FBG-C induces effective tolerance to this stimulus on both IL-6 and TNF (Fig. 4.16 B). As many of the employed triggers could not induce production of TNF or IL-6 in human monocytes, and thus establishment of memory could not be assessed, release of IL-8 in culture media at day 7 was also quantified. Cells re-stimulated with all of the tested triggers could produce IL-8, with LPS, P3CSK4 and flagellin inducing higher levels, and poly(I:C), CpG, β-glucan and MDP inducing lower levels of the cytokine. FBG-C induced tolerance towards LPS EH100 could be observed again, with lower levels of IL-8 secreted by FBG-C primed than unprimed cells. However, IL-8 release was higher in FBG-C primed cells compared to the unprimed controls upon re-stimulation with poly(I:C), β-glucan and MDP, suggesting FBG-C can also train monocyte response to these triggers. Response to CpG was also potentiated in primed cells, however this effect was not statistically significant (Fig. 4.16 C). Moderate differences in cell viability measured by MTT assay in primed versus unprimed cells were detected, with MTT signal being significantly higher in unprimed samples re-stimulated with LPS EH100, P3CSK4, poly(I:C) and flagellin (Fig. 4.16 D).

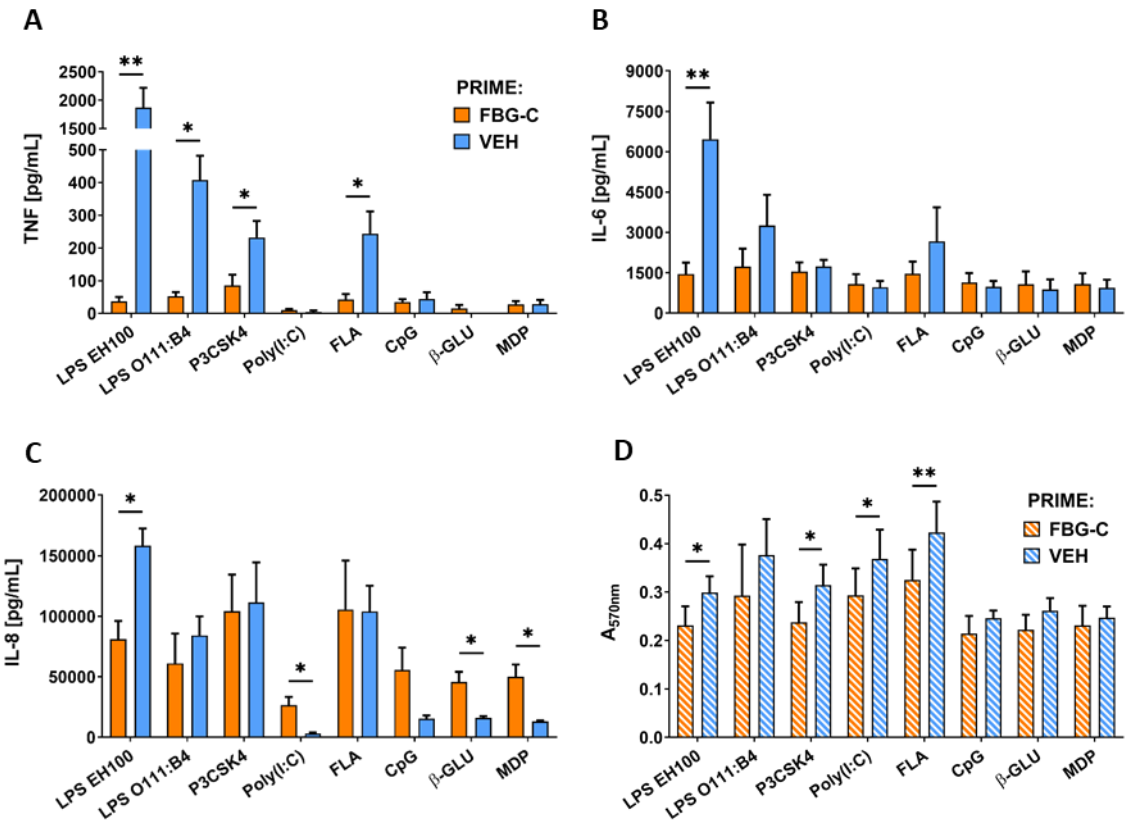


Figure 4.16 FBG-C induced memory is not contained to the activation of TLR4 pathway I. Cells were primed for 24h with FBG-C at 1 µm, or treated with protein vehicle control (TN buffer with PMB) [VEH] in serum free medium. After 5 days of rest in medium supplemented with 10% human serum cells were then re-stimulated with various TLR ligands. TNF (**A**), IL-6 (**B**) and IL-8 (**C**) levels in media at the end of the protocol were measured by ELISA. MTT assay was performed to asses cell viability at the end of the experiment (**D**). Data are shown as mean ± SEM from 3-5 independent donors. Data was analysed using paired T-test, *p < 0.05, **p < 0.01.

In the second part of this experiment, the highest levels of TNF were produced by unprimed cells re-stimulated with heat killed *E. coli* (HKEC), although the observed data spread was large. Low levels of TNF were measured following re-stimulation with heat killed *S. aureus* (HKSA) and FBG domain from fibrinogen ɣ (FIB-G), and the remaining triggers induced very low levels of the cytokine, or none at all. Inhibition of TNF release in FBG-C primed compared to unprimed samples was detected following re-stimulation with HKEC and HKSA, however this was only significant for HKSA (Fig. 4.17 A). Similarly, the most potent induction of IL-6 secretion was observed in HKEC re-stimulated samples, and other triggers induced low levels of IL-6. Decrease in IL-6

production was measured in FBG-C primed cells re-stimulated with HKEC compared to the unprimed control, however this was not deemed statistically significant. A minor, but significant increase in IL-6 release was found in primed cells re-stimulated with FIB-G, in comparison to the unprimed sample, indicating FBG-C induces a weak training of IL-6 response to that trigger (Fig. 4.17 B). Monocytes were shown to produce IL-8 in response to the tested triggers, with the highest levels of this cytokine induced by HKEC. Significant potentiation of IL-8 secretion in primed versus unprimed cells was quantified in samples re-stimulated with HKCA, oxidised LDL (oxLDL) and TNF, demonstrating FBG-C induced training towards these stimuli. Increase of IL-8 production in primed cells in response to HKSA and IL-1α, and decrease in response to HKEC were also detected, however these effects were not significant (Fig. 4.17 C). Minor decrease in cell viability between unprimed and primed samples were identified in HKEC and HKSA re-stimulated cells, while no differences could be observed for the other tested stimuli (Fig. 4.17 D.

Hence, FBG-C was demonstrated to induce innate immune memory to ligands of various PRRs. What is more, FBG-C was shown to generate not only tolerance, but also training, depending on the trigger used for re-stimulation.

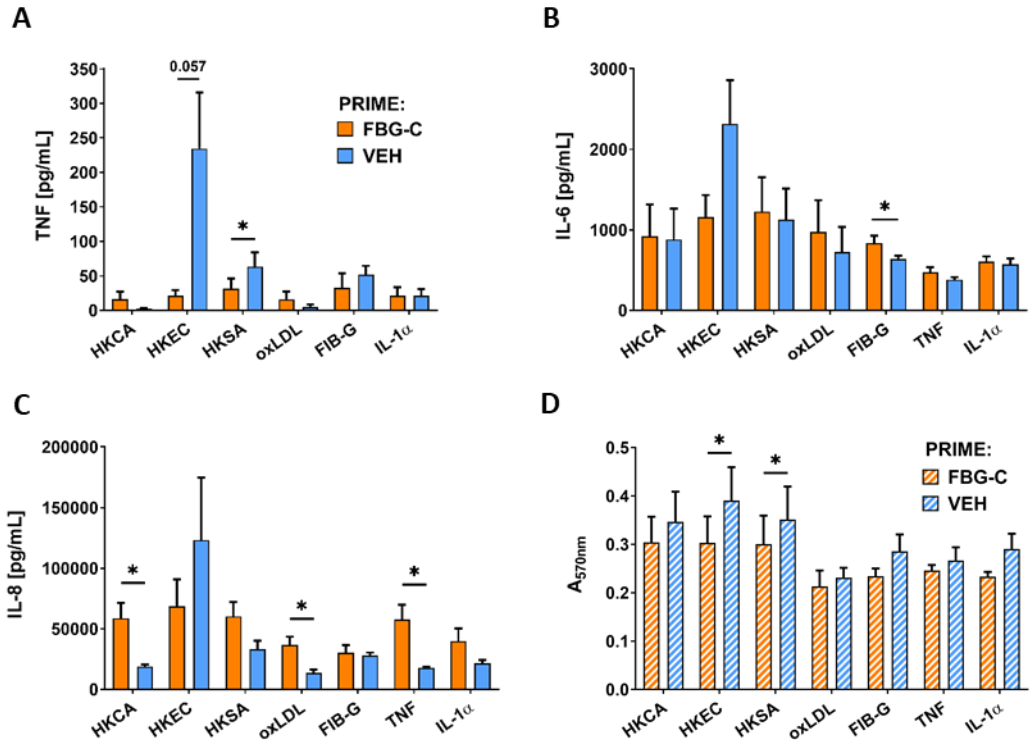


Figure 4.17 FBG-C induced memory is not contained to the activation of TLR4 pathway II. Cells were primed for 24h with FBG-C at 1 μm, treated with protein vehicle control (TN buffer with PMB) [VEH] in serum free medium. After 5 days of rest in medium supplemented with 10% human serum cells were then re-stimulated with whole heat killed pathogens, endogenous TLR ligands, or cytokines. TNF (**A**), IL-6 (**B**) and IL-8 (**C**) levels in media at the end of the protocol were measured by ELISA. MTT assay was performed to asses cell viability at the end of the experiment (**D**). Data are shown as mean ± SEM from 3-5 independent donors. Data was analysed using paired T-test, *p < 0.05.

4.2.6 FBG-C induced memory is effector-specific and temporally regulated

Published data indicates that LPS tolerance can be observed already in cells primed for at least 6h and then re-stimulated immediately after [185]; and cells primed with LPS for 24h were shown to remain tolerised following 5 days of rest [39]. In a study investigating β-glucan training, different duration of priming (2/4/24h) and rest (1/3/6 days) was tested, revealing a minimum of 3 days of rest are required to observe trained cytokine response, and the effect is still detected after 6 days of rest. With regards to the priming, 2h stimulation with β-glucan was sufficient for the induction of training, however maximum cytokine secretion potentiation was achieved with 24h priming [107].

The above findings on FBG-C induced innate immune memory in human monocytes were obtained using a 7 day protocol, including a 5 day rest step between the stimulations. In paragraph 4.2.1 inhibition of response induced by FBG-C and LPS in macrophages was observed in a considerably shorter timescale, with re-stimulation performed immediately post priming. To better understand when FBG-C induced memory develops and how long it persists, the memory assay was modified to facilitate a time course experiment, with variable length of rest (0 – 7 days) between the PRIME and TRIGGER steps (Fig. 4.18).

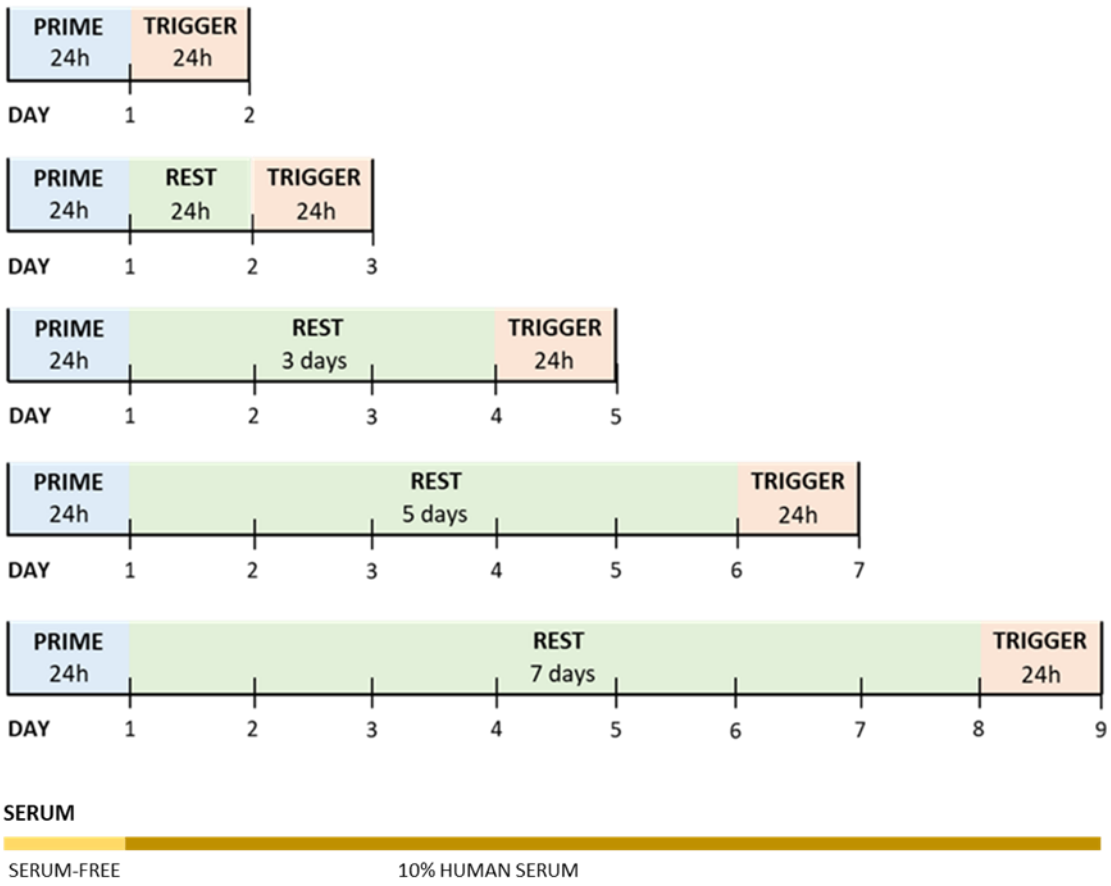


Figure 4.18 Time course memory assay protocol. Primary human monocytes were seeded in a 96 well plate and stimulated for 24h with training or tolerizing agents in serum free medium (PRIME). Medium was then collected, cells washed with PBS and fresh medium supplemented with 10% human serum added. Cells were rested for 0-7 days (REST), with one medium change during the resting period (at day 4, only for 5 and 7 day rest protocols). Following REST step, cells were re-stimulated with LPS (TRIGGER) for 24h, after which time medium was collected for analysis and cell viability assay was performed.

Analysis of TNF release demonstrated FBG-C tolerance was induced in cells re-stimulated immediately following priming, with a fold change over unprimed, re-stimulated control of approximately 0.6. However, following 1 day of rest the tolerance was more effective, and the cells displayed nearly complete suppression of TNF secretion. A similar magnitude of FBG-C tolerance was also observed after resting the cells for 3, 5 or 7 days (Fig. 4.19 A). Maximal LPS tolerance was detected already in cells re-stimulated directly after the 24h of priming, and comparable tolerance efficiency was retained in cells rested for 1, 3, 5 or 7 days (Fig. 4.19 B). β-glucan training was found in the no rest protocol, though the potentiation of TNF response was further increased

with 1 day of rest, reaching maximum effectiveness (fold change of 1.5 with no rest and 2.0 with 1 day of rest). Cells were still trained following 3, 5 and 7 days of rest (fold change of more than 1), however the magnitude of β-glucan training was gradually decreasing in these samples (Fig. 4.19 C).

A striking observation was made following the measurement of IL-6 release. Production of this cytokine in cells re-stimulated without any rest was 10 times higher in FBG-C primed cells compared to the unprimed control, demonstrating induction of FBG-C training to LPS. Superinduction of IL-6 was still detected in a 1 day rest protocol (fold change of 3), however the magnitude of this effect was decreasing the longer cells were rested before re-stimulation. IL-6 secretion by primed and unprimed cells rested for 3 days was similar, and tolerance was detected in samples rested for 5 and 7 days (Fig. 4.19 D). Superinduction was also observed in LPS primed sample in a no rest protocol, with primed cells producing 5 times more IL-6 than the unprimed control. After 1 and 3 days of rest IL-6 was no longer induced and similar levels of the cytokine were produced by primed and unprimed cells (fold change of approximately 1).When rested for longer periods of time, 5 or 7 days, cells demonstrated tolerised IL-6 response to re-stimulation with LPS (Fig. 4.19 E). 1 day of rest was required to detect β-glucan induced potentiation of IL-6 secretion, and training was the most potent in cells rested for 3 days before re-stimulation (3 times increase in primed versus unprimed sample). β-glucan training of lower magnitude was measured after 5 and 7 days of rest (fold change of 1.5) (Fig. 4.19 F).

Therefore, FBG-C and LPS were demonstrated to generate TNF tolerance that is maintained in monocytes for up to 8 days, while IL-6 response is initially superinduced, and only later tolerised. Such a biphasic manner of regulation was not reported before

either for LPS or FBG-C, and substantiates effector-specific nature of innate immune memory, first hinted in paragraph 4.2.5.

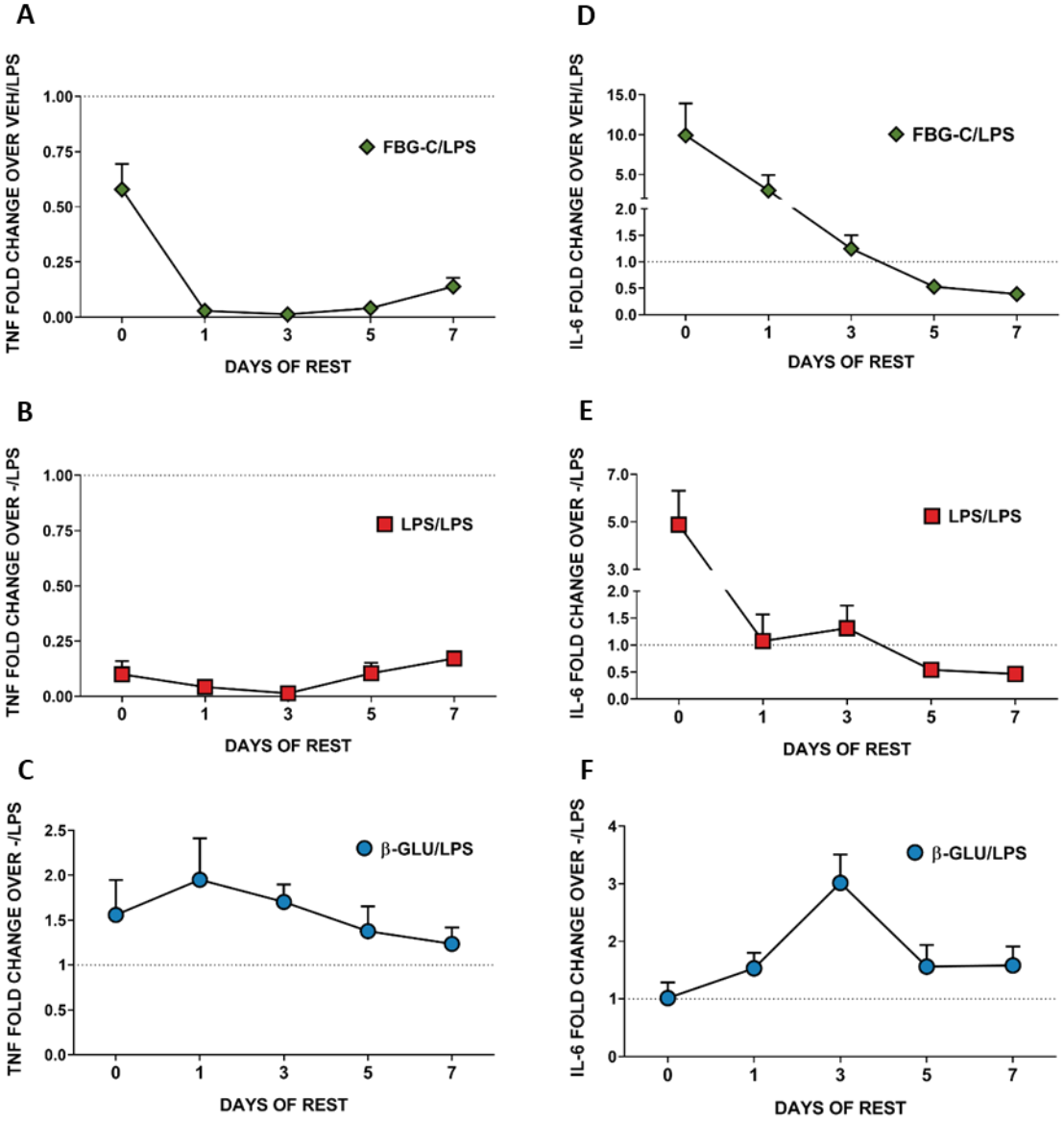


Figure 4.19 Memory effects are effector-specific and temporally regulated. Cells were primed for 24h with FBG-C at 1 μM, LPS at 100 ng/mL, β-glucan at 10 μg/mL [β-GLU], protein vehicle control [VEH], or left unprimed [-] in serum free medium. After 0-7 days of rest in medium supplemented with 10% human serum cells were then re-stimulated with LPS at 10 ng/mL (protocol outline presented in Fig. 4.18). TNF (**A**, **B**, **C**) and IL-6 (**D**, **E**, **F**) release in culture media at the end of the protocol were measured by ELISA. Data are shown as mean fold change over vehicle control treated, re-stimulated ([VEH/LPS], for FBG-C) or unprimed, re-stimulated ([-/LPS], for LPS) ± SEM from 3 independent donors.

4.2.7 Transcriptional analysis of effector molecules in FBG-C induced memory

All data thus far has assessed cytokine release by ELISA of cell culture supernatant in memory protocols. The observed inhibition of cytokine release upon secondary stimulation following FBG-C priming may be mediated via a number of mechanisms. These include reduced cytokine mRNA transcription, reduced mRNA stability, or reduced cytokine secretion, for example by sequestering of effector molecules inside the cell. To further investigate the mechanisms underpinning FBG-C induced memory, TNF and IL6 mRNA levels were quantified at various time points throughout PRIME and TRIGGER steps, in two different memory protocols – one in which there was no rest period between PRIME and TRIGGER, and the classis 5 day rest memory protocol (Fig. 4.20).

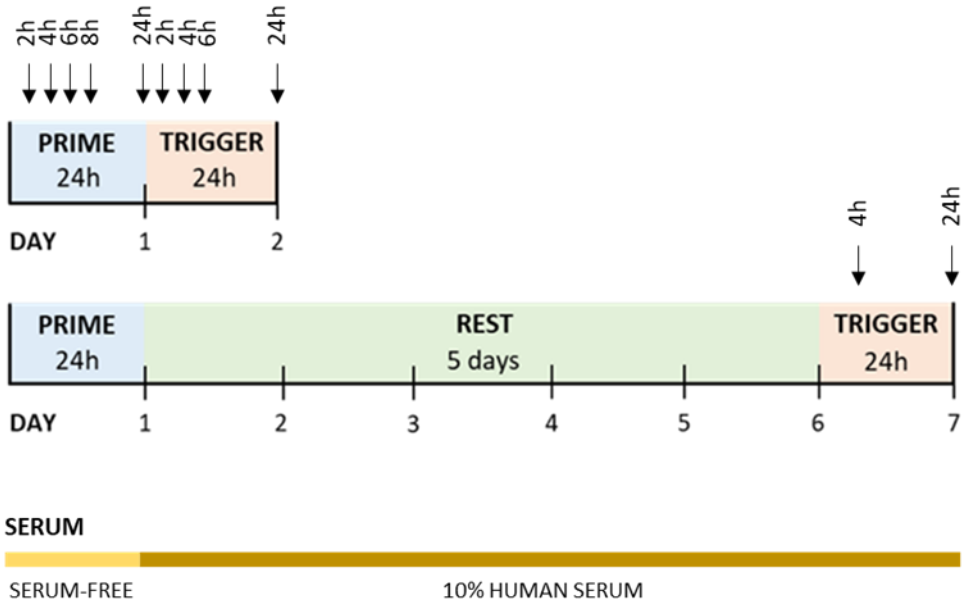


Figure 4.20 Transcriptional regulation of memory - assay protocol. Primary human monocytes were seeded in a 96 well plate and stimulated for 24h with FBG-C or LPS in serum free medium (PRIME). Medium was then collected, cells washed with PBS and fresh medium supplemented with 10% human serum added. Cells were not rested, or rested for 5 days (REST) with one medium change during the resting period (at day 4). Next, cells were re-stimulated with LPS (TRIGGER) for 24h. Cell lysates and culture media for analysis were collected at (timepoints marked with arrows): 2, 4, 6, 8, and 24h into PRIME step; 2, 4, 6, and 24h into TRIGGER step (no REST protocol); 4 and 24h into TRIGGER step (5 day REST protocol).

First, mRNA levels and cytokine secretion following primary stimulation with FBG-C and LPS were analysed in the same cells. No induction of cytokine mRNA could be detected in cells that were left unstimulated [-], or treated with protein vehicle control [VEH]. Stimulation with FBG-C and LPS induced expression of TNF and IL-6, with mRNA levels reaching maximum at 6h. FBG-C generated higher peak levels of mRNA than LPS, however this effect was not statistically significant ($p = 0.079$; relative expression of 300 versus 140 for TNF, and 670 versus 180 for IL-6). The kinetics of induction were comparable for TNF and IL-6, however upregulation of TNF by both stimuli was faster, with mRNA levels elevated already at 2h, whilst 4h were needed to detect an increase in IL-6 mRNA. By 24h levels of TNF mRNA decreased back to baseline, yet expression of IL-6 was still induced (relative expression of 35 for FBG-C and 25 for LPS) (Fig. 4.21 A). No cytokine release could be detected in unstimulated [-] and vehicle treated [VEH] samples. FBG-C and LPS induced secretion of TNF and IL-6 that was delayed in time compared to the observed mRNA induction. Cytokine levels were increasing over time, up to 24h. While the kinetics of cytokine release induced by both stimuli were similar, significantly higher maximal amounts of TNF and IL-6 were detected at 24h in FBG-C stimulated than LPS stimulated samples ($p = 0.006$ and 11,000 pg/mL versus 8,000 pg/mL for TNF; $p = 0.016$ and 65,000 pg/mL versus 38,000 pg/mL for IL-6) (Fig. 4.21 B).

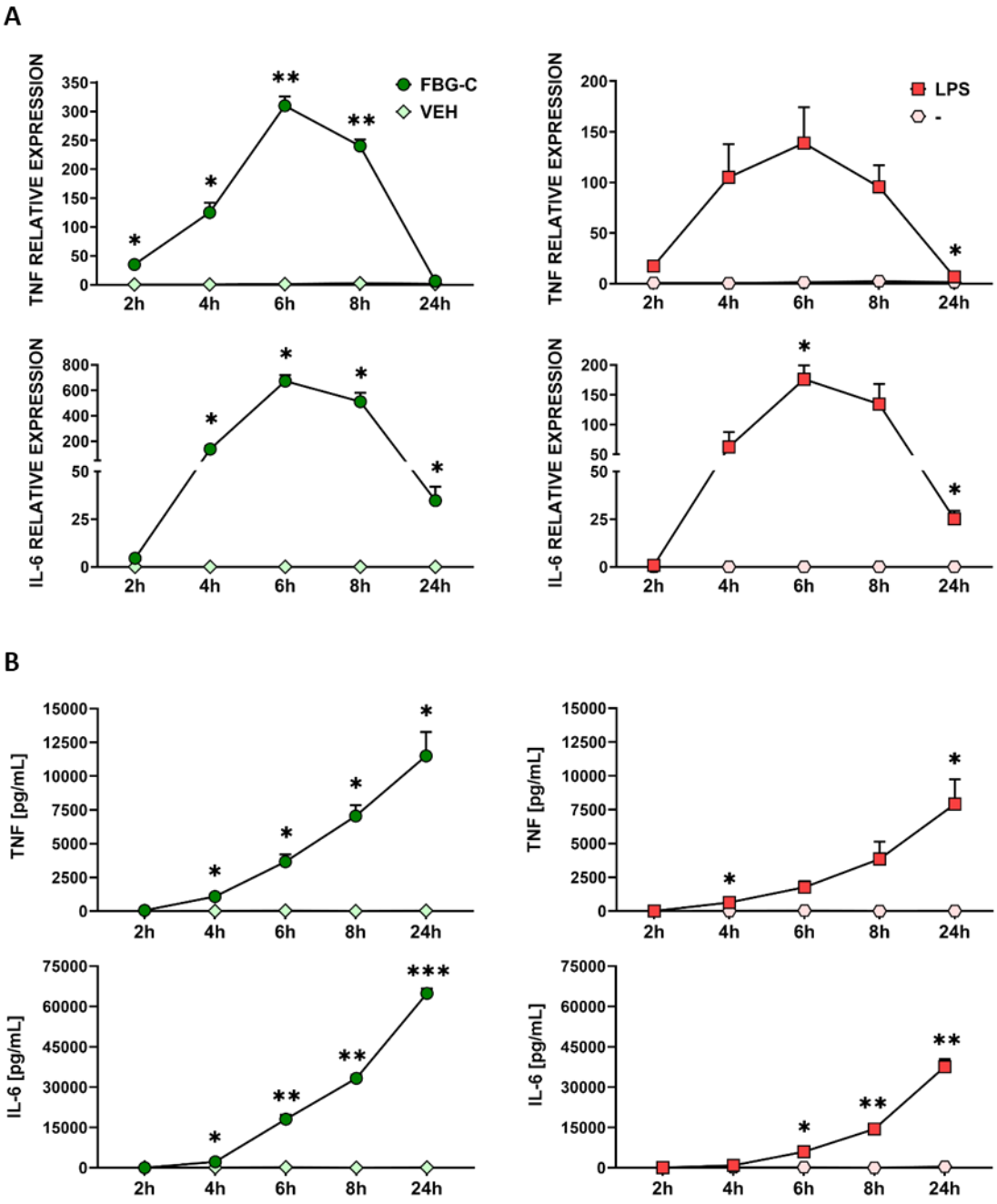


Figure 4.21 Transcriptional regulation of memory - primary response. Cells were primed for 2/4/6/8/24h with FBG-C at 1 µM, LPS at 100 ng/mL, protein vehicle control [VEH], or left unstimulated [-] in serum free medium (protocol outline presented in Fig. 4.20). TNF and IL-6 transcription was measured in cell lysates by TaqMan based qPCR (**A**) and protein release in culture media was measured by ELISA (**B**). Data are shown as mean ± SEM from 3 independent donors. Data was analysed using paired T-test between primed and vehicle treated (FBG-C), or primed and unstimulated (LPS); *p < 0.05, **p < 0.01, ***p < 0.001.

Next, cytokine mRNA and secretion following secondary stimulation with no rest in between PRIME and TRIGGER were analysed. During re-stimulation, cells which were not primed with FBG or LPS ([VEH/LPS] and [-/LPS]) exhibited a fast induction of TNF transcript. Levels of TNF mRNA reached maximum at 2h, and began decreasing thereafter, returning to baseline by 24h. Kinetics of TNF induction observed in vehicle treated [VEH] and unstimulated [-] samples were comparable, however peak mRNA levels were higher in vehicle treated cells ($p = 0.045$, relative expression of 700 versus 550). No significant TNF induction at any time point could be detected in re-stimulated cells primed with FBG-C or LPS ([FBG/LPS] and [LPS/LPS]). Induction of IL-6 expression in samples treated with vehicle control, or untreated, and re-stimulated ([VEH/LPS] and [-/LPS]) was slower than TNF, with mRNA levels elevated at 4h and peaking at 6h, before decreasing back to baseline by 24h. Quantified maximal IL-6 mRNA was comparable in these two samples ($p = 0.5$, relative expression of 25 and 21). In FBG-C and LPS primed cells cytokine mRNA levels were elevated at the start of the TRIGGER step, as described previously. *De novo* transcription was activated following re-stimulation, inducing further increase in IL-6 expression that reached maximum at 2h. Subsequently, IL-6 mRNA levels started decreasing and returned to baseline by 24h. Peak levels of IL-6 transcript in FBG-C and LPS primed cells were not significantly different ($p = 0.16$, relative expression of 53 and 38, respectively) (Fig. 4.22 A). Secretion of TNF was observed in vehicle treated and untreated cells re-stimulated with LPS ([VEH/LPS] and [-/LPS]) at 2h, and was further increased by 4h, after which remained at a similar level until 24h (3,000 – 4,000 pg/mL for vehicle treated, and 2,500 – 3,000 pg/mL for untreated). Low levels of TNF were detected in FBG-C and LPS primed samples ([FBG/LPS] and [LPS/LPS]) at all time points. Induction of IL-6 release following re-stimulation of cells which were not primed with FBG or LPS ([VEH/LPS]

and [-/LPS]) was slower than TNF, detected by 6h and peaking at 24h. Quantified at 24h maximum IL-6 levels were higher in vehicle treated than untreated sample, however this was not statistically significant ($p = 0.10$, 4,500 pg/mL for vehicle treated, and 2,800 pg/mL for untreated). Secretion of IL-6 by primed cells ([FBG/LPS] and [LPS/LPS]) was observed at 2h, and gradually increased with time, reaching maximum at 24h. IL-6 release by primed cells was higher than the vehicle treated, or untreated control, and a little higher maximum levels were measured in LPS primed than FBG-C primed cells ($p = 0.16$, 14,000 pg/mL versus 11,000 pg/mL) (Fig. 4.22 B).

Finally, secondary responses on cytokine transcription and secretion were measured in a protocol involving 5 days of rest. Expression of TNF and IL-6 in vehicle treated and untreated cells ([VEH/LPS] and [-/LPS]) was observed at 4h, with similar levels of mRNA detected in both conditions (relative expression of 190 versus 160 for TNF, and 50 versus 45 for IL-6), and then declined to baseline by 24h. Low levels of cytokine transcripts were found in primed cells at 4h, lower in FBG-C [FBG/LPS] than LPS [LPS/LPS] primed, however this difference was only significant for TNF ($p = 0.003$ and relative expression of 9.5 versus 22.5 for TNF, $p = 0.135$ and relative expression of 16.5 versus 23.5 for IL-6). Thereafter, TNF and IL-6 mRNA levels returned to baseline by 24h (Fig. 4.23 A). Secretion of TNF was observed in samples treated with vehicle control, or untreated, and re-stimulated ([VEH/LPS] and [-/LPS]) at 4h (5,500 pg/mL for vehicle, and 4,400 pg/mL for untreated), and a small decrease was measured at 24h (3,600 pg/mL and 3,300 pg/mL). Very low or low levels of TNF were detected in FBG-C and LPS primed cells ([FBG/LPS] and [LPS/LPS]), respectively. Induction of IL-6 release in unprimed control samples ([VEH/LPS] and [-/LPS]) was seen at 4h (4,000 pg/mL for vehicle and 3,300 pg/mL for untreated), and cytokine levels peaked at 24h (9,000 pg/mL and 8,700 pg/mL, respectively). In primed cells, production of IL-6 was

also observed at 4h and increased at 24h (from 1,500 pg/mL to 2,300 pg/mL for FBG-C primed sample [FBG-C/LPS], and from 2,800 pg/mL to 3,600 pg/mL for LPS primed sample [LPS/LPS]). Peak IL-6 levels were not significantly different between the primed samples ($p = 0.07$) (Fig. 4.23 B).

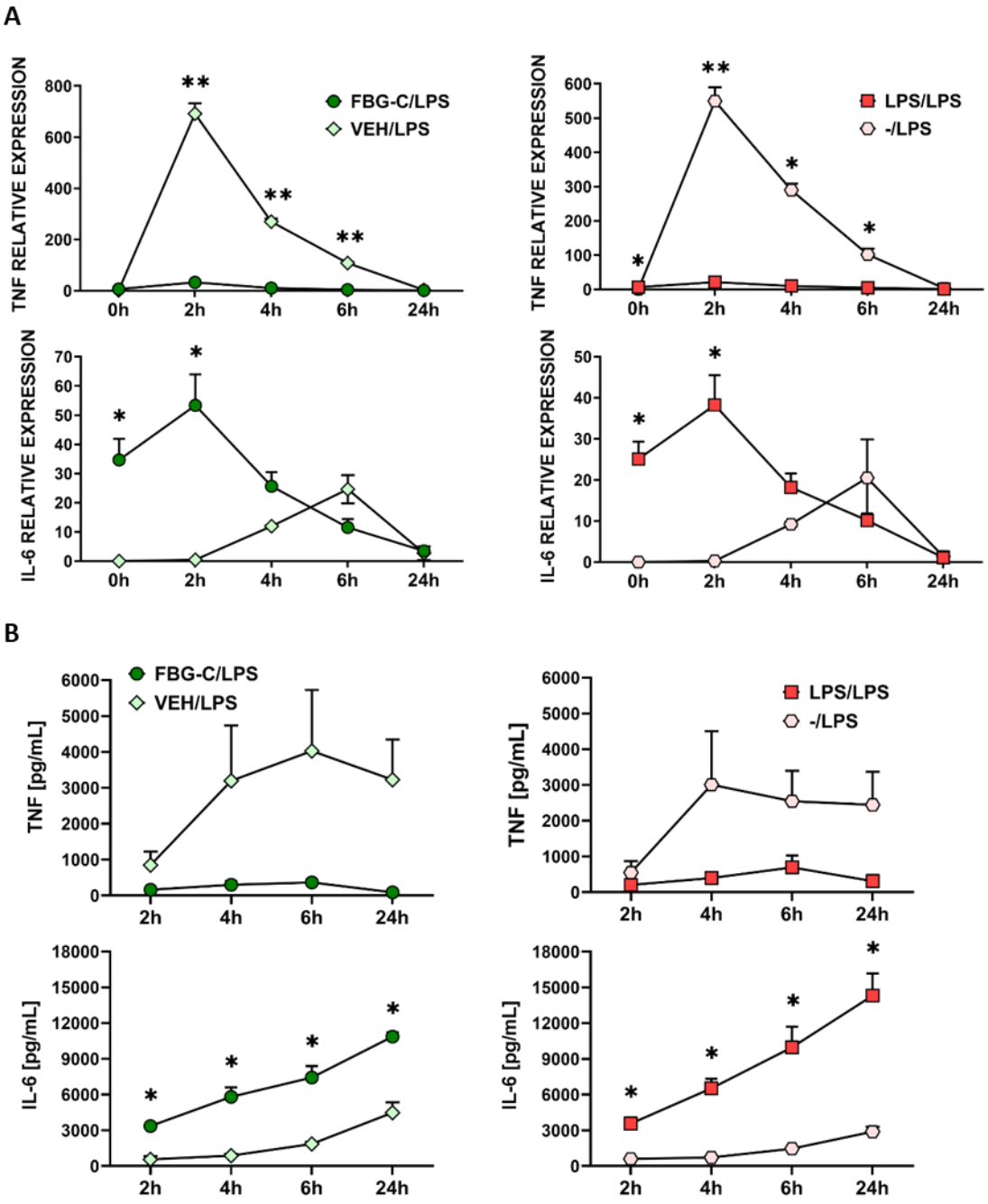


Figure 4.22 Transcriptional regulation of memory – secondary response I. Cells were primed for 24h with FBG-C at 1 µM, LPS at 100 ng/mL, protein vehicle control [VEH], or left unstimulated [-] in serum free medium. Immediately after, cells were re-stimulated with LPS at 10 ng/mL in medium supplemented with 10% human serum (protocol outline presented in Fig. 4.20). TNF and IL-6 transcription was measured by TaqMan based qPCR in cell lysates (**A**), and secretion was measured by ELISA in culture media (**B**), collected at different time points into the second stimulus. Data are shown as mean ± SEM from 3 independent donors. Data was analysed using paired T-test between primed and vehicle primed (FBG-C), or primed and unprimed (LPS); *p < 0.05, **p < 0.01.

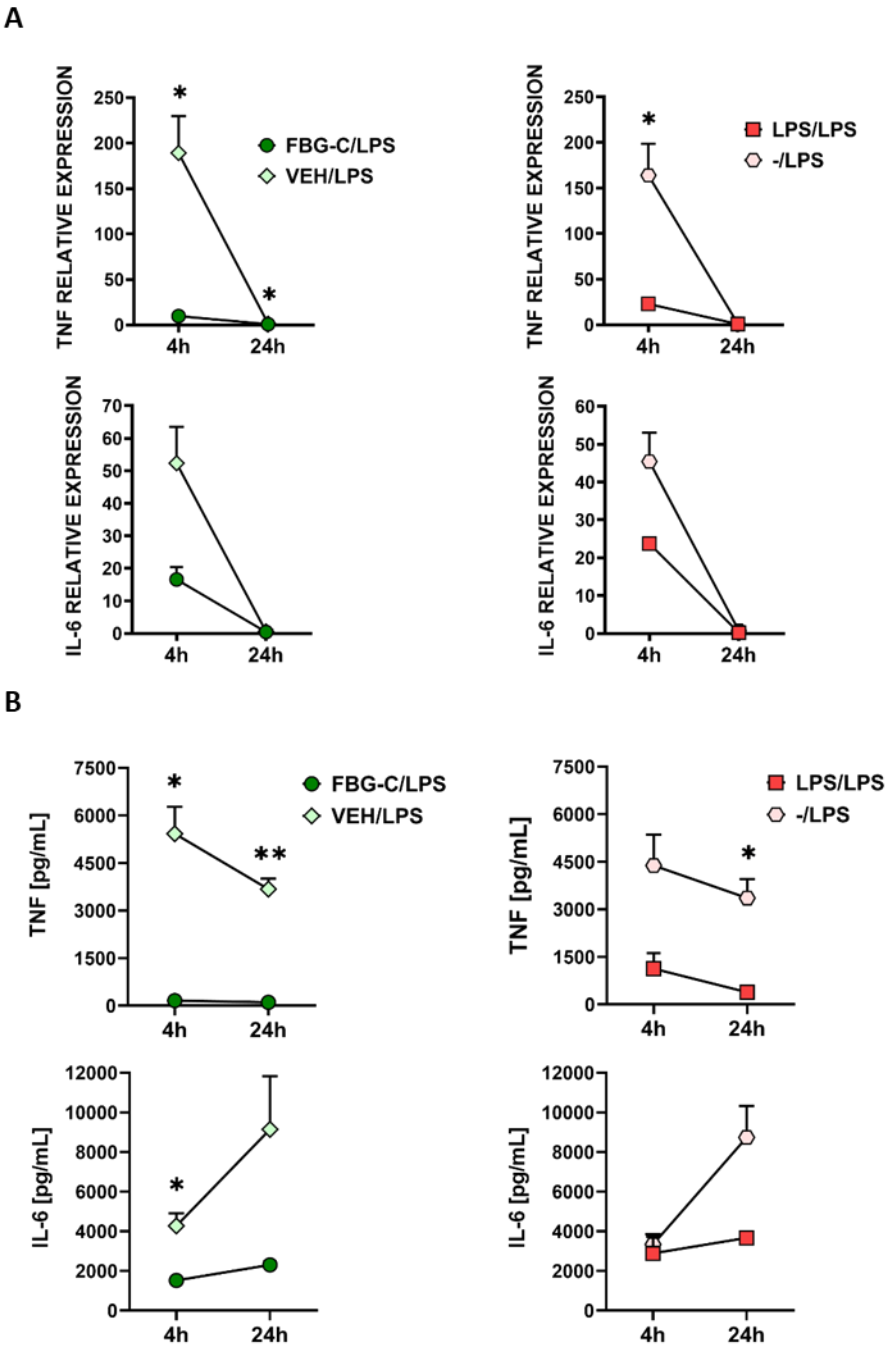


Figure 4.23 Transcriptional regulation of memory – secondary response II. Cells were primed for 24h with FBG-C at 1 μM, LPS at 100 ng/mL, protein vehicle control [VEH], or left unstimulated [-] in serum free medium. Following 5 days of rest, cells were re-stimulated with LPS at 10 ng/mL in medium supplemented with 10% human serum (protocol outline presented in Fig. 4.20). TNF and IL-6 transcription was measured by TaqMan based qPCR in cell lysates (**A**), and secretion was measured by ELISA in culture media (**B**), collected at different time points into the second stimulus. Data are shown as mean ± SEM from 3 independent donors. Data was analysed using paired T-test between primed and vehicle primed (FBG-C), or primed and unprimed (LPS); *$p < 0.05$, **$p < 0.01$.

The above study verified FBG-C induced memory to be transcriptionally controlled, and implied IL-6 superinduction might be driven both by mRNA remaining in the cells from the PRIME step, and *de novo* transcription induced at re-stimulation. To elucidate the contribution of the secondary stimulus, a control memory experiment was performed, where alongside re-stimulated primed [+/+], and unprimed [VEH/+ or -/+] cells, additional sample was included, which was primed, but did not receive the secondary stimulus [+/-]. Analysis of TNF secretion revealed induction of tolerance in FBG-C and LPS primed cells, as expected. In the FBG-C and LPS primed, but not stimulated cells [+/-], TNF release was not different from the respective tolerised samples [+/+], and at the level of, or lower than, the unstimulated control [-/-] (Fig. 4.24 A). Significant IL-6 superinduction following re-stimulation was observed between the vehicle treated [VEH/+] and FBG-C primed [FBG-C +/+], and untreated [-/+] and LPS primed [LPS +/+] cells. Then, IL-6 levels in the FBG-C primed, unstimulated [FBG-C +/-] sample were significantly lower than the superinduction measured in FBG-C primed, re-stimulated cells [FBG-C +/+]. Production of IL-6 in LPS primed, unstimulated cells [LPS +/-] was a little lower than in the re-stimulated cells primed with LPS [LPS +/+], however this was not a statistically significant difference (Fig. 4.24 B). Altogether, this data indicates that secondary challenge is necessary to obtain the full extent of FBG-C generated IL-6 superinduction. On the other hand, IL-6 potentiation observed in LPS primed cells is largely a passive process, with little contribution from the secondary stimulus.

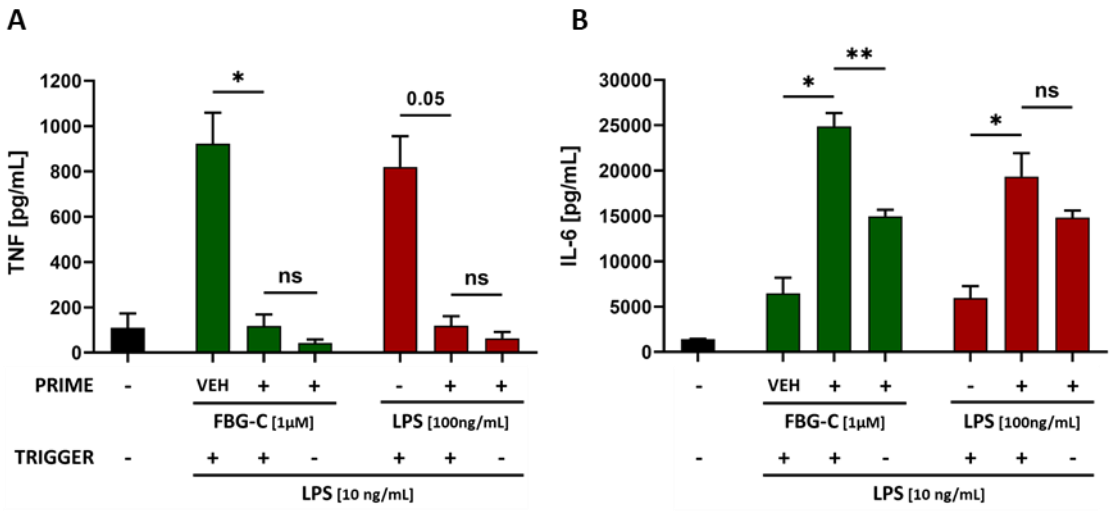


Figure 4.24 Secondary challenge contributes to the FBG-C generated IL-6 superinduction. Cells were primed for 24h with FBG-C at 1 µM, LPS at 100 ng/mL, protein vehicle control [VEH], or left unprimed [-] in serum free medium. Immediately after cells were re-stimulated with LPS at 10 ng/mL, or left unstimulated [-] in medium supplemented with 10% human serum. TNF (**A**) and IL-6 (**B**) release was measured by ELISA in culture media collected at the end of the protocol. Data are shown as mean ± SEM from 4 independent donors. Data was analysed using paired T-test; *p < 0.05, **p < 0.01.

Finally, to prove that TNF tolerance and IL-6 superinduction observed in the no rest protocol is FBG-C dependent, thermal denaturation of the protein was performed prior to priming. Analysis of TNF secretion following re-stimulation with LPS demonstrated effective induction of tolerance by FBG-C, however inhibition of TNF release was no longer observed in the cells primed with boiled protein, which responded similarly to the vehicle treated control. LPS induced tolerance was also generated as expected, and boiling of LPS did not abolish its capability to tolerise the cells (Fig. 4.25 A). Superinduction of IL-6 was observed in FBG-C primed sample, but not in the cells primed with boiled FBG-C that secreted levels of IL-6 similar to the vehicle treated, re-stimulated control. Both LPS and boiled LPS generated similar IL-6 superinduction (Fig. 4.25 B). This experiment demonstrates that intact protein structure is necessary for FBG-C to induce TNF tolerance and IL-6 superinduction.

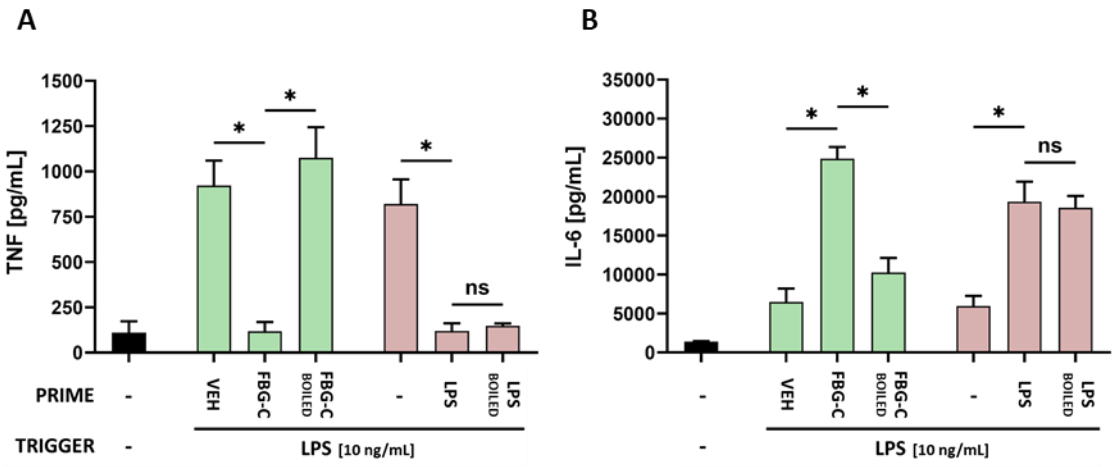


Figure 4.25 FBG-C induced tolerance/superinduction is protein dependent. Cells were primed for 24h with FBG-C at 1 μM, boiled FBG-C, LPS at 100 ng/mL, boiled LPS, protein vehicle control [VEH], or left unprimed [-] in serum free medium. Immediately after cells were re-stimulated with LPS at 10 ng/mL in medium supplemented with 10% human serum. TNF (**A**) and IL-6 (**B**) release was measured by ELISA in culture media collected at the end of the protocol. Data are shown as mean ± SEM from 4 independent donors. Data was analysed using paired T-test; *$p < 0.05$.

In summary, the data presented above demonstrates that FBG-C induced innate immune memory is mediated at the level of cytokine transcription, as it was previously described for LPS tolerance. Production of TNF was found to be quickly and effectively tolerised, with induction of mRNA arrested. IL-6 response is first potentiated, and only then becomes suppressed, however this phenomenon is not regulated in the same way for FBG-C and LPS. FBG-C priming allows for *de novo* transcription to be activated by the secondary challenge, accounting for the higher IL-6 superinduction peak, whereas LPS does not, and the observed LPS superinduction effect is transcriptionally passive, resulting from lingering mRNA. Therefore, it was discovered that FBG-C and LPS innate immune memory, whilst producing similar cytokine effects, are in fact differently controlled phenomena.

4.2.8 Epigenetic re-programing in FBG-C induced memory

For the effector proteins to be transcribed, chromatin, that is the template DNA wrapped around the histone proteins, needs to acquire an open conformation, allowing access of RNA polymerase II. The state of chromatin is regulated through various chemical tags, such as DNA methylation and post-translational modifications of histone tail proteins (e.g. methylation, acetylation, phosphorylation) [75]. These marks are placed by a specific group of enzymes called writers, and can be removed by erasers. Finally, another group of proteins, readers, are responsible for identifying the marks [329]. Together, this protein machinery facilitates transition between heterochromatin (closed) and euchromatin (open), and thus controls gene transcription.

Research conducted on the LPS tolerance and β-glucan training demonstrates extensive chromatin remodelling is a pivotal mechanism underlying induction of innate memory [39, 74, 76]. To advance the understanding of epigenetic re-programming by FBG-C, a library of 58 small molecule probes targeting various epigenetic pathway proteins (readers, writers, erasers) was tested in a modified memory protocol (full list of probes used and their targets is presented in Table 2.15) (Fig. 4.26).

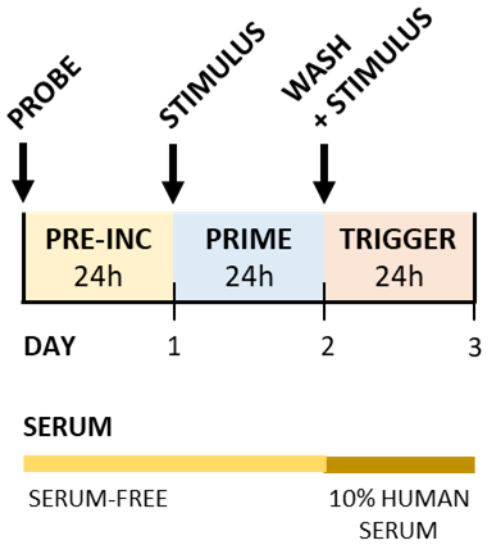


Figure 4.26 Epigenetic probe library testing – assay protocol. Primary human monocytes were seeded in a 96 well plate and pre-incubated with epigenetic probes for 24h in serum free medium (PRE-INC). Then, FBG-C or LPS was added for 24h (PRIME). Medium was then collected, cells washed with PBS and fresh medium supplemented with 10% human serum added. Cells were then re-stimulated with LPS for 24h (TRIGGER), after which time medium was collected for analysis and cell viability assay was performed.

Pre-treatment with the probes affected TNF inhibition (Fig. 4.27) and IL-6 potentiation (Fig. 4.28) in FBG-C and LPS primed monocytes. Both increase in efficiency and rescue of the memory effects could be observed. To understand the functional interactions between the protein targets of probes inducing a significant alteration in tolerance and training efficiency, STRING (Search Tool for the Retrieval of Interacting Genes/Proteins) analysis was performed. Interaction networks were generated for TNF tolerance and IL-6 superinduction, revealing interacting epigenetic pathway proteins and complexes involved in the establishment of the memory phenotypes. Both FBG-C and LPS induced TNF tolerance was associated with extensive methytransferase functionality, and formation of the histone methylating COMPASS family complexes. Furthermore, MOZ/MORF complexes conducting histone tail modifications through KAT6A acetyltransferase, as well as KAT2A/2B acetyltransferases were identified to be involved. Activity of PAD4, a peptidyl arginine deiminase citrulinating histones and other proteins, was also found to be important for the establishment of efficient tolerance (Fig. 4.29).

Analysis of IL-6 data also demonstrated involvement of COMPASS family proteins, suggesting these complexes are linked with both types of the described memory phenomena, tolerance and superinduction. Moreover, activity of CBP/p300 transcriptional coactivators and acetyltransferases was associated with efficient potentiation of IL-6. These features were shared between the FBG-C and LPS induced superinduction, however considerable differences were also observed. For LPS driven superinduction of IL-6 there was additional requirement for chromatin remodelling BAF-type complexes, and an overall high dependence on bromodomain functionality. On the other hand, activity of PAD4 was needed for FBG-C, but not LPS, induced superinduction (Fig. 4.30).

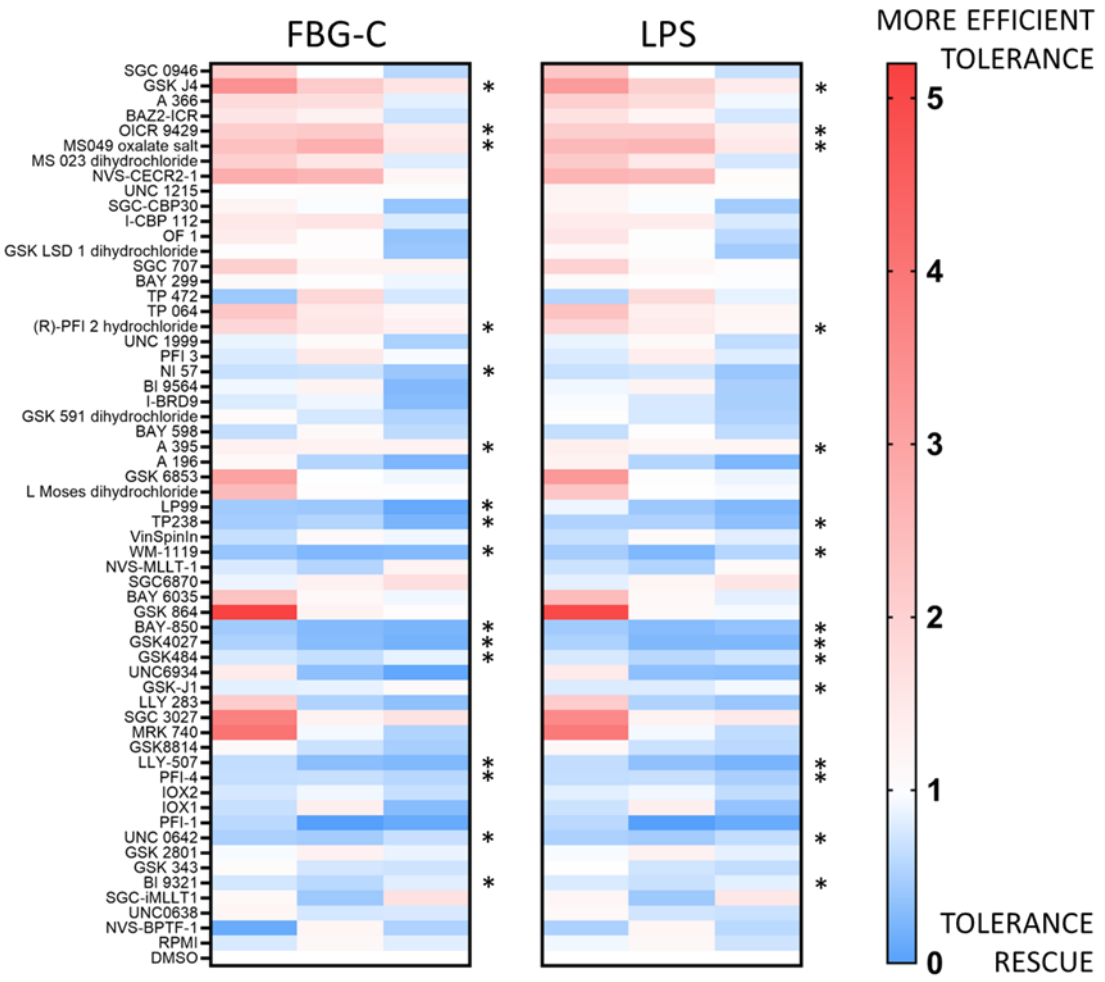


Figure 4.27 Epigenetic probes alter TNF tolerance. Cells were pre-incubated with epigenetic probes, DMSO control [DMSO], or left untreated [RPPMI] for 24h in serum free medium. Next, FBG-C at 1 μM, LPS at 100 ng/mL, or no stimuli was added for 24h. Medium was then collected, cells washed with PBS and fresh medium supplemented with 10% human serum added. Cells were then re-stimulated with LPS at 10 ng/mL for 24h. TNF release was measured by ELISA in culture media collected at the end of the protocol. MTT assay was performed to asses cell viability at the end of the experiment. Data are presented as TNF tolerance (decrease in TNF secretion between unprimed, re-stimulated and primed, re-stimulated) fold change over DMSO control, normalized to MTT, from 3 independent donors. Data was analysed using paired T-test vs DMSO control; *$p < 0.05$.

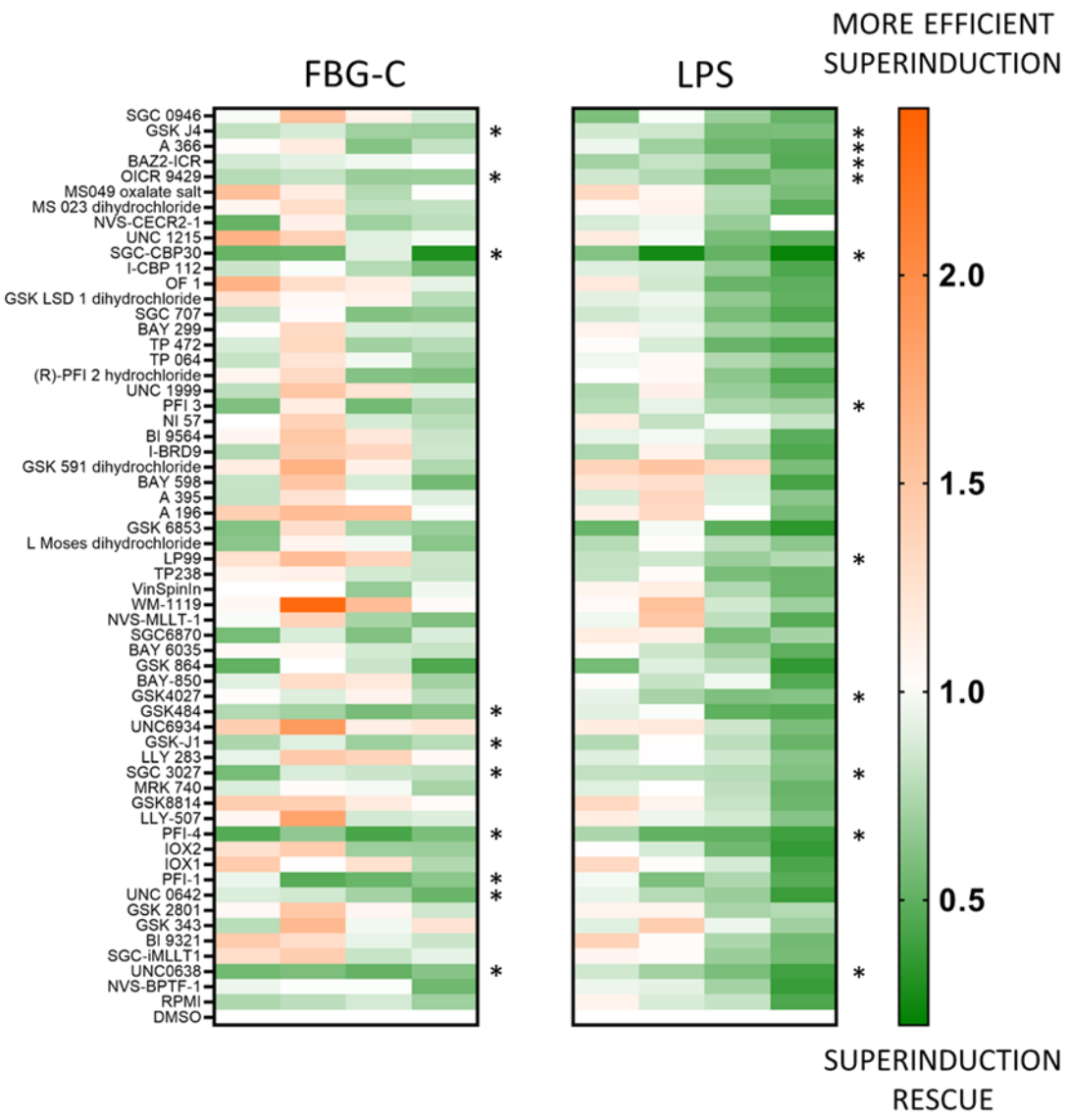


Figure 4.28 Epigenetic probes alter IL-6 superinduction. Cells were pre-incubated with epigenetic probes, DMSO control [DMSO], or left untreated [RPPMI] for 24h in serum free medium. Next, FBG-C at 1 µM, LPS at 100 ng/mL, or no stimuli was added for 24h. Medium was then collected, cells washed with PBS and fresh medium supplemented with 10% human serum added. Cells were then re-stimulated with LPS at 10 ng/mL for 24h. IL-6 release was measured by ELISA in culture media collected at the end of the protocol. MTT assay was performed to asses cell viability at the end of the experiment. Data are presented as IL-6 superinduction (increase in IL-6 secretion between unprimed, re-stimulated and primed, re-stimulated) fold change over DMSO control, normalized to MTT, from 4 independent donors. Data was analysed using paired T-test vs DMSO control; *$p < 0.05$.

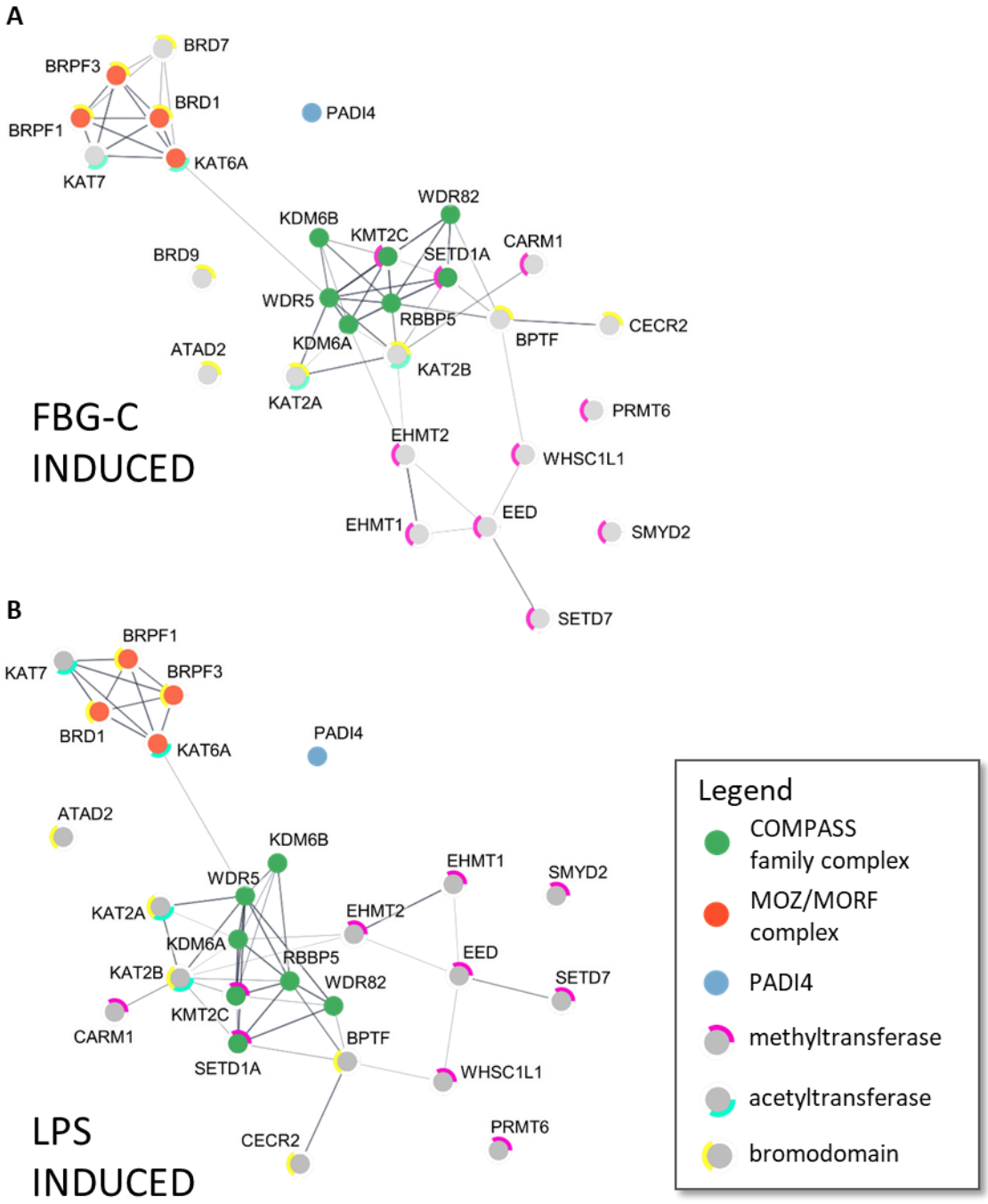


Figure 4.29 STRING interaction network analysis of proteins involved in the establishment of TNF tolerance. Physical subnetworks of the targets of small molecule probes significantly altering establishment of FBG-C (**A**) and LPS (**B**) induced TNF tolerance and 5 best predicted interaction partners were generated using STRING. The thickness of the line indicates the degree of confidence of predicted functional association between the proteins. The nodes represent proteins in the network and were coloured according to their involvement in the formation of chromatin remodelling complexes and their catalytic functions.

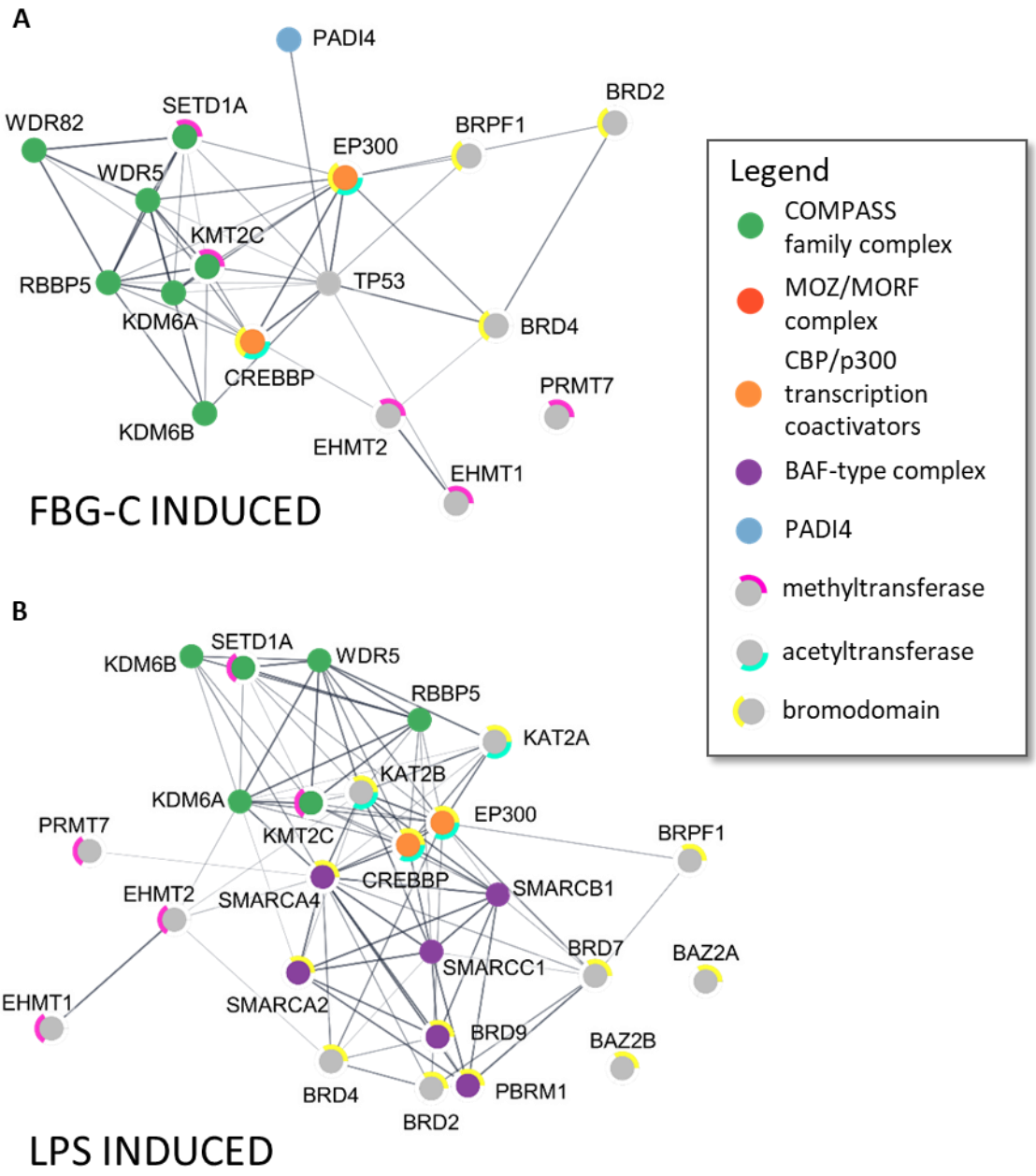


Figure 4.30 STRING interaction network analysis of proteins involved in the establishment of IL-6 superinduction. Physical subnetworks of the targets of small molecule probes significantly altering establishment of FBG-C (**A**) and LPS (**B**) induced IL-6 superinduction and 5 best predicted interaction partners were generated using STRING. The thickness of the line indicates the degree of confidence of predicted functional association between the proteins. The nodes represent proteins in the network and were coloured according to their involvement in the formation of chromatin remodelling complexes and their catalytic functions.

Finally, Gene Ontology (GO) analysis was performed to uncover pathway enrichment in TNF tolerance and IL-6 superinduction. GO biological process terms over-represented for TNF tolerance induced by both FBG-C or LPS were mostly associated

with chromatin structure (e.g. chromatin remodeling, histone methylation/acetylation). However, proteins required for efficient TNF tolerance were also linked with cellular metabolism, specifically upregulation of gluconeogenesis (Fig. 4.31 A). Biological processes affected in IL-6 superinduction were predominantly related to chromatin conformation and histone modifications, with the addition of DNA methylation. Interestingly, a number of terms were also enriched specifically in FBG-C or LPS primed samples. IL-6 superinduction induced by FBG-C requires proteins involved in upregulation of TGFβ receptor signalling pathway and cellular response to stress; while positive regulation of viral transcription by host and upregulation of gluconeogenesis were overrepresented in targets identified for LPS superinduction (Fig. 4.31 B).

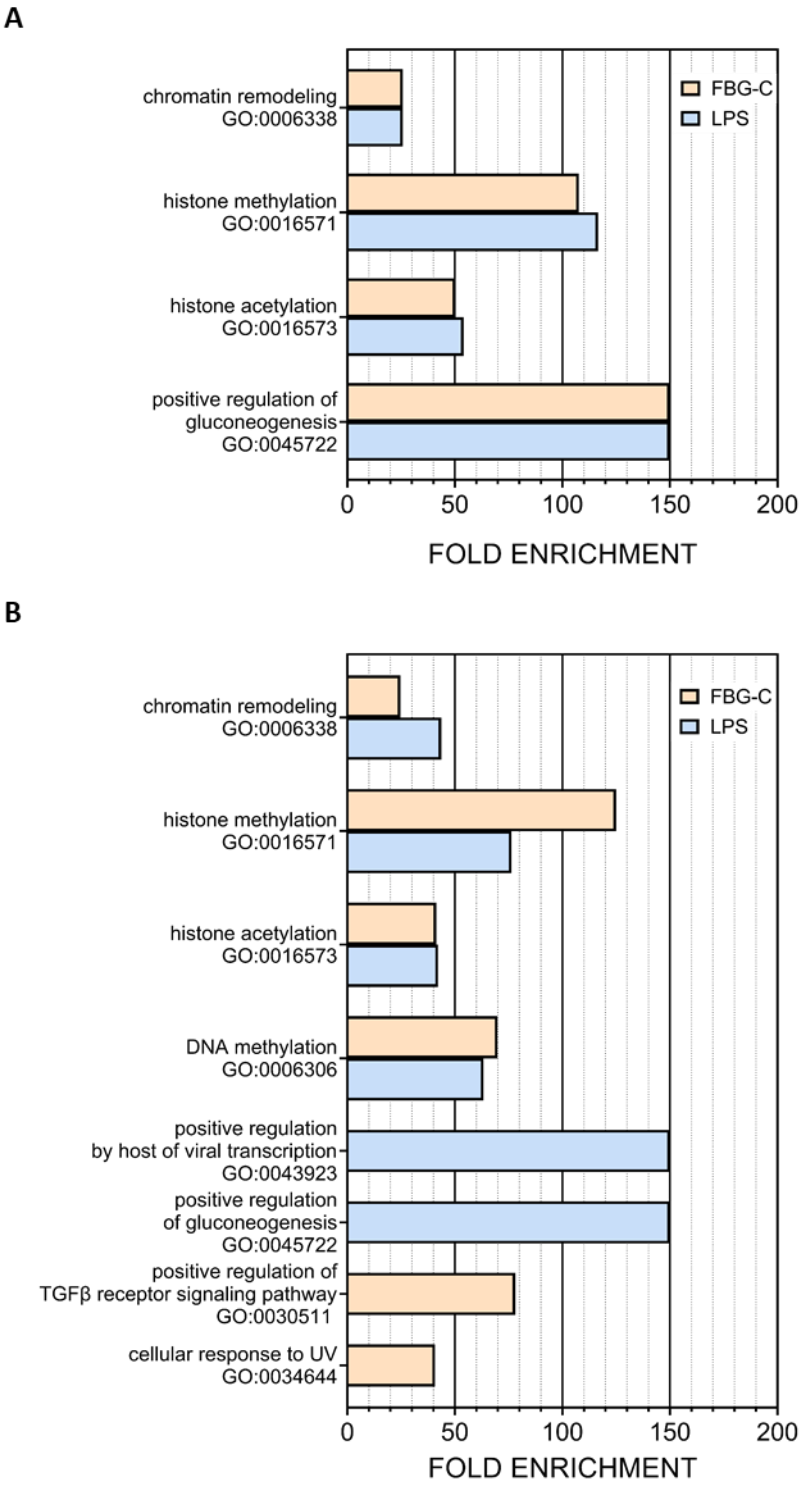


Figure 4.31 Gene ontology (GO) enrichment analysis. GO analysis was performed for the targets of small molecule probes significantly altering establishment of FBG-C and LPS induced TNF tolerance (**A**) and IL-6 superinduction (**B**). Bar charts depict fold enrichment of selected significantly enriched (FDR < 0.05) GO terms for biological process.

Chromatin immunoprecipitation (ChIP) is a technique that allows for selective enrichment of DNA bound to target proteins, such as modified histones or transcription factors [330]. Combined with RNA sequencing (ChIP-seq) or quantitative real-time PCR (ChIP-qPCR), it enables to study chromatin structure and epigenetic modifications acquired for example during, and following mounting of the cell immune response. To gain a better understanding of epigenetic remodelling underlying FBG-C induced memory, samples were collected throughout the memory protocol (Fig. 4.32) and ChIP was performed using antibodies against histone H3 lysine 4 tri-methylation (H3K4me3; a mark associated with euchromatin), histone H3 lysine 27 tri-methylation (H3K27me3; characteristic for heterochromatin), and CCCTC-binding factor (CTCF; a zinc-finger transcription factor involved in regulation of chromatin structure). Additionally, RNA polymerase II antibody was used to detect de-novo transcription of the effector cytokine mRNA. Stored immunoprecipitated DNA will be analysed by qPCR in the near future.

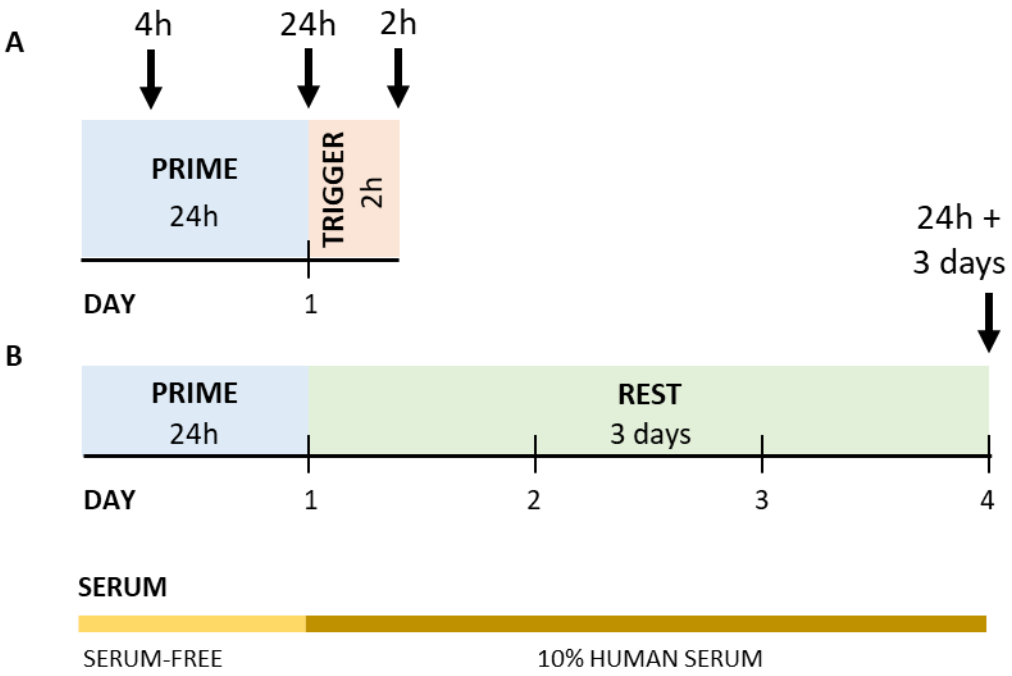


Figure 4.32 Chromatin immunoprecipitation – assay protocol. Primary human monocytes were seeded in 10 cm dishes and stimulated for 24h with FBG-C or LPS in serum free medium (PRIME). After that, medium was removed, cells washed with PBS and fresh medium supplemented with 10% human serum added. Cells were then immediately re-stimulated with LPS for 2h (TRIGGER; **A**), or rested for 3 days (REST; **B**). To perform chromatin analysis, cells were fixed in culture medium 4h and 24h into the PRIME step, 2h into the TRIGGER step (**A**); and after 3 days of REST (**B**). Next, nuclei were isolated, chromatin sheared, and chromatin immunoprecipitation performed.

4.3 Discussion

In this chapter, the FBG domain from tenascin-C was demonstrated to induce innate immune memory. Exposure of primary human macrophages and monocytes to FBG-C prevented cytokine release in response to further stimulation with LPS, similar to what has been previously described as endotoxin tolerance. This response was rapid, occurring within hours of priming, and was sustained beyond 7 days. Suppressed cytokine synthesis in monocytes primed with FBG-C was not limited to subsequent activation of TLR4 by LPS, but was evident in response to a variety of pathogenic ligands detected by a number of different pattern recognition receptors, and in response to cell stimulation with cytokines and DAMPs, including re-exposure to FBG-C. Different cytokines exhibited distinct responses; TNF release was immediately suppressed, whilst IL-6 demonstrated bi-phasic regulation, with initial superinduction followed by dampening from day 3 onwards. Transcript analysis revealed that this pattern is due to *de novo* transcription in FBG-C primed cells, while similar effects induced by LPS could be attributed to mRNA stability. Finally, chromatin immunoprecipitation and a library of small molecule epigenetic probes were employed with an intent of gaining an insight into FBG-C-mediated changes in chromatin organization and histone modifications underpinning cytokine rewiring, and this data will be analysed in the near future.

Overall, FBG-C induced innate immune memory was described as a complex functional adaptation modulating immune cell responses to future challenges. While generating effects similar to LPS, FBG-C induced memory was found to be regulated by different mechanisms, and thus constitutes a distinct phenomenon.

4.3.1 Investigating memory effects *in vitro* in human immune cells

Innate immune memory generated by pathogenic triggers, particularly LPS, is a phenomenon extensively studied *in vitro*. Endotoxin (or LPS) tolerance is typically described as downregulation of TNF synthesis and has been reported widely in murine peritoneal macrophages [26-31], splenocytes [28, 32] and bone marrow derived macrophages [33, 34], as well as macrophage-like cell lines [30, 41]. In humans, this was demonstrated predominantly in peripheral blood mononuclear cells [35-37] and monocytes [38-40], monocyte derived macrophages [35, 40], and monocytic THP-1 cell line [36, 38, 40, 42, 43]. While these published studies agree on the inhibition of TNF secretion in endotoxin tolerance, expression of other pro-inflammatory cytokines, such as IL-6, was sometimes reported to be suppressed, and sometimes augmented in different studies (reviewed in [44]). This is perhaps not so surprising, taking into account the various cellular models, and the lack of consistency in the methods employed. All reported endotoxin tolerance protocols comprise sequential LPS stimulation, yet they differ substantially in the duration of the primary and secondary stimuli, in the inclusion of a rest step in between, and in the concentration and source of the LPS used. Thus, selecting the right setup to study memory effects can be troublesome.

In this study, initial observations were made in a double stimulation 24h/24h, no rest protocol in human MCSF-derived macrophages. However, the protocol outline chosen later on, containing a 5 day rest step between the two 24h stimulations, was based on the more recently published reports detailing whole genome remodelling in primary human monocytes during LPS tolerance and β-glucan training [39, 76, 331]. Such protocol allows to simulate a naïve monocyte encountering a stranger or danger signal after being drawn to the tissue from blood, and its response to future threats in the tissue in the coming days (e.g. reinfection or further tissue damage), and thus can be valuable

for the study of pathogenic, as well as endogenous triggers of inflammation, for example tenascin-C, and for better understanding the molecular mechanisms in the pathology of rheumatoid arthritis.

As mentioned before, LPS used previously to study endotoxin tolerance was of various origin (and often not described in detail), which could play a role in the reported differential regulation of some of the effector molecules. Activation of inflammatory pathways can be affected by the use of different LPS serotypes [332]. What is more, insufficient purification process of commercially available LPS might result in residual endotoxin protein contamination that can trigger signalling through TLR2 [333]. Here, endotoxin tolerance was induced using LPS from *E. coli* serotype O55:B5 that was phenol extracted and further purified by ion-exchange chromatography, resulting in negligible (< 1%) protein contamination guarantying signalling limited to TLR4. β-glucan utilized in this project was endotoxin-free insoluble particulate preparation of β-1,3-(D)-glucan from *C. albicans*, obtained curtesy of Prof David Williams (East Tennessee State University), also used in the model studies mentioned above [39, 76, 331]. Due to the differences in the reported concentration of stimuli employed to induce the memory effects, LPS and β-glucan were tested experimentally to find an optimal dose. A set LPS concentration of 10 ng/mL was used as the secondary challenge. Interestingly, a few published reports claim that LPS can induce both dampening and potentiation of cytokine responses, depending on the dose used [320, 321, 323, 334]. LPS generated potentiation was so far observed exclusively in mouse cells, using doses in the range of 1 ng/mL - 5 pg/mL [320-323], and the molecular mechanisms responsible for this effect are not well understood. In my human monocyte protocol, despite examining a wide range of LPS concentrations, increase of TNF could not be found even with a very low dose of 10 fg/mL. In the course of this project potentiation of IL-6 was identified,

however it was induced by higher concentration of LPS (100 ng/mL), and was observed in protocols with no rest, or short rest between the primary and secondary stimulation. The studies mentioned above reporting augmented TNF and IL-6 secretion were indeed performed using short protocols, with re-stimulation following immediately after 4/6/20h of priming. Overall, consensus could not be found on the capability of LPS to induce dose-dependent potentiation of cytokine release.

In general, circulating human monocytes are short lived cells, with a lifespan of about one day, during which they either infiltrate tissue at sites of inflammation and undergo differentiation, or die [335]. Thus, to execute longer term cultures implementation of growth factors or serum supplementation is necessary. Addition of autologous serum, that is serum derived from the same individual as the cells, was shown to be particularly efficient at sustaining cell viability [336]. Here, culture medium was supplemented with pooled human serum, aiming at providing close to physiological levels of hormones, and growth and differentiation factors, such as M-CSF.

As the methods described in the literature differ on the serum supplementation throughout the memory protocol, two alternative versions were compared: priming with or without serum. Cells primed in the presence of serum displayed increased secretion of TNF and IL-6 in response to primary LPS stimulation. Such effect can be likely attributed to the natural serum levels of LPS binding protein, which facilitates LPS sensing by TLR4-MD2 complexes [47], thus explaining a more potent response. However, quite surprisingly, addition of serum during the PRIME step also resulted in diminished cell viability and cytokine secretion following re-stimulation. This is contrary to expected serum induced enhanced culture maintenance. Therefore, it was decided to perform priming in serum free medium.

In conclusion, inconsistency in the methodology applied in innate immune memory research may be a contributing factor behind the different patterns of regulation described for some of the effector molecules. In this study, a systematic approach was adopted, and memory protocol was first optimised to achieve clear TNF and IL-6 response alteration for the classic tolerance and training controls, in a biologically relevant model. This protocol outline could be subsequently used to examine the memory effects induced by tenascin-C.

4.3.2 FBG-C vs LPS in innate immune memory: same, but different?

Priming with FBG-C was found to generate tolerised TNF and IL-6 responses in the 7 day protocol, both to re-stimulation with LPS and FBG-C. Dampening of cytokine secretion was striking; priming cells with as little as 0.1 µM FBG-C induced a potent inhibitory effect. A wide range of FBG-C concentrations was tested, from 5 µM and reaching as low as 1 nM, a dose no longer capable of inducing cytokine release in the priming step. As observed previously for LPS, no potentiation of cytokine synthesis could be detected, even in cells primed with low FBG-C doses.

FBG-C generated tolerance to re-challenge with FBG-C was not induced below 0.1 µM, with lower doses used during prime resulting in secondary responses comparable to unprimed, re-stimulated samples. However, cells primed with FBG-C at very low levels (0.1 and 1 nM) still secreted lower levels of TNF and IL-6 in response to LPS than the unprimed control. This could imply certain differences between the signalling triggered by secondary challenge with FBG-C and LPS. However, donor variability and impact of protein vehicle (Tris and sodium chloride buffer with PMB) is also possible. Thus, in the next experiments proper vehicle control was always used alongside FBG-C priming.

Not only was FBG-C discovered to induce tolerance to LPS, but LPS was also demonstrated to tolerise monocytes to FBG-C. Response of LPS primed cells to FBG-C at 1 and 0.5 µM was significantly inhibited. These data suggest similarity in the signalling induced by the two triggers possibly results in cross-interaction in the induction and triggering of innate immune tolerance.

Nevertheless, a striking difference was revealed in β-glucan trained cells. Unlike LPS, response to FBG-C was not augmented following β-glucan priming. This is a

remarkable observation, indicating that differences must exist in the pathways activated by the two triggers in β-glucan treated monocytes. Pro-inflammatory gene expression induced following binding of LPS to TLR4 is a result of signalling through the MyD88-dependent pathway and NF-κB activation [337]. Sensing of LPS by TLR also triggers the MyD88-independent pathway via the adaptor protein TRIF. Signalling through TRIF leads to IRF3 induced expression of type I interferons, but it also interacts with the NF-κB cascade and contributes to upregulation of pro-inflammatory cytokines such as TNF [338]. Induction of cytokine synthesis in human and mouse fibroblasts by FBG-C requires engagement of MyD88 [136], however it is not clear if the TRIF-dependent pathway is also being activated by this trigger. What is more, FBG-C and LPS were shown to both activate NF-κB and MAPK pathways upon recognition by TLR4, yet induce two distinct phenotypes in human monocyte derived macrophages [191], also suggesting differences in the signalling via the same receptor induced by the two triggers. One can thus speculate that response potentiation generated by β-glucan depends on activation of particular components of the TLR4 pathway (e.g. the TRIF pathway?) that are not triggered by FBG-C. MD-2 and CD14, co-receptors involved in LPS signalling via TLR4 [339], are not required for FBG-C to activate the receptor [136]. However, it is possible that another, currently unknown co-receptor is necessary for the activation of TLR4 by FBG-C, and that this co-receptor is downregulated in β-glucan trained cells, decreasing FBG-C detection sensitivity.

In the big picture, this investigation constitutes yet another clue that while FBG-C and LPS signal through the same pattern recognition receptor and induce pro-inflammatory cytokine secretion, they are being distinguished as different cues by the molecular machinery of our innate immune system. This in turn likely allows for triggering of a tailored set of signalling pathways to meet biological demands specific for

the threat detected. In the context of innate immune memory, it appears that fungal infection induces a cell programme involving reinforcement of protection against bacterial re-infection, but allows mounting of unaltered response to tissue damage.

4.3.3 The importance of cell viability in innate immune memory research

Literature studying immune memory has so far centered on assessing the alteration of cytokine secretion measured in a relatively long term culture of human primary monocytes. As such, the question of loss of cell viability is a crucial matter. Monocytes are not commonly considered to proliferate in culture without growth factor supplementation, and some reduction in cell numbers after 7 days can be expected. However, if a trigger employed during the PRIME step significantly affects cell viability, is cytotoxic or possesses adherence altering properties, then comparing cytokine release in primed cells and unprimed controls can lead to false conclusions. Regrettably, so far this issue has been poorly addressed in the published literature on the subject with many papers not showing cell viability data.

Many different techniques are used to assess cell viability, for example quantifying ATP levels or ability to enzymatically process a substrate. Viability can also be tested through cytotoxicity assays that detect cellular membrane damage. Here, a combination of two different techniques was used to determine the amounts of healthy, living cells during the memory protocol: MTT assay and LDH assay. The MTT assay is a colorimetric cell viability assay that involves reduction of yellow tetrazolium dye (3-(4,5-dimethylthiazol-2-yl)-2,5-diphenyltetrazolium bromide, or MTT) to purple formazan product by mitochondrial succinate dehydrogenase in live cells. The LDH assay depends on the activity of lactate dehydrogenase, a cytoplasmic enzyme processing pyruvate to L-lactate and NADH to NAD+ during glycolysis. As a result of the enzymatic activity of LDH, a tetrazolium salt (iodonitrotetrazolium violet) is converted into a red formazan product that is detected colorimetrically. In a classic cytotoxicity assay LDH release into culture medium following loss of membrane integrity is measured. This was combined with quantification of enzymatic activity in cell lysate, allowing for direct

evaluation of cell viability. It is important to mention that both techniques, as the majority of cell viability assays, depend on the metabolic activity of the cells. Thus, alteration of cellular metabolism might be incorrectly interpreted as change in viability. To avoid this, the three different measurements were combined and further supported by observation of cell density under a bright-field microscope.

This analysis revealed a decrease in monocyte viability with time over the 7 days of the assay, as anticipated. However, at re-challenge cell viability is not significantly different in FBG-C and LPS primed samples, as well as the unprimed control. Therefore, FBG-C induced memory effects are unlikely to be caused by significant loss of cell viability, and are further strengthened by proven lack of influence by potential endotoxin contamination, and dependence on structural integrity of the protein.

On the other hand, β-glucan priming consistently showed a significant impact on cell viability. Undistinguishable during PRIME step, upon re-stimulation with LPS β-glucan primed cells demonstrated an increased viability both in MTT and LDH (in the cell lysate). The culture was also visibly more dense, and the cells larger. Consequently, cytokine secretion potentiation observed in β-glucan treated sample in comparison to unprimed control might be partially attributed to the differences in cell numbers. A similar observation in primary human monocytes was made previously by Bekkering *et al.* [107], who additionally described a β-glucan induced increase of metabolic activity (glycolysis). Since, a number of published studies described alteration of metabolism in β-glucan trained cells [112, 113, 325, 331, 340]. The above results highlight how important it is to meticulously consider even simple confounding factors and perform all fundamental controls when aiming to investigate such complex phenomena.

4.3.4 Complexity of FBG-C induced tolerance/training

Cross-tolerance defines a phenomenon where a stimulus reduces the response to another different stimulus, which typically activates a different receptor to the priming stimulus. It has been described in the context of LPS tolerance for a number of secondary triggers, such as TLR2 ligands lipoteichoic acid [85] and Pam3CSK4 [31], poly(I:C) (TLR3) [341], flagellin (TLR5) [342], S-27609 (synthetic TLR7 ligand) [341] and CpG DNA (TLR9) [343]. Activation of TLR2 [85, 344], TLR3 [345], TLR7 [346], TLR9 [347], as well as pre-treatment with TNF [185] and IL-1β [348] was also shown to induce cross-tolerance to LPS. However, flagellin [342] and muramyl dipeptide (NOD2 agonist) [349] did not induce cross-tolerance to LPS. If one would like to adapt a similar terminology, the reported β-glucan training is actually not a self-sensitization, but rather a cross-training to LPS. β-glucan cross-training was also documented in response to Pam3CSK4 [100].

Here, FBG-C was demonstrated to induce memory effects in response to a variety of PRR ligands and cytokines. FBG-C primed cells exhibited cross-tolerance to Pam3CSK4, flagellin and whole heat killed pathogens, as well as cross-training to poly(I:C), β-glucan, muramyl dipeptide, oxidised LDL and TNF. Interestingly, the observed augmented response to poly(I:C) does not align with previously reported cross-tolerance between LPS and poly(I:C), albeit this was measured in an *ex vivo* experiment in whole blood [341]. A question arises, how to explain this apparently intricate network of connections?

The study of molecular mechanisms behind endotoxin tolerance revealed a number of negative regulators of TLR4 signalling involved in the inhibition of response to secondary challenge. IRAK-M, upregulated in monocytes and macrophages upon TLR activation, inhibits dissociation of kinases IRAK and IRAK-4 from MyD88, and the

following binding of IRAK to TRAF6, blocking downstream signalling [67]. Bone marrow derived macrophages from IRAK-M deficient mice display impaired induction of endotoxin tolerance, with a delayed inhibition of pro-inflammatory cytokine secretion [67]. What is more, priming of primary human monocytes with LPS caused a quicker and more potent induction of IRAK-M in response to re-stimulation with LPS [350]. Another NF-κB inhibitor, SHIP-1, targeting phosphatidylinositol 3-kinase (PI3K) [61], was shown to be necessary for the generation of LPS tolerance in $SHIP^{-/-}$ bone marrow derived macrophages [62], and following shRNA knockdown of SHIP-1 in THP-1 cells [64]. In fact, cell lacking SHIP-1 have markedly reduced IRAK-M expression, and all this seems to depend on TGF-β1 signalling [64]. SOCS-1 and SOCS-3 affect several targets both upstream and downstream the TLR MyD88-dependent pathway, suppressing NF-κB induced pro-inflammatory gene expression (reviewed in [351]). In turn, peritoneal macrophages from SOCS-1 knockout mice are more sensitive to LPS stimulation, and show disrupted endotoxin tolerance [68]. Finally, zinc finger protein A20 (also called TNFAIP3) is an off switch shutting down NF-κB activation induced by TNF [352], and also terminating TLR signalling through deubiquitination of TRAF6 [353]. As demonstrated in THP-1 cells, A20 silencing abolished establishment of tolerance to LPS [69]. It is important to indicate that the aforementioned regulatory molecules were shown to be still upregulated in spleen and peritoneal mouse macrophages a day post LPS administration [65], however in human blood cells they peaked only hours following the infusion, and were completely down by 24h [354]. Furthermore, studies summarized in this paragraph all employed short memory protocols, comprising a few hours to a maximum of 24h of priming, followed by immediate, or nearly immediate, re-stimulation. Several microRNAs have been also implicated as important for generating and sustaining endotoxin tolerance, particularly

miR-146a (reviewed in [83]). Recently, another microRNA, miR–9-5p, was also shown to be a contributing factor in β-glucan training [355].

The inhibitors described so far in endotoxin tolerance preferentially target MyD88, but not TRIF-dependent pathway. This is puzzling in the context of LPS cross-tolerance to poly(I:C), a ligand of TLR3, the only Toll-like receptor not utilizing the MyD88-dependent pathway. More work is needed to comprehensively elucidate the extent of negative regulation of PRR signalling in tolerance, particularly with the use of longer memory protocols. However, it is important to remember that while TLRs, and also other PRRs and cytokine receptors, share many components of their signalling cascades, such as MyD88, IRAK or TRIF, they utilise different combination of signal transduction molecules, producing unique signalling blueprints to mount response targeted to detected trigger (reviewed in [10]). For example, activation of TLR3 leads to induction of type I interferons through the TRIF/TRAF3/IRF3 pathway, though it can also stimulate NF-κB translocation to the nucleus and consecutive pro-inflammatory cytokine expression following recruitment of TRAF6 and RIP1 by TRIF. Thus, the observed tolerance and cross-tolerance induced by various triggers, including FBG-C, might involve regulation by repressors described already for LPS, although this is likely a non-exhaustive list. Moreover, it remains to be seen if a comparable mechanism will be proposed to explain the augmentation of responses in training, e.g. downregulation of signalling inhibitors.

A further fascinating aspect of FBG-C induced memory is the secondary trigger- and effector-specific mode of response regulation. TNF was visibly tolerised following re-stimulation with LPS serotypes EH100 and O111:B4, Pam3CSK4, and flagellin. However, the same inhibitory effect on IL-6 and IL-8 was only statistically significant for LPS EH100. The other three molecules induced similar levels of IL6 and IL-8 in both

primed and unprimed cells. Another group of triggers, poly(I:C), CpG, β-glucan, muramyl dipeptide, heat killed *C. albicans* and oxidised LDL, induced low levels of IL-6 and no TNF at all, regardless of priming. Then, IL-8 response was clearly induced by these triggers in primed cells, compared with close to no release in unprimed samples. Similar IL-8 effect was also observed upon re-stimulation with TNF. This demonstrates an intriguing adjustment of cells exposed to FBG-C, a tissue damage/inflammation marker, comprising a compartmentalized protective programme. These cells appear to initiate a strict control of highly pro-inflammatory TNF, and a more loose regulation of IL-6 and IL-8, in response to bacterial invasion days later, as simulated by engagement of TLR2, TLR4 and TLR5. Such control of mechanisms fuelling inflammation might be aimed at preventing excessive aggravation and potential resulting tissue damage. On the other hand, fungal (β-glucan, heat killed *C. albicans*) or viral (poly(I:C)) infection, as well bacterial components detected inside the cell (CpG, muramyl dipeptide), and endogenous molecules (oxidised LDL, TNF), activate a potentiated IL-8 response. IL-8 (or CXCL8) is a potent chemoattractant responsible for neutrophil recruitment and activation [356]. Neutrophils have a well-established role in defence against fungi and extracellular bacteria [357], and evidence is emerging they might also contribute to immune responses targeted at intracellular pathogens [358, 359] and viruses [360]. It is conceivable that this preferential activation of IL-8 in FBG-C primed cells is evoked to produce a targeted antimicrobial response orchestrated by neutrophils.

Yet another, albeit very different, example of effector-specific regulation in FBG-C induced memory was discovered through the analysis of variable resting time memory protocols. Induction of TNF was tolerised in FBG-C and LPS primed cells already at 24h, and still maintained with 7 days of rest. More than 3 days of rest were needed to achieve IL-6 inhibition in FBG-C and LPS treated samples, and moreover this

response was initially superinduced, revealing a unique temporal regulation pattern. No study reporting a similar phenomenon could be found despite thorough literature search, suggesting bi-phasic regulation of cytokine response to be a novel mechanism. With regards to biological relevance, this result might indicate that the cellular programmes adapted during induction of innate immune memory are not only customised towards the type of secondary threat encountered, but also to how soon this new danger for the system emerges. For instance, it might be required to immediately switch off aggressively pro-inflammatory TNF following mounting of response to FBG-C to prevent accumulation of the cytokine that could cause inflammation-induced damage. However, IL-6 is a pleiotropic cytokine, with pro-inflammatory activity and a role in acute phase response, but is also important in the resolution of inflammation and tissue regeneration (reviewed in [361]). This was demonstrated for example in IL-6 knockout mice, which display impaired liver regeneration [362] and delayed cutaneous wound healing [363, 364], while overexpression of IL-6 caused accelerated nerve regeneration [365]. Therefore, early superinduction of this cytokine, apart from providing protection from opportunistic infections, might also promote activation of tissue repair, helping to return the system to homeostasis.

Interestingly, β-glucan primed TNF augmentation was also found to be fast, observed immediately following the completion of PRIME step, and peaks with 1 day of rest. This is not in accordance with a previous report, claiming 3 days are needed to induce full β-glucan training effect [107]. However, 3 days of rest were indeed necessary to achieve the maximal β-glucan potentiation of IL-6 response in this study as well.

4.3.5 Understanding re-programming underlying FBG-C induced memory

It is a consensus by now that innate immune memory involves a tailored re-adjustment of the cell responses, and not complete anergy or hyper-activity, which could not be explained by simple inhibition of TLR signalling pathways. In 2007, Medzhitov and colleagues published an elegant study proposing two classes of effector molecules distinctly regulated in endotoxin tolerance: tolerisable, inhibited in LPS primed cells, and non-tolerisable, still expressed in response to secondary trigger [74]. For example, induction of pro-inflammatory mediator IL-6 is blocked, but host defence peptide CRAMP (cathelicidin-related antimicrobial peptide) continues to be expressed following re-exposure to LPS. This regulation is executed at a transcriptional level through epigenetic pathways modifying chromatin accessibility. We now understand that similar chromatin re-modelling allows for cytokine superinduction observed in β-glucan training [100]. Here, for the first time effector was shown to undergo a time-dependent bi-phasic regulation that was reflected in transcription.

Analysis performed in the course of this study demonstrated a diverse kinetics in the induction of TNF and IL-6 in response to FBG-C and LPS. Both cytokines reached maximal upregulation around 6h, but TNF mRNA was cleared by 24h, while IL-6 could still be detected. A similar effect was reported previously in human monocytes [366]. Following re-stimulation with LPS, peak IL-6 mRNA levels at 2h were higher in FBG-C than LPS primed cells, yet this was not a statistically significant difference. Additionally, secretion of IL-6 was found to be similar in these two samples at 2h. However, control ELISA data demonstrated that observed IL-6 superinduction in FBG-C primed cells is fuelled by the secondary stimulus, while cytokine levels in LPS primed cells are similar whether they are re-challenged or not. These data suggest that FBG-C generated IL-6 superinduction might be a result of both *de novo* transcription and mRNA stability, whilst

this effect in LPS primed cells is predominantly due to the stability of IL-6 transcript (proposed model of regulation is presented in Fig. 4.33).

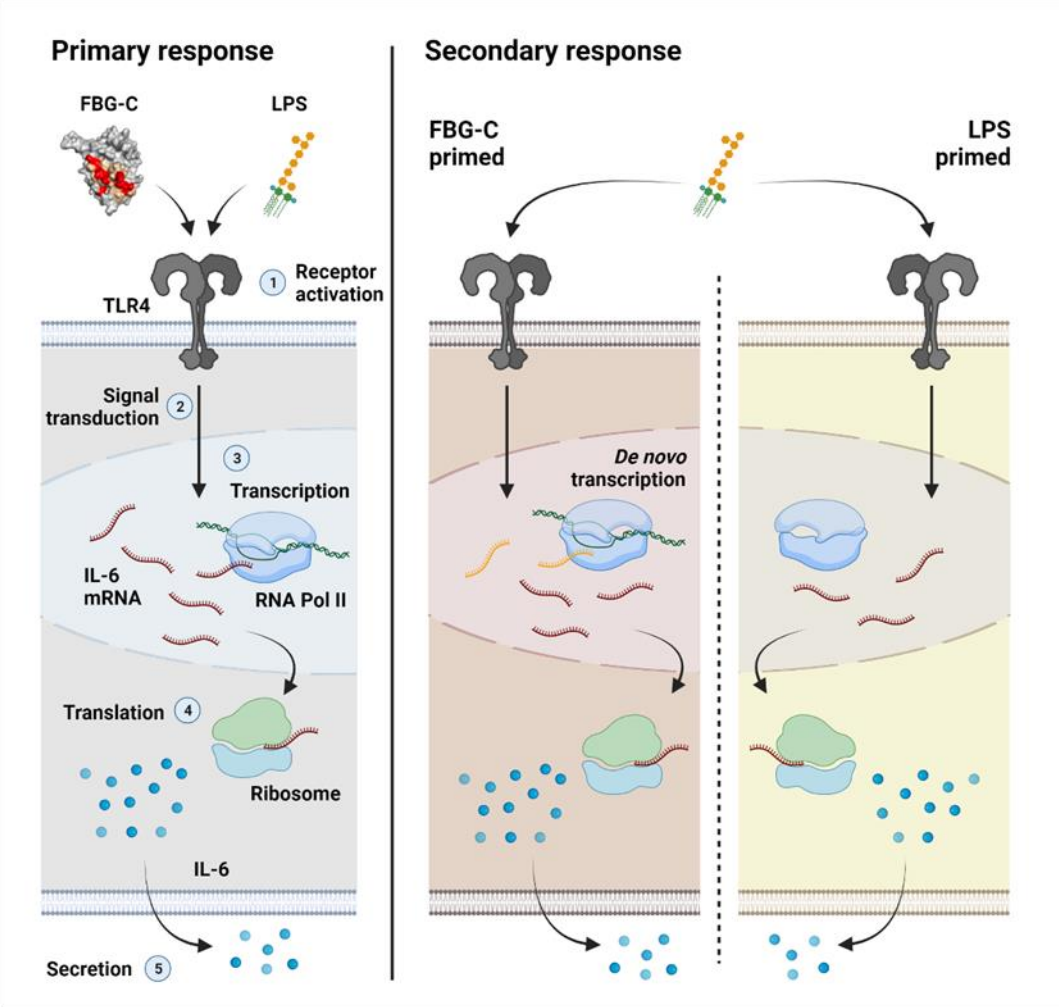


Figure 4.33 Proposed regulation mechanisms of FBG-C and LPS generated IL-6 superinduction. Primary response to FBG-C and LPS involves activation of TLR4, followed by signal transduction and transcription of IL-6 mRNA by RNA Polymerase II (RNA Pol II). Protein translation is then performed by ribosomes, and produced IL-6 secreted into the extracellular space. In FBG-C primed cells, secondary challenge with LPS re-activates transcription, and *de novo* transcripts together with stable mRNA remaining from the primary response serve as template for protein translation. However, in LPS primed cells *de novo* transcription does not happen, and protein is produced from leftover mRNA.

Thus, extended (or reduced) half-life of cytokine mRNA induced by the primary stimulus could potentially influence the levels of said cytokines secreted following the secondary challenge. This is a novel, previously unreported, aspect of innate immune memory regulation, reaching beyond the inhibition of signalling pathways and

modification of chromatin accessibility. Such a regulation could be of particular importance with regards to data collected in short protocols, where primary and secondary responses might partially overlay on transcriptional level.

More work is required to understand the differential regulation of IL-6 superinduction generated by FBG-C and LPS. Measurement of RNA polymerase II occupancy is predicted to be particularly valuable, allowing quantification of *de novo* transcription activated during the TRIGGER step. Furthermore, completion of the ChIP experiment will be indispensable to uncover the remodelling of histone marks responsible for chromatin structure. Together with a more in depth interpretation of epigenetic probe dataset, the above will help decipher transcriptomic and epigenetic rewiring behind the FBG-C induced memory.

4.3.6 Conclusions

Herein, innate immune memory induced by the endogenous TLR4 agonist FBG-C, the inflammation inducing domain derived from tenascin-C, was demonstrated in human monocytes and macrophages. FBG-C generated memory effects were described, and novel processes, unreported in LPS tolerance and β-glucan training, were discovered, including dual aspect, effector-specific cross-tolerance/training, and temporal biphasic regulation of IL-6. Foundations were laid for the investigation of epigenetic, transcriptomic, and potentially also metabolic re-programming behind FBG-C induced memory, albeit significantly more work is still needed to fully understand these mechanisms.

Investigation of innate immune memory produced by factors of endogenous origin is still in its infancy. The majority of published studies on the subject report memory effects generated by priming with TNF (reviewed in [181]). TNF induced tolerance was observed as protection from TNF-induced lethality *in vivo*, and inhibition of pro-inflammatory gene expression in human and mouse cells in response to re-stimulation with TNF or LPS (cross-tolerance). Mechanistically, TNF induced tolerance has been attributed to signalling repression by augmented glycogen synthase kinase 3 (GSK3) and A20 [185] and chromatin remodelling [367]. Thus, it could be speculated that autocrine TNF signalling plays a role in LPS induced tolerance. However, this was refuted in TNFR deficient mice, which presented a normal induction of endotoxin tolerance [185]. A number of alarmins activating TLR4, high mobility group box 1 (HMGB1) [167], high mobility group nucleosome binding protein 1 (HMGN1) [168], S100 proteins [170], and extracellular cold-inducible RNA-binding protein (eCIRP) [169] have been also implicated as tolerance inducing molecules. In another paper, authors claimed that priming of monocytes with a number of DAMPs (S100 proteins,

HMGB1, HSP90, fibrinogen, citrullinated fibrinogen, tenascin-C, biglycan and ATP) could induce both training and tolerance, depending on the concentration employed. It is though important to mention that the stimulation protocol is not described clearly and consistently throughout the manuscript, and not sufficient information is provided on the source of stimuli used. What is more, levels of LPS contamination in the stimuli were not reported, and PMB control was not performed in this study. With regards to the tenascin-C, recombinant protein employed is likely a truncated version, lacking the TLR4 activating FBG domain (although not enough data is given to establish this definitely) [368]. All things considered, results of this investigation should be treated with caution.

In this study, FBG-C was demonstrated to induce innate immune tolerance and training, and these effects were verified to be protein dependent, and not due to endotoxin contamination or change in cell viability. Most importantly, collected data shows for the first time that a DAMP can induce effector-specific, bi-phasic, temporally regulated memory, which is controlled on transcriptional level. These findings are novel, and shed a new light on our understanding of not only endogenously driven, but innate immune memory in general.

As innate immune tolerance is believed to be a protective mechanism, preventing from excessive inflammation and resulting tissue damage, it is logical that such regulatory mechanism would also exist for DAMPs. While necessary for induction of inflammation and activation of repair programmes, DAMPs can also accumulate in the tissue and contribute to persistent inflammation [369]. It remains to be elucidated if this off-switch mechanism is in some way impaired in diseases driven by dysregulated endogenously driven inflammation. An insight into this matter will be presented in the next chapter, where induction of tolerance by FBG-C will be investigated in the context

of rheumatoid arthritis, a chronic inflammatory disease characterized by elevated articular tissue and blood levels of tenascin-C [370].

5

Tenascin-C induced memory in the context of rheumatoid arthritis

Contents

5.1 Introduction 229

5.2 Results 235

5.2.1 Induction of memory in sustained model of inflammation 235

5.2.2 Innate immune memory in RA blood monocytes 244

5.3 Discussion 249

5.3.1 RA-specific extrinsic factors are not enough to block memory 250

5.3.2 RA cells: intrinsically different, but tolerised as well 253

5.1 Introduction

Rheumatoid arthritis (RA) is an incurable chronic autoimmune disease of synovial joints, affecting approximately 1% of the population [371] and creating significant socioeconomic burdens [372]. The disease is manifested by pain, swelling and stiffness of the joints, and results in progressive functional disability of the individual [373]. The aetiology of RA is not well understood, however certain susceptibility genes, particularly the human leukocyte antigen (HLA) DRB1 locus [374], and environmental factors, such as smoking [375] and periodontitis [376], have been associated with increased risk of acquiring the disease, as well as its severity and rate of progression.

RA immunopathology is complex and thus far no consensus has been agreed on the exact sequence of events that causes the catastrophic destruction of the joint tissue. A well-known hallmark of the disease is the generation of autoantibodies, rheumatoid factors (RFs) [377] and anti-citrullinated protein antibodies (ACPAs) [378]. RFs target the Fc region of IgG, while ACPAs bind post-translationally modified epitopes containing citrullines in a number of endogenous proteins, including fibrinogen [312], vimentin [379], α-enolase [380], and tenascin-C [264]. Presence of ACPAs can be detected years prior to symptom manifestation, and is associated with an aggressive disease phenotype and severe joint damage [381], making them a useful predictive and diagnostic marker in the clinics. Nevertheless, up to one third of individuals suffering from RA are classified as seronegative and present with disease characterized by a more heterogeneous clinical spectrum, different genetic and environmental risk factors, and efficacy of treatment strategies [382].

In conjunction with the systemic breach of tolerance to altered endogenous molecules, chronic synovitis resulting from massive influx and activation of leukocytes in the joint is a key feature in the pathogenesis of RA. Infiltrating cells include T and B

lymphocytes, monocytes, mast cells, and dendritic cells. In the adaptive immune compartment, B cells contribute to the disease development through production of autoreactive antibodies, such as ACPAs and RFs, cytokine secretion, mainly IL-1, IL-6 and TNF, and antigen presentation to $CD4^+$ T cells [383]. Due to various intrinsic differences (e.g. in HLA and DNA repair genes), following activation naïve $CD4^+$ T lymphocytes differentiate into highly inflammatory and proliferating effector cells [384]. Th1 helper cells producing IFN-γ and TNF, and activating monocytes/macrophages to act as antigen presenting cells, have been long considered the dominant subset driving RA pathology. However, IFN-γ levels in diseased joints are not universally upregulated [385, 386], and IFN-γ receptor deficient mice can still develop arthritis [387, 388], indicating Th1 are likely not indispensable for RA progression. More recently, an important role was assigned to Th17 cells due to their capability to produce IL-17, a cytokine abundant in RA synovial fluid [389], activating synovial fibroblasts, and promoting tissue destruction [390]. Despite disease exacerbation caused by IL-17 overexpression [391], and promising protective effects of IL-17 signalling ablation [392-394] in mouse models of arthritis, targeting the cytokine in RA patients yielded ambivalent results so far [395]. Other lymphocyte subsets, for example $CD8^+$ T cells, were also implicated in the pathogenesis of arthritis, yet their exact role in disease initiation and maintenance remains poorly understood [396].

Historically, humoral and cellular adaptive immunity were focal points of study in the field of RA and other joint diseases. Nowadays, innate immune cells are also recognized as crucial players contributing to pathological processes in RA. Dendritic cells, mast cells and neutrophils were demonstrated to promote pathological immune responses responsible for disease progression [397-399]. Yet, infiltrating monocytes and differentiated synovial macrophages are the most extensively studied innate immune

component in RA. Present in high numbers in diseased tissue, macrophages are the major producers of pro-inflammatory mediators, such as TNF, IL-6 and IL-1β, thus propelling the initiation and perpetuation of synovitis. Furthermore, macrophages serve as antigen presenting cells, stimulating T cell differentiation. Systemic depletion of macrophages in a rat model of arthritis was demonstrated to alleviate inflammation and reduce joint tissue destruction [400]. While specific targeting of inflammatory synovial macrophages as RA therapeutic has not been achieved so far, biological disease-modifying antirheumatic drugs (DMARDs), targeting cytokines released by activated macrophages, are currently routinely used in clinics. The importance of macrophages in the pathogenesis of arthritis is corroborated in particular through the efficacy of anti-TNF agents, as macrophages are the number one producers of pathogenic TNF in RA joint. What is more, numbers of synovial macrophages have been shown to correlate with the extent of tissue damage in the joint [401], and can be used as a biomarker of clinical outcome, regardless of the employed treatment [402]. However, macrophages in the arthritic joint are not homogenous. In a recent study, two distinct populations of synovial tissue macrophages were identified. MerTK^{neg} macrophages, abundant in active RA, were demonstrated to produce pro-inflammatory mediators and drive pathological activation of synovial fibroblasts. These cells could also mount a potent response following activation of TLR4. On the other hand, MerTK^{pos} population, associated with disease remission, were characterized by secretion of mediators promoting resolution of inflammation, and could induce repair programmes in fibroblasts [403].

As alluded to in the previous paragraph, stromal cells also participate in the development of joint pathology. The aggravated inflammatory response of interacting immune cells promotes the acquisition of an aggressive phenotype by resident synovial fibroblasts, which in turn release tissue degrading enzymes and stimulate chondrocyte

catabolism. Moreover, the pro-inflammatory milieu of the synovium, comprising cytokines produced by both immune cells and the stroma, induces differentiation of the bone-resorbing cells, osteoclasts [404]. Tissue breakdown is launched, releasing molecules further stimulating immune responses [405]. Altogether, positive feedback loops are established and inflammation spirals out of control, ultimately leading to severe cartilage destruction and bone resorption.

Signalling through PRRs, and in particular TLRs, is considered important for the pro-inflammatory phenotype of innate immune cells and fibroblasts in the synovium. A number of studies demonstrated synovial cells express high levels of TLRs, and become activated following receptor ligation in vitro (reviewed in [160, 406]). For example, upregulation of TLR4 was reported in RA synovial macrophages, and LPS-induced TNF production in these cells was significantly higher compared to healthy control [407]. In addition, peripheral blood monocytes isolated from RA patients were shown to express functional TLR2, TLR4, TLR5, TLR7, TLR8 and TLR9 [408-411]. Interestingly, an investigation of 110 RA patients revealed polymorphisms in TLR4, TLR9 and NF-κB1 genes were associated with disease susceptibility and progression, as well as response to anti-TNF treatment [412]. Moreover, experimental models of arthritis indicate TLR signalling is fuelling chronic inflammation. In a K/BxN serum transfer model, TLR4 deficiency significantly delayed symptom onset and severity [413].

It has been speculated that pathogens, for example periodontal bacteria *P. gingivalis*, could play a role in the initiation of RA. However, no persistent infection could be found in the joint tissue, and thus it seems unlikely that PAMPs drive TLR induced inflammation. On the other hand, TLR-activating DAMPs have been detected in RA synovium and synovial fluid. These include HMGB1, S100 proteins, heat shock proteins, hyaluronic acid, fibronectin, and tenascin-C (reviewed in [369]). Furthermore,

many DAMPs were strongly implicated in RA pathogenesis, both using experimental animal models and clinical data. For instance, HMGB1 can induce mouse arthritis following intraarticular administration [414], and targeting the molecule alleviates disease symptoms in a collagen-antibody induced arthritis model [415]. Similarly, injection of FBG domain from tenascin-C (FBG-C) stimulated mouse joint inflammation, and tenascin-C KO animals were protected from antigen-induced arthritis [136]. Furthermore, monoclonal antibody blocking activation of TLR4 by FBG-C prevented disease progression in a rat model of collagen-induced arthritis [416]. Finally, serum levels of tenascin-C [263], HMGB1 [417], and S100A8/S100A9 proteins [418] in patients suffering from RA were shown to correlate with disease severity. Altogether, published data suggests DAMP-TLR axis provides a significant contribution to the pathological pro-inflammatory response in RA.

It remains to be elucidated if the disordered uncontrolled innate response is simply fuelled by the deleterious positive feedback loops specific to the RA joint microenvironment, or whether crucial mechanisms responsible for preventing excessive inflammation are inherently defective in RA patient cells. That is, do higher levels of joint DAMPS cause excessive myeloid cell activation, and/or do cells from people with RA respond differently to DAMP activation. I hypothesized that one or both cell intrinsic or extrinsic changes may be at play. As described in chapter 4, FBG-C, an endogenous TLR4 ligand derived from tenascin-C, is capable of generating innate immune memory, including dampening of TNF production. In this chapter, I aimed to investigate if FBG-C induced tolerance is as a protective mechanism that is broken, or malfunctions, in people who develop RA.

First, I devised a new type of innate immune memory assay using healthy human monocytes. Rather than a single stimulation, followed by a rest period and a re-challenge,

that I used in chapter 4 and which was designed to mimic infection, and a subsequent re-infection, this model involved sustained challenge with FBG-C, with the intent to mimic cell exposure to accumulating levels of this pro-inflammatory stimulus as occurs in the DAMP rich milieu of the joints of people with RA. I discovered that in such a model of chronic inflammation tolerance is established, and persists throughout the duration of the assay. Moreover, I employed the classic memory assay optimized in chapter 4 to examine the effects of RA-specific post-translational modification of FBG-C, and demonstrated citrullination does not preclude induction of FBG-C-mediated tolerance. Finally, I investigated immune responses to FBG-C in primary monocytes isolated from the blood of RA patients. My analysis revealed that the capability to induce innate immune memory is not affected in diseased cells, however secretion of TNF and IL-6 following stimulation with FBG-C is elevated in RA compared to healthy control monocytes. Therefore, my data suggest that tolerance in healthy cells is not lost upon exposure to accumulating, high levels of DAMPs and that DAMP-induced memory remains functional in monocytes from people with RA. However, cells from people with RA exhibit altered primary responses that might account for exacerbated myeloid cell behaviour in disease.

5.2 Results

5.2.1 Induction of memory in sustained model of inflammation

Tenascin-C levels are upregulated in the joint of RA patients [262, 419, 420]. Thus, peripheral blood monocytes infiltrating the joint will likely encounter tenascin-C, and will remain exposed to the molecule as they differentiate in the synovium. To investigate the influence of prolonged stimulation with FBG-C, a novel "sustained" memory assay was designed. In this assay, healthy primary human monocytes were first stimulated with various concentrations of FBG-C for 24h in serum free medium (STIMULUS I, SI), and then the stimulus was replenished in serum supplemented medium at day 1 (STIMULUS II, SII), day 3 (STIMULUS III, SIII), and day 5 (STIMULUS IV, SIV). In this way cells are exposed to FBG throughout the duration of the model. Monocytes were stimulated for 7 days with a constant dose of FBG-C at 1, 0.1, 0.01, or 0.001 μM; or with an ascending dose of the stimulus, starting with 0.001 μM during SI, and then 0.01 μM (SII), 0.1 μM (SIII), and finally 1 μM (SIV), aimed at mimicking gradual accumulation of the protein in the joint microenvironment. Additionally, a control sample was included to assess late response to stimulation, where cells were left unstimulated for the first 5 days (SI – SIII), and then treated with 1 μM of FBG-C for 48h (SIV). To quantify the response during the 7 day exposure to FBG-C, TNF secretion was measured in culture media by ELISA at the end of day 1 (after SI), day 3 (SII), day 5 (SIII), and day 7 (SIV) (Fig. 5.1 A).

As previously observed, unstimulated monocytes [-] secreted little TNF after culture for 1 day (SI, pink bar), and low levels of TNF were detected in these cells throughout the duration of the protocol (SII, green bar; SIII, blue bar; and SIV, orange bar). Priming with a constant dose of FBG-C for 24h (SI, pink bars) induced TNF release in a dose dependent manner, with high levels produced following activation with 1 μM,

and little secretion observed in samples stimulated with 0.1, 0.01, and 0.001 µM. In all cells treated with a constant dose of the protein, analysis of conditioned media at day 3 (SII, green bars), day 5 (SIII, blue bars), and day 7 (SIV, orange bars) revealed no TNF secretion at any of the tested time points, demonstrating that priming with FBG-C renders cells unable to secrete TNF following re-challenge with FBG-C, and that sustained exposure does not break this tolerance. No TNF was detected in samples stimulated with ascending dose of FBG-C at all assayed time points (SI, SII, SIII and SIV), indicating that exposure to increasing concentrations of the stimulus also does not break tolerance. Finally, in a late response control sample, little or no cytokine release was detected in the first 5 days (SI, pink bar; SII, green bar; and SIII, blue bar) while cells were left unstimulated. When exposed to FBG-C at 1 µM in the last 48h, these cells were still capable to respond to stimulation by releasing TNF (SIV, orange bar), although the signal was weaker than the primary response to the molecule quantified in the first 24h in cells stimulated with a constant dose of FBG-C at 1 µM (SI, pink bar) (Fig. 5.1 B). An MTT assay performed at the end of day 7 demonstrated cell viability was not affected by stimulation with FBG-C in this model (Fig. 5.1 C).

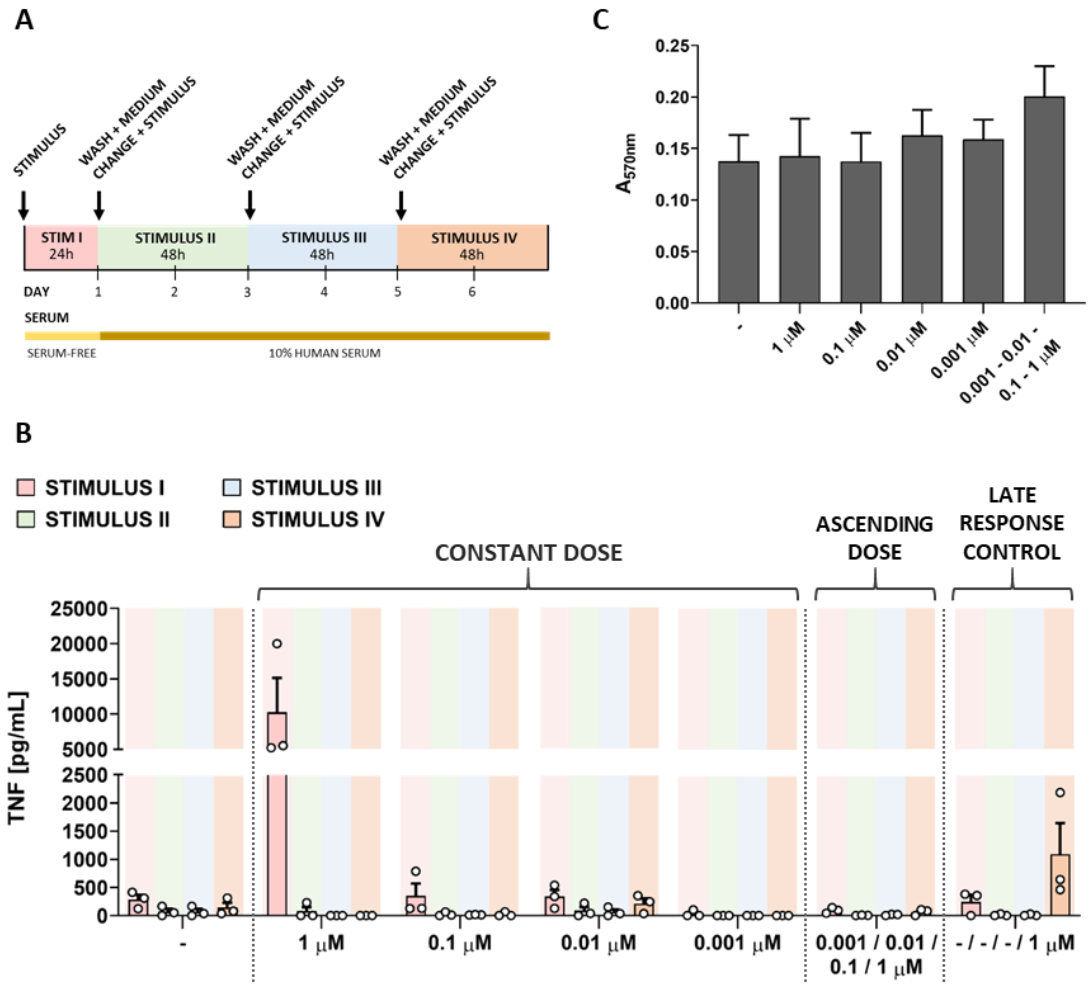


Figure 5.1 Tolerance during prolonged exposure to FBG-C I. A Protocol outline. Cells were exposed to FBG-C for 7 days divided into 4 steps: STIMULUS I (SI, 24h), STIMULUS II (SII, 48h), STIMULUS III (SIII, 48h) and STIMULUS IV (SIV, 48h). After each step medium was collected, cells were washed and fresh medium with appropriate dose of FBG-C added. SI was performed in serum free medium, medium supplemented with 10% human serum was used for next 3 steps. Cells were stimulated for 7 days with constant dose of FBG-C at 1 µM, 0.1 µM, 0.01 µM, and 0.001 µM; or with ascending dose at 0.001 µM (SI), then 0.01 µM (SII), 0.1 µM (SIII), and 1 µM (SIV) [0.001/0.01/0.1/1 µM]. Additionally, a late response control was performed where cells were left unstimulated for SI – SIII, and then stimulated with FBG-C at 1 µM for SIV [-/-/-/1 µM]. Sample unstimulated for the 7 days [-] was also included. TNF levels in media after each step were measured by ELISA (**B**). MTT assay was performed to asses cell viability at the end of the experiment (**C**). Data are shown as mean ± SEM from 3 independent donors.

Therefore, tolerance was not shown to be broken during sustained exposition to FBG-C. However, in the previous experiment change of medium performed with each addition of the stimulus resulted in removal of all immune mediators and metabolites produced by the cells, which would not happen in physiological conditions. To test if soluble factors released by monocytes in response to stimulation with FBG-C have an

effect on the maintenance of tolerance during prolonged exposure, “sustained spiked” memory assay was employed. In this protocol, monocytes were exposed to FBG-C for 24h in serum free medium (STIMULUS I, SI), and then additional doses of the stimulus were added to the same medium (“spiked”) at day 1 (STIMULUS II, SII), day 3 (STIMULUS III, SIII), and day 5 (STIMULUS IV, SIV), without removing the medium and replacing it with fresh medium as in Figure 5.1. Cells were spiked with a constant dose of FBG-C at 1 μM; or with ascending doses of the protein, starting with 0.001 μM during SI, and then 0.01 μM (SII), 0.1 μM (SIII), and finally 1 μM (SIV). Additionally, a control sample was included to assess late response to stimulation, where cells were left unstimulated for the first 5 days (SI – SIII), and then spiked with 1 μM of FBG-C for 48h (SIV). Two versions of this protocol were tested. In the first, serum was added to a final concentration of 10% at day 1, and maintained at 10% throughout (HIGH SERUM). The second, aimed at assessing if high level of serum impacts the ability of cells to respond to FBG-C, involved a gradual increase from serum levels of 1% to 2.5% between day 1 and day 7 (LOW SERUM). TNF release was measured in culture media by ELISA at the end of day 1 (end of SI), day 3 (SII), day 5 (SIII), and day 7 (SIV) (Fig. 5.2 A).

Unstimulated cells [-] in both versions of the protocol produced no TNF at all assayed time points (SI, pink bars; SII, green bars; SIII, blue bars; SIV, orange bars). Similarly high levels of TNF secretion were detected after 24h in response to FBG-C at 1 μM in serum high and low protocols (SI, pink bars). Release of TNF in culture medium collected at day 3 (SII, green bars), day 5 (SII, blue bars), and day 7 (SIV, orange bars), following subsequent spikes with 1 μM doses decreased gradually. This TNF signal dampening was more pronounced in serum high compared to serum low version of the protocol. In cells spiked with ascending doses of FBG-C [0.001/0.01/0.1/1 μM], no TNF

release throughout the duration of the assay was detected (SI, pink bars; SII, green bars; SIII, blue bars; SIV, orange bars). Interestingly, in the late response control cells, left unstimulated for SI-SIII, and then spiked with FBG-C at 1 µM for 48h [-/-/-/1 µM], negligible cytokine secretion was observed in all measured time points (SI, pink bars; SII, green bars; SIII, blue bars; SIV, orange bars) and in both versions of the protocol, suggesting cells are no longer capable to respond to FBG-C from day 5 onwards (Fig 5.2 B). Finally, cell viability assessed with an MTT assay was not significantly different between the tested samples, albeit overall higher in the serum high protocol (Fig. 5.2 C). Altogether, these data indicate that certain products of monocyte metabolism, released by cultured cells, suppress their capability to respond to FBG-C, and that this effect is not due to high levels of human serum present in culture medium.

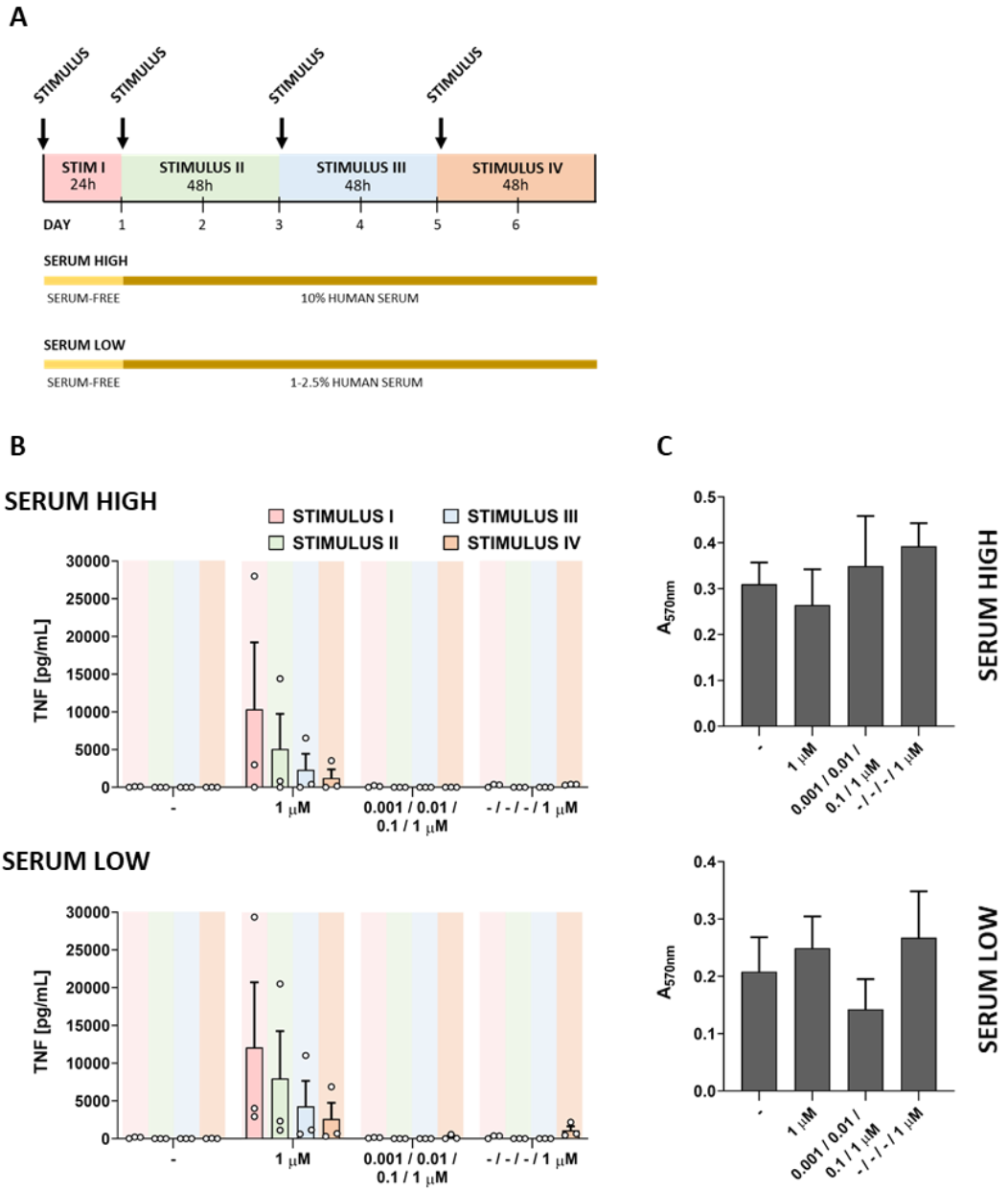


Figure 5.2 Tolerance during prolonged exposure to FBG-C II. A. Protocol outline. Cells were exposed to FBG-C for 7 days divided into 4 steps: STIMULUS I (SI, 24h), STIMULUS II (SII, 48h), STIMULUS III (SIII, 48h) and STIMULUS IV (SIV, 48h). After each step 40 µL of medium was collected and volume was topped with stimulating reagent and medium supplemented with 10% human serum. SI was performed in serum free medium. Prior to SII serum levels were adjusted to 10% (SERUM HIGH), or were gradually increasing from 1% at SII to 2.5% at SIV (SERUM LOW). Cells were stimulated for 7 days with constant dose of FBG-C at 1 µM, or with ascending dose at 0.001 µM (SI), then 0.01 µM (SII), 0.1 µM (SIII), and 1 µM (SIV) [0.001/0.01/0.1/1 µM]. Additionally, a late response control was performed where cells were left unstimulated for SI – SIII, and then stimulated with FBG-C at 1 µM for SIV [-/-/-/1 µM]. Sample unstimulated for the 7 days [-] was also included. TNF levels in media after each step were measured by ELISA (**B**). MTT assay was performed to asses cell viability at the end of the experiment (**C**). Data are shown as mean ± SEM from 3 independent donors.

Citrullination (or deimination) is a type of post-translational modification of proteins, whereby arginine residues in the polypeptide chain are converted to citrullines by protein arginine deiminase (PAD) enzymes [8]. Citrullinated epitopes are not uncommon in human organism, for example citrullination of histones is involved in regulation of chromatin accessibility [9]. However, in people with RA, generation of autoantibodies against citrullinated epitopes is a well-established biomarker of the disease [421]. In particular, antibodies recognizing the FBG domain of tenascin-C are present at high levels in people with RA [264, 422], whilst citrullination in the FBG-C domain protein was detected in RA synovial fluid [423].

I hypothesized that citrullination of FBG-C may affect its ability to induce tolerance, and that accumulating levels of modified protein in the RA joint may contribute to exacerbated myeloid cell activation. In order to determine the impact of this post-translational modification on the induction of innate immune memory, citrullinated FBG-C was applied in the classic memory assay (priming with FBG for 24h, resting for 5 days and then re-challenge with LPS) using healthy human blood monocytes (Fig. 5.3 A). Cells were primed with decreasing concentrations of the citrullinated FBG domain, or by unmodified control FBG-C treated with inactive PAD enzyme, kindly provided by Dr Anja Schwenzer (Midwood Group, Kennedy Institute, University of Oxford). Cytokine release in culture media was measured by ELISA after 24h, demonstrating both stimuli induce production of TNF at 2 – 0.5 μM. Citrullinated FBG-C (orange bars) induced more TNF that the control FBG-C (green bars), consistent with unpublished data from the Midwood lab This was most apparent, although not statistically significant, at 0.1 μM, where control FBG-C induced negligible amounts of TNF, while citrullinated protein could still generate TNF secretion. No TNF could be

detected following stimulation with both versions of FBG-C at 100 nM and 1 nM, and in the unprimed sample [-] (Fig. 5.3 B).

After 5 days of rest cells were re-stimulated with LPS and TNF levels were measured by ELISA. No spontaneous cytokine release was detected in unstimulated control [-/-], and unprimed cells responded to stimulation by secreting TNF [-/+]. In samples primed with citrullinated, or sham citrullinated FBG-C at 100 nM and 1 nM production of TNF was comparable to the unprimed, re-stimulated control. Priming with 2 – 0.5 μM of either of the stimuli resulted in nearly complete inhibition of TNF secretion following secondary challenge with LPS. Corresponding to the difference in primary response registered between the stimuli, at 0.1 μM cells primed with citrullinated FBG-C were already partially tolerised towards LPS, whereas priming using FBG-C treated with inactive PAD enzyme had no effect on cytokine release ($p = 0.001$) (Fig. 5.3 C). MTT assay was performed at the end of the protocol and revealed no significant changes in cell viability in this assay, although a modest increase in absorbance was detected in samples primed with both types of FBG-C at 0.1 μM (Fig. 5.3 D).

In summary, this series of experiments, aimed at modelling the RA-specific microenvironment of the joint, demonstrated that FBG-C induced tolerance is not broken by persistent exposure to the stimuli, or to increasing concentration of the stimuli, and that induction of tolerance is not hindered as a result of protein citrullination.

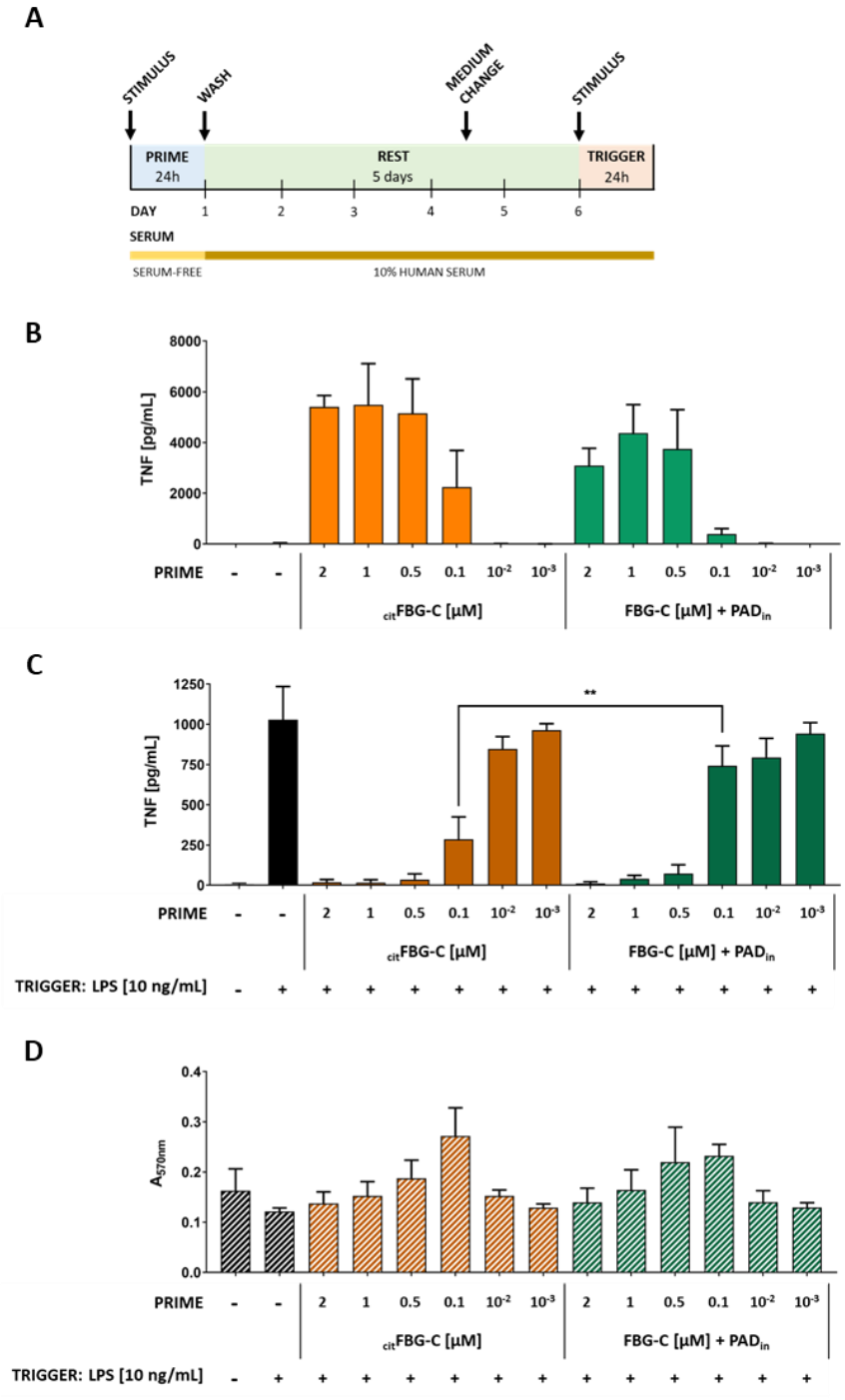


Figure 5.3 Induction of tolerance by citrullinated FBG-C. A. Protocol outline. Cells were primed for 24h with decreasing concentrations of citrullinated FBG-C [$_{cit}$FBG-C], decreasing concentrations of FBG-C treated with inactive PAD enzyme [FBG-C + PAD$_{in}$] or left unprimed [-] in serum free medium. After 5 days of rest in medium supplemented with 10% human serum cells were then re-stimulated with LPS at 10 ng/mL or left unstimulated [-/-]. TNF levels in media at 24h (**B**) and the end of the protocol (**C**) were measured by ELISA. MTT assay was performed to asses cell viability at the end of the experiment (**D**). Data are shown as mean ± SEM from 3 independent donors. Data was analysed using two-way ANOVA; **p < 0.01.

5.2.2 Innate immune memory in RA blood monocytes

The identification of genetic risk factors associated with disease susceptibility indicates individuals who develop RA are inherently different from the healthy population. It is thus not inconceivable that due to some currently undetermined alterations in cellular physiology, mechanisms limiting immune responses are compromised in diseased immune cells. One such mechanism could be innate immune tolerance, and I hypothesised that induction of FBG-C tolerance is impaired in cells of individuals that developed RA. To explore this hypothesis, monocytes isolated from peripheral blood of RA patients were examined in the classical memory assay. Monocytes were primed with FBG, LPS, or β-glucan, and either re-challenged immediately with LPS, or rested for 5 days before re-stimulation with LPS.

In collaboration with Prof. Karim Raza (Institute for Inflammation and Ageing, NIHR Birmingham Biomedical Research Center and Clinical Research Facility, University of Birmingham), whole blood was obtained from 8 patients diagnosed with RA and monocytes were isolated as described in chapter 2. The cohort was predominantly female (six females, two males), with age distribution between 41 and 81 years, median age of 63.5 years. Four treatment naïve and four conventional DMARD treated (methotrexate and/or hydroxychloroquine) individuals were recruited. As a control, monocytes were isolated from blood of six healthy volunteers (female, median age of 54.5 years). Due to lower cells numbers isolated from blood of 3 donors, classic 5 days rest protocol was performed on all 8 RA samples, but the short, no rest protocol was tested in only 5 donors.

Healthy control (HC) and diseased (RA) cells were stimulated for 24h with FBG-C at 1 μM, LPS at 100 ng/mL, or β-glucan at 10 μg/mL, and culture media were assayed for TNF and IL-6 release by ELISA. No spontaneous cytokine secretion was

detected in the unstimulated samples at 24h, whereas stimulation with LPS and FBG induced TNF and IL6 in both HC and RA cells. In comparison to HC, mean levels of cytokines released by RA cells in response to both triggers were 2-3 times higher, although due to large data spread this was only statistically significant for LPS induced IL-6 production. β-glucan did not induce production of these two cytokines in either HC (as demonstrated in chapter 4) or in RA cells. No significant difference could be detected between untreated (white dots) and DMARD treated (grey dots) RA donors in secretion of TNF ($p = 0.92$ for LPS, and $p = 0.41$ for FBG-C) and IL-6 ($p = 0.88$ for LPS, and $p = 0.96$ for FBG-C) (Fig. 5.4).

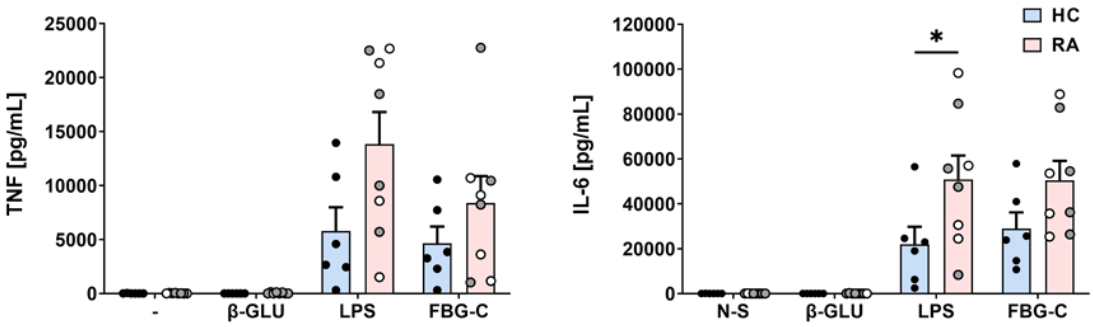


Figure 5.4 Primary immune response in rheumatoid arthritis patients blood monocytes. Rheumatoid arthritis patients (RA) or healthy controls (HC) cells were primed for 24h with FBG-C at 1 μM, LPS at 100 ng/mL, β-glucan at 10 μg/mL [β-GLU], or left unstimulated [-] in serum free medium. TNF levels in culture media were measured by ELISA. Data are shown as mean ± SEM from 6 (HC) or 8 (RA) independent donors. Black dots, HC donors; white dots, RA donors not receiving treatment; grey dots, RA donors treated with DMARDs. Data was analysed using unpaired T-test; *$p < 0.05$.

After re-challenge of the cells in the classic long protocol (5 day rest, Fig. 5.5 A), priming with β-glucan induced training in HC and RA cells and this was observed for both TNF and IL-6. The mean fold induction of TNF and IL6 was higher in HC cells compared to RA cells (8.5 versus 3.6 for TNF, and 4.9 versus 3.5 for IL-6), though this was not statistically significant due to marked donor to donor variability. Priming with LPS induced inhibition of both TNF and IL6 secretion following re-stimulation. The degree of tolerance was significantly greater in RA cells compared to HC for both

cytokines (fold change of 0.08 in RA versus 0.33 in HC for TNF, and 0.44 in RA versus 0.68 in HC for IL-6). Production of TNF and IL-6 was also inhibited in FBG-C primed cells in response to secondary stimulation with LPS, and this effect was comparable for both HC and RA cells (fold change of 0.01 in RA versus 0.0.2 in HC for TNF, and 0.24 in RA versus 0.34 in HC for IL-6) (Fig. 5.5 B).

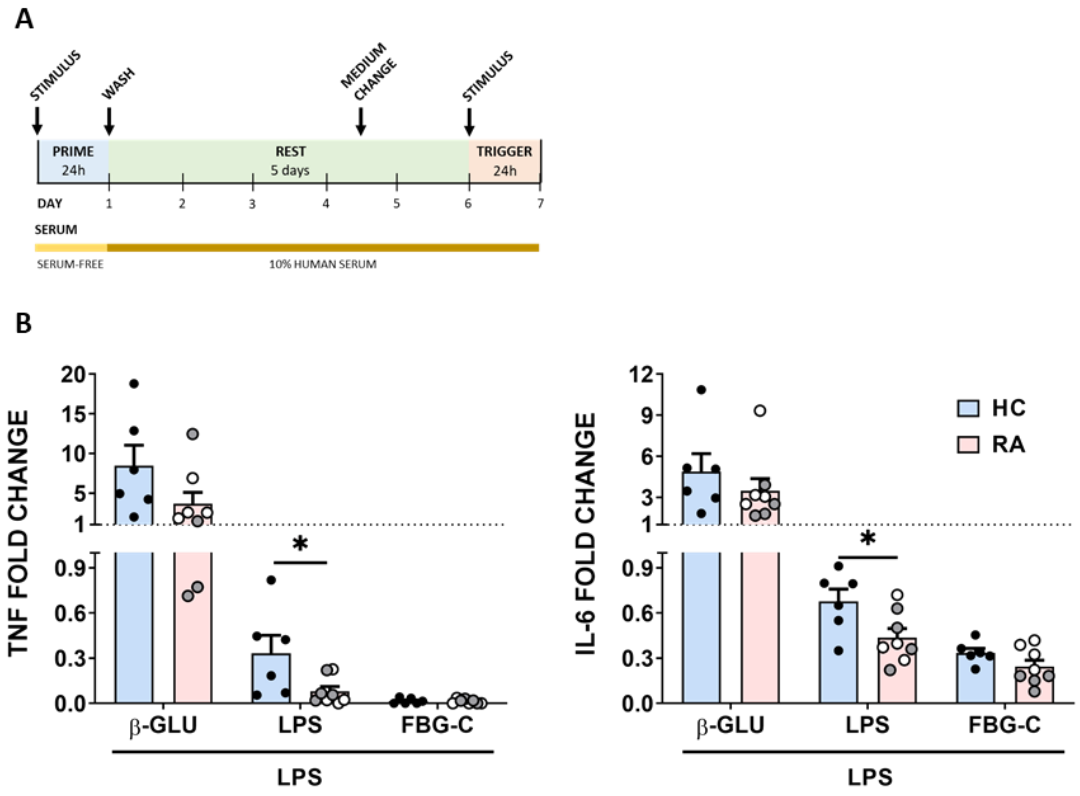


Figure 5.5 Innate immune memory effects in rheumatoid arthritis patients blood monocytes I. **A** Protocol outline. Cells were primed for 24h with FBG-C at 1 μM [FBG-C], protein vehicle control (VEH, TN buffer with PMB), LPS at 100 ng/mL [LPS], β-glucan at 10 μg/mL [β-GLU], or left unprimed in serum free medium. After 5 days of rest in medium supplemented with 10% human serum cells were re-stimulated with LPS at 10 ng/mL. TNF and IL-6 levels in media at the end of the protocol were measured by ELISA (**B**). Data are shown as mean fold change over VEH (for FBG-C) or unprimed (for LPS and β-GLU) ± SEM from 6 (HC) or 8 (RA) independent donors. Black dots, HC donors; white dots, RA donors not receiving treatment; grey dots, RA donors treated with DMARDs. Data was analysed using unpaired T-test; *p < 0.05.

In the short protocol (Fig. 5.6 A), β-glucan primed HC and RA cells re-challenged immediately following the end of PRIME step displayed a trained TNF response. The potentiation of TNF secretion was more evident in HC than RA cells (mean fold change of 2.9 for HC and 1.6 for RA), however this difference was not statistically

significant. Release of IL-6 in these cells was not increased compared to respective unprimed control (mean fold change of below 1). Tolerised TNF response to re-stimulation with LPS was observed in LPS and FBG-C primed samples, with a similar degree of inhibition quantified in RA and HC cells. Superinduction of IL-6 secretion was detected in cells primed with LPS, with a higher mean fold change for RA than HC (2.6 for RA versus 1.9 for HC). Production of IL-6 was also superinduced in FBG-C primed cells, although the level of cytokine induction was comparable between the RA and HC (Fig. 5.6 B).

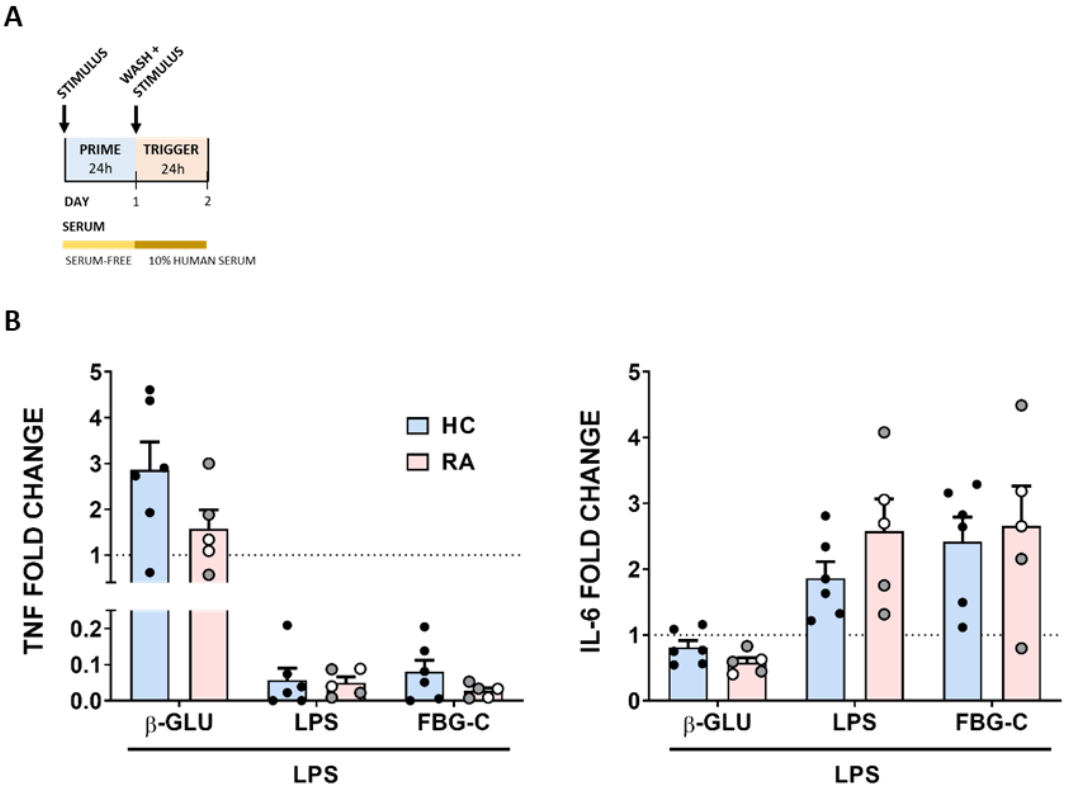


Figure 5.6 Innate immune memory effects in rheumatoid arthritis patients blood monocytes II. **A** Protocol outline. Cells were primed for 24h with FBG-C at 1 μM [FBG-C], protein vehicle control (VEH, TN buffer with PMB), LPS at 100 ng/mL [LPS], β-glucan at 10 μg/mL [β-GLU], or left unprimed in serum free medium. Immediately after the PRIME step cells were re-stimulated with LPS at 10 ng/mL. TNF and IL-6 levels in media at the end of the protocol were measured by ELISA (**B**). Data are shown as mean fold change over VEH (for FBG-C) or unprimed (for LPS and β-GLU) ± SEM from 6 (HC) or 5 (RA) independent donors. Black dots, HC donors; white dots, RA donors not receiving treatment; grey dots, RA donors treated with DMARDs. Data was analysed using unpaired T-test.

In summary, RA monocytes were demonstrated to be intrinsically different than healthy controls due to their potentiated capacity to produce pro-inflammatory cytokines in response to DAMPs and PAMPs. However, innate immune tolerance can be invoked in diseased cells in a manner similar to healthy control monocytes, albeit with a trend towards weaker training and more effective tolerance.

5.3 Discussion

In this chapter, I investigated whether alterations to innate immune memory may contribute to RA pathogenesis by causing loss of key regulatory mechanisms designed to limit myeloid cell activation. Tolerance induced by FBG-C, an immunogenic domain from tenascin-C, was found to be sustained in models mimicking characteristics of the chronic inflammation persisting in the rheumatic joint. The capability to become tolerised and trained was present in innate immune cells from RA patients, however these cells were distinguished by augmented primary response to threats of both endogenous (FBG-C) and pathogenic (LPS) origin. Therefore, innate immune memory was demonstrated to remain functional in a model of chronic inflammation and in diseased cells.

5.3.1 RA-specific extrinsic factors are not enough to block memory

The investigation of innate immune memory induced by FBG-C presented in chapter 4 revealed it is an intricate, temporally regulated phenomenon. The classic, 7 day memory assay emulates a situation where the primary trigger of inflammation is cleared and immune response switched off by the time the secondary threat arrives. However, this is not the most relevant setup for the study of RA. In the microenvironment of rheumatic joint, inflammation remains unresolved, and infiltrating blood monocytes are persistently exposed to DAMPs such as tenascin-C. It was speculated that such constant stimulation might finally lead to breaking of established tolerance. Yet, employment of sustained protocols, involving prolonged exposure to FBG-C for 7 days, did not result in reinstating of TNF responsiveness. Increasing concentration of FBG-C were equally not sufficient to overcome induced memory, suggesting tolerance is not a threshold limited effect. Furthermore, in protocols performed without medium changes monocytes were no longer sensitive to stimulation in the final 48h. This could be a result of certain immune mediators, or products of cell metabolism accumulating in culture medium, and preventing cell activation. Collectively, these data suggest that chronic exposition to DAMPs in RA might be insufficient to cause tolerance breakdown. However, the tested model was simplified, involving only one DAMP, FBG-C. In RA joint environment, a variety of DAMPs, cytokines, and other immune mediators is present. Therefore, potentially interesting follow up experiment could comprise RA synovial fluid applied in the sustained protocol, as a more complex and disease relevant source of immune triggers.

Together with high abundance of DAMPs, citrullination is another characteristic of the arthritic joint milieu. More than 100 different citrullinated proteins were identified in the synovial fluid collected from RA patients [423-425]. Under normal circumstances,

citrullination is a tightly controlled physiological process, requiring high calcium levels and redox conditions when happening outside of the cell [426]. The mechanisms behind RA hypercitrullination are not fully understood, however disruption of membrane integrity as a result of perforin and complement pathway activation have been implicated [427]. In addition to creating epitopes for ACPA generation, citrullination can have a profound impact on the function of modified molecules. Creation of neutral citrulline from cationic arginine changes local charge distribution, and this can affect formation and stability of both intra- and intermolecular protein interactions. For example, citrullination of vimentin and α-enolase, known targets of ACPAs in RA, resulted in inhibition of their physiological activities [428, 429], and could even promote proteolytic degradation [429]. Citrullinated FBG-C was also detected in RA synovial fluid [423], albeit the identified modification is located away from the TLR4-binding cationic ridge, on the other side of the molecule. Data generated by Dr Anja Schwenzer indicates *in vitro* citrullination of FBG-C does not inactivate the protein, but rather improves its capability to induce pro-inflammatory cytokine production in human monocyte derived macrophages (unpublished). A similar observation was made in this study, with citrullinated FBG-C eliciting modestly increased levels of TNF compared to control, sham citrullinated samples. Subsequently, lower concentrations of citrullinated FBG-C were sufficient to induce tolerance to re-stimulation with LPS. Thus, such RA characteristic post-translational modification appears to only improve innate immune memory sensitivity.

In conclusion, data acquired in the course of this study did not allow to confirm that DAMP accumulation or modification initiates innate immune tolerance breakdown, contributing to development of RA pathology. One might thus ask, do highly pro-inflammatory conditions in the synovial tissues indeed impact acquisition of tolerance?

It is of course possible that DAMP induced protective tolerance remains functional in RA, yet is insufficient to restrain overblown inflammation. However, tolerance might be also affected by some of the many other factors present in the RA synovium, not addressed in the scope of this report. An interesting candidate for this deleterious role is IFN-γ, cytokine secreted by T cells and contributing to ACPAs generation and synovial inflammation, as well as bone loss (reviewed in [430]). In human monocytes, treatment with IFN-γ was demonstrated to inhibit induction of LPS tolerance and rescue TNF production [431]. Thus, incorporation of IFN-γ in the memory protocols poses a next promising avenue in the study of innate immune memory. Other RA-specific factors, potentially responsible for the breakdown of tolerance in RA, could be also probed through the use of synovial fluid collected from diseased joints. This would be a worthwhile future endeavour, as identification of tolerance disruption and its molecular cause could allow for development of targeted therapeutic intervention, reinstating control over DAMP induced inflammation in cells of RA joint.

5.3.2 RA cells: intrinsically different, but tolerised as well

Genetic predisposition is a widely accepted causative factor underlying RA pathogenesis (reviewed in [432]). Disease susceptibility associates strongly with a number of HLA-DRB1 alleles, coding for major histocompatibility complex (MHC) class II molecule. Professional antigen presenting cells, such as macrophages, use MHC class II to present processed peptides to $CD4^+$ T cells. Single nucleotide polymorphisms conferring RA susceptibility were also identified in more than 30 non-HLA genes [432]. These include PADI4, citrullination executing enzyme; PTPN22, protein tyrosine phosphatase negatively regulating T cell-receptor signalling; TRAF1, signalling adaptor downstream of the TNF receptor superfamily, and negative regulator of TLR and NLR receptor signalling; STAT4, transcription factor mediating response to IL-12 and Th1 cell differentiation; as well as various cytokines, chemokines and other immune mediators, cytokine receptors and co-stimulatory molecules. While the exact functional results of the above loci remain controversial, likely due to significant heterogeneity in the human population, they are predominantly linked to various immune response signalling mechanisms.

It is therefore also possible that genetically determined, intrinsic differences in cell physiology in individuals who develop RA are the cause of impaired tolerance acquisition and contribute to increased disease susceptibility. In this study, analysis of blood monocytes from a small cohort of RA patients revealed induction of innate immune memory by PAMPs (LPS, β-glucan) and DAMPs (FBG-C) is not compromised. This experiment indicates generation of innate immune tolerance in patients with active disease is not obstructed, and inherent defects in mechanisms necessary for the initiation of this regulatory off switch are unlikely a meaningful factor driving dysregulated inflammation in RA.

However, diseased cells secreted substantially more TNF and IL-6 when first exposed to FBG-C and LPS. Increased TNF production following LPS stimulation was reported previously in RA blood monocytes [433] and synovial macrophages [407]. Although, other published studies show LPS induced secretion of this cytokine by monocytes isolated from RA patients is not different from healthy controls [434, 435]. This discrepancy might be a result of natural variability observed in human monocytes, heterogeneity of RA pathology, and also different treatment regimens used by examined patients, as all of these factors can affect cell capabilities to secrete cytokines. Hydroxycholoroquine and chloroquine, conventional DMARDs, were demonstrated to inhibit TNF and IL-6 release in LPS stimulated healthy human mononuclear cells [436-438]. What is more, both compounds were recently found to block innate immune training by heat killed *C. albicans* [439]. The patient cohort recruited in this project consisted individuals receiving hydroxychloroquine and/or methotrexate, and treatment naïve, yet no differences in primary cytokine response and induction of memory correlating with therapy could be observed.

My data demonstrates for the first time that blood monocytes from patients with active RA have enhanced capacity to produce pro-inflammatory cytokines in response to a DAMP. This characteristic can have a profound impact with regards to RA pathogenesis, as monocytes entering tenascin-C rich joint milieu would initially become cytokine super-producers, promoting the development of synovitis. Question remains, what is the reason for such heightened activity of RA monocytes? One might speculate that it is a consequence of inherent physiological differences specific for RA cells, as discussed in previous paragraphs. RA is a systemic disease, thus it is also possible that monocytes undergo priming in blood, or even in bone marrow, resulting in such augmented cytokine response. Sensitisation of healthy human monocytes in the context

of RA was described before. IgG immunocomplexes precipitated from RA sera were shown to prime monocytes for a potentiated TNF release in response to LPS, but also a number of DAMPs (C-reactive protein, HMGB1 and fibrinogen) [440]. Furthermore, pathogenic (BCG, β-glucan) end endogenous (Western diet) triggers of innate immune memory were demonstrated to induce re-programming in hematopoietic progenitor cells in bone marrow, resulting in long-term trained phenotype of mature myeloid cells and consecutive improved protection from infection [178, 441, 442]. Therefore, observed *in vitro* enhanced primary response of RA monocytes might be a manifestation of innate immune training generated by exposure of the cells, or cell progenitors, to immunocomplexes or other RA specific factors. Further work is necessary to fully understand functional programmes adapted by circulating monocytes in RA, however reversing of monocyte trained phenotype to allow for mitigation of cytokine release poses an attractive potential therapeutic strategy.

6

Final discussion

Contents

6.1 Conclusions 257

6.2 Clinical relevance 261

6.3 Future work 264

6.1 Conclusions

It is nearly three decades since the danger theory was proposed [443], and the term ‘DAMP’ was subsequently coined [444]. Nowadays, the concept of endogenously driven immune response is widely accepted and remains to be studied extensively. However, many outstanding biological questions on the nature of endogenous immune triggers remain unanswered. This work was aimed at advancing our understanding of the molecular basis of danger, and exploring the role of DAMPs reaching beyond the primary activation of myeloid cells. For this purpose, immune responses elicited by endogenous triggers were investigated, and control mechanisms that shape these responses were identified. Finally, the regulatory mechanisms guiding DAMP induced inflammation were studied in the context of autoimmune diseases, such as RA.

Tenascin-C was examined as an exemplar DAMP, previously demonstrated to bind to TLR4 and activate immune responses through a cationic ridge exposed on the surface of the C-terminal FBG domain. In this study, this positively charged feature was also identified in FBG domains from other proteins, and its presence was confirmed to be required for receptor activation. Therefore, in chapter 3 the cationic ridge was found to be a relatively widespread, universal TLR4 binding epitope in stress response proteins containing structurally conserved FBG domains (data published in [193]). The FBG domain from tenascin-C was also demonstrated to have functions beyond activation of the first wave of inflammation. In chapter 4, FBG-C was discovered to induce innate immune memory in human monocytes and macrophages, modulating cell responses to secondary challenges of various origin. The study of memory generated by FBG-C allowed to identify how these second wave responses are adapted to both limit inflammation, and also re-direct the flavour of the immune response in a temporally orchestrated manner. Hence, FBG-C induced memory was demonstrated to be both an

inflammation off switch, and a kinetic evolution, allowing for a modulated response as the changing environment requires. The predominant focus of the published work in the field of innate immunity is simply the initiation of inflammation. However, little is known about how the immune responses develop over time, are shaped and controlled by the immune system, and how they are eventually turned off. These processes are of paramount importance, being an essential part of a physiological, resolvable immune response. Conclusions presented in chapter 4 take us a step closer towards understanding these burning questions.

Data acquired in the course of this investigation adds to evidence on the many similarities in how our bodies sense and respond to infection and injury. Pathogenic and endogenous triggers can ligate the same receptors, and activate the same downstream signalling cascades, for example TLR4 is bound by bacterial LPS [47], and FBG domain cationic ridge-containing stress response proteins, such as tenascin-C [136, 193]. Both LPS [337] and tenascin-C [136] are known to activate the MyD88-dependent pathway, and induce production of pro-inflammatory cytokines. Here, FBG-C was demonstrated to re-program the cells to induce tolerance in a manner similar to LPS, limiting expression of immune mediators that drive inflammation in order to protect from excessive tissue damage.

However, PAMPs and DAMPs are signals of very different threats, which require tailored responses to return the system to homeostasis. Thus, it would be inconceivable for the immune system not to discern between such triggers. Indeed, we know that infection and sterile inflammation stimulate distinct modes of activation of innate immune cells. While LPS induces production of pro-inflammatory cytokines and proteases in human macrophages, FBG-C generates a different phenotype, characterized by secretion of a separate cytokine subset, and enhanced expression and phosphorylation

of matrix molecules [191]. This diversification is likely a result of trigger specific alterations in the signalling through common pathways. Firstly, specific co-receptors, CD14 and MD-2, are engaged to sense LPS [47], but are not necessary for FBG-C to activate TLR4 [136]. Secondly, selection of adaptor molecules recruited by these microbe-derived and host-derived stimuli are not identical. For example, NF-κB and MAPK signalling are activated by both LPS and FBG-C [191], and responses generated by both triggers involve MyD88-dependent pathway stimulation. However, only LPS was confirmed to signal via the non-classical, TRIF-dependent pathway, and induce expression of type I interferons [445]. Furthermore, as illustrated in this study, LPS and FBG-C both offer cross-protection from bacterial infection and injury induced tissue damage through induction of tolerance, though FBG-C was also demonstrated to potentiate cytokine response to certain pathogenic triggers.

Overall, the analysis of memory induced in the context of injury, contrasted to the previously described pathogenic LPS tolerance and β-glucan training, offers an insight into the fascinating complexities of cellular programmes induced by these various triggers. Bacterial invasion generates a strong, widespread tolerant state. Yeast infection, simulated by the use of β-glucan, strengthens resistance to opportunistic bacterial infection, however it does not alter response to injury, as demonstrated for the first time in this study. Finally, cells exposed to FBG domain of tenascin-C, an archetypal tissue damage marker, were shown to acquire a sophisticated memory phenotype, involving effector specific modulation of responses, distinct for the various types of subsequent threat encountered. Injury induces suppression of pro-inflammatory cytokine secretion in response to further injury, and to bacterial invasion; however secondary exposure to intracellular pathogens and fungi results in potentiated release of certain immune mediators. Moreover, FBG-C induced memory is temporally regulated, with initial

superinduction of IL-6, followed by acquisition of tolerance later on. Such biphasic control of secondary immune response was identified in LPS primed cells as well, although mediated by different processes at a transcriptional level.

In conclusion, regulatory mechanisms employed to control responses to infections are also present during sterile inflammation, however they are not a one-to-one copy, but rather are differentially controlled, and tailored to offer most efficient, context dependent protection.

In conclusion, research presented in this thesis describes molecular determinants of danger, and elucidates how immune responses triggered by these stimuli evolve over time to protect from opportunistic infection following tissue damage, and from further tissue damage ensuing as a result of exacerbated immune response. These regulatory mechanisms ensure immune response proceeds in a regulated manner, avoiding destructive inflammation, but allowing for repair and regeneration, before being switched off completely.

6.2 Clinical relevance

The main underlying cause of symptoms in RA is persistent synovitis, manifesting in joint swelling and pain, and ultimately leading to cartilage destruction and bone loss [446]. Thus, treatment strategies aim at suppressing inflammation to alleviate the symptoms and prevent structural damage. Patients newly diagnosed with RA are recommended to promptly start therapy using disease modifying anti-rheumatic drugs (DMARDs) [447], a class of medications with immunosuppressive and immunomodulatory properties. DMARDs can be divided into two major groups: conventional synthetic and biological. Conventional DMARDs, for example methotrexate and hydroxychloroquine, are small molecule broad spectrum immunosupressants. Biological DMARDs target specific pathways involved in propagation of joint inflammation, through inhibiting TNF signalling, inhibiting IL-6 receptor activation, blocking of T cell co-stimulation and depletion of B cells (reviewed in [448]).

Modern combination DMARD therapies, including short-term use of glucocorticoids, allow for good disease management, and in 20-40% patients sustained clinical remission can be achieved [449]. However, these strategies require personalised approach, and frequent monitoring and therapy adjustments, which can be inconvenient for the patient. What is more, administration of DMARDs can produce adverse effects such as gastrointestinal problems, stomatitis, alopecia and various skin reactions [450]. Some DMARDs can cause bone marrow suppression [451], hepatotoxicity [452], or increase risk of serious infections [453]. Unfortunately, with currently available treatment options long term, drug-free remission is not impossible, yet remains elusive [454]. Therefore, novel therapeutics that could compliment currently used treatment strategies are still in high demand.

What is more, despite our current understanding of genetic and environmental risk factors, still very little is known about the exact sequence of events resulting in dysregulation of inflammation in the joint and the development of RA. The disease is usually diagnosed when synovitis is already established, and causing severe discomfort for the patient. We are yet to identify molecular and cellular culprits, as well as impaired regulatory mechanisms, underlying the exacerbated immune processes leading to the initiation and perpetuation of inflammation in early arthritis.

Tenascin-C is a protein with a highly restricted expression pattern, that is absent in most healthy adult tissues, yet upregulated locally in response to injury and inflammation [189]. In the context of RA, tenascin-C levels are elevated in patient blood, and correlate with joint erosion [263]; and expression in the inflamed joint is not switched off, but persists, with protein accumulating in the tissue [419, 420]. Furthermore, in a mouse model, tenascin-C deficiency protected the animals from erosive arthritis, and administration of FBG-C induced joint damage [136]. In addition, monoclonal anti-FBG-C antibodies, neutralizing activation of TLR4 by the protein, prevented progression of experimental arthritis in rats [416]. Therefore, tenascin-C, and in particular its immunogenic domain, FBG-C, remains an attractive candidate for innovative RA treatments.

Herein, in chapter 5, immune responses induced by FBG-C were investigated in a model of chronic inflammation and in cells from people with RA. Protective FBG-C tolerance was demonstrated to be maintained during prolonged exposure to the molecule, and not impaired by citrullination, a posttranslational modification frequent in the RA joint. Moreover, induction of innate immune memory by FBG-C was not obstructed in diseased cells, although, more potent cytokine responses to both endogenous and pathogenic triggers was observed in patient cells, compared to healthy controls.

More extensive work is required to validate if DAMP induced tolerance in myeloid cells indeed remains fully functional in RA, and is not broken by other components present in inflamed joint milieu. However, the detected potentiation of response to primary stimulation of diseased monocytes *ex vivo* might suggest that a trained phenotype is induced in these cells by soluble agents circulating in the blood of RA patients. Augmented production of cytokines, for example pathogenic TNF, following exposure to FBG-C (and potentially other triggers) by such trained cells infiltrating arthritic joint might promote accelerated disease development. Therefore, innate immune memory could be a new prospective mechanism with relevance for the treatment of RA. Reverting of the trained phenotype observed in diseased cells could limit the excessive production of pro-inflammatory cytokines, help regain control over the deleterious chronic inflammation, and thus impact disease progression.

6.3 Future work

Research presented in this thesis broadens our knowledge on the immune responses and innate memory induced in tissue damage by endogenous triggers, such as tenascin-C. The cellular effects of innate immune tolerance and training induced by FBG-C, including qualitative, quantitative and temporal regulation of effector molecules, were described in chapter 4, however to further elucidate the underlying cellular re-programming, the following work will be performed in the near future:

- Chromatin immunoprecipitation was performed in memory protocols to measure epigenetic modifications induced by FBG-C, in comparison to LPS. Now, collected data will be analysed to verify if the state of chromatin, influenced by re-modelling of histone marks, is responsible for the observed transcriptional regulation.
- A library of small molecule inhibitors was used to target epigenetic remodelling induced by FBG-C or by LPS. Bioinformatic analysis of this dataset is now required to identify probes that selectively modulate memory induced by FBG, LPS, or both stimuli. The top 3-5 probes of interest will be then validated using negative control probes and in dose response repeats.

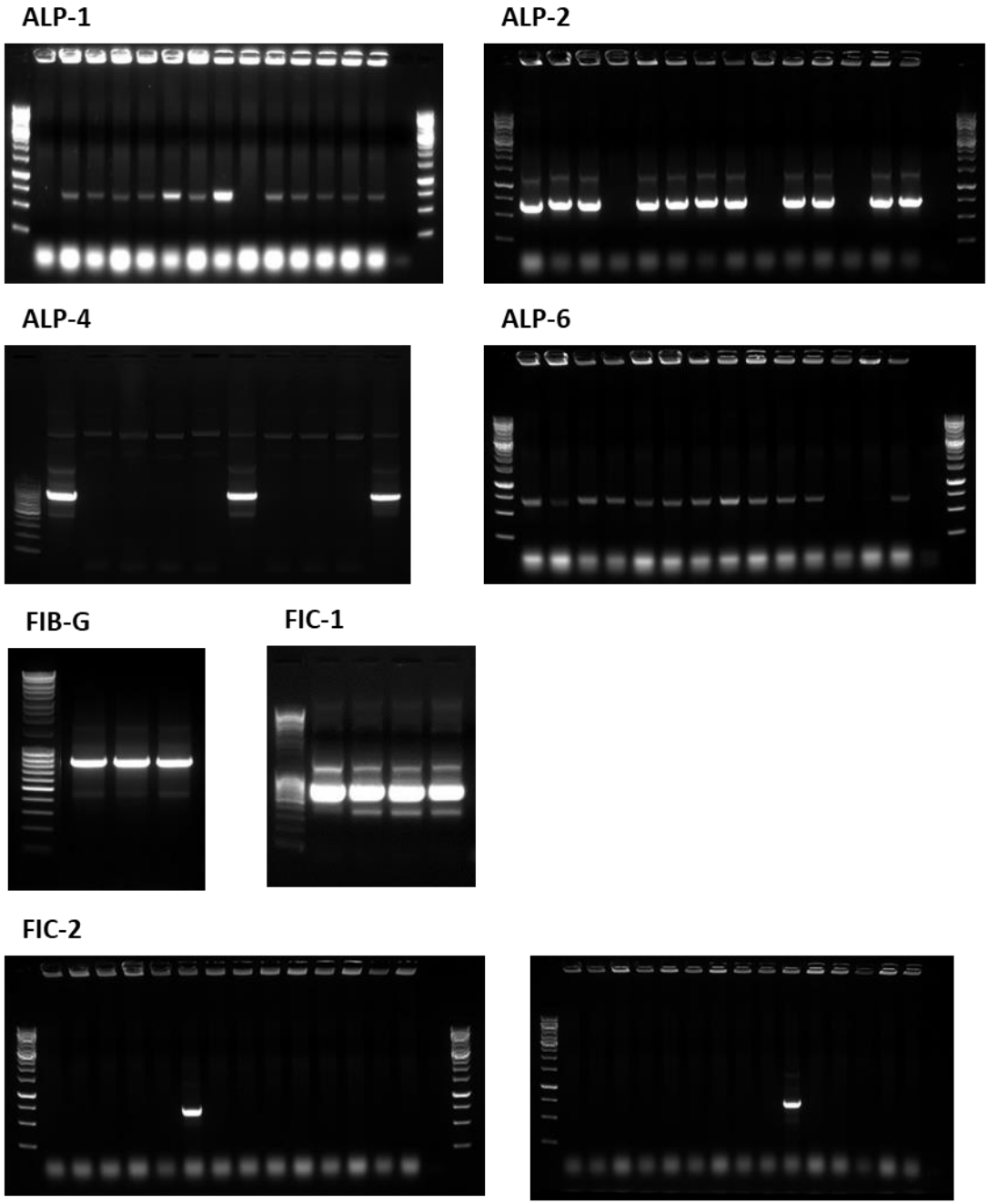
A number of other puzzling questions emerged in the course of this research that would be fascinating to address in the longer term. These include:

– What is the exact mode of TLR4 activation by FBG-C (and other FBG domains), and co-receptor requirements, as well as downstream signalling cascades employed to elicit immune responses?

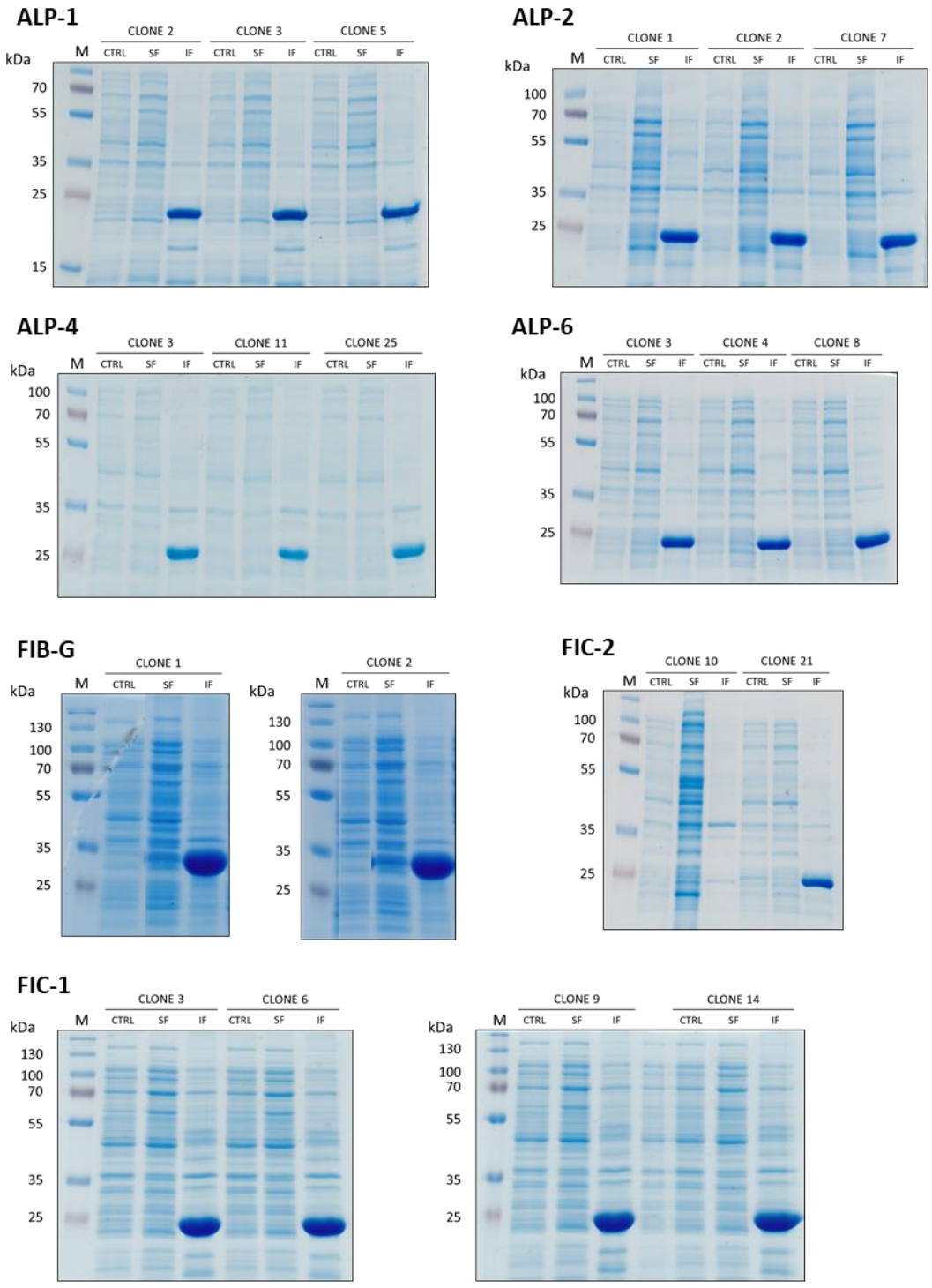
– Are other FRePs inducing a similar pattern of innate immune memory, or is there an FBG domain specificity?

- Are upstream events, such as diminished receptor availability on the cell surface or blockade of NF-κB activation by negative regulators of signalling, contributing to the observed FBG-C tolerance?
- Could FBG-C memory phenotype be recapitulated *in vivo*?
- Are other, RA specific DAMPs (e.g. HMGB1, S100 proteins) also inducing innate immune tolerance in sterile conditions? Is this tolerance impacted in chronic inflammation, or in people who develop RA?
- Is DAMP tolerance broken in RA due to soluble factors present in the synovial fluid (e.g. IFN-γ)?
- Could selected epigenetic probes be used to revert memory phenotypes in the clinic?

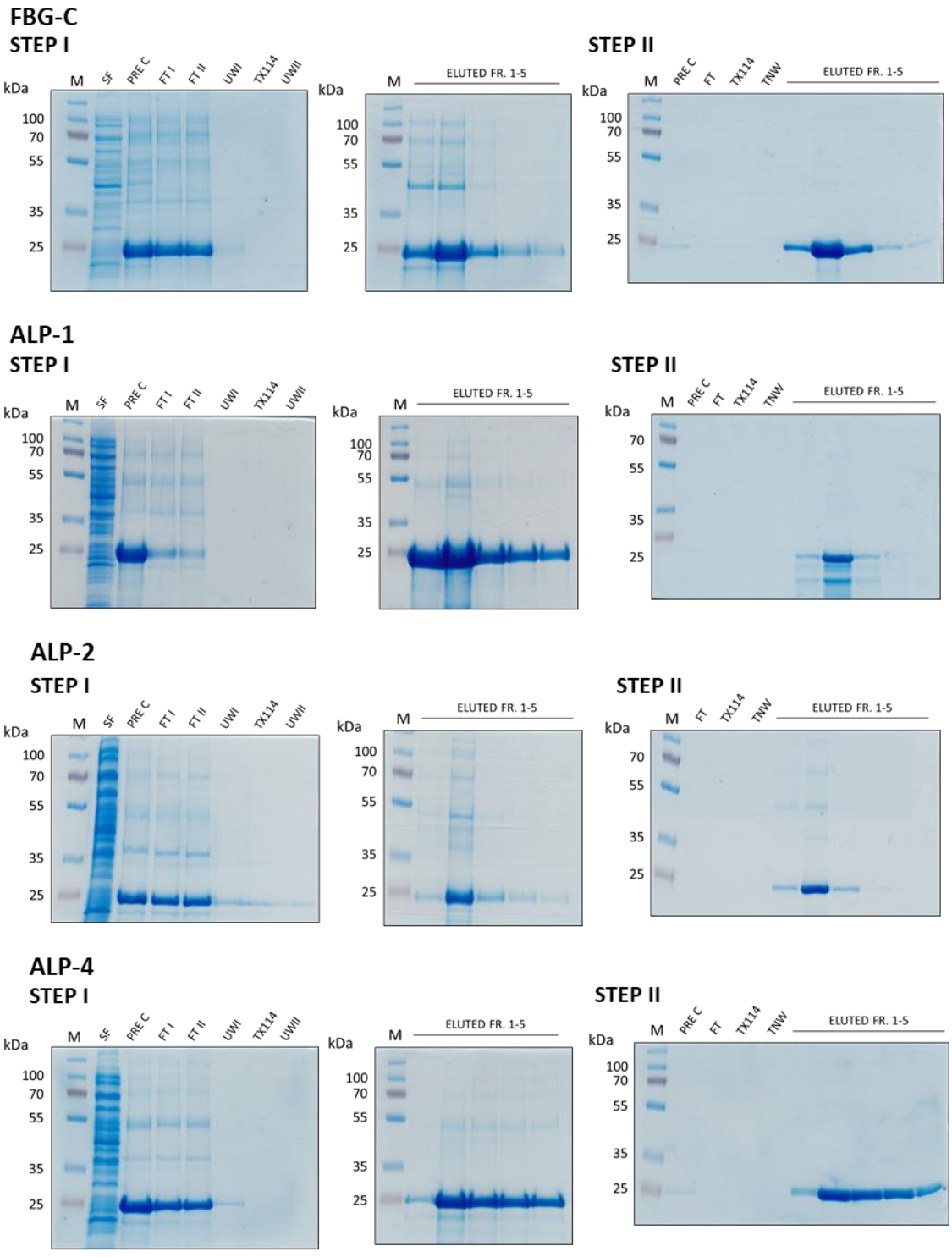
Appendix



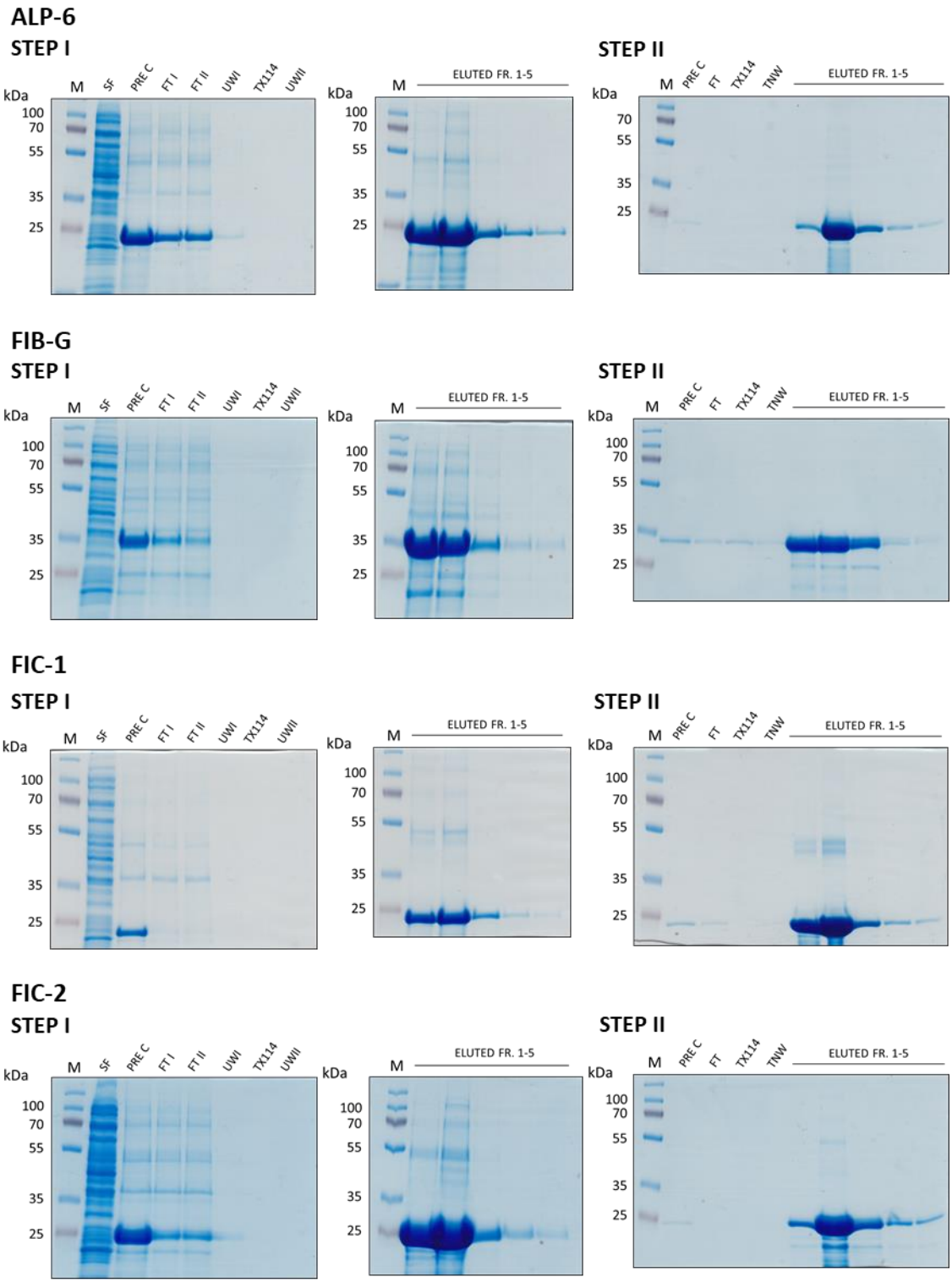
Supplementary figure 1 Successful cloning confirmation by PCR/colony PCR. To identify clones containing insert, colony PCR with insert-specific primers was performed. Clones that gave PCR products of the expected insert size were then confirmed by sequencing to ensure complete DNA identity.



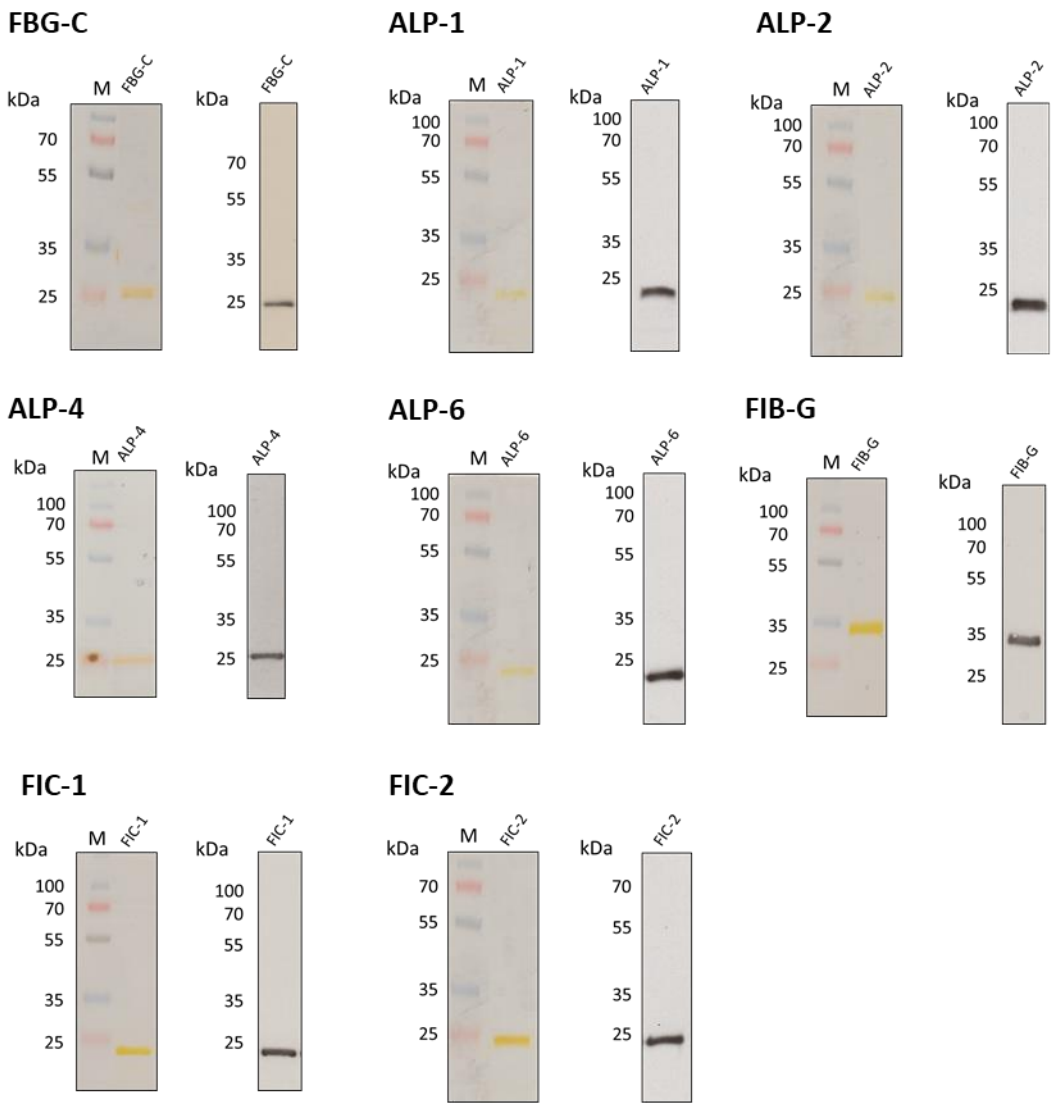
Supplementary figure 2 Test expression of cloned FBG domains. Positive clones were transformed into *E. coli* BL21 cells and small scale test expression was performed. Expression efficiency was assessed with SDS-PAGE. CTRL, unstimulated control; SF, soluble fraction; IF, insoluble fraction.



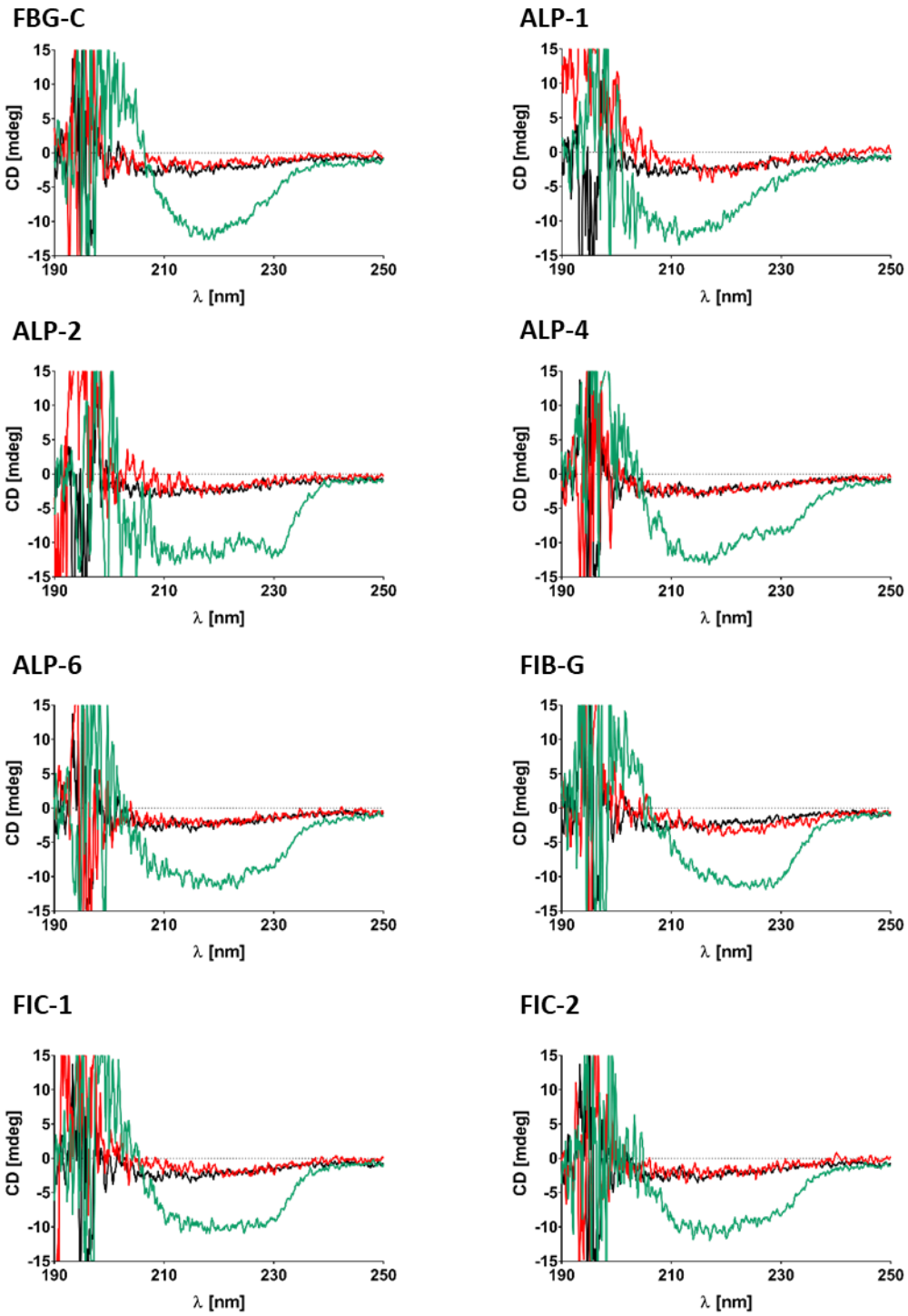
Supplementary figure 3 FBG protein purification: FBG-C, ALP-1, ALP-2 and ALP-4. Selected well-expressing clones were used to produce recombinant FBG domains on a larger scale. Efficiency of the purification protocol was assessed with SDS-PAGE. SF, soluble fraction; PRE C, pre-column sample; FT, flow through; UW, urea wash; TX114, Triton X-114 wash; TNW, Tris-NaCl wash.



Supplementary figure 4 FBG protein purification: ALP-6, FIB-G, FIC-1 and FIC-2. Selected well-expressing clones were used to produce recombinant FBG domains on a larger scale. Efficiency of the purification protocol was assessed with SDS-PAGE. SF, soluble fraction; PRE C, pre-column sample; FT, flow through; UW, urea wash; TX114, Triton X-114 wash; TNW, Tris-NaCl wash.



Supplementary figure 5 FBG protein purity control. The purity of obtained recombinant proteins was assessed by silver staining and western blotting with anti-His Tag antibody of 1 μg protein.



Supplementary figure 6 FBG protein folding control. Folding of purified proteins was assessed by circular dichroism. Folded FBG domains generate a distinct negative peak between 210 nm and 230 nm, which is no longer observed following thermal denaturation of the protein. Green line, protein sample; red line, protein sample boiled; black line, buffer.

Bibliography

1. Cooper, S. and C.E. Helmstetter, *Chromosome replication and the division cycle of Escherichia coli.* Journal of Molecular Biology, 1968. **31**(3): p. 519-540.
2. Medzhitov, R., *Recognition of microorganisms and activation of the immune response.* Nature, 2007. **449**(7164): p. 819-826.
3. Proksch, E., J.M. Brandner, and J.M. Jensen, *The skin: an indispensable barrier.* Exp Dermatol, 2008. **17**(12): p. 1063-72.
4. Belkaid, Y. and T.W. Hand, *Role of the microbiota in immunity and inflammation.* Cell, 2014. **157**(1): p. 121-41.
5. Dunkelberger, J.R. and W.C. Song, *Complement and its role in innate and adaptive immune responses.* Cell Res, 2010. **20**(1): p. 34-50.
6. Ganz, T., *Defensins: antimicrobial peptides of innate immunity.* Nat Rev Immunol, 2003. **3**(9): p. 710-20.
7. Bals, R. and J.M. Wilson, *Cathelicidins--a family of multifunctional antimicrobial peptides.* Cell Mol Life Sci, 2003. **60**(4): p. 711-20.
8. Mogensen, T.H., *Pathogen Recognition and Inflammatory Signaling in Innate Immune Defenses.* Clinical Microbiology Reviews, 2009. **22**(2): p. 240-+.
9. Bertani, B. and N. Ruiz, *Function and Biogenesis of Lipopolysaccharides.* EcoSal Plus, 2018. **8**(1).
10. Takeuchi, O. and S. Akira, *Pattern recognition receptors and inflammation.* Cell, 2010. **140**(6): p. 805-20.
11. Alberts, B., Johnson, A., Lewis, J., et al., *Molecular Biology of the Cell. 4th edition.* 2002.
12. Purvis, A. and A. Hector, *Getting the measure of biodiversity.* Nature, 2000. **405**(6783): p. 212-9.
13. Albert, M.R., *Fever therapy for general paresis.* Int J Dermatol, 1999. **38**(8): p. 633-7.
14. Lehner, M.D. and T. Hartung, *Endotoxin tolerance-mechanisms and beneficial effects in bacterial infection.* Rev Physiol Biochem Pharmacol, 2002. **144**: p. 95-141.
15. Beeson, P.B. and R. Technical Assistance of Elizabeth, *Tolerance to Bacterial Pyrogens : I. Factors Influencing Its Development.* J Exp Med, 1947. **86**(1): p. 29-38.
16. Greisman, S.E., F.A. Carozza, Jr., and J.D. Hills, *Mechanisms of endotoxin tolerance. I. Relationship between tolerance and reticuloendothelial system phagocytic activity in the rabbit.* J Exp Med, 1963. **117**: p. 663-74.
17. Watson, D.W. and Y.B. Kim, *Modification of Host Responses to Bacterial Endotoxins. I. Specificity of Pyrogenic Tolerance and the Role of Hypersensitivity in Pyrogenicity, Lethality, and Skin Reactivity.* J Exp Med, 1963. **118**: p. 425-46.
18. Freudenberg, M.A. and C. Galanos, *Induction of tolerance to lipopolysaccharide (LPS)-D-galactosamine lethality by pretreatment with LPS is mediated by macrophages.* Infect Immun, 1988. **56**(5): p. 1352-7.
19. Lehner, M.D., et al., *Improved innate immunity of endotoxin-tolerant mice increases resistance to Salmonella enterica serovar typhimurium infection despite attenuated cytokine response.* Infect Immun, 2001. **69**(1): p. 463-71.
20. Williams, J.F., *Induction of tolerance in mice and rats to the effect of endotoxin to decrease the hepatic microsomal mixed-function oxidase system. Evidence for a possible macrophage-derived factor in the endotoxin effect.* International Journal of Immunopharmacology, 1985. **7**(4): p. 501-509.
21. Sanchez-Cantu, L., H.N. Rode, and N.V. Christou, *Endotoxin tolerance is associated with reduced secretion of tumor necrosis factor.* Arch Surg, 1989. **124**(12): p. 1432-5; discussion 1435-6.
22. Mengozzi, M., et al., *Reversal of defective IL-6 production in lipopolysaccharide-tolerant mice by phorbol myristate acetate.* The Journal of Immunology, 1991. **147**(3): p. 899.

23. Erroi, A., et al., *Differential regulation of cytokine production in lipopolysaccharide tolerance in mice.* Infect Immun, 1993. **61**(10): p. 4356-9.
24. Wakabayashi, G., et al., *Altered interleukin-1 and tumor necrosis factor production and secretion during pyrogenic tolerance to LPS in rabbits.* Am J Physiol, 1994. **267**(1 Pt 2): p. R329-36.
25. Astiz, M.E., et al., *Pretreatment of normal humans with monophosphoryl lipid A induces tolerance to endotoxin: A prospective, double-blind, randomized, controlled trial.* Critical Care Medicine, 1995. **23**(1): p. 9-17.
26. Takasuka, N., T. Tokunaga, and K.S. Akagawa, *Preexposure of macrophages to low doses of lipopolysaccharide inhibits the expression of tumor necrosis factor-alpha mRNA but not of IL-1 beta mRNA.* The Journal of Immunology, 1991. **146**: p. 3824-3830.
27. Tominaga, K., et al., *Lipopolysaccharide tolerance in murine peritoneal macrophages induces downregulation of the lipopolysaccharide signal transduction pathway through mitogen-activated protein kinase and nuclear factor-κB cascades, but not lipopolysaccharide-incorporation steps.* Biochimica et Biophysica Acta (BBA) - Molecular Cell Research, 1999. **1450**(2): p. 130-144.
28. Wysocka, M., et al., *IL-12 suppression during experimental endotoxin tolerance: dendritic cell loss and macrophage hyporesponsiveness.* J Immunol, 2001. **166**(12): p. 7504-13.
29. Porta, C., et al., *Tolerance and M2 (alternative) macrophage polarization are related processes orchestrated by p50 nuclear factor kappaB.* Proc Natl Acad Sci U S A, 2009. **106**(35): p. 14978-83.
30. Rajaiah, R., et al., *Dissociation of endotoxin tolerance and differentiation of alternatively activated macrophages.* J Immunol, 2013. **190**(9): p. 4763-72.
31. Dobrovolskaia, M.A., et al., *Induction of in vitro reprogramming by Toll-like receptor (TLR)2 and TLR4 agonists in murine macrophages: effects of TLR "homotolerance" versus "heterotolerance" on NF-kappa B signaling pathway components.* J Immunol, 2003. **170**(1): p. 508-19.
32. Julian, M.W., et al., *Tolerance and Cross-Tolerance following Toll-Like Receptor (TLR)-4 and -9 Activation Are Mediated by IRAK-M and Modulated by IL-7 in Murine Splenocytes.* PLoS One, 2015. **10**(7): p. e0132921.
33. O'Carroll, C., et al., *Identification of a unique hybrid macrophage-polarization state following recovery from lipopolysaccharide tolerance.* J Immunol, 2014. **192**(1): p. 427-36.
34. Butcher, S.K., et al., *Toll-Like Receptors Drive Specific Patterns of Tolerance and Training on Restimulation of Macrophages.* Front Immunol, 2018. **9**: p. 933.
35. Pena, O.M., et al., *Endotoxin tolerance represents a distinctive state of alternative polarization (M2) in human mononuclear cells.* J Immunol, 2011. **186**(12): p. 7243-54.
36. Weisheit, C.K., et al., *Sustained Immunoparalysis in Endotoxin-Tolerized Monocytic Cells.* Mediators Inflamm, 2020. **2020**: p. 8294342.
37. Randow, F., et al., *Mechanism of endotoxin desensitization: involvement of interleukin 10 and transforming growth factor beta.* J Exp Med, 1995. **181**(5): p. 1887-92.
38. Widdrington, J.D., et al., *Exposure of Monocytic Cells to Lipopolysaccharide Induces Coordinated Endotoxin Tolerance, Mitochondrial Biogenesis, Mitophagy, and Antioxidant Defenses.* Front Immunol, 2018. **9**: p. 2217.
39. Saeed, S., et al., *Epigenetic programming of monocyte-to-macrophage differentiation and trained innate immunity.* Science, 2014. **345**(6204): p. 1251086.
40. Petes, C., et al., *The effects of CD14 and IL-27 on induction of endotoxin tolerance in human monocytes and macrophages.* J Biol Chem, 2018. **293**(45): p. 17631-17645.
41. Virca, G.D., et al., *Lipopolysaccharide Induces Hyporesponsiveness to Its Own Action in RAW 264.7 Cells.* Journal of Biological Chemistry, 1989. **264**(36): p. 21951-21956.

42. El Gazzar, M., et al., *Epigenetic silencing of tumor necrosis factor alpha during endotoxin tolerance.* J Biol Chem, 2007. **282**(37): p. 26857-64.
43. Muller, M.M., et al., *Global analysis of glycoproteins identifies markers of endotoxin tolerant monocytes and GPR84 as a modulator of TNFalpha expression.* Sci Rep, 2017. **7**(1): p. 838.
44. West, M.A. and W. Heagy, *Endotoxin tolerance: a review.* Crit Care Med, 2002. **30**(1 Suppl): p. S64-73.
45. Seatter, S.C., et al., *ENDOTOXIN PRETREATMENT OF HUMAN MONOCYTES ALTERS SUBSEQUENT ENDOTOXIN-TRIGGERED RELEASE OF INFLAMMATORY MEDIATORS.* Shock, 1995. **3**(4).
46. del Fresno, C., et al., *Potent phagocytic activity with impaired antigen presentation identifying lipopolysaccharide-tolerant human monocytes: demonstration in isolated monocytes from cystic fibrosis patients.* J Immunol, 2009. **182**(10): p. 6494-507.
47. Park, B.S. and J.O. Lee, *Recognition of lipopolysaccharide pattern by TLR4 complexes.* Exp Mol Med, 2013. **45**: p. e66.
48. Akira, S. and K. Takeda, *Toll-like receptor signalling.* Nat Rev Immunol, 2004. **4**(7): p. 499-511.
49. Nomura, F., et al., *Cutting edge: endotoxin tolerance in mouse peritoneal macrophages correlates with down-regulation of surface toll-like receptor 4 expression.* J Immunol, 2000. **164**(7): p. 3476-9.
50. Adib-Conquy, M. and J.M. Cavaillon, *Gamma interferon and granulocyte/monocyte colony-stimulating factor prevent endotoxin tolerance in human monocytes by promoting interleukin-1 receptor-associated kinase expression and its association to MyD88 and not by modulating TLR4 expression.* J Biol Chem, 2002. **277**(31): p. 27927-34.
51. Medvedev, A.E., et al., *Induction of tolerance to lipopolysaccharide and mycobacterial components in Chinese hamster ovary/CD14 cells is not affected by overexpression of Toll-like receptors 2 or 4.* J Immunol, 2001. **167**(4): p. 2257-67.
52. Fan, H. and J.A. Cook, *Molecular mechanisms of endotoxin tolerance.* J Endotoxin Res, 2004. **10**(2): p. 71-84.
53. Labeta, M.O., et al., *CD14 and tolerance to lipopolysaccharide: biochemical and functional analysis.* Immunology, 1993. **80**(3): p. 415-423.
54. Ziegler-Heitbrock, H.W., et al., *Tolerance to lipopolysaccharide involves mobilization of nuclear factor kappa B with predominance of p50 homodimers.* 1994(0021-9258 (Print)).
55. Martin, M., et al., *Differential induction of endotoxin tolerance by lipopolysaccharides derived from Porphyromonas gingivalis and Escherichia coli.* J Immunol, 2001. **167**(9): p. 5278-85.
56. Medvedev, A.E., et al., *Dysregulation of LPS-induced Toll-like receptor 4-MyD88 complex formation and IL-1 receptor-associated kinase 1 activation in endotoxin-tolerant cells.* J Immunol, 2002. **169**(9): p. 5209-16.
57. Medvedev, A.E., K.M. Kopydlowski, and S.N. Vogel, *Inhibition of lipopolysaccharide-induced signal transduction in endotoxin-tolerized mouse macrophages: dysregulation of cytokine, chemokine, and toll-like receptor 2 and 4 gene expression.* J Immunol, 2000. **164**(11): p. 5564-74.
58. Shi, L., et al., *Endotoxin tolerance in monocytes can be mitigated by alpha2-interferon.* J Leukoc Biol, 2015. **98**(4): p. 651-9.
59. Shalova, I.N., et al., *Human monocytes undergo functional re-programming during sepsis mediated by hypoxia-inducible factor-1alpha.* Immunity, 2015. **42**(3): p. 484-98.
60. Biswas, S.K. and E. Lopez-Collazo, *Endotoxin tolerance: new mechanisms, molecules and clinical significance.* Trends Immunol, 2009. **30**(10): p. 475-87.

61. Kalesnikoff, J., et al., *SHIP negatively regulates IgE + antigen-induced IL-6 production in mast cells by inhibiting NF-kappa B activity.* J Immunol, 2002. **168**(9): p. 4737-46.
62. Sly, L.M., et al., *LPS-induced upregulation of SHIP is essential for endotoxin tolerance.* Immunity, 2004. **21**(2): p. 227-39.
63. Piao, W., et al., *Endotoxin tolerance dysregulates MyD88- and Toll/IL-1R domain-containing adapter inducing IFN-beta-dependent pathways and increases expression of negative regulators of TLR signaling.* J Leukoc Biol, 2009. **86**(4): p. 863-75.
64. Pan, H., et al., *SMAD4 is required for development of maximal endotoxin tolerance.* J Immunol, 2010. **184**(10): p. 5502-9.
65. Xiong, Y. and A.E. Medvedev, *Induction of endotoxin tolerance in vivo inhibits activation of IRAK4 and increases negative regulators IRAK-M, SHIP-1, and A20.* J Leukoc Biol, 2011. **90**(6): p. 1141-8.
66. Nakagawa, R., et al., *SOCS-1 Participates in Negative Regulation of LPS Responses.* Immunity, 2002. **17**(5): p. 677-687.
67. Kobayashi, K., et al., *IRAK-M Is a Negative Regulator of Toll-like Receptor Signaling.* Cell, 2002. **110**(2): p. 191-202.
68. Kinjyo, I., et al., *SOCS1/JAB Is a Negative Regulator of LPS-Induced Macrophage Activation.* Immunity, 2002. **17**(5): p. 583-591.
69. Xiong, Y., et al., *Endotoxin tolerance impairs IL-1 receptor-associated kinase (IRAK) 4 and TGF-beta-activated kinase 1 activation, K63-linked polyubiquitination and assembly of IRAK1, TNF receptor-associated factor 6, and IkappaB kinase gamma and increases A20 expression.* J Biol Chem, 2011. **286**(10): p. 7905-7916.
70. Adib-Conquy, M., et al., *Up-regulation of MyD88s and SIGIRR, molecules inhibiting Toll-like receptor signaling, in monocytes from septic patients.* Crit Care Med, 2006. **34**(9): p. 2377-85.
71. Adib-Conquy, M., et al., *NF-kappaB expression in mononuclear cells of patients with sepsis resembles that observed in lipopolysaccharide tolerance.* Am J Respir Crit Care Med, 2000. **162**(5): p. 1877-83.
72. Adib-Conquy, M., et al., *Long-term-impaired expression of nuclear factor-κB and IκBα in peripheral blood mononuclear cells of trauma patients.* Journal of Leukocyte Biology, 2001. **70**(1): p. 30-38.
73. Foster, S.L. and R. Medzhitov, *Gene-specific control of the TLR-induced inflammatory response.* Clin Immunol, 2009. **130**(1): p. 7-15.
74. Foster, S.L., D.C. Hargreaves, and R. Medzhitov, *Gene-specific control of inflammation by TLR-induced chromatin modifications.* Nature, 2007. **447**(7147): p. 972-8.
75. Bannister, A.J. and T. Kouzarides, *Regulation of chromatin by histone modifications.* Cell Res, 2011. **21**(3): p. 381-95.
76. Novakovic, B., et al., *beta-Glucan Reverses the Epigenetic State of LPS-Induced Immunological Tolerance.* Cell, 2016. **167**(5): p. 1354-1368 e14.
77. El Gazzar, M., et al., *G9a and HP1 couple histone and DNA methylation to TNFalpha transcription silencing during endotoxin tolerance.* J Biol Chem, 2008. **283**(47): p. 32198-208.
78. Mino, T. and O. Takeuchi, *Post-transcriptional regulation of cytokine mRNA controls the initiation and resolution of inflammation.* Biotechnol Genet Eng Rev, 2013. **29**: p. 49-60.
79. El Gazzar, M. and C.E. McCall, *MicroRNAs distinguish translational from transcriptional silencing during endotoxin tolerance.* J Biol Chem, 2010. **285**(27): p. 20940-51.
80. Dan, C., et al., *Modulation of TNF-alpha mRNA stability by human antigen R and miR181s in sepsis-induced immunoparalysis.* EMBO Mol Med, 2015. **7**(2): p. 140-57.
81. Zhang, W., et al., *MicroRNA-181b regulates endotoxin tolerance by targeting IL-6 in macrophage RAW264.7 cells.* J Inflamm (Lond), 2015. **12**: p. 18.

82. Learn, C.A., S.B. Mizel, and C.E. McCall, *mRNA and protein stability regulate the differential expression of pro- and anti-inflammatory genes in endotoxin-tolerant THP-1 cells.* J Biol Chem, 2000. **275**(16): p. 12185-93.
83. Nahid, M.A., M. Satoh, and E.K. Chan, *MicroRNA in TLR signaling and endotoxin tolerance.* Cell Mol Immunol, 2011. **8**(5): p. 388-403.
84. Ifrim, D.C., et al., *Trained immunity or tolerance: opposing functional programs induced in human monocytes after engagement of various pattern recognition receptors.* Clin Vaccine Immunol, 2014. **21**(4): p. 534-45.
85. Lehner, M.D., et al., *Induction of cross-tolerance by lipopolysaccharide and highly purified lipoteichoic acid via different Toll-like receptors independent of paracrine mediators.* J Immunol, 2001. **166**(8): p. 5161-7.
86. Seeley, J.J. and S. Ghosh, *Molecular mechanisms of innate memory and tolerance to LPS.* J Leukoc Biol, 2017. **101**(1): p. 107-119.
87. Melillo, D., et al., *Innate Immune Memory in Invertebrate Metazoans: A Critical Appraisal.* Front Immunol, 2018. **9**: p. 1915.
88. Netea, M.G., J. Quintin, and J.W. van der Meer, *Trained immunity: a memory for innate host defense.* Cell Host Microbe, 2011. **9**(5): p. 355-61.
89. Ross, A.F., *Systemic acquired resistance induced by localized virus infections in plants.* Virology, 1961. **14**(3): p. 340-358.
90. Gaffney, T., et al., *Requirement of salicylic Acid for the induction of systemic acquired resistance.* Science, 1993. **261**(5122): p. 754-6.
91. Delaney, T.P., et al., *A central role of salicylic Acid in plant disease resistance.* Science, 1994. **266**(5188): p. 1247-50.
92. Durrant, W.E. and X. Dong, *Systemic acquired resistance.* Annu Rev Phytopathol, 2004. **42**: p. 185-209.
93. Pham, L.N., et al., *A specific primed immune response in Drosophila is dependent on phagocytes.* PLoS Pathog, 2007. **3**(3): p. e26.
94. Butkeviciute, E., C.E. Jones, and S.G. Smith, *Heterologous effects of infant BCG vaccination: potential mechanisms of immunity.* Future Microbiol, 2018. **13**: p. 1193-1208.
95. Blok, B.A., et al., *Trained innate immunity as underlying mechanism for the long-term, nonspecific effects of vaccines.* J Leukoc Biol, 2015. **98**(3): p. 347-56.
96. Sher, N.A., et al., *Effects of BCG, Corynebacterium parvum, and methanol-extration residue in the reduction of mortality from Staphylococcus aureus and Candida albicans infections in immunosuppressed mice.* Infection and Immunity, 1975. **12**(6): p. 1325-1330.
97. Tribouley, J., J. Tribouley-Duret, and M. Appriou, *[Effect of Bacillus Callmette Guerin (BCG) on the receptivity of nude mice to Schistosoma mansoni].* C R Seances Soc Biol Fil, 1978. **172**(5): p. 902-4.
98. Kleinnijenhuis, J., et al., *Bacille Calmette-Guerin induces NOD2-dependent nonspecific protection from reinfection via epigenetic reprogramming of monocytes.* Proc Natl Acad Sci U S A, 2012. **109**(43): p. 17537-42.
99. Bistoni, F., et al., *Immunomodulation by a low-virulence, agerminative variant of Candida albicans. Further evidence for macrophage activation as one of the effector mechanisms of nonspecific anti-infectious protection.* J Med Vet Mycol, 1988. **26**(5): p. 285-99.
100. Quintin, J., et al., *Candida albicans infection affords protection against reinfection via functional reprogramming of monocytes.* Cell Host Microbe, 2012. **12**(2): p. 223-32.
101. Di Luzio, N.R. and D.L. Williams, *Protective effect of glucan against systemic Staphylococcus aureus septicemia in normal and leukemic mice.* Infect Immun, 1978. **20**(3): p. 804-10.

102. Chedid, L., et al., *Enhancement of nonspecific immunity to Klebsiella pneumoniae infection by a synthetic immunoadjuvant (N-acetylmuramyl-L-alanyl-D-isoglutamine) and several analogs.* Proc Natl Acad Sci U S A, 1977. **74**(5): p. 2089-93.
103. Chedid, L., et al., *Enhancement of certain biological activities of muramyl dipeptide derivatives after conjugation to a multi-poly(DL-alanine)--poly(L-lysine) carrier.* Proc Natl Acad Sci U S A, 1979. **76**(12): p. 6557-61.
104. Cummings, N.P., M.J. Pabst, and R.B. Johnston, Jr., *Activation of macrophages for enhanced release of superoxide anion and greater killing of Candida albicans by injection of muramyl dipeptide.* J Exp Med, 1980. **152**(6): p. 1659-69.
105. Bistoni, F., et al., *Evidence for macrophage-mediated protection against lethal Candida albicans infection.* Infect Immun, 1986. **51**(2): p. 668-74.
106. Vecchiarelli, A., et al., *Protective immunity induced by low-virulence Candida albicans: Cytokine production in the development of the anti-infectious state.* Cellular Immunology, 1989. **124**(2): p. 334-344.
107. Bekkering, S., et al., *In Vitro Experimental Model of Trained Innate Immunity in Human Primary Monocytes.* Clin Vaccine Immunol, 2016. **23**(12): p. 926-933.
108. Netea, M.G., et al., *Trained immunity: A program of innate immune memory in health and disease.* Science, 2016. **352**(6284): p. aaf1098.
109. Arts, R.J.W., et al., *Immunometabolic Pathways in BCG-Induced Trained Immunity.* Cell Rep, 2016. **17**(10): p. 2562-2571.
110. Taylor, P.R., et al., *Dectin-1 is required for beta-glucan recognition and control of fungal infection.* Nat Immunol, 2007. **8**(1): p. 31-8.
111. Girardin, S.E., et al., *Nod2 is a general sensor of peptidoglycan through muramyl dipeptide (MDP) detection.* J Biol Chem, 2003. **278**(11): p. 8869-72.
112. Cheng, S.C., et al., *mTOR- and HIF-1alpha-mediated aerobic glycolysis as metabolic basis for trained immunity.* Science, 2014. **345**(6204): p. 1250684.
113. Arts, R.J., et al., *Glutaminolysis and Fumarate Accumulation Integrate Immunometabolic and Epigenetic Programs in Trained Immunity.* Cell Metab, 2016. **24**(6): p. 807-819.
114. Acosta-Rodriguez, E.V., et al., *Interleukins 1beta and 6 but not transforming growth factor-beta are essential for the differentiation of interleukin 17-producing human T helper cells.* Nat Immunol, 2007. **8**(9): p. 942-9.
115. Zhou, L., et al., *IL-6 programs T(H)-17 cell differentiation by promoting sequential engagement of the IL-21 and IL-23 pathways.* Nat Immunol, 2007. **8**(9): p. 967-74.
116. Kleinnijenhuis, J., et al., *Long-lasting effects of BCG vaccination on both heterologous Th1/Th17 responses and innate trained immunity.* J Innate Immun, 2014. **6**(2): p. 152-8.
117. Quinn, S.M., et al., *Anti-inflammatory Trained Immunity Mediated by Helminth Products Attenuates the Induction of T Cell-Mediated Autoimmune Disease.* Front Immunol, 2019. **10**: p. 1109.
118. Hsu, P., et al., *IL-10 Potentiates Differentiation of Human Induced Regulatory T Cells via STAT3 and Foxo1.* J Immunol, 2015. **195**(8): p. 3665-74.
119. Guo, B., *IL-10 Modulates Th17 Pathogenicity during Autoimmune Diseases.* J Clin Cell Immunol, 2016. **7**(2).
120. Dinarello, C.A., *Overview of the IL-1 family in innate inflammation and acquired immunity.* Immunol Rev, 2018. **281**(1): p. 8-27.
121. Jacobson, N.G., et al., *Interleukin 12 signaling in T helper type 1 (Th1) cells involves tyrosine phosphorylation of signal transducer and activator of transcription (Stat)3 and Stat4.* J Exp Med, 1995. **181**(5): p. 1755-62.
122. Flach, R., et al., *Interleukin-10 is downregulated in mononuclear cells from endotoxin tolerant humans.* Journal of Endotoxin Research, 2016. **4**(3): p. 189-195.

123. Frankenberger, M., H. Pechumer, and H.W. Ziegler-Heitbrock, *Interleukin-10 is upregulated in LPS tolerance.* Journal of inflammation, 1995. **45**(1): p. 56-63.
124. Karp, C.L., et al., *Potent suppression of IL-12 production from monocytes and dendritic cells during endotoxin tolerance.* European Journal of Immunology, 1998. **28**(10): p. 3128-3136.
125. Wolk, K., et al., *Impaired antigen presentation by human monocytes during endotoxin tolerance.* Blood, 2000. **96**(1): p. 218-223.
126. Arts, R.J.W., L.A.B. Joosten, and M.G. Netea, *The Potential Role of Trained Immunity in Autoimmune and Autoinflammatory Disorders.* Front Immunol, 2018. **9**: p. 298.
127. Schaefer, L., *Complexity of Danger: The Diverse Nature of Damage-associated Molecular Patterns.* Journal of Biological Chemistry, 2014. **289**(51): p. 35237-35245.
128. Bryant, C.E., et al., *Advances in Toll-like receptor biology: Modes of activation by diverse stimuli.* Critical Reviews in Biochemistry and Molecular Biology, 2015. **50**(5): p. 359-379.
129. Dostert, C., et al., *Innate immune activation through Nalp3 inflammasome sensing of asbestos and silica.* Science, 2008. **320**(5876): p. 674-677.
130. Halle, A., et al., *The NALP3 inflammasome is involved in the innate immune response to amyloid-beta.* Nature Immunology, 2008. **9**(8): p. 857-865.
131. Duewell, P., et al., *NLRP3 inflammasomes are required for atherogenesis and activated by cholesterol crystals.* Nature, 2010. **464**(7293): p. 1357-U7.
132. Woo, S.R., L. Corrales, and T.F. Gajewski, *Innate Immune Recognition of Cancer*, in *Annual Review of Immunology Vol 33*, D.R. Littman and W.M. Yokoyama, Editors. 2015, Annual Reviews: Palo Alto. p. 445-474.
133. Schaefer, L., et al., *The matrix component biglycan is proinflammatory and signals through Toll-like receptors 4 and 2 in macrophages.* J Clin Invest, 2005. **115**(8): p. 2223-33.
134. Okamura, Y., et al., *The extra domain A of fibronectin activates Toll-like receptor 4.* J Biol Chem, 2001. **276**(13): p. 10229-33.
135. Smiley, S.T., J.A. King, and W.W. Hancock, *Fibrinogen stimulates macrophage chemokine secretion through toll-like receptor 4.* J Immunol, 2001. **167**(5): p. 2887-94.
136. Midwood, K., et al., *Tenascin-C is an endogenous activator of Toll-like receptor 4 that is essential for maintaining inflammation in arthritic joint disease.* Nat Med, 2009. **15**(7): p. 774-80.
137. Zhang, Q., et al., *Circulating mitochondrial DAMPs cause inflammatory responses to injury.* Nature, 2010. **464**(7285): p. 104-7.
138. Jiang, D., et al., *Regulation of lung injury and repair by Toll-like receptors and hyaluronan.* Nat Med, 2005. **11**(11): p. 1173-9.
139. Funderburg, N., et al., *Human -defensin-3 activates professional antigen-presenting cells via Toll-like receptors 1 and 2.* Proceedings of the National Academy of Sciences, 2007. **104**(47): p. 18631-18635.
140. Babelova, A., et al., *Biglycan, a danger signal that activates the NLRP3 inflammasome via toll-like and P2X receptors.* J Biol Chem, 2009. **284**(36): p. 24035-48.
141. Park, J.S., et al., *Involvement of toll-like receptors 2 and 4 in cellular activation by high mobility group box 1 protein.* J Biol Chem, 2004. **279**(9): p. 7370-7.
142. Klune, J.R., et al., *HMGB1: endogenous danger signaling.* Mol Med, 2008. **14**(7-8): p. 476-84.
143. Park, J.S., et al., *High mobility group box 1 protein interacts with multiple Toll-like receptors.* Am J Physiol Cell Physiol, 2006. **290**(3): p. C917-24.
144. Devaney, J.M., et al., *Neutrophil elastase up-regulates interleukin-8 via toll-like receptor 4.* FEBS Letters, 2003. **544**(1-3): p. 129-132.
145. Vogl, T., et al., *Mrp8 and Mrp14 are endogenous activators of Toll-like receptor 4, promoting lethal, endotoxin-induced shock.* Nat Med, 2007. **13**(9): p. 1042-9.

146. Xia, C., et al., *S100 Proteins As an Important Regulator of Macrophage Inflammation.* Front Immunol, 2017. **8**: p. 1908.
147. Sorci, G., et al., *The danger signal S100B integrates pathogen- and danger-sensing pathways to restrain inflammation.* PLoS Pathog, 2011. **7**(3): p. e1001315.
148. He, R.L., et al., *Serum amyloid A induces G-CSF expression and neutrophilia via Toll-like receptor 2.* Blood, 2009. **113**(2): p. 429-37.
149. Sandri, S., et al., *Is serum amyloid A an endogenous TLR4 agonist?* J Leukoc Biol, 2008. **83**(5): p. 1174-80.
150. Kariko, K., et al., *mRNA is an endogenous ligand for Toll-like receptor 3.* J Biol Chem, 2004. **279**(13): p. 12542-50.
151. Vollmer, J., et al., *Immune stimulation mediated by autoantigen binding sites within small nuclear RNAs involves Toll-like receptors 7 and 8.* J Exp Med, 2005. **202**(11): p. 1575-85.
152. Chen, G.Y. and G. Nunez, *Sterile inflammation: sensing and reacting to damage.* Nat Rev Immunol, 2010. **10**(12): p. 826-37.
153. Zelenay, S. and C. Reis e Sousa, *Adaptive immunity after cell death.* Trends Immunol, 2013. **34**(7): p. 329-35.
154. Zindel, J. and P. Kubes, *DAMPs, PAMPs, and LAMPs in Immunity and Sterile Inflammation.* Annu Rev Pathol, 2020. **15**: p. 493-518.
155. Ellis, S., E.J. Lin, and D. Tartar, *Immunology of Wound Healing.* Curr Dermatol Rep, 2018. **7**(4): p. 350-358.
156. Song, J. and S.N. Abraham, *TLR-mediated immune responses in the urinary tract.* Curr Opin Microbiol, 2008. **11**(1): p. 66-73.
157. Brooks, L.R.K. and G.I. Mias, *Streptococcus pneumoniae's Virulence and Host Immunity: Aging, Diagnostics, and Prevention.* Front Immunol, 2018. **9**: p. 1366.
158. Gowda, D.C. and X. Wu, *Parasite Recognition and Signaling Mechanisms in Innate Immune Responses to Malaria.* Front Immunol, 2018. **9**: p. 3006.
159. Gong, T., et al., *DAMP-sensing receptors in sterile inflammation and inflammatory diseases.* Nat Rev Immunol, 2020. **20**(2): p. 95-112.
160. Goh, F.G. and K.S. Midwood, *Intrinsic danger: activation of Toll-like receptors in rheumatoid arthritis.* Rheumatology (Oxford), 2012. **51**(1): p. 7-23.
161. Liu, T., M. Son, and B. Diamond, *HMGB1 in Systemic Lupus Erythematosus.* Front Immunol, 2020. **11**: p. 1057.
162. Shin, J.J., et al., *Damage-associated molecular patterns and their pathological relevance in diabetes mellitus.* Ageing Res Rev, 2015. **24**(Pt A): p. 66-76.
163. Zimmer, S., A. Grebe, and E. Latz, *Danger signaling in atherosclerosis.* Circ Res, 2015. **116**(2): p. 323-40.
164. Venegas, C. and M.T. Heneka, *Danger-associated molecular patterns in Alzheimer's disease.* J Leukoc Biol, 2017. **101**(1): p. 87-98.
165. Pajares, M., et al., *Inflammation in Parkinson's Disease: Mechanisms and Therapeutic Implications.* Cells, 2020. **9**(7).
166. Anders, H.J. and L. Schaefer, *Beyond tissue injury-damage-associated molecular patterns, toll-like receptors, and inflammasomes also drive regeneration and fibrosis.* J Am Soc Nephrol, 2014. **25**(7): p. 1387-400.
167. Aneja, R.K., et al., *Preconditioning with high mobility group box 1 (HMGB1) induces lipopolysaccharide (LPS) tolerance.* J Leukoc Biol, 2008. **84**(5): p. 1326-34.
168. Arts, R.J.W., et al., *High-Mobility Group Nucleosome-Binding Protein 1 as Endogenous Ligand Induces Innate Immune Tolerance in a TLR4-Sirtuin-1 Dependent Manner in Human Blood Peripheral Mononuclear Cells.* Front Immunol, 2018. **9**: p. 526.
169. Zhou, M., et al., *Extracellular CIRP induces macrophage endotoxin tolerance through IL-6R-mediated STAT3 activation.* JCI Insight, 2020. **5**(5).

170. Austermann, J., et al., *Alarmins MRP8 and MRP14 induce stress tolerance in phagocytes under sterile inflammatory conditions.* Cell Rep, 2014. **9**(6): p. 2112-23.
171. Yang, H., H. Wang, and U. Andersson, *Targeting Inflammation Driven by HMGB1.* Front Immunol, 2020. **11**: p. 484.
172. Robert, S.M., et al., *Preconditioning with high mobility group box 1 (HMGB1) induces lipoteichoic acid (LTA) tolerance.* J Immunother, 2010. **33**(7): p. 663-71.
173. Yang, et al., *High-mobility group nucleosome binding domain 1 (HMGN1) functions as a Th1-polarizing alarmin.* Semin Immunol, 2018. **38**: p. 49-53.
174. Aziz, M., M. Brenner, and P. Wang, *Extracellular CIRP (eCIRP) and inflammation.* J Leukoc Biol, 2019. **106**(1): p. 133-146.
175. Wang, S., et al., *S100A8/A9 in Inflammation.* Front Immunol, 2018. **9**: p. 1298.
176. Obermayer, G., T. Afonyushkin, and C.J. Binder, *Oxidized low-density lipoprotein in inflammation-driven thrombosis.* J Thromb Haemost, 2018. **16**(3): p. 418-428.
177. Bekkering, S., et al., *Oxidized low-density lipoprotein induces long-term proinflammatory cytokine production and foam cell formation via epigenetic reprogramming of monocytes.* Arterioscler Thromb Vasc Biol, 2014. **34**(8): p. 1731-8.
178. Christ, A., et al., *Western Diet Triggers NLRP3-Dependent Innate Immune Reprogramming.* Cell, 2018. **172**(1-2): p. 162-175 e14.
179. Fraker, D.L., et al., *Tolerance to tumor necrosis factor in rats and the relationship to endotoxin tolerance and toxicity.* J Exp Med, 1988. **168**(1): p. 95-105.
180. Fraker, D.L., B.C. Sheppard, and J.A. Norton, *Impact of Tolerance on Antitumor Efficacy of Tumor Necrosis Factor in Mice.* Cancer Research, 1990. **50**(8): p. 2261-2267.
181. Huber, R., et al., *TNF Tolerance in Monocytes and Macrophages: Characteristics and Molecular Mechanisms.* J Immunol Res, 2017. **2017**: p. 9570129.
182. Gunther, J., et al., *Identification of two forms of TNF tolerance in human monocytes: differential inhibition of NF-kappaB/AP-1- and PP1-associated signaling.* J Immunol, 2014. **192**(7): p. 3143-55.
183. Takahashi, N., P. Brouckaert, and W. Fiers, *Mechanism of tolerance to tumor necrosis factor: receptor-specific pathway and selectivity.* Am J Physiol, 1995. **269**(2 Pt 2): p. R398-405.
184. Weber, M., et al., *Transcriptional inhibition of interleukin-8 expression in tumor necrosis factor-tolerant cells: evidence for involvement of C/EBP beta.* J Biol Chem, 2003. **278**(26): p. 23586-93.
185. Park, S.H., et al., *Tumor necrosis factor induces GSK3 kinase-mediated cross-tolerance to endotoxin in macrophages.* Nat Immunol, 2011. **12**(7): p. 607-15.
186. Loosbroock, C. and K.W. Hunter, *Inhibiting TNF-alpha signaling does not attenuate induction of endotoxin tolerance.* J Inflamm Res, 2014. **7**: p. 159-67.
187. Chiquet-Ehrismann, R. and M. Chiquet, *Tenascins: regulation and putative functions during pathological stress.* Journal of Pathology, 2003. **200**(4): p. 488-499.
188. Udalova, I.A., et al., *Expression and Immune Function of Tenascin-C.* Critical Reviews in Immunology, 2011. **31**(2): p. 115-145.
189. Midwood, K.S., et al., *Tenascin-C at a glance.* Journal of Cell Science, 2016. **129**(23): p. 4321-4327.
190. Yu, L., L.T. Wang, and S.W. Chen, *Endogenous toll-like receptor ligands and their biological significance.* Journal of Cellular and Molecular Medicine, 2010. **14**(11): p. 2592-2603.
191. Piccinini, A.M., et al., *Distinct microenvironmental cues stimulate divergent TLR4-mediated signaling pathways in macrophages.* Science Signaling, 2016. **9**(443): p. 16.
192. Benbow, J.H., et al., *Diet-Induced Obesity Enhances Progression of Hepatocellular Carcinoma through Tenascin-C/Toll-Like Receptor 4 Signaling.* American Journal of Pathology, 2016. **186**(1): p. 145-158.

193. Zuliani-Alvarez, L., et al., *Mapping tenascin-C interaction with toll-like receptor 4 reveals a new subset of endogenous inflammatory triggers.* Nature Communications, 2017.
194. Machino-Ohtsuka, T., et al., *Tenascin-C Aggravates Autoimmune Myocarditis via Dendritic Cell Activation and Th17 Cell Differentiation.* Journal of the American Heart Association, 2014. **3**(6): p. 15.
195. Maqbool, A., et al., *Tenascin C upregulates interleukin-6 expression in human cardiac myofibroblasts via toll-like receptor 4.* World Journal of Cardiology, 2016. **8**(5): p. 340-350.
196. Patel, L., et al., *Tenascin-C induces inflammatory mediators and matrix degradation in osteoarthritic cartilage.* Bmc Musculoskeletal Disorders, 2011. **12**: p. 14.
197. Broz, P. and V.M. Dixit, *Inflammasomes: mechanism of assembly, regulation and signalling.* Nature Reviews Immunology, 2016. **16**(7): p. 407-420.
198. Jo, E.K., et al., *Molecular mechanisms regulating NLRP3 inflammasome activation.* Cellular & Molecular Immunology, 2016. **13**(2): p. 148-159.
199. Hesse, J., et al., *CD73-derived adenosine and tenascin-C control cytokine production by epicardium-derived cells formed after myocardial infarction.* Faseb Journal, 2017. **31**(7): p. 3040-3053.
200. Ruhmann, M., et al., *Endogenous activation of adaptive immunity: Tenascin-C drives interleukin-17 synthesis in murine arthritic joint disease.* Arthritis and Rheumatism, 2012. **64**(7): p. 2179-2190.
201. Boniface, K., et al., *Prostaglandin E2 regulates Th17 cell differentiation and function through cyclic AMP and EP2/EP4 receptor signaling.* Journal of Experimental Medicine, 2009. **206**(3): p. 535-548.
202. Napolitani, G., et al., *Prostaglandin E2 enhances Th17 responses via modulation of IL-17 and IFN-gamma production by memory CD4(+) T cells.* European Journal of Immunology, 2009. **39**(5): p. 1301-1312.
203. Kuriyama, N., et al., *Tenascin-C: A Novel Mediator of Hepatic Ischemia and Reperfusion Injury.* Hepatology, 2011. **54**(6): p. 2125-2136.
204. Liu, R., et al., *Tenascin-C Produced by Oxidized LDL-Stimulated Macrophages Increases Foam Cell Formation through Toll-like Receptor-4.* Molecules and Cells, 2012. **34**(1): p. 35-41.
205. Bhattacharyya, S., et al., *Tenascin-C drives persistence of organ fibrosis.* Nature Communications, 2016. **7**: p. 14.
206. Kanayama, M., et al., *alpha(9) Integrin and Its Ligands Constitute Critical Joint Microenvironments for Development of Autoimmune Arthritis.* Journal of Immunology, 2009. **182**(12): p. 8015-8025.
207. Kanayama, M., et al., *alpha(9)beta(1) Integrin-Mediated Signaling Serves as an Intrinsic Regulator of Pathogenic Th17 Cell Generation.* Journal of Immunology, 2011. **187**(11): p. 5851-5864.
208. Shimojo, N., et al., *Tenascin-C May Accelerate Cardiac Fibrosis by Activating Macrophages via the Integrin alpha V beta 3/NuclearFactor-kappa B/Interleukin-6 Axis.* Hypertension, 2015. **66**(4): p. 757-766.
209. Prieto, A.L., G.M. Edelman, and K.L. Crossin, *MULTIPLE INTEGRINS MEDIATE CELL ATTACHMENT TO CYTOTACTIN TENASCIN.* Proceedings of the National Academy of Sciences of the United States of America, 1993. **90**(21): p. 10154-10158.
210. Yokoyama, K., et al., *Identification of amino acid sequences in fibrinogen gamma-chain and tenascin CC-terminal domains critical for binding to integrin alpha(v)beta(3).* Journal of Biological Chemistry, 2000. **275**(22): p. 16891-16898.
211. Ruiz, C., et al., *Dilfferential gene expression analysis reveals activation of growth promoting signaling pathways by tenascin-C.* Cancer Research, 2004. **64**(20): p. 7377-7385.

212. Hendaoui, S., et al., *Tenascin-C is required for normal Wnt/beta-catenin signaling in the whisker follicle stem cell niche.* Matrix Biology, 2014. **40**: p. 46-53.
213. Ma, B. and M.O. Hottiger, *Crosstalk between wnt/beta-Catenin and NF-kappa B Signaling Pathway during Inflammation.* Frontiers in Immunology, 2016. **7**: p. 14.
214. Piccinini, A.M. and K.S. Midwood, *Endogenous Control of Immunity against Infection: Tenascin-C Regulates TLR4-Mediated Inflammation via MicroRNA-155.* Cell Reports, 2012. **2**(4): p. 914-926.
215. Mansour, R.G., et al., *The Presence and Anti-HIV-1 Function of Tenascin C in Breast Milk and Genital Fluids.* Plos One, 2016. **11**(5): p. 16.
216. Chiovaro, F., R. Chiquet-Ehrismann, and M. Chiquet, *Transcriptional regulation of tenascin genes.* Cell Adhesion & Migration, 2015. **9**(1-2): p. 34-47.
217. De Laporte, L., et al., *Tenascin C Promiscuously Binds Growth Factors via Its Fifth Fibronectin Type III-Like Domain.* Plos One, 2013. **8**(4): p. 9.
218. Kelly, A., et al., *Regulation of Innate and Adaptive Immunity by TGF beta*, in *Advances in Immunology, Vol 134*, F.W. Alt, Editor. 2017, Elsevier Academic Press Inc: San Diego. p. 137-233.
219. Ruegg, C.R., R. Chiouetehrismann, and S.S. Alkan, *TENASCIN, AN EXTRACELLULAR-MATRIX PROTEIN, EXERTS IMMUNOMODULATORY ACTIVITIES.* Proceedings of the National Academy of Sciences of the United States of America, 1989. **86**(19): p. 7437-7441.
220. Hemesath, T.J., L.S. Marton, and K. Stefansson, *INHIBITION OF T-CELL ACTIVATION BY THE EXTRACELLULAR-MATRIX PROTEIN TENASCIN.* Journal of Immunology, 1994. **152**(11): p. 5199-5207.
221. Hibino, S., et al., *Tenascin suppresses CD3-mediated T cell activation.* Biochemical and Biophysical Research Communications, 1998. **250**(1): p. 119-124.
222. Navazo, M.D.P., D. Valmori, and C. Ruegg, *The alternatively spliced domain TnFnIII A1A2 of the extracellular matrix protein tenascin-C suppresses activation-induced T lymphocyte proliferation and cytokine production.* Journal of Immunology, 2001. **167**(11): p. 6431-6440.
223. Jachetti, E., et al., *Tenascin-C Protects Cancer Stem-like Cells from Immune Surveillance by Arresting T-cell Activation.* Cancer Research, 2015. **75**(10): p. 2095-2108.
224. Saga, Y., et al., *MICE DEVELOP NORMALLY WITHOUT TENASCIN.* Genes & Development, 1992. **6**(10): p. 1821-1831.
225. Forsberg, E., et al., *Skin wounds and severed nerves heal normally in mice lacking tenascin-C.* Proceedings of the National Academy of Sciences of the United States of America, 1996. **93**(13): p. 6594-6599.
226. Matsuda, A., et al., *Corneal wound healing in tenascin knockout mouse.* Investigative Ophthalmology & Visual Science, 1999. **40**(6): p. 1071-1080.
227. Sumioka, T., et al., *Impaired cornea wound healing in a tenascin C-deficient mouse model.* Laboratory Investigation, 2013. **93**(2): p. 207-217.
228. Tamaoki, M., et al., *Tenascin-C regulates recruitment of myofibroblasts during tissue repair after myocardial injury.* American Journal of Pathology, 2005. **167**(1): p. 71-80.
229. Xie, K., et al., *Tenascin-C deficiency ameliorates Alzheimer's disease-related pathology in mice.* Neurobiology of Aging, 2013. **34**(10): p. 2389-2398.
230. Fujimoto, M., et al., *Deficiency of tenascin-C and attenuation of blood-brain barrier disruption following experimental subarachnoid hemorrhage in mice.* Journal of Neurosurgery, 2016. **124**(6): p. 1693-1702.
231. Fujimoto, M., et al., *Effects of Tenascin-C Knockout on Cerebral Vasospasm After Experimental Subarachnoid Hemorrhage in Mice.* Mol Neurobiol, 2017.
232. Momcilovic, M., et al., *Tenascin-C deficiency protects mice from experimental autoimmune encephalomyelitis.* Journal of Neuroimmunology, 2017. **302**: p. 1-6.

233. Nakahara, H., et al., *Deficiency of tenascin C attenuates allergen-induced bronchial asthma in the mouse.* European Journal of Immunology, 2006. **36**(12): p. 3334-3345.
234. Busse, W.W. and R.F. Lemanske, *Advances in immunology - Asthma.* New England Journal of Medicine, 2001. **344**(5): p. 350-362.
235. van den Berg, W.B. and P. Miossec, *IL-17 as a future therapeutic target for rheumatoid arthritis.* Nature Reviews Rheumatology, 2009. **5**(10): p. 549-553.
236. Petermann, F. and T. Korn, *Cytokines and effector T cell subsets causing autoimmune CNS disease.* Febs Letters, 2011. **585**(23): p. 3747-3757.
237. Yamamoto, K., et al., *Tenascin-C is an essential factor for neointimal hyperplasia after aortotomy in mice.* Cardiovascular Research, 2005. **65**(3): p. 737-742.
238. Sawada, Y., et al., *Tenascin-C synthesized in both donor grafts and recipients accelerates artery graft stenosis.* Cardiovascular Research, 2007. **74**(3): p. 366-376.
239. Nishioka, T., et al., *Tenascin-C may aggravate left ventricular remodeling and function after myocardial infarction in mice.* American Journal of Physiology-Heart and Circulatory Physiology, 2010. **298**(3): p. H1072-H1078.
240. El-Karef, A., et al., *Deficiency of tenascin-C attenuates liver fibrosis in immune-mediated chronic hepatitis in mice.* Journal of Pathology, 2007. **211**(1): p. 86-94.
241. Carey, W.A., et al., *Tenascin-C deficiency attenuates TGF-beta-mediated fibrosis following murine lung injury.* American Journal of Physiology-Lung Cellular and Molecular Physiology, 2010. **299**(6): p. L785-L793.
242. Pohlers, D., et al., *TGF-beta and fibrosis in different organs - molecular pathway imprints.* Biochimica Et Biophysica Acta-Molecular Basis of Disease, 2009. **1792**(8): p. 746-756.
243. Nakao, N., et al., *Tenascin-C promotes healing of habu-snake venom-induced glomerulonephritis - Studies in knockout congenic mice and in culture.* American Journal of Pathology, 1998. **152**(5): p. 1237-1245.
244. Koyama, Y., et al., *Effect of tenascin-C deficiency on chemically induced dermatitis in the mouse.* Journal of Investigative Dermatology, 1998. **111**(6): p. 930-935.
245. Okamura, N., et al., *Deficiency of tenascin-C delays articular cartilage repair in mice.* Osteoarthritis and Cartilage, 2010. **18**(6): p. 839-848.
246. Ohta, M., et al., *Suppression of hematopoietic activity in tenascin-C-deficient mice.* Blood, 1998. **91**(11): p. 4074-4083.
247. Nakamura-Ishizu, A., et al., *Extracellular matrix protein tenascin-C is required in the bone marrow microenvironment primed for hematopoietic regeneration.* Blood, 2012. **119**(23): p. 5429-5437.
248. Song, L., et al., *Bone Marrow-Derived Tenascin-C Attenuates Cardiac Hypertrophy by Controlling Inflammation.* Journal of the American College of Cardiology, 2017. **70**(13): p. 1601-1615.
249. Talts, J.F., et al., *Tenascin-C modulates tumor stroma and monocyte macrophage recruitment but not tumor growth or metastasis in a mouse strain with spontaneous mammary cancer.* Journal of Cell Science, 1999. **112**(12): p. 1855-1864.
250. Tanaka, K., et al., *Tenascin-C regulates angiogenesis in tumor through the regulation of vascular endothelial growth factor expression.* International Journal of Cancer, 2004. **108**(1): p. 31-40.
251. Saupe, F., et al., *Tenascin-C Downregulates Wnt Inhibitor Dickkopf-1, Promoting Tumorigenesis in a Neuroendocrine Tumor Model.* Cell Reports, 2013. **5**(2): p. 482-492.
252. Zhao, Y.L., et al., *Exome Sequencing and Linkage Analysis Identified Tenascin-C (TNC) as a Novel Causative Gene in Nonsyndromic Hearing Loss.* Plos One, 2013. **8**(7): p. 8.
253. Matsuda, A., et al., *Coding SNP in tenascin-C Fn-III-D domain associates with adult asthma.* Human Molecular Genetics, 2005. **14**(19): p. 2779-2786.

254. Orsmark-Pietras, C., et al., *Biological and genetic interaction between Tenascin C and Neuropeptide S receptor 1 in allergic diseases.* Human Molecular Genetics, 2008. **17**(11): p. 1673-1682.
255. Saunders, C.J., et al., *Investigation of variants within the COL27A1 and TNC genes and Achilles tendinopathy in two populations.* Journal of Orthopaedic Research, 2013. **31**(4): p. 632-637.
256. Lowy, C.M. and T. Oskarsson, *Tenascin C in metastasis: A view from the invasive front.* Cell Adhesion & Migration, 2015. **9**(1-2): p. 112-124.
257. Orak, U., et al., *Tenascin C levels in patients with mild and severe preeclampsia.* Journal of Maternal-Fetal & Neonatal Medicine, 2016. **29**(2): p. 270-273.
258. Schenk, S., et al., *TENASCIN-C IN SERUM - A QUESTIONABLE TUMOR-MARKER.* International Journal of Cancer, 1995. **61**(4): p. 443-449.
259. Riedl, S., et al., *Serum tenascin-C is an indicator of inflammatory bowel disease activity.* International Journal of Colorectal Disease, 2001. **16**(5): p. 285-291.
260. Zavada, J., et al., *Serum tenascin-C discriminates patients with active SLE from inactive patients and healthy controls and predicts the need to escalate immunosuppressive therapy: a cohort study.* Arthritis Research & Therapy, 2015. **17**: p. 11.
261. Hasegawa, M., et al., *Tenascin-C concentration in synovial fluid correlates with radiographic progression of knee osteoarthritis.* Journal of Rheumatology, 2004. **31**(10): p. 2021-2026.
262. Hasegawa, M., et al., *Expression of large tenascin-C splice variants in synovial fluid of patients with rheumatoid arthritis.* Journal of Orthopaedic Research, 2007. **25**(5): p. 563-568.
263. Page, T.H., et al., *Raised circulating tenascin-C in rheumatoid arthritis.* Arthritis Research & Therapy, 2012. **14**(6): p. 9.
264. Schwenzer, A., et al., *Identification of an immunodominant peptide from citrullinated tenascin-C as a major target for autoantibodies in rheumatoid arthritis.* Annals of the Rheumatic Diseases, 2016. **75**(10): p. 1876-1883.
265. Raza, K., et al., *Detection of antibodies to citrullinated tenascin-C in patients with early synovitis is associated with the development of rheumatoid arthritis.* RMD Open, 2016. **2**(2).
266. Franz, M., et al., *Tenascin-C in cardiovascular remodeling: potential impact for diagnosis, prognosis estimation and targeted therapy.* Cell Adhesion & Migration, 2015. **9**(1-2): p. 90-95.
267. Okuma, Y., et al., *Serum Tenascin-C as a Novel Predictor for Risk of Coronary Artery Lesion and Resistance to Intravenous Immunoglobulin in Kawasaki Disease - A Multicenter Retrospective Study.* Circulation Journal, 2016. **80**(11): p. 2376-2381.
268. Kitaoka, H., et al., *Serum tenascin-C levels as a prognostic biomarker of heart failure events in patients with hypertrophic cardiomyopathy.* Journal of Cardiology, 2012. **59**(2): p. 209-214.
269. Saiwai, H., et al., *Ly6C+ Ly6G- Myeloid-derived suppressor cells play a critical role in the resolution of acute inflammation and the subsequent tissue repair process after spinal cord injury.* J Neurochem, 2013. **125**(1): p. 74-88.
270. Kumar, V., et al., *The Nature of Myeloid-Derived Suppressor Cells in the Tumor Microenvironment.* Trends in Immunology, 2016. **37**(3): p. 208-220.
271. Boros, P., J. Ochando, and M. Zeher, *Myeloid derived suppressor cells and autoimmunity.* Human Immunology, 2016. **77**(8): p. 631-636.
272. Baniyash, M., *Myeloid-derived suppressor cells as intruders and targets: clinical implications in cancer therapy.* Cancer Immunology Immunotherapy, 2016. **65**(7): p. 857-867.

273. Ray, A., K. Chakraborty, and P. Ray, *Immunosuppressive MDSCs induced by TLR signaling during infection and role in resolution of inflammation.* Frontiers in Cellular and Infection Microbiology, 2013. **3**: p. 8.
274. Arora, M., et al., *TLR4/MyD88-induced CD11b(+)Gr-1(int)F4/80(+) non-migratory myeloid cells suppress Th2 effector function in the lung.* Mucosal Immunology, 2010. **3**(6): p. 578-593.
275. Sinha, P., et al., *Proinflammatory S100 proteins regulate the accumulation of myeloid-derived suppressor cells.* Journal of Immunology, 2008. **181**(7): p. 4666-4675.
276. Spenle, C., et al., *Tenascin-C: Exploitation and collateral damage in cancer management.* Cell Adhesion & Migration, 2015. **9**(1-2): p. 141-153.
277. Weisel, J.W. and R.I. Litvinov, *Fibrin Formation, Structure and Properties.* Subcell Biochem, 2017. **82**: p. 405-456.
278. Kollman, J.M., et al., *Crystal structure of human fibrinogen.* Biochemistry, 2009. **48**(18): p. 3877-86.
279. Kamath, S. and G.Y. Lip, *Fibrinogen: biochemistry, epidemiology and determinants.* QJM, 2003. **96**(10): p. 711-29.
280. Davalos, D. and K. Akassoglou, *Fibrinogen as a key regulator of inflammation in disease.* Semin Immunopathol, 2012. **34**(1): p. 43-62.
281. Doolittle, R.F., K. McNamara, and K. Lin, *Correlating structure and function during the evolution of fibrinogen-related domains.* Protein Sci, 2012. **21**(12): p. 1808-23.
282. Zuliani-Alvarez, L. and K.S. Midwood, *Fibrinogen-Related Proteins in Tissue Repair: How a Unique Domain with a Common Structure Controls Diverse Aspects of Wound Healing.* Adv Wound Care (New Rochelle), 2015. **4**(5): p. 273-285.
283. Zuliani-Alvarez, L., et al., *Mapping tenascin-C interaction with toll-like receptor 4 reveals a new subset of endogenous inflammatory triggers.* Nature Communications, 2017. **8**(1): p. 1595.
284. Chapin, J.C. and K.A. Hajjar, *Fibrinolysis and the control of blood coagulation.* Blood Rev, 2015. **29**(1): p. 17-24.
285. Matsushita, M. and T. Fujita, *Ficolins and the lectin complement pathway.* Immunol Rev, 2001. **180**: p. 78-85.
286. Fagiani, E. and G. Christofori, *Angiopoietins in angiogenesis.* Cancer Lett, 2013. **328**(1): p. 18-26.
287. Yee, V.C., et al., *Crystal structure of a 30 kDa C-terminal fragment from the γ chain of human fibrinogen.* Structure, 1997. **5**(1): p. 125-138.
288. Sheinerman, F., *Electrostatic aspects of protein–protein interactions.* Current Opinion in Structural Biology, 2000. **10**(2): p. 153-159.
289. Ye, S., K. Patel, and C.P. Hodgkinson, *Functional Toll-like receptor 4 mutations modulate the response to fibrinogen.* Thrombosis and Haemostasis, 2017. **100**(08): p. 301-307.
290. Carbone, C., et al., *Angiopoietin-Like Proteins in Angiogenesis, Inflammation and Cancer.* Int J Mol Sci, 2018. **19**(2).
291. Zimmerman, T., et al., *Simultaneous metal chelate affinity purification and endotoxin clearance of recombinant antibody fragments.* J Immunol Methods, 2006. **314**(1-2): p. 67-73.
292. Matsunaga, N., et al., *TAK-242 (resatorvid), a small-molecule inhibitor of Toll-like receptor (TLR) 4 signaling, binds selectively to TLR4 and interferes with interactions between TLR4 and its adaptor molecules.* Mol Pharmacol, 2011. **79**(1): p. 34-41.
293. Giblin, S.P., A. Schwenzer, and K.S. Midwood, *Alternative splicing controls cell lineage-specific responses to endogenous innate immune triggers within the extracellular matrix.* Matrix Biol, 2020. **93**: p. 95-114.
294. Sievers, F., et al., *Fast, scalable generation of high-quality protein multiple sequence alignments using Clustal Omega.* Mol Syst Biol, 2011. **7**: p. 539.

295. Guex, N., M.C. Peitsch, and T. Schwede, *Automated comparative protein structure modeling with SWISS-MODEL and Swiss-PdbViewer: a historical perspective.* Electrophoresis, 2009. **30 Suppl 1**: p. S162-73.
296. Coker, J., et al., *Structure and function of ANGPTLs as TLR4-activating endogenous DAMPs. Manuscript in preparation.*
297. Dhanabal, M., et al., *Angioarrestin: an antiangiogenic protein with tumor-inhibiting properties.* Cancer Res, 2002. **62**(13): p. 3834-41.
298. Morelli, M.B., C. Chavez, and G. Santulli, *Angiopoietin-like proteins as therapeutic targets for cardiovascular disease: focus on lipid disorders.* Expert Opin Ther Targets, 2020. **24**(1): p. 79-88.
299. Teodorowicz, M., et al., *Optimized Triton X-114 assisted lipopolysaccharide (LPS) removal method reveals the immunomodulatory effect of food proteins.* PLoS One, 2017. **12**(3): p. e0173778.
300. Duff, G.W. and E. Atkins, *The inhibitory effect of polymyxin B on endotoxin-induced endogenous pyrogen production.* Journal of Immunological Methods, 1982. **52**(3): p. 333-340.
301. Cardoso, L.S., et al., *Polymyxin B as inhibitor of LPS contamination of Schistosoma mansoni recombinant proteins in human cytokine analysis.* Microb Cell Fact, 2007. **6**: p. 1.
302. Donovan, J.W. and E. Mihalyi, *Clotting of fibrinogen. 1. Scanning calorimetric study of the effect of calcium.* Biochemistry, 1985. **24**(14): p. 3434-43.
303. Folch, B., Y. Dehouck, and M. Rooman, *Thermo- and mesostabilizing protein interactions identified by temperature-dependent statistical potentials.* Biophys J, 2010. **98**(4): p. 667-77.
304. Koch, C., et al., *A comparison of the immunogenicity of the native and denatured forms of a protein.* APMIS, 1996. **104**(2): p. 115-25.
305. Bogahawaththa, D., et al., *In vitro immunogenicity of various native and thermally processed bovine milk proteins and their mixtures.* J Dairy Sci, 2018. **101**(10): p. 8726-8736.
306. Ebeling, W., et al., *Proteinase K from Tritirachium album Limber.* Eur J Biochem, 1974. **47**(1): p. 91-7.
307. Moreth, K., et al., *Biglycan-triggered TLR-2- and TLR-4-signaling exacerbates the pathophysiology of ischemic acute kidney injury.* Matrix Biol, 2014. **35**: p. 143-51.
308. Yamada, C., et al., *Surfactant protein A directly interacts with TLR4 and MD-2 and regulates inflammatory cellular response. Importance of supratrimeric oligomerization.* J Biol Chem, 2006. **281**(31): p. 21771-80.
309. Akashi, S., et al., *Lipopolysaccharide interaction with cell surface Toll-like receptor 4-MD-2: higher affinity than that with MD-2 or CD14.* J Exp Med, 2003. **198**(7): p. 1035-42.
310. Marzeda, A.M. and K.S. Midwood, *Internal Affairs: Tenascin-C as a Clinically Relevant, Endogenous Driver of Innate Immunity.* J Histochem Cytochem, 2018. **66**(4): p. 289-304.
311. Flick, M.J., et al., *Leukocyte engagement of fibrin(ogen) via the integrin receptor alphaMbeta2/Mac-1 is critical for host inflammatory response in vivo.* J Clin Invest, 2004. **113**(11): p. 1596-606.
312. Nielen, M.M., et al., *Antibodies to citrullinated human fibrinogen (ACF) have diagnostic and prognostic value in early arthritis.* Ann Rheum Dis, 2005. **64**(8): p. 1199-204.
313. Banda, N.K., et al., *Deconstructing the Lectin Pathway in the Pathogenesis of Experimental Inflammatory Arthritis: Essential Role of the Lectin Ficolin B and Mannose-Binding Protein-Associated Serine Protease 2.* J Immunol, 2017. **199**(5): p. 1835-1845.
314. Katayama, M., et al., *Ficolin-1 is a promising therapeutic target for autoimmune diseases.* Int Immunol, 2019. **31**(1): p. 23-32.

315. Vander Cruyssen, B., et al., *Polymorphisms in the ficolin 1 gene (FCN1) are associated with susceptibility to the development of rheumatoid arthritis.* Rheumatology (Oxford), 2007. **46**(12): p. 1792-5.
316. Millien, V.O., et al., *Cleavage of fibrinogen by proteinases elicits allergic responses through Toll-like receptor 4.* Science, 2013. **341**(6147): p. 792-6.
317. Alexander, C. and E.T. Rietschel, *Bacterial lipopolysaccharides and innate immunity.* Journal of Endotoxin Research, 2001. **7**(3): p. 167-202.
318. Morrison, D.C. and J.L. Ryan, *Endotoxins and disease mechanisms.* Annu Rev Med, 1987. **38**: p. 417-32.
319. Cavaillon, J.M. and M. Adib-Conquy, *Bench-to-bedside review: endotoxin tolerance as a model of leukocyte reprogramming in sepsis.* Crit Care, 2006. **10**(5): p. 233.
320. Deng, H., et al., *Molecular mechanism responsible for the priming of macrophage activation.* J Biol Chem, 2013. **288**(6): p. 3897-906.
321. Henricson, B.E., et al., *Dissociation of lipopolysaccharide (LPS)-inducible gene expression in murine macrophages pretreated with smooth LPS versus monophosphoryl lipid A.* Infect Immun, 1993. **61**(6): p. 2325-33.
322. Hirohashi, N. and D.C. Morrison, *Low-dose lipopolysaccharide (LPS) pretreatment of mouse macrophages modulates LPS-dependent interleukin-6 production in vitro.* Infect Immun, 1996. **64**(3): p. 1011-5.
323. Zhang, X. and D.C. Morrison, *Lipopolysaccharide-induced selective priming effects on tumor necrosis factor alpha and nitric oxide production in mouse peritoneal macrophages.* J Exp Med, 1993. **177**(2): p. 511-6.
324. Benn, C.S., et al., *A small jab - a big effect: nonspecific immunomodulation by vaccines.* Trends Immunol, 2013. **34**(9): p. 431-9.
325. Bekkering, S., et al., *Metabolic Induction of Trained Immunity through the Mevalonate Pathway.* Cell, 2018. **172**(1-2): p. 135-146 e9.
326. Netea, M.G., et al., *Differential requirement for the activation of the inflammasome for processing and release of IL-1beta in monocytes and macrophages.* Blood, 2009. **113**(10): p. 2324-35.
327. Decker, T. and M.-L. Lohmann-Matthes, *A quick and simple method for the quantitation of lactate dehydrogenase release in measurements of cellular cytotoxicity and tumor necrosis factor (TNF) activity.* Journal of Immunological Methods, 1988. **115**(1): p. 61-69.
328. Riss, T.L., et al., *Cell Viability Assays*, in *Assay Guidance Manual*, S. Markossian, et al., Editors. 2004, Eli Lilly & Company and the National Center for Advancing Translational Sciences: Bethesda (MD).
329. Gillette, T.G. and J.A. Hill, *Readers, writers, and erasers: chromatin as the whiteboard of heart disease.* Circ Res, 2015. **116**(7): p. 1245-53.
330. Kuo, M.H. and C.D. Allis, *In vivo cross-linking and immunoprecipitation for studying dynamic Protein:DNA associations in a chromatin environment.* Methods, 1999. **19**(3): p. 425-33.
331. Dominguez-Andres, J., et al., *The Itaconate Pathway Is a Central Regulatory Node Linking Innate Immune Tolerance and Trained Immunity.* Cell Metab, 2019. **29**(1): p. 211-220 e5.
332. Migale, R., et al., *Specific Lipopolysaccharide Serotypes Induce Differential Maternal and Neonatal Inflammatory Responses in a Murine Model of Preterm Labor.* Am J Pathol, 2015. **185**(9): p. 2390-401.
333. Hirschfeld, M., et al., *Cutting edge: repurification of lipopolysaccharide eliminates signaling through both human and murine toll-like receptor 2.* J Immunol, 2000. **165**(2): p. 618-22.

334. West, M.A. and A. Koons, *Endotoxin tolerance in sepsis: concentration-dependent augmentation or inhibition of LPS-stimulated macrophage TNF secretion by LPS pretreatment.* J Trauma, 2008. **65**(4): p. 893-8; discussion 898-900.
335. Patel, A.A., et al., *The fate and lifespan of human monocyte subsets in steady state and systemic inflammation.* J Exp Med, 2017. **214**(7): p. 1913-1923.
336. Safi, W., et al., *Differentiation of human CD14+ monocytes: an experimental investigation of the optimal culture medium and evidence of a lack of differentiation along the endothelial line.* Exp Mol Med, 2016. **48**: p. e227.
337. Lu, Y.C., W.C. Yeh, and P.S. Ohashi, *LPS/TLR4 signal transduction pathway.* Cytokine, 2008. **42**(2): p. 145-151.
338. Sakai, J., et al., *Lipopolysaccharide-induced NF-kappaB nuclear translocation is primarily dependent on MyD88, but TNFalpha expression requires TRIF and MyD88.* Sci Rep, 2017. **7**(1): p. 1428.
339. Fitzgerald, K.A., D.C. Rowe, and D.T. Golenbock, *Endotoxin recognition and signal transduction by the TLR4/MD2-complex.* Microbes Infect, 2004. **6**(15): p. 1361-7.
340. Keating, S.T., et al., *The Set7 Lysine Methyltransferase Regulates Plasticity in Oxidative Phosphorylation Necessary for Trained Immunity Induced by beta-Glucan.* Cell Rep, 2020. **31**(3): p. 107548.
341. de Vos, A.F., et al., *In vivo lipopolysaccharide exposure of human blood leukocytes induces cross-tolerance to multiple TLR ligands.* J Immunol, 2009. **183**(1): p. 533-42.
342. Mizel, S.B. and J.A. Snipes, *Gram-negative flagellin-induced self-tolerance is associated with a block in interleukin-1 receptor-associated kinase release from toll-like receptor 5.* J Biol Chem, 2002. **277**(25): p. 22414-20.
343. Yeo, S.J., et al., *CpG DNA induces self and cross-hyporesponsiveness of RAW264.7 cells in response to CpG DNA and lipopolysaccharide: alterations in IL-1 receptor-associated kinase expression.* J Immunol, 2003. **170**(2): p. 1052-61.
344. Hu, J., et al., *A20 is critical for the induction of Pam3CSK4-tolerance in monocytic THP-1 cells.* PLoS One, 2014. **9**(1): p. e87528.
345. Jiang, W., et al., *Toll-like receptor 3 ligand attenuates LPS-induced liver injury by down-regulation of toll-like receptor 4 expression on macrophages.* Proc Natl Acad Sci U S A, 2005. **102**(47): p. 17077-82.
346. Sato, S., et al., *A variety of microbial components induce tolerance to lipopolysaccharide by differentially affecting MyD88-dependent and -independent pathways.* Int Immunol, 2002. **14**(7): p. 783-91.
347. Dalpke, A.H., et al., *Differential effects of CpG-DNA in Toll-like receptor-2/-4/-9 tolerance and cross-tolerance.* Immunology, 2005. **116**(2): p. 203-12.
348. Nahid, M.A., M. Satoh, and E.K. Chan, *Interleukin 1beta-Responsive MicroRNA-146a Is Critical for the Cytokine-Induced Tolerance and Cross-Tolerance to Toll-Like Receptor Ligands.* J Innate Immun, 2015. **7**(4): p. 428-40.
349. Lee, K.H., et al., *Proteasomal degradation of Nod2 protein mediates tolerance to bacterial cell wall components.* J Biol Chem, 2012. **287**(47): p. 39800-11.
350. Escoll, P., et al., *Rapid up-regulation of IRAK-M expression following a second endotoxin challenge in human monocytes and in monocytes isolated from septic patients.* Biochem Biophys Res Commun, 2003. **311**(2): p. 465-72.
351. Yoshimura, A., T. Naka, and M. Kubo, *SOCS proteins, cytokine signalling and immune regulation.* Nat Rev Immunol, 2007. **7**(6): p. 454-65.
352. Lee, E.G., et al., *Failure to regulate TNF-induced NF-kappaB and cell death responses in A20-deficient mice.* Science, 2000. **289**(5488): p. 2350-4.
353. Boone, D.L., et al., *The ubiquitin-modifying enzyme A20 is required for termination of Toll-like receptor responses.* Nat Immunol, 2004. **5**(10): p. 1052-60.

354. van 't Veer, C., et al., *Induction of IRAK-M is associated with lipopolysaccharide tolerance in a human endotoxemia model.* J Immunol, 2007. **179**(10): p. 7110-20.
355. Su, H., et al., *miR-9-5p regulates immunometabolic and epigenetic pathways in beta-glucan-trained immunity via IDH3alpha.* JCI Insight, 2021. **6**(9).
356. Russo, R.C., et al., *The CXCL8/IL-8 chemokine family and its receptors in inflammatory diseases.* Expert Rev Clin Immunol, 2014. **10**(5): p. 593-619.
357. Mayadas, T.N., X. Cullere, and C.A. Lowell, *The multifaceted functions of neutrophils.* Annu Rev Pathol, 2014. **9**: p. 181-218.
358. Witter, A.R., B.M. Okunnu, and R.E. Berg, *The Essential Role of Neutrophils during Infection with the Intracellular Bacterial Pathogen Listeria monocytogenes.* J Immunol, 2016. **197**(5): p. 1557-65.
359. Appelberg, R., *Neutrophils and intracellular pathogens: beyond phagocytosis and killing.* Trends Microbiol, 2007. **15**(2): p. 87-92.
360. Naumenko, V., et al., *Neutrophils in viral infection.* Cell Tissue Res, 2018. **371**(3): p. 505-516.
361. Scheller, J., et al., *The pro- and anti-inflammatory properties of the cytokine interleukin-6.* Biochim Biophys Acta, 2011. **1813**(5): p. 878-88.
362. Cressman, D.E., et al., *Liver failure and defective hepatocyte regeneration in interleukin-6-deficient mice.* Science, 1996. **274**(5291): p. 1379-83.
363. Gallucci, R.M., et al., *Impaired cutaneous wound healing in interleukin-6-deficient and immunosuppressed mice.* FASEB J, 2000. **14**(15): p. 2525-31.
364. Lin, Z.Q., et al., *Essential involvement of IL-6 in the skin wound-healing process as evidenced by delayed wound healing in IL-6-deficient mice.* J Leukoc Biol, 2003. **73**(6): p. 713-21.
365. Hirota, H., et al., *Accelerated Nerve Regeneration in Mice by upregulated expression of interleukin (IL) 6 and IL-6 receptor after trauma.* J Exp Med, 1996. **183**(6): p. 2627-34.
366. Agarwal, S., et al., *Differential expression of IL-1 beta, TNF-alpha, IL-6, and IL-8 in human monocytes in response to lipopolysaccharides from different microbes.* J Dent Res, 1995. **74**(4): p. 1057-65.
367. Park, S.H., et al., *Type I interferons and the cytokine TNF cooperatively reprogram the macrophage epigenome to promote inflammatory activation.* Nat Immunol, 2017. **18**(10): p. 1104-1116.
368. Neidhart, M., et al., *Oligomeric S100A4 Is Associated With Monocyte Innate Immune Memory and Bypass of Tolerance to Subsequent Stimulation With Lipopolysaccharides.* Front Immunol, 2019. **10**: p. 791.
369. Piccinini, A.M. and K.S. Midwood, *DAMPening inflammation by modulating TLR signalling.* Mediators Inflamm, 2010. **2010**.
370. Hasegawa, M., T. Yoshida, and A. Sudo, *Tenascin-C in Osteoarthritis and Rheumatoid Arthritis.* Front Immunol, 2020. **11**: p. 577015.
371. Silman, A.J. and J.E. Pearson, *Epidemiology and genetics of rheumatoid arthritis.* Arthritis Res, 2002. **4 Suppl 3**: p. S265-72.
372. Cross, M., et al., *The global burden of rheumatoid arthritis: estimates from the global burden of disease 2010 study.* Ann Rheum Dis, 2014. **73**(7): p. 1316-22.
373. Birch, J.T., Jr. and S. Bhattacharya, *Emerging trends in diagnosis and treatment of rheumatoid arthritis.* Prim Care, 2010. **37**(4): p. 779-92, vii.
374. Viatte, S., et al., *Association of HLA-DRB1 haplotypes with rheumatoid arthritis severity, mortality, and treatment response.* JAMA, 2015. **313**(16): p. 1645-56.
375. Klareskog, L., L. Padyukov, and L. Alfredsson, *Smoking as a trigger for inflammatory rheumatic diseases.* Curr Opin Rheumatol, 2007. **19**(1): p. 49-54.
376. Scher, J.U., D.R. Littman, and S.B. Abramson, *Microbiome in Inflammatory Arthritis and Human Rheumatic Diseases.* Arthritis Rheumatol, 2016. **68**(1): p. 35-45.

377. Dorner, T., et al., *Rheumatoid factor revisited.* Curr Opin Rheumatol, 2004. **16**(3): p. 246-53.
378. Wu, C.Y., H.Y. Yang, and J.H. Lai, *Anti-Citrullinated Protein Antibodies in Patients with Rheumatoid Arthritis: Biological Effects and Mechanisms of Immunopathogenesis.* Int J Mol Sci, 2020. **21**(11).
379. Bang, H., et al., *Mutation and citrullination modifies vimentin to a novel autoantigen for rheumatoid arthritis.* Arthritis Rheum, 2007. **56**(8): p. 2503-11.
380. Mahdi, H., et al., *Specific interaction between genotype, smoking and autoimmunity to citrullinated alpha-enolase in the etiology of rheumatoid arthritis.* Nat Genet, 2009. **41**(12): p. 1319-24.
381. Suwannalai, P., et al., *Anti-citrullinated protein antibodies (ACPA) in early rheumatoid arthritis.* Mod Rheumatol, 2012. **22**(1): p. 15-20.
382. Pratt, A.G. and J.D. Isaacs, *Seronegative rheumatoid arthritis: pathogenetic and therapeutic aspects.* Best Pract Res Clin Rheumatol, 2014. **28**(4): p. 651-9.
383. Wu, F., et al., *B Cells in Rheumatoid ArthritisPathogenic Mechanisms and Treatment Prospects.* Front Immunol, 2021. **12**: p. 750753.
384. Weyand, C.M. and J.J. Goronzy, *The immunology of rheumatoid arthritis.* Nat Immunol, 2021. **22**(1): p. 10-18.
385. Firestein, G.S., J.M. Alvaro-Gracia, and R. Maki, *Quantitative analysis of cytokine gene expression in rheumatoid arthritis.* J Immunol, 1990. **144**(9): p. 3347-53.
386. Chen, E., E.C. Keystone, and E.N. Fish, *Restricted cytokine expression in rheumatoid arthritis.* Arthritis Rheum, 1993. **36**(7): p. 901-10.
387. Vermeire, K., et al., *Accelerated collagen-induced arthritis in IFN-gamma receptor-deficient mice.* J Immunol, 1997. **158**(11): p. 5507-13.
388. Matthys, P., et al., *Anti-IL-12 antibody prevents the development and progression of collagen-induced arthritis in IFN-γ receptor-deficient mice.* European Journal of Immunology, 1998. **28**(7): p. 2143-2151.
389. Raza, K., et al., *Early rheumatoid arthritis is characterized by a distinct and transient synovial fluid cytokine profile of T cell and stromal cell origin.* Arthritis Res Ther, 2005. **7**(4): p. R784-95.
390. Yang, P., et al., *Th17 cell pathogenicity and plasticity in rheumatoid arthritis.* J Leukoc Biol, 2019. **106**(6): p. 1233-1240.
391. Lubberts, E., et al., *Overexpression of IL-17 in the knee joint of collagen type II immunized mice promotes collagen arthritis and aggravates joint destruction.* Inflamm Res, 2002. **51**(2): p. 102-4.
392. Nakae, S., et al., *Suppression of immune induction of collagen-induced arthritis in IL-17-deficient mice.* J Immunol, 2003. **171**(11): p. 6173-7.
393. Lubberts, E., et al., *Treatment with a neutralizing anti-murine interleukin-17 antibody after the onset of collagen-induced arthritis reduces joint inflammation, cartilage destruction, and bone erosion.* Arthritis Rheum, 2004. **50**(2): p. 650-9.
394. Zwerina, K., et al., *Anti IL-17A therapy inhibits bone loss in TNF-alpha-mediated murine arthritis by modulation of the T-cell balance.* Eur J Immunol, 2012. **42**(2): p. 413-23.
395. Kellner, H., *Targeting interleukin-17 in patients with active rheumatoid arthritis: rationale and clinical potential.* Ther Adv Musculoskelet Dis, 2013. **5**(3): p. 141-52.
396. Petrelli, A. and F. van Wijk, *CD8(+) T cells in human autoimmune arthritis: the unusual suspects.* Nat Rev Rheumatol, 2016. **12**(7): p. 421-8.
397. Khan, S., J.D. Greenberg, and N. Bhardwaj, *Dendritic cells as targets for therapy in rheumatoid arthritis.* Nat Rev Rheumatol, 2009. **5**(10): p. 566-71.
398. Rivellese, F., et al., *Mast cells in rheumatoid arthritis: friends or foes?* Autoimmun Rev, 2017. **16**(6): p. 557-563.

399. O'Neil, L.J. and M.J. Kaplan, *Neutrophils in Rheumatoid Arthritis: Breaking Immune Tolerance and Fueling Disease.* Trends Mol Med, 2019. **25**(3): p. 215-227.
400. Richards, P.J., et al., *Liposomal clodronate eliminates synovial macrophages, reduces inflammation and ameliorates joint destruction in antigen-induced arthritis.* Rheumatology (Oxford), 1999. **38**(9): p. 818-25.
401. Mulherin, D., O. Fitzgerald, and B. Bresnihan, *Synovial tissue macrophage populations and articular damage in rheumatoid arthritis.* Arthritis Rheum, 1996. **39**(1): p. 115-24.
402. Haringman, J.J., et al., *Synovial tissue macrophages: a sensitive biomarker for response to treatment in patients with rheumatoid arthritis.* Annals of the Rheumatic Diseases, 2005. **64**: p. 834-838.
403. Alivernini, S., et al., *Distinct synovial tissue macrophage subsets regulate inflammation and remission in rheumatoid arthritis.* Nat Med, 2020. **26**(8): p. 1295-1306.
404. McInnes, I.B. and G. Schett, *Cytokines in the pathogenesis of rheumatoid arthritis.* Nat Rev Immunol, 2007. **7**(6): p. 429-42.
405. Foell, D., H. Wittkowski, and J. Roth, *Mechanisms of disease: a 'DAMP' view of inflammatory arthritis.* Nat Clin Pract Rheumatol, 2007. **3**(7): p. 382-90.
406. Unterberger, S., et al., *Contribution of Toll-Like Receptors and the NLRP3 Inflammasome in Rheumatoid Arthritis Pathophysiology.* Immunotargets Ther, 2021. **10**: p. 285-298.
407. Huang, Q., et al., *Increased macrophage activation mediated through toll-like receptors in rheumatoid arthritis.* Arthritis Rheum, 2007. **56**(7): p. 2192-201.
408. Chamberlain, N.D., et al., *TLR5, a novel and unidentified inflammatory mediator in rheumatoid arthritis that correlates with disease activity score and joint TNF-alpha levels.* J Immunol, 2012. **189**(1): p. 475-83.
409. Chamberlain, N.D., et al., *Ligation of TLR7 by rheumatoid arthritis synovial fluid single strand RNA induces transcription of TNFalpha in monocytes.* Ann Rheum Dis, 2013. **72**(3): p. 418-26.
410. Lacerte, P., et al., *Overexpression of TLR2 and TLR9 on monocyte subsets of active rheumatoid arthritis patients contributes to enhance responsiveness to TLR agonists.* Arthritis Res Ther, 2016. **18**: p. 10.
411. Thwaites, R.S., et al., *TLR1/2 and 5 induce elevated cytokine levels from rheumatoid arthritis monocytes independent of ACPA or RF autoantibody status.* Rheumatology (Oxford), 2020. **59**(11): p. 3533-3539.
412. Gebura, K., et al., *Polymorphisms within Genes Involved in Regulation of the NF-kappaB Pathway in Patients with Rheumatoid Arthritis.* Int J Mol Sci, 2017. **18**(7).
413. Kim, H.S. and D.H. Chung, *TLR4-mediated IL-12 production enhances IFN-gamma and IL-1beta production, which inhibits TGF-beta production and promotes antibody-induced joint inflammation.* Arthritis Res Ther, 2012. **14**(5): p. R210.
414. Pullerits, R., et al., *High mobility group box chromosomal protein 1, a DNA binding cytokine, induces arthritis.* Arthritis Rheum, 2003. **48**(6): p. 1693-700.
415. Biscetti, F., et al., *The role of high-mobility group box protein 1 in collagen antibody-induced arthritis is dependent on vascular endothelial growth factor.* Clin Exp Immunol, 2016. **184**(1): p. 62-72.
416. Aungier, S.R., et al., *Targeting early changes in the synovial microenvironment: a new class of immunomodulatory therapy?* Annals of the Rheumatic Diseases, 2019. **78**: p. 186-191.
417. Goldstein, R.S., et al., *Cholinergic anti-inflammatory pathway activity and High Mobility Group Box-1 (HMGB1) serum levels in patients with rheumatoid arthritis.* Mol Med, 2007. **13**(3-4): p. 210-5.
418. Jarlborg, M., et al., *Serum calprotectin: a promising biomarker in rheumatoid arthritis and axial spondyloarthritis.* Arthritis Res Ther, 2020. **22**(1): p. 105.

419. Salter, D.M., *Tenascin is increased in cartilage and synovium from arthritic knees.* Br J Rheumatol, 1993. **32**(9): p. 780-6.
420. Chevalier, X., et al., *Tenascin distribution in articular cartilage from normal subjects and from patients with osteoarthritis and rheumatoid arthritis.* Arthritis Rheum, 1994. **37**(7): p. 1013-22.
421. de Brito Rocha, S., D.C. Baldo, and L.E.C. Andrade, *Clinical and pathophysiologic relevance of autoantibodies in rheumatoid arthritis.* Adv Rheumatol, 2019. **59**(1): p. 2.
422. Song, J., et al., *Shared recognition of citrullinated tenascin-C peptides by T and B cells in rheumatoid arthritis.* JCI Insight, 2021. **6**(5).
423. Tutturen, A.E., B. Fleckenstein, and G.A. de Souza, *Assessing the citrullinome in rheumatoid arthritis synovial fluid with and without enrichment of citrullinated peptides.* J Proteome Res, 2014. **13**(6): p. 2867-73.
424. van Beers, J.J., et al., *The rheumatoid arthritis synovial fluid citrullinome reveals novel citrullinated epitopes in apolipoprotein E, myeloid nuclear differentiation antigen, and beta-actin.* Arthritis Rheum, 2013. **65**(1): p. 69-80.
425. Wang, F., et al., *Identification of citrullinated peptides in the synovial fluid of patients with rheumatoid arthritis using LC-MALDI-TOF/TOF.* Clin Rheumatol, 2016. **35**(9): p. 2185-94.
426. Darrah, E. and F. Andrade, *Rheumatoid arthritis and citrullination.* Curr Opin Rheumatol, 2018. **30**(1): p. 72-78.
427. Romero, V., et al., *Immune-mediated pore-forming pathways induce cellular hypercitrullination and generate citrullinated autoantigens in rheumatoid arthritis.* Sci Transl Med, 2013. **5**(209): p. 209ra150.
428. Inagaki, M., et al., *Ca2+-dependent deimination-induced disassembly of intermediate filaments involves specific modification of the amino-terminal head domain.* Journal of Biological Chemistry, 1989. **264**(30): p. 18119-18127.
429. Jang, B., et al., *Peptidylarginine deiminase modulates the physiological roles of enolase via citrullination: links between altered multifunction of enolase and neurodegenerative diseases.* Biochem J, 2012. **445**(2): p. 183-92.
430. Kato, M., *New insights into IFN-gamma in rheumatoid arthritis: role in the era of JAK inhibitors.* Immunol Med, 2020. **43**(2): p. 72-78.
431. Chen, J. and L.B. Ivashkiv, *IFN-gamma abrogates endotoxin tolerance by facilitating Toll-like receptor-induced chromatin remodeling.* Proc Natl Acad Sci U S A, 2010. **107**(45): p. 19438-43.
432. Karami, J., et al., *Genetic implications in the pathogenesis of rheumatoid arthritis; an updated review.* Gene, 2019. **702**: p. 8-16.
433. Leirisalo-Repo, M., et al., *Production of TNF by monocytes of patients with early rheumatoid arthritis is increased.* Scand J Rheumatol, 1995. **24**(6): p. 366-71.
434. Rossol, M., et al., *The contact-mediated response of peripheral-blood monocytes to preactivated T cells is suppressed by serum factors in rheumatoid arthritis.* Arthritis Res Ther, 2005. **7**(6): p. R1189-99.
435. Fabris, M., et al., *Mononuclear cell response to lipopolysaccharide in patients with rheumatoid arthritis: relationship with tristetraprolin expression.* J Rheumatol, 2005. **32**(6): p. 998-1005.
436. Sperber, K., et al., *Selective regulation of cytokine secretion by hydroxychloroquine: inhibition of interleukin 1 alpha (IL-1-alpha) and IL-6 in human monocytes and T cells.* J Rheumatol, 1993. **20**(5): p. 803-8.
437. vandenBorne, B., et al., *Chloroquine and hydroxychloroquine equally affect tumor necrosis factor-alpha, interleukin 6, and interferon-gamma production by peripheral blood mononuclear cells.* Journal of Rheumatology, 1997. **24**(1): p. 55-60.

438. Jang, C.H., et al., *Chloroquine inhibits production of TNF-alpha, IL-1beta and IL-6 from lipopolysaccharide-stimulated human monocytes/macrophages by different modes.* Rheumatology (Oxford), 2006. **45**(6): p. 703-10.
439. Rother, N., et al., *Hydroxychloroquine Inhibits the Trained Innate Immune Response to Interferons.* Cell Rep Med, 2020. **1**(9): p. 100146.
440. Zhong, Q., et al., *IgG Immunocomplexes Sensitize Human Monocytes for Inflammatory Hyperactivity via Transcriptomic and Epigenetic Reprogramming in Rheumatoid Arthritis.* J Immunol, 2018. **200**(12): p. 3913-3925.
441. Mitroulis, I., et al., *Modulation of Myelopoiesis Progenitors Is an Integral Component of Trained Immunity.* Cell, 2018. **172**(1-2): p. 147-161 e12.
442. Kaufmann, E., et al., *BCG Educates Hematopoietic Stem Cells to Generate Protective Innate Immunity against Tuberculosis.* Cell, 2018. **172**(1-2): p. 176-190 e19.
443. Matzinger, P., *Tolerance, danger, and the extended family.* Annu Rev Immunol, 1994. **12**: p. 991-1045.
444. Seong, S.Y. and P. Matzinger, *Hydrophobicity: an ancient damage-associated molecular pattern that initiates innate immune responses.* Nat Rev Immunol, 2004. **4**(6): p. 469-78.
445. Yamamoto, M., et al., *Role of adaptor TRIF in the MyD88-independent toll-like receptor signaling pathway.* Science, 2003. **301**(5633): p. 640-3.
446. Lee, D.M. and M.E. Weinblatt, *Rheumatoid arthritis.* The Lancet, 2001. **358**(9285): p. 903-911.
447. Smolen, J.S., et al., *EULAR recommendations for the management of rheumatoid arthritis with synthetic and biological disease-modifying antirheumatic drugs: 2019 update.* Ann Rheum Dis, 2020. **79**(6): p. 685-699.
448. Smolen, J.S., D. Aletaha, and I.B. McInnes, *Rheumatoid arthritis.* The Lancet, 2016. **388**(10055): p. 2023-2038.
449. Nagy, G. and R.F. van Vollenhoven, *Sustained biologic-free and drug-free remission in rheumatoid arthritis, where are we now?* Arthritis Res Ther, 2015. **17**: p. 181.
450. Scott, D.L., *CHAPTER 70 - Arthritis in the Elderly*, in *Brocklehurst's Textbook of Geriatric Medicine and Gerontology (Seventh Edition)*, H.M. Fillit, K. Rockwood, and K. Woodhouse, Editors. 2010, W.B. Saunders: Philadelphia. p. 566-576.
451. Sosin, M. and S. Handa, *Low dose methotrexate and bone marrow suppression.* BMJ, 2003. **326**(7383): p. 266-7.
452. Shergy, W.J., et al., *Methotrexate-associated hepatotoxicity: retrospective analysis of 210 patients with rheumatoid arthritis.* The American Journal of Medicine, 1988. **85**(6): p. 771-774.
453. Riley, T.R. and M.D. George, *Risk for infections with glucocorticoids and DMARDs in patients with rheumatoid arthritis.* RMD Open, 2021. **7**(1).
454. van den Broek, M., et al., *Drug-free remission: is it already possible?* Curr Opin Rheumatol, 2011. **23**(3): p. 266-72.